

**PERFORMANCE OF CROSS-LAMINATED TIMBER SHEAR WALLS FOR
PLATFORM CONSTRUCTION UNDER LATERAL LOADING**

by

Md Shahnewaz

MASc, The University of British Columbia, 2013

A THESIS SUBMITTED IN PARTIAL FULFILLMENT OF
THE REQUIREMENTS FOR THE DEGREE OF

DOCTOR OF PHILOSOPHY

in

THE FACULTY OF GRADUATE AND POSTDOCTORAL STUDIES

(Civil Engineering)

THE UNIVERSITY OF BRITISH COLUMBIA

(Vancouver)

April 2018

© Md Shahnewaz, 2018

Abstract

Cross-laminated timber (CLT) is gaining popularity in residential and non-residential applications in the North American construction market. CLT is very effective in resisting lateral forces resulting from wind and seismic loads. This research investigated the in-plane performance of CLT shear wall for platform-type buildings under lateral loading.

Analytical models were proposed to estimate the in-plane stiffness of CLT wall panels with openings based on experimental and numerical investigations. The models estimate the in-plane stiffness under consideration of panel thickness, aspect ratios, and size and location of the openings. A sensitivity analysis was conducted to reduce the number of model parameters to those that have a significant impact on the stiffness reduction of CLT wall panels with openings.

Finite element models of CLT wall connections were developed and calibrated against experimental tests. The results were incorporated into models of CLT single and coupled shear walls. Finite element analyses were conducted on CLT shear walls and the results in terms of peak displacements, peak loads and energy dissipation were in good agreement when compared against full-scale shear wall tests. A parametric study on single and coupled CLT shear walls was conducted with variation of number and type of connectors. The seismic performance of 56-single and 40-coupled CLT shear walls' assemblies for platform-type construction were evaluated.

Deflection formulas were proposed for both single and coupled CLT shear walls loaded laterally in-plane that in addition to the contributions of CLT panels and connections, also account for the influence of adjacent perpendicular walls and floors above and illustrated with examples.

Analytical equations were proposed to calculate the resistance of CLT shear walls accounting for the kinematic behaviour of the walls observed in experimental investigations (sliding, rocking and

combined sliding-rocking) and illustrated with examples. Different configurations (number and location of hold-downs) of single and coupled CLT walls were considered. The findings presented in this thesis will contribute to the scientific body of knowledge and furthermore will be a useful tool for practitioners for the successful seismic design of CLT platform buildings in-line with the current CSA O86 provisions.

Lay Summary

Cross-laminated timber (CLT) is an engineered wood product consisting of several layers of lumber boards stacked crosswise and glued together to form a solid panel. CLT offers new design possibilities to architects and engineers being a light and sustainable material. CLT panels can be used as the main structural component to resist wind and earthquake loading in platform-type buildings. This research investigated the performance of CLT shear walls for platform-type buildings under loads applied along the length or height of a wall (in-plane). This research proposed simplified formulas to estimate the in-plane stiffness of CLT wall panels with openings based on experimental and numerical investigations. This research also developed simplified procedures to estimate the deflection and resistance of CLT shear walls which are required for a successful design of CLT buildings. The findings presented in this thesis provide design guidance for engineers and practitioners.

Preface

This research was initiated from a collaborative project in partnership with the FPInnovations and the University of British Columbia. I, the author of this thesis, am the principal investigator of this research project. Some findings have been published and others have been submitted for publication in conference proceedings and journals. I am the primary author of these manuscripts and my co-authors (Dr. Thomas Tannert, Dr. M. Shahria Alam, and Dr. Marjan Popovski) have provided technical input and reviewing the research findings.

Shahnewaz, M., Tannert, T., Alam, M. S. & Popovski, M. (2017). In-Plane Stiffness of Cross Laminated Timber Panels with Openings. *Structural Engineering International, IABSE*, 27(2), 217-223. DOI: 10.2749/101686617X14881932436131.

Shahnewaz, M., Tannert, T., Alam, M. S. & Popovski, M. (2017). Performance of Cross Laminated Timber Shear walls under Cyclic Loading. 6th International Conference on Engineering Mechanics and Materials, CSCE, May 31-June 3 2017, Vancouver, BC, Canada.

Shahnewaz, M., Tannert, T., Alam, M. S. & Popovski, M. (2017). Capacity-Based Design for Platform-Framed Cross-Laminated Timber Buildings. *Structures Congress 2017, ASCE*, April 6-8, 2017, Denver, CO, USA.

Shahnewaz, M., Tannert, T., Alam, M. S. & Popovski, M. (2017). Sensitivity Analysis of In-Plane Stiffness of CLT Walls with Openings. 16th World Conference on Earthquake Conference, WCEE 2017, 9-13th January 2017, Santiago, Chile.

Shahnewaz, M., Tannert, T., Alam, M. S. & Popovski, M. (2016). In-plane stiffness of CLT walls with and without opening. *World Conference on Timber Engineering, WCTE 2016*, 22-25th August, Vienna, Austria.

Shahnewaz, M., Tannert, T., Alam, M. S. & Popovski, M. (2016). CLT walls with openings: in-plane stiffness using finite element and its sensitivity analysis. 5th International Structural Specialty Conference, CSCE 2016, 1-4th June 2016, London, ON, Canada.

Shahnewaz, M., Tannert, T., Alam, M. S. & Popovski, M. (2015). Experimental and Finite Element Analysis of Cross Laminated Timber (CLT) Panels. In First International Conference on Advances in Civil Infrastructure and Construction Materials 2015, 14-15th December 2015, Dhaka, Bangladesh.

Shahnewaz, M., Tannert, T., Alam, M. S. & Popovski, M. Deflection of Cross Laminated Timber Shear Walls in Platform Construction. World Conference on Timber Engineering, WCTE 2018, 20-23th August, Seoul, Rep. of Korea (Submitted).

Shahnewaz, M., Tannert, T., Alam, M. S. & Popovski, M. Strength and Stiffness of Cross Laminated Timber Shear Walls in Platform Construction. World Conference on Timber Engineering, WCTE 2018, 20-23th August, Seoul, Rep. of Korea (Submitted).

Shahnewaz, M., Tannert, T., Alam, M. S. & Popovski, M. In-plane Strength and Stiffness of Cross Laminated Timber Shear Walls. (manuscript in preparation).

Shahnewaz, M., Tannert, T., Alam, M. S. & Popovski, M. In-plane Deflection of Cross Laminated Timber Shear Walls with Perpendicular Walls and Floor Above for Platform-Type Construction. (manuscript in preparation).

Shahnewaz, M., Tannert, T., Alam, M. S. & Popovski, M. Lateral Resistance of Cross Laminated Timber Shear Walls for Platform-Type Construction. (manuscript in preparation).

Table of Contents

Abstract.....	ii
Lay Summary	iv
Preface.....	v
Table of Contents	vii
List of Tables	xii
List of Figures.....	xiii
List of Symbols and Abbreviations	xviii
Acknowledgements	xxii
Dedication	xxiii
Chapter 1: Introduction	1
1.1 Background.....	1
1.2 Cross-laminated timber	2
1.3 In-Plane Stiffness of CLT Panels	4
1.4 In-Plane Stiffness of CLT Panels with Openings.....	11
1.5 In-Plane Strength and Stiffness of CLT Shear Walls.....	15
1.5.1 Connections for CLT Shear-Walls in Platform-type Construction	16
1.5.2 CLT Shear Walls in Platform-type Construction	18
1.6 CLT Buildings under Lateral Loading	25
1.6.1 CLT Structural Systems	25
1.6.2 European Studies on CLT Buildings.....	27
1.6.3 North American Studies on CLT Buildings	30
1.6.4 Asian Studies on CLT Buildings.....	32

1.7	Code Provision for CLT Platform Building Design	34
1.7.1	CSA O86	34
1.7.2	Capacity-based design approached considered in CSA O86	35
1.7.3	IBC 2015 & NDS 2015	36
1.8	Research Need	37
1.9	Objectives	38
1.10	Thesis Outline.....	38
Chapter 2:	In-Plane Stiffness of CLT Panels with Openings	40
2.1	Introduction	40
2.2	Finite Element Analysis for CLT panels with openings	42
2.2.1	Model Development	42
2.3	Model Validation.....	43
2.4	Parametric Study on 3-ply CLT Wall Panels with Openings.....	45
2.4.1	Effect of opening size.....	45
2.4.2	Effect of opening-to-wall height ratio	48
2.4.3	Effect of opening offset.....	49
2.4.4	Effect of panel aspect ratio.....	51
2.5	Sensitivity Analysis on 3-ply CLT Wall Panels with Openings	52
2.5.1	Methods	52
2.5.2	Results of Sensitivity Analyses	54
2.6	In-plane Stiffness of 5-ply and 7-ply CLT Wall Panels with Openings.....	57
2.6.1	Numerical Study on 5-ply and 7-ply CLT Walls	57
2.6.2	Parametric Study on 5-ply and 7-ply CLT Wall Panels with Openings	58
2.6.3	Results and Discussion.....	59
2.7	Summary.....	60

Chapter 3: Strength and Stiffness of Single and Coupled CLT Shear Walls	62
3.1 Introduction	62
3.2 Finite Element Analysis of CLT Connections.....	64
3.2.1 Tests on CLT Connections	64
3.2.2 FEA Model for Connections	65
3.2.3 Hysteresis Pinching4 Model.....	66
3.2.4 Model Validation for CLT Connections	67
3.3 Finite Element Analysis of CLT Shear Walls	70
3.3.1 Experimental Tests on CLT Shear Walls	70
3.3.2 Shear Wall Model Formulation.....	72
3.3.3 CLT Walls Model Validation.....	73
3.4 Parametric Study for Single and Coupled CLT Walls	77
3.4.1 Single CLT Shear Walls.....	77
3.4.2 Coupled CLT Shear Walls	79
3.5 Summary.....	81
Chapter 4: Deflection of Cross-Laminated Timber Shear Walls.....	82
4.1 Introduction	82
4.2 Single and Coupled Shear Walls and their Connections	83
4.3 Deflection of Single CLT Shear Walls without Perpendicular Walls	88
4.3.1 Bending Deflection	89
4.3.2 Shear Deflection	90
4.3.3 Sliding Deflection	91
4.3.4 Rocking Deflection	92
4.3.5 Total Deflection of Single CLT Shear Wall without perpendicular walls	93
4.4 Deflection of Single CLT Shear Walls with Perp. Walls and Floors above	94

4.4.1	Perpendicular Wall Configuration 1	94
4.4.2	Perpendicular Wall Configuration 2	99
4.5	Deflection of Coupled CLT Shear Walls	102
4.5.1	Deflection of Coupled Shear Walls (4 HDs) without Perp. Walls.....	104
4.5.2	Deflection of Coupled Shear Walls (4 HDs) with Perp. Walls and Floor Above.	106
4.5.3	Deflection of Coupled CLT Shear Walls with 2-HDs	109
4.6	Overview of Equations to Estimate the Deflection of CLT Shear Walls.....	112
4.7	Summary.....	118
Chapter 5: Lateral Resistance of CLT Single and Coupled Shear Walls.....		119
5.1	Introduction	119
5.2	Assumptions	121
5.3	Resistance of Single CLT Shear Walls	122
5.3.1	Overview	122
5.3.2	CLT shear wall with brackets only	123
5.3.3	Single CLT shear wall with brackets and hold-downs.....	129
5.4	Resistance of Coupled CLT Shear Walls	135
5.4.1	Coupled CLT shear wall with brackets only	136
5.4.2	CLT coupled shear wall with brackets and 2-hold-downs	142
5.4.3	CLT coupled shear wall with brackets and 4-hold-downs	147
5.5	Yielding of Vertical Shear Connectors in Coupled CLT Shear Wall	151
5.6	Overview of equations to estimate the resistance of CLT shear walls.....	152
5.7	Parametric study	154
5.7.1	Parametric study on single CLT shear walls	154
5.7.2	Parametric study on coupled CLT shear walls	156
5.8	Summary.....	158

Chapter 6: Conclusion.....	160
6.1 Key Contributions	160
6.2 Future Research	162
Bibliography	164
Appendix A: Parameter studies.....	173
Appendix A1: CLT single shear walls	173
Appendix A2: CLT coupled shear walls.....	175
Appendix B: Examples on Deflection of CLT Shear Walls	177
Appendix B1: Single CLT shear wall	177
Appendix B2: Single CLT shear wall connected to a perpendicular wall	180
Appendix B3: Coupled CLT shear wall with 4-HDs	185
Appendix B4: Coupled CLT shear wall with 4-HDs connected to a perpendicular wall	188
Appendix B5: Coupled CLT shear wall with 2-HDs connected to a perpendicular wall	193
Appendix C: Examples on Lateral Resistance of CLT Shear Walls.....	195
Appendix C1: Single CLT Shear Wall with Brackets	195
Appendix C2: Single CLT Shear Wall with Brackets and Hold-downs.....	202
Appendix C3: Coupled CLT Shear Wall with Brackets and 2-HDs.....	204
Appendix C4: Coupled CLT Shear Wall with Brackets and 4-HDs.....	208
Appendix D: Parametric studies on Resistance of CLT Shear Walls	211
Appendix D1: CLT single shear walls	211
Appendix D2: CLT coupled shear walls.....	213

List of Tables

Table 1.1 Composition factors k_i for CLT panels (Blass & Fellmoser 2004)	5
Table 1.2 Effective strength and stiffness for CLT panels (Blass & Fellmoser 2004)	6
Table 2.1 CLT material properties	43
Table 2.2 Parameter ranges and importance for sensitivity analysis	57
Table 3.1 CLT connection Types and IDs	65
Table 3.2 CLT Connection's FEA results and estimated parameters from EEEP curve.....	69
Table 3.3 Comparison of CLT Connection's FEA vs test results.....	70
Table 3.4 Experimental data set for single and coupled CLT shear walls.....	74
Table 3.5 CLT single and coupled shear walls parameters from EEEP curve	75
Table 3.6 Comparison of CLT shear walls FEA vs test results	76
Table 4.1 Deflection formulas for Single CLT walls	112
Table 4.2 Deflection formulas for Coupled CLT walls with 4-HDs	114
Table 4.3 Deflection formulas for Coupled CLT walls with 2-HDs	116

List of Figures

Figure 1.1 CLT panel.....	3
Figure 1.2 CLT panel with opening.....	4
Figure 1.3 CLT wall parameters for Eq. (1.5)	12
Figure 1.4 CLT wall parameters for Eq. (1.7)	14
Figure 1.5 Diekmann Model: (a) wall with opening, (b) free body diagram of various sheathed areas and (c) horizontal and vertical cuts for internal shears	15
Figure 1.6 Lateral resistance of CLT shear wall from Gavric and Popovski (2014): model D1 to D5 (with permission).....	21
Figure 1.7 Lateral resistance of coupled CLT shear wall from Gavric and Popovski (2014) (with permission)	23
Figure 1.8 CLT structural system: (a) platform-type and (b) balloon-type construction	26
Figure 1.9 Connection detail of CLT floor as a coupling beam (Reproduced from Pei et al. 2017)	32
Figure 2.1 Three-ply CLT panel with door and window	41
Figure 2.2 (a) Experimental and (b) schematic test setup for CLT beams and walls, (c) FE models, and (d) experimental versus FEA load-deflection curves	44
Figure 2.3 Experimental versus FEA load-deflection curves	44
Figure 2.4 Typical openings in CLT Walls and description of parameters	46
Figure 2.5 Effect of opening on CLT wall stiffness; normalized stiffness versus a) % reduction in wall area; b) ratio of opening to wall area (A_o/A_w); c) product of opening aspect ratio (r_o) and opening to wall area (A_o/A_w); and d) aspect ratio of opening to wall ($r_{o/w}$)	47
Figure 2.6 FEA vs. calculated stiffness of CLT walls from this study compared to previous studies	48

Figure 2.7 Bending stiffness calculation from the cross section of m-ply CLT panel	50
Figure 2.8 Effect of opening offset (a) and aspect ratio (b) on CLT wall stiffness	51
Figure 2.9 Algorithm for sensitivity Analysis in optiSLang.....	54
Figure 2.10 (a) MLS approximation of the CLT wall stiffness, k with respect to the two input parameters, A_o/A_w (x_1) and $r_{o/w}$ (x_2); (b) and CoP values of each parameter.....	56
Figure 2.11 CLT panels with openings: (a) 3-layer, (b) 5-layer, and (c) 7-layer	58
Figure 2.12 Effect of opening on the reduction of 3, 5, and 7-ply CLT walls stiffness	59
Figure 3.1 CLT shear walls: (a) single, (b) coupled with lap joint, (c) coupled with spline joint, (d) bracket and hold-down connectors, (e) fasteners, (f) half-lap joint, (g) spline joint.....	63
Figure 3.2 CLT connection's tests configuration: (a) cyclic tension test and FE model, and (b) shear test and FE model	66
Figure 3.3 Pinching4 Model	67
Figure 3.4 CLT Connection's test vs FEA model: (a) bracket B_1 - shear, (b) bracket B_1 - tension, (c) hold-down HD_1 -tension, and (d) STS connector WW_1 -shear (one connector).....	68
Figure 3.5 CLT shear wall's test setup: (a) single wall and (b) coupled wall; and Schematic of FE models: (c) single wall and (d) coupled wall	71
Figure 3.6 CLT shear wall's FEA vs Test: (a) single shear wall-CA-SN-00 (Popovski et al. 2010), (b) coupled shear wall-II.1 (Gavric et al. 2015).....	73
Figure 3.7 Single walls with brackets: (a) capacity, (b) stiffness, (c) ductility, and (d) energy; Single walls with brackets and HDs: (e) capacity, (f) stiffness, (g) ductility, and (h) energy	78
Figure 3.8 Coupled CLT shear walls with half-lap vs spline joints: (a) capacity, (b) stiffness, (c) ductility, and (d) energy; coupled CLT shear walls with 2-HDs vs 4-HDs: (e) capacity, (f) stiffness, (g) ductility, and (h) energy	80
Figure 4.1 Components of (a) single and (b) coupled CLT shear wall.....	83

Figure 4.2 CLT shear walls in a typical floor plan	84
Figure 4.3 Top view of in-plane connections to perpendicular walls: Configuration 1 (a) STSs connection, (b) bracket; Configuration 2 by (c) STSs connection, (d) bracket.....	85
Figure 4.4 Influence of perpendicular wall and floor on CLT shear wall's deflection	86
Figure 4.5 Cross section of in-plane connections floor to in-plane walls: (a) STSs connection and (b) bracket connection	87
Figure 4.6 The deflection calculation of the CLT shear wall under lateral loading	88
Figure 4.7 Deflection due to bending of CLT panel	89
Figure 4.8 Cross section of m-ply CLT panel.....	90
Figure 4.9 Deflection due to shear deformation of CLT panel	90
Figure 4.10 deflection due to sliding of CLT shear wall	91
Figure 4.11 Deflection due to rocking of CLT shear wall	92
Figure 4.12 Force distribution due to CLT wall's rocking in presence of perpendicular wall and floor above.....	95
Figure 4.13 Modified sliding deflection of CLT shear wall	98
Figure 4.14 (a) CLT shear wall with perpendicular wall in configuration 2, (b) walls under rocking, and (c) walls under sliding	100
Figure 4.15 Coupled shear wall with: (a) 4-HDs and half-lap, (b) 4-HDs and spline joints, (c) 2-HDs and half-lap, (d) 2-HDs and spline joint, (e) half-lap schematic, (f) spline joint schematic	103
Figure 4.16 Deflection of coupled CLT shear wall with 4-HDs.....	104
Figure 4.17 Deflection of coupled CLT shear wall with 2-HDs.....	111
Figure 5.1 Typical configuration of single CLT shear walls with: (a) configuration 1-brackets only and (b) configuration 2 -hold-downs and brackets.....	122

Figure 5.2 Kinematic behaviour of single shear walls with brackets subjected to: (a) sliding, (b) rocking and (c) combined rocking-sliding	123
Figure 5.4 (a) Interaction diagram for bracket connection and (b) force-deformation relation for brackets under sliding and rocking.....	127
Figure 5.5 Ratio of sliding to rocking deformation with variation of aspect ratio in CLT shear walls with brackets	129
Figure 5.6 Kinematic behaviour of shear walls with brackets and HDs subjected to: (a) sliding, (b) rocking and (c) combined rocking-sliding	131
Figure 5.7 Elastic force-displacement relation among hold-down and bracket.....	133
Figure 5.8 Ratio of sliding to rocking deformation with variation of aspect ratio in CLT shear walls with brackets and HDs	135
Figure 5.9 Resistance of coupled CLT shear walls: (a) with brackets only, (b) with 2-HDs and brackets, and (c) with 4-HDs and brackets	136
Figure 5.10 Kinematic behaviour of coupled shear wall with brackets subjected to: (a) sliding, (b) rocking, and (c) combined rocking-sliding	138
Figure 5.11 Kinematic behaviour of coupled shear wall with brackets and 2-hold-downs subjected to: (a) sliding, (b) rocking and (c) combined rocking-sliding	143
Figure 5.12 Kinematic behaviour of coupled shear wall with brackets and 4-hold-downs subjected to: (a) sliding, (b) rocking, and (c) combined rocking-sliding	149
Figure 5.13 Equations for resistance of single CLT shear walls	152
Figure 5.14 Equations for resistance of coupled CLT shear walls	153
Figure 5.15 Peak vs resistance of single CLT shear wall with brackets only.....	155
Figure 5.16 Peak vs resistance of single CLT shear wall (with brackets and hold-downs)	155
Figure 5.17 Peak vs resistance of coupled CLT shear wall with brackets and two hold-downs	157
Figure 5.18 Peak vs resistance of coupled CLT shear wall with brackets and four hold-downs	157

Figure B.1 Deflection calculation in a single CLT shear wall.....	177
Figure C.2 Deflection calculation in a single CLT shear wall with perp. wall and floor above: (a) schematic of wall with connections; (b) properties of connections	181
Figure B.3 (a) wall-to-perp. wall connections and (b) in-plane wall-to-floor connections	182
Figure B.4 (a) In-plane wall-to-perp. wall's configuration 2 and (b) connections between in-plane wall-to-perp. wall in configuration 2.....	183
Figure B.5 Geometry and properties of coupled CLT shear walls with 4-HDs	185
Figure B.6 Geometry and properties of coupled CLT shear walls with 4-HDs connected to pepr. wall and floor above	188
Figure B.7 Geometry and properties of coupled CLT shear walls with 2-HDs connected to pepr. wall and floor above	193
Figure C.1 Lateral resistance calculation in a single CLT shear wall with brackets	195
Figure C.2 Lateral resistance calculation in a single CLT shear wall with brackets and HDs ...	202
Figure C.3 Lateral resistance calculation in a coupled CLT shear wall with brackets and 2-HDs	204
Figure C.4 Lateral resistance calculation in a coupled CLT shear wall with brackets and 4-HDs	208

List of Symbols and Abbreviations

A_o	= area of walls with opening
A_w	= area of walls without opening
a_m	= total thickness of the m-ply CLT panel
ALHS	= Advanced Latin Hypercube Sampling
b	= width of the wall
b_1	= width of the left panel in coupled wall
b_2	= width of the right panel in coupled wall
CLT	= cross laminated timber
CoD	= coefficient of determination
CoI	= coefficients of importance
d_{yi}	= vertical deformation of the i^{th} wall-to-floor connectors
E_o	= modulus of elasticity in parallel to grain directions
E_{90}	= modulus of elasticity in perpendicular to grain directions
EI_{eff}	= effective bending stiffness of the CLT panel
F	= lateral force on the wall
F'	= resultant force on CLT shear wall
F_{sl}	= sliding resistance of CLT shear wall
F_r	= rocking resistance of CLT shear wall
F_{r-sl}	= combined rocking-sliding resistance of CLT shear wall
F_N	= normal force on CLT shear wall due to friction
f_{fi}	= reaction forces of wall-to-floor connections
f_{wi}	= reaction forces of wall-to-perpendicular wall connections

G_{CLT} (or G^*)	= shear modulus of CLT panel (or equivalent shear modulus of CLT panel)
G_{\perp}	= shear modulus perpendicular to the grain
G_{\parallel} (or G)	= shear modulus parallel to the grain
G_Q	= transverse (out-of-plane) shear modulus
G_{eff}	= effective shear modulus = $(G_{\perp} + G_{\parallel}) / 2$
H	= wall height
h_o	= opening height
K_b	= bending stiffness of the CLT wall
K_s	= shear stiffness of the CLT wall
K_{sl}	= sliding stiffness of the CLT wall
K_r	= rocking stiffness of the CLT wall
$K_{opening}$	= stiffness of walls with opening
K_{full}	= stiffness of walls without opening
$K_{rectangular}$	= stiffness of rectangular walls
K_{square}	= stiffness of square walls
k_B	= stiffness of the bracket connections in wall-to-floor/foundation underneath
k_{HD}	= stiffness of the hold-down connections
k_f	= stiffness of the connection in CLT wall-to-floor above
k_w	= stiffness of the of the connections in CLT wall-to-perpendicular wall
k_{fi}	= stiffness of the i^{th} wall-to-floor connectors
k_{wi}	= stiffness of the i^{th} wall-to-perpendicular wall connectors

$k_{t,P}$	= tensile stiffness of the brackets in perpendicular wall-to-foundation or floor below
$k_{s,P}$	= shear stiffness of the brackets in perpendicular wall-to-foundation or floor below
L	= wall length
l_o	= opening length
MOP	= Meta-model of Optimal Prognosis
N	= number of sample points
N_B	= factored resistance of the bracket connections
N_B^*	= modified factored resistance of the bracket under combined rocking-sliding
N_{HD}	= factored resistance of the hold-down connections
$N_{B,sl}$	= sliding reaction of the brackets
$N_{B,r}$	= rocking reaction of the brackets
N_{ix}	= reaction force of the i^{th} fasteners in x-direction
N_{iy}	= reaction force of the i^{th} fasteners in y-direction
N_S	= resistance of the vertical joints in coupled wall
n_B	= number of brackets on the wall connecting wall-to-floor/foundation underneath
n_f	= total number of in-plane CLT wall-to-floor connections
n_w	= total number of in-plane CLT wall-to-perpendicular wall connections
p	= number of regression co-efficients
q	= vertical load on the shear wall
R	= reaction forces at the corner connections of CLT shear wall
r	= reduction factor of rocking deflection in coupled wall due to perpendicular walls
r_o	= aspect ratio of the opening (smaller to larger dimension)

$r_{o/w}$	= maximum aspect ratio of opening to wall dimension (max of l_o/L or h_o/H)
r_w	= wall aspect ratio = L/H
r_{off}	= ratio of wall offset to wall dimension (x_{off}/L or y_{off}/H)
SS_T	= total variance
SS_R	= variation due to the regression
SS_E	= unexplained variation
t_{CLT}	= total thickness of CLT panel
x_i	= distance of connection i from the edge of the wall
x_{off}	= opening offset along the length of the wall
x_{fi}	= distance of the wall-to-floor connectors from lower right corner of the wall
y_{off}	= opening offset along the height of the wall
y_{wi}	= distance of the wall-to-perpendicular wall connectors from lower right corner
α	= rotation of the CLT shear wall
γ	= shear strain
δ	= total wall deflection
δ_b	= deflection due to bending
δ_s	= deflection due to shear
δ_{sl}	= deflection due to sliding
δ_r	= deflection due to rocking
μ	= frictional co-efficient
τ	= shear stress

Acknowledgements

First, I would like to express my special thanks and appreciation to my supervisor Dr. Thomas Tannert for his positive support, awesome guidance, and excellent mentorship.

I would like to express my deep sense of gratitude to Dr. Marjan Popovski for not only initiating this research, but for also providing funding from FPInnovations and lending his valuable technical guidance and suggestions throughout the project.

Likewise, my sincere thanks to Dr. M. Shahria Alam for his encouragement and support and to Dr. Carlos Ventura for his valuable comments and guidance with respect to my project proposal defense and yearly committee meetings.

Thanks to my colleagues Hercend, Kuldeep, Alex, Xiaoyue, Afrin and Thomas for their encouragement and support for the success of this project.

I would like to express a very special thanks to Dr. Igor Gavric and Dr. Johannes Schneider for sharing with me their test results on CLT connections and walls.

I am deeply grateful to the University of British Columbia and FPInnovations for their generous funding for this research.

Lastly, I'd like to thank my parents and wife for their love, their sacrifices, and their unwavering support for my educational pursuits.

Dedication

For my wife and parents.

Chapter 1: Introduction

1.1 Background

With an increase in pollution, climate change and a diminishing amount of available fossil fuel, the global demand is increasingly moving towards sustainable construction. Unsurprisingly, the construction industry has begun to utilize materials such as timber that has a low-carbon footprint in their life cycle. High-strength mass timber products, innovative ductile connections, and fast computer-numerically-controlled (CNC) pre-fabrication create an opportunity to build mid- to high-rise timber buildings. The 18-storey UBC's Brock Commons is a good example of a mass timber high-rise showcase building constructed in less than 70 days (UBC News 2016). In 2009, British Columbia (BC) was the first Canadian jurisdiction to allow 6-storey timber structures and later amended its provincial building code (BCBC 2012). According to BC's Wood First Act, all government buildings are required to consider timber as the primary building material (Parliament of British Columbia 2009). This encouraged building of more mid-rise timber buildings; currently more than 200 mid-rise timber buildings have been built or are under construction in BC (ReNew Canada, The Infrastructure Magazine 2016).

Other Canadian provinces have embraced the knowledge and experience from BC and have allowed the construction of timber buildings of up to 6-storey. In spring 2013, Quebec became the second province allowing up to 6-storey timber building. Ontario followed the same path and amended its building code to allow 6-storey wood buildings in 2015. In August 2015, the Quebec Government published a technical guide for construction of mass-timber buildings of up to 12-storey. And the Quebec Building Act now approves 12-storey mass-timber buildings with a

condition that the buildings must have the same quality and safety standards equivalent to what is required by the National Building of Canada (Veilleux et al. 2015).

More recently, the Ontario legislature has introduced the Ontario Forestry Revitalization Act 2017 to allow construction of timber frame buildings of up to 14-storeys (Bill 169 2017). The Bill aims to amend the Building Code Act, stating that “The building code shall not prohibit a building that is 14-storey or less in building height from being of wood frame construction”. The Bill has received First Reading in the Legislative Assembly of Ontario on October 18, 2017. If passed, the change will boost the entire forestry industry in the province.

The Government of Canada has launched a federal program, Green Construction Through Wood (GCWood), aimed at encouraging high-rise wood projects (GCWood 2017). The program allocates a budget of \$39.8 million over four years with a maximum of \$5 million per project to support up to 100% of non-payable projects cost for the demonstration of innovative mass timber products and systems. The program aims to address the technical gaps that prevent the construction of tall timber buildings and to facilitate revisions to the 2025 NBCC.

1.2 Cross-laminated timber

Cross-laminated timber (CLT) was first developed in the early 1990s in Austria and Germany (Gagnon and Pirvu 2011) and ever since has been gaining popularity in residential and non-residential applications throughout Europe. As production of CLT has begun in North America, this product can now be used as a viable wood-based structural solution for the shift towards sustainable densification of urban and suburban centres in North America.

CLT panels consist of several layers of boards stacked crosswise and glued together. A CLT element has usually three to nine glued layers of boards placed orthogonally to each other (90°) to

form a solid panel (see Figure 1.1). Such panels can then be used for wall, floor and roof assemblies. Using CLT for wall and floor panels offers many advantages: the cross-lamination itself provides improved dimensional stability to the product and allows for prefabrication of long floor slabs and single storey walls.

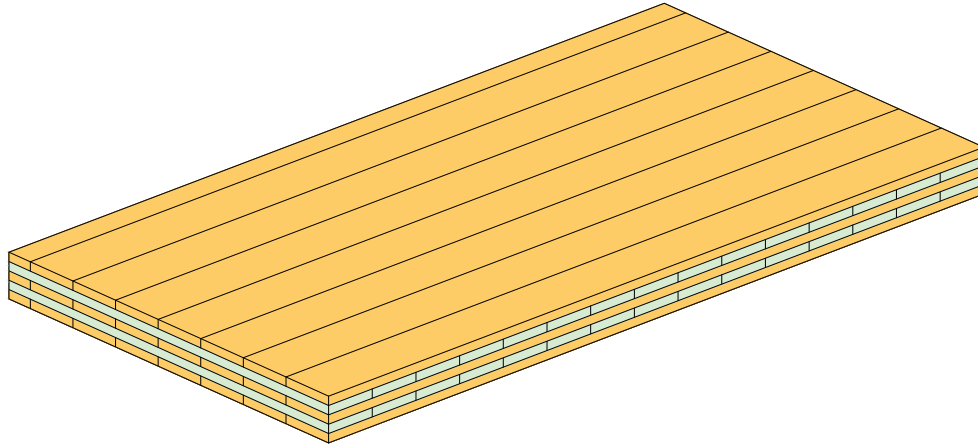


Figure 1.1 CLT panel

CLT panels are easy to process and can be assembled with ordinary tools. The pre-cut wall and floor panels are assembled on the construction site using various types of screws and steel connectors to form the structural system (Gagnon and Pirvu 2011). Quick erection of solid and durable structures is possible even when using low-skilled manpower. The good thermal insulation and a fairly good response in case of fire are added benefits resulting from the massiveness of the wood elements. Furthermore, CLT is a clean product to work with, resulting in little waste and dust produced on site which is preferable in terms of health and safety. Openings for windows and doors (see Figure 1.2) can be pre-cut using either hand-tools or, more commonly, computer controlled CNC machines.

In 2012, the American National Standards Institute (ANSI) approved the first standard for CLT (ANSI/APA PRG 320 2017). The PRG 320 standard covers the manufacturing, qualification and quality assurance requirements for performance-rated CLT. The manufacturing requirements of CLT such as lamination process, lumber species and grades, moisture content, adhesives and joints in laminations are described in detail. The standard includes seven stress classes covering major wood species in North America and provides requirements for CLT qualification tests to meet the structural performance levels specified in the codes. CLT shall meet the minimum structural performance and must be evaluated by an approved agency.

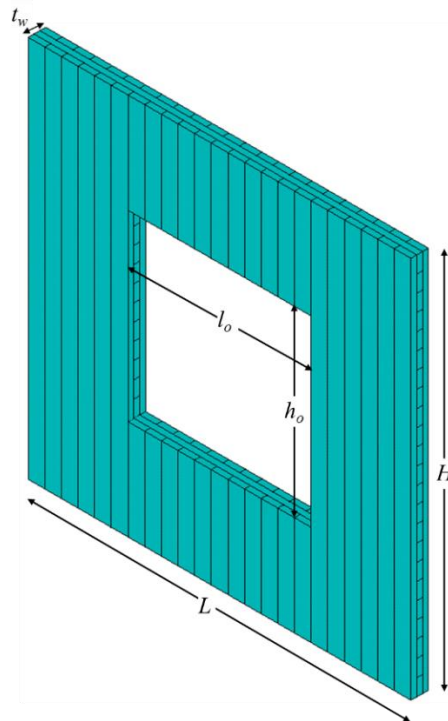


Figure 1.2 CLT panel with opening

1.3 In-Plane Stiffness of CLT Panels

In designing CLT shear walls, understanding of the mechanical properties of CLT panels and the connectors is needed. Several studies aimed to predict the properties of CLT panels loaded in-

plane. Blass and Fellmoser (2004) developed a methodology for the design of CLT panels under in-plane loading based on the composite theory. The composition factors (k-factors) were proposed to calculate the strength and stiffness of CLT panels in various directions based on single layer properties. The composition factors, k_i are the ratio of the strength/stiffness of the considered CLT cross-section to the strength/stiffness of a fictitious homogeneous cross-section where the grain direction of all layers is parallel to the direction of the stress. The stress distribution and the deformation of solid wood panels with different cross sections were determined from the effective strength and stiffness values. The effective stiffness equations were derived for both in-plane and out-of-plane loading. The composition factors are listed in Table 1.1 with different configurations of loading. The effective strength and stiffness can be calculated using formulas in Table 1.2.

Table 1.1 Composition factors k_i for CLT panels (Blass & Fellmoser 2004)

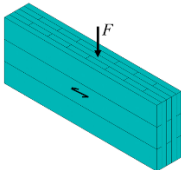
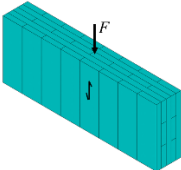
Load Configuration	Composition Factors, k_i
	$k_3 = 1 - \left(1 - \frac{E_{90}}{E_0}\right) \frac{a_{m-2} - a_{m-4} + \dots \pm a_1}{a_m}$
	$k_4 = \frac{E_{90}}{E_0} + \left(1 - \frac{E_{90}}{E_0}\right) \frac{a_{m-2} - a_{m-4} + \dots \pm a_1}{a_m}$

Table 1.2 Effective strength and stiffness for CLT panels (Blass & Fellmoser 2004)

Loading Direction	To the grain of outer skins	Effective strength value	Effective stiffness value
In-plane loading			
Bending	Parallel	$f_{m,0.ef} = f_{m,0} \cdot k_3$	$E_{m,0.ef} = E_0 \cdot k_3$
	Perpendicular	$f_{m,90.ef} = f_{m,0} \cdot k_4$	$E_{m,90.ef} = E_0 \cdot k_4$
Tension	Parallel	$f_{t,0.ef} = f_{t,0} \cdot k_3$	$E_{t,0.ef} = E_0 \cdot k_3$
	Perpendicular	$f_{t,90.ef} = f_{t,0} \cdot k_4$	$E_{t,90.ef} = E_0 \cdot k_4$
Compression	Parallel	$f_{c,0.ef} = f_{c,0} \cdot k_3$	$E_{c,0.ef} = E_0 \cdot k_3$
	Perpendicular	$f_{c,90.ef} = f_{c,0} \cdot k_4$	$E_{c,90.ef} = E_0 \cdot k_4$

Moosbrugger et al. (2006) proposed a model based on the regular periodic internal geometry of CLT wall elements, considering uniform shear loading on the boundaries. They defined the complex internal structure of CLT elements with a unit cell called Representative Volume Element (RVE). The RVE extends over the whole plate thickness and is sub-divided into sub-elements called Representative Volume Sub-Element (RVSE). The RVSE considers two orthogonal boards extending over half the board thickness neglecting boundary effects by considering infinite periodical boards in the thickness direction. The complete state of shear loading was decomposed into two basic mechanisms: pure shear in a single board (mechanism I); and torsional-like behaviour in the glue interface between two boards (mechanism II). Two equations were proposed to estimate the in-plane shear modulus based on simplified analytical models for panels without (Eq. 1.1) and with (Eq. 1.2) spacing between the individual boards:

$$\frac{G^*}{G} = \frac{1}{1 + 3(G / G_{\text{eff}})(t_i / a)^2} \quad (1.1)$$

$$\frac{G^*}{G} = \left(1 + (u / a) \left(1 + 2(G / G_Q) \right) + 2(G / E)(u / a)^3 + 3(G / G_{\text{eff}})(1 + u / a)^2 (t_i / a)^2 \right)^{-1} \quad (1.2)$$

where $G_{\text{eff}} = (G_{\perp} + G_{\parallel}) / 2$, is the effective shear modulus, G_{\perp} is the shear moduli perpendicular to the grain, G_{\parallel} or G is the shear moduli parallel to the grain, G^* is the equivalent shear modulus, G_Q is the transverse shear modulus, t_i/a is the board thickness-to-width ratio and u/a is the board-spacing to board-width ratio.

Eqs. (1.1) and (1.2) depict that the equivalent shear modulus of a CLT panel depends on the shear moduli (parallel and perpendicular to the grain direction) and the geometric aspect ratio of the panels (i.e., t_i/a , u/a). Both shear moduli and aspect ratio are main parameters that affect in-plane behaviour of CLT panels. Moosbrugger et al. (2006) verified the proposed analytical models by finite element analyses (FEA) and a practical range of the thickness-to-width ratio for CLT panels was recommended.

Bogensperger et al. (2007) investigated the in-plane behaviour of CLT panels and carried out 3-point bending and shear tests according to EN 384 (2004). The test configuration consists of a rigid steel frame with pin-connections at all edges. Three different configurations with two replicates each were tested. The results were verified with FEA using the same boundary conditions as those in the experiment. The effective shear modulus was calculated as described in Eq. (1.1) and a deviation of the shear modulus of up to 26% was reported comparing tests and FEA results. In addition, a discrepancy in stresses and strains was observed between an ideal CLT structure and the test configuration under shear load. Therefore, a calibration factor of 0.9 was recommended to calculate the shear stiffness.

Other research regarding appropriate test set-ups focused on the shear strength of diaphragms, beams and small CLT elements. Jobstl et al. (2008) argued that the Common Understanding of Assessment Procedure (CUAP)¹ that uses 4-point bending tests to determine the in-plane shear strength of CLT panels, does not lead to shear failure in most cases. To validate this claim, 90 CLT specimens consisting of 3 and 5 layers were tested using the CUAP test configuration. It was observed that none of them failed in shear parallel to the grain with few exceptions that failed in rolling shear. Therefore, a new symmetric test configuration was proposed and subsequently used for determining the shear properties of 20 CLT panels. All test specimens failed in shear with large deformations. The average shear strength was found to be 12.8 MPa with a COV of 11.3%.

Bogensperger et al. (2010) performed FEA to achieve better correlation with the experimental results and to further verify the studies by Moosbrugger et al. (2006) and Jobstl et al. (2008). They investigated the effect of boundary conditions on the shear stiffness of the CLT elements, introduced a correction factor for the shear modulus in Eq. (1.1) for three, five, and seven layer CLT panels, and accurately predicted the effective shear stiffness of CLT panels. In addition, the shear and torsional stresses in the gluing interface were presented for the RVSE for the ultimate limit state. From their test results, they proposed a shear strength of 8-10 MPa and a torsional strength of 2.5 MPa for CLT panels.

Brandner et al. (2013) investigated the influence of test configuration and other parameters affecting the shear strength of CLT panels loaded in-plane and identified three failure modes of

¹In Europe, each new product requires an approval from European Organization for Technical Approvals (EOTA) following the European Technical Approval Guidelines (ETAGs). Given the logistical hurdles involved in developing ETAGs for all possible construction products, EOTA has developed an alternate path, CUAP, for securing approvals for construction products not covered by an existing ETAG.

CLT elements: Mode I: “net shear” –i.e. shear perpendicular to grain; Mode II: “torsion” and mode III: “gross shear” –i.e. shear parallel to grain. However, their study only focused on the shear resistance of CLT elements perpendicular to grain (Mode I). They proposed a new test configuration with a modification from the test configuration used by Jobstl et al. (2008) rotating the specimen by 14° from its original configuration so that the resultant loading and support force remained in-plane. The test setup and specimen configuration allowed to develop for only one shear failure plane compared to two shear planes in the previous test setup. A total of 150 specimens in two series were prepared and tested from Norway spruce of nominal strength class C24. The obtained net shear strength ranged from 7.2-11.7 MPa for different series. A net shear resistance of CLT element –i.e. shear strength perpendicular to grain of $f_{v,net} = 5.5$ Mpa was recommended for lamella thickness of 40mm or less. The study also showed that parameters that significantly affect the shear strength of CLT elements are the core lamella thickness, the annual ring orientation and the width of the gap between the boards.

More recently, Brandner et al. (2017) presented research on a novel test configuration and evaluated the net- and gross-shear modulus and strength and shear failures in CLT diaphragms. The configuration consist of column-shaped rectangular specimens cut after rotating the main orientation of CLT elements by 45° . They tested 23 series featuring various parameters: number of layers, ratio between the sum of layer thicknesses in weak plane direction to that in the strong plane direction, edge gluing, board thickness and board width. The specimens were 3-7-ply CLT panels with the variation of thickness from 60-210 mm. CLT layer thickness and gap execution were the main parameters that influenced significantly the in-plane shear modulus and strength. Net-shear modulus and strength of the CLT elements were found to be 450 MPa and 5.5 MPa,

respectively while the values for gross-shear modulus and strength were found to be 650 MPa and 3.5 MPa, respectively.

Flaig and Blass (2013) developed a new methodology for shear design of CLT beams loaded in-plane. They proposed analytical equations for shear stress and stiffness and verified them with test results. Three different failure modes for the CLT beams subjected to in-plane transverse loading were reported.

- Mode I: shear failure parallel to the grain in the gross cross section of the beam;
- Mode II: shear failure perpendicular to the grain in the net cross section of the beam; and
- Mode III: shear failure within the crossing areas between orthogonally bonded lamellae.

An analytical approach was presented for the shear stresses occurring in the lamellae and the crossing areas of CLT beams. The shear strength properties were verified based on their test results along with results from the literature. An expression for the effective shear strength (Eq. 1.3) of CLT beams was derived. It was observed that the effective shear strength of CLT beams is strongly dependent on cross sectional arrangement, thickness ratio of longitudinal and transversal layers and on the lamellae width. Finally, a closed form solution for the effective shear stiffness (effective shear modulus) was obtained by the superposition of strain components resulting from shear stresses (Eq. 1.4). The expression accounts for the lamellae width and their cross sectional arrangement. The proposed equations were then verified with tests performed on prismatic beams, notched beams and beams with holes, showing good agreement. The proposed effective shear modulus $G_{\text{eff,CLT}}$ of CLT beams is:

$$G_{\text{eff,CLT}} = \left(\frac{1}{G_{\text{lam}}} + \frac{1}{G_{\text{eff,CA}}} \right)^{-1} \quad (1.3)$$

where G_{lam} is the shear modulus of the lamellae parallel to grain and $G_{\text{eff,CA}}$ is the shear modulus in the crossing areas between adjacent layers that is related to gross cross section (see Eq. 1.4):

$$G_{\text{eff,CA}} = \frac{6V}{5A_{\text{gross}}(\gamma_{\text{tor}} + \gamma_{\text{yx}})} = \frac{Kb^2}{5} \frac{n_{\text{CA}}}{t_{\text{gross}}} \frac{m^2}{(m^2 + 1)} \quad (1.4)$$

where V is the transversal force, m is the number of longitudinal lamellae within the beam height, b is the width of lamellae, γ_{tor} and γ_{yx} are the shear strain component within crossing areas, t_{gross} is the overall thickness of the CLT element and n_{CA} number of glue lines between longitudinal and transversal layers within the element.

Eq. (1.3) was derived based on the experimental and analytical investigations on CLT beams loaded in-plane under four-point bending. Therefore, this equation is restricted to CLT beams only. By contrast, the Eqs. (1.1) and (1.2) were proposed from an experimental investigation on CLT elements tested following a configuration (-i.e. orientation at an angle of 14° with the loading direction) such that they failed under pure shear. Therefore, these equations are suitable for CLT panels subjected to in-plane loading.

1.4 In-Plane Stiffness of CLT Panels with Openings

Openings for doors and windows are very common in CLT walls. The areas around an opening experience stress concentrations that can reduce in-plane stiffness and load bearing capacity of the panel. In case of light-frame wood shear walls, often only the full wall segments are taken into consideration when determining the wall resistance. While this approach may be appropriate for light-frame wood shear walls, it can lead to significant underestimation of the stiffness and resistance of CLT walls (Dujic et al. 2007). Another approach is the coupled-beam analogy where

the panels above and below the opening are considered as coupled-beams (Diekmann 1995). The concept is based on rigorous mechanics which may be not practical for design purposes.

Moosbrugger et al. (2006) performed FEA to quantify the stiffness of a CLT panel with a quadratic opening at the centre. This study determined the reduced stiffness of a CLT panel with openings by considering the ratio of the effective wall area (A_{wall}) to total area (A_{total}), where $A_{\text{wall}} = A_{\text{total}} - A_{\text{opening}}$, and proposed a formula to calculate the reduced stiffness of CLT walls with an opening:

$$\frac{G_{\text{wall}}}{G^*} = \exp^{-6(b/B)^{2.5}} \quad (1.5)$$

where G_{wall} is the shear stiffness of the wall and G^* is the equivalent shear modulus for the panel, B is the half of wall width, and b is the half of the opening width as seen in Figure 1.3. However, it should be noted that Eq. (1.5) was developed for square CLT walls with square openings.

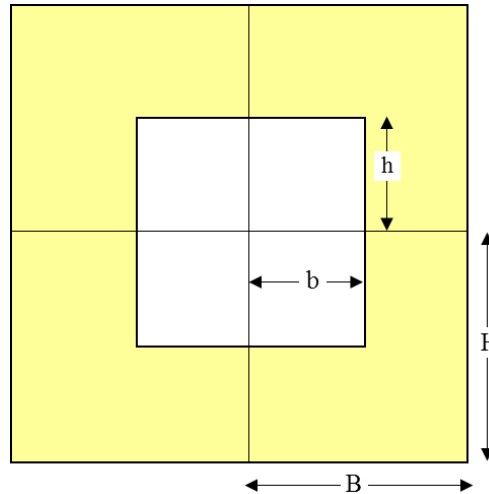


Figure 1.3 CLT wall parameters for Eq. (1.5)

Dujic et al. (2007) experimentally investigated the behaviour of CLT walls with different opening locations. Four cyclic tests were performed on two CLT walls with and without openings. The walls were composed of 3-ply panel produced from European Spruce with dimensions of $3.2\text{m} \times$

2.72m × 0.094m. Four BMF angle brackets of 105mm height were used to connect wall to concrete foundation where ten annularly nails (4.0/40mm) were used for fixing connectors-to-wall and two M12 steel bolts were used for fixing connectors-to-foundation. The boundary conditions (loading and connections between wall-to-foundation) were kept the same for walls with and without openings. The wall segment with opening contained a door and a window as openings. It was observed that for a wall with an opening equal to 30% of the wall area, the strength of the wall did not change. However, the stiffness was reduced by about 50%. A parametric study was conducted using FEA to determine the influence of the size and layout of openings on the strength and stiffness of CLT walls. The shear strength and stiffness properties of 36 different wall configurations were determined. Finally, analytical equation (Eq. 1.6) was proposed to calculate the reduced stiffness of the CLT walls:

$$K_{opening} = K_{full} \frac{r}{2 - r} \quad (1.6)$$

where $K_{opening}$ and K_{full} are the stiffness of CLT wall with opening and without and opening, respectively, and r is the panel area ratio:

$$r = \frac{H \sum L_i}{H \sum L_i + \sum A_i} \quad (1.7)$$

where H is the height of wall, $\sum L_i$ is the summation of length of full height wall segments (excluding length of openings from total length), and $\sum A_i$ is the summation of openings area. The parameters for Eq. (1.7) are illustrated in Figure 1.4.

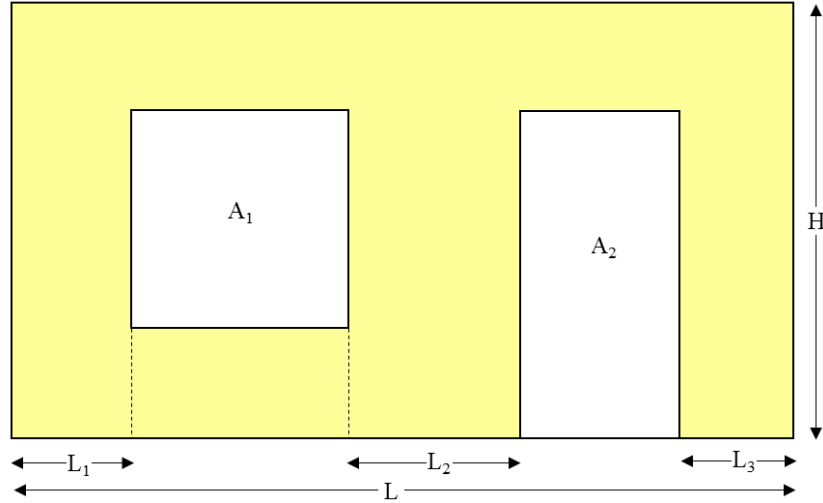


Figure 1.4 CLT wall parameters for Eq. (1.7)

Ashtari (2012) analyzed the in-plane stiffness of four different CLT floor diaphragm configurations with and without openings using FEA. A smeared panel-to-panel connection model was developed by calibrating it with experimental results (Yawalata and Lam 2011). However, the tests from Yawalata and Lam (2011) were conducted with a connection using proprietary self-tapping screws (STS); therefore, the model's applicability was limited to those connections. The FEA was extended to a parametric study to identify the parameters affecting the in-plane behaviour of CLT floor diaphragms. It was observed that the CLT panel-to-panel connections, the in-plane shear modulus of CLT panels, the stiffness of shear walls and the floor diaphragm configuration were the main parameters affecting the in-plane behaviour of CLT floor diaphragm.

Pai et al. (2016) investigated the mechanism of force transfer around CLT shear walls with openings and potential reinforcement requirements for the corners of the opening. The stress concentration around openings due to lateral in-plane loads was called the transfer force. Four different models from literature calculating the transfer forces in wood frame shear walls were evaluated. Among them, Diekmann's model (Diekmann 1995) was found to be the most suitable

for CLT shear walls with openings. This method assumes that the wall behaves as a monolith and unit shear above and below the openings is uniform. The internal forces in each pier adjacent to that specific opening can be calculated by creating a series of free body diagrams, see Figure 1.5.

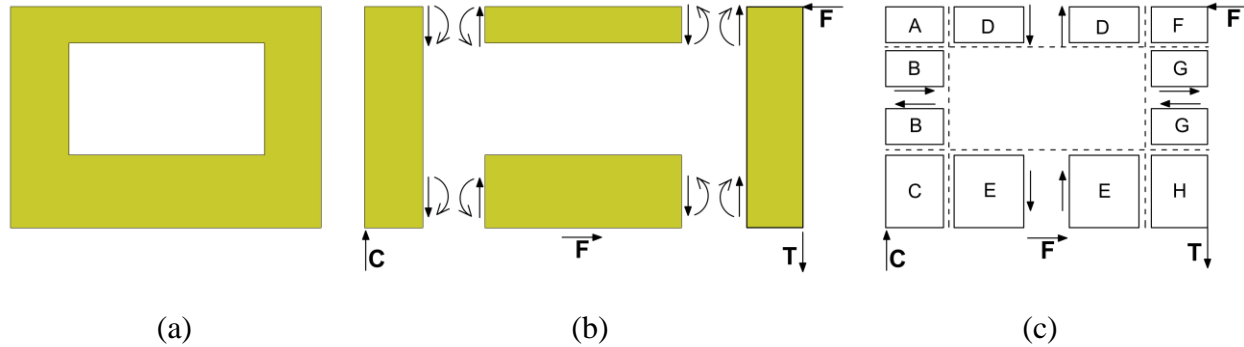


Figure 1.5 Diekmann Model: (a) wall with opening, (b) free body diagram of various sheathed areas and (c) horizontal and vertical cuts for internal shears

Pai et al. (2016) developed a numerical model of CLT shear walls with openings was developed to evaluate the forces around corners. Solid elements were used for CLT laminae where the glue-line contact between laminates was considered as rigid. The analyses showed no axial stress concentration around opening corners. However, high shear stress concentrations were found which indicated that there is a possibility of a shear failure. Therefore, reinforcement around the opening was suggested.

1.5 In-Plane Strength and Stiffness of CLT Shear Walls

Understanding the in-plane behaviour of CLT shear wall systems is essential for the reliable design of CLT buildings under lateral loads. CLT panels are very rigid in comparison to the connections connecting them. Therefore, the flexibility of CLT systems mostly depends on the behaviour of the connections. As discussed in the previous sections, no universal agreement has been reached

for determining the in-plane stiffness and resistance of CLT walls. Furthermore, in CLT shear walls, assemblies and structures, there is a wide variety of fasteners that are used for connecting roof-to-wall, wall-to-floor, wall-to-wall and floor-to-floor CLT panels. Examples include long STS, regular wood screws, smooth, spiral and annular ring nails, lag screws, rivets, bolts and dowels. The lateral resistance of CLT wall assemblies can be assumed to be a simple summation of the resistance of all connections connecting the walls to the floors (Gavric and Popovski 2014). While this approach is simple, the kinematic motion of the walls (sliding, rocking or a combination of rocking and sliding) should be considered when determining the resistance of CLT walls. A limited number of studies have been conducted on CLT connections and wall systems to determine their in-plane strength and stiffness. Some of the most important studies and findings are discussed in the following section.

1.5.1 Connections for CLT Shear-Walls in Platform-type Construction

In a platform construction, the CLT shear walls under lateral loading can be designed for rocking or sliding or combined of both. To do so, the hold-downs are designed to resist rocking forces and the brackets are designed to resist sliding forces. Test results showed that the rocking capacity of bracket connections is similar to their sliding capacity (Gavric et al. 2015a). On the contrary, the sliding capacity of hold-downs were found to be only one-fifth to their rocking capacity.

For an efficient design of CLT shear walls in platform construction, it is important to evaluate the actual behaviour of different CLT connectors. Tomasi and Smith (2014) investigated the mechanical behaviour of angle brackets connecting CLT walls to the foundation. Five different types of brackets with two proprietary fasteners (annular nails: 4×40 mm and 4×60 mm) were tested under monotonic and cyclic loading on 98 mm thick 3-ply CLT panels. The angle brackets were rigidly connected with foundations using one or two steel bolts. They found that the

connection's capacity depended on the geometries of bracket (i.e., length, shape, presence of ribs and corrugation) and the fasteners connected to CLT panels (e.g., annular nails) and foundation (e.g., bolts). They recommended relying upon the test results for determining the design strength of CLT connections because the behaviour of the metal connectors is far too complex to predict using simplified analytical methods. However, it should be noted that other researchers suggested designing CLT connectors such that only the fasteners connecting the bracket to CLT panels should experience plastic deformation (Schneider et al 2015, Gavric et al 2015a).

Gavric et al. (2015a) conducted monotonic and cyclic tests on two different types of hold-downs and brackets connections with 4×60 mm annular nails. They tested both wall-to-foundation and wall-to-floor connections using 5-ply 85 mm thick wall panels and 5-ply 142 mm thick floor panels. They observed that brackets have similar capacity and stiffness in under-tension and shear tests. On the contrary, hold-downs showed higher strength and stiffness in tension compared to bracket connections and their sliding resistance was negligible. For the design of CLT building, they recommended overstrength factors of 1.3 and 1.25-1.45 for hold-down and bracket connections, respectively.

A similar study was conducted by Schneider et al. (2015) on bracket connections using three different types of fasteners: spiral nails, ring nails and STS. They performed tests on CLT connections under monotonic and cyclic loading, developed FEA models in OpenSees (McKenna et al. 2000) and calculated connection's stiffness, strength, deformation capacity and ductility based on the equivalent energy elastic plastic (EEEP) curve (ASTM 2126 2011). The results from tests and FEA (ductility, elastic shear stiffness and strength) showed good correlation. However, the damage index of the connections calculated using an energy-based damage accumulation method (Kraetzig et al. 1989) showed significant differences between tests and FEA.

Gavric et al. (2015b) also performed monotonic and cyclic tests on shear connectors for the application of CLT wall-to-wall and floor-to-floor assembly. The shear connectors were tested in two configurations of half-lap joint (50 mm overlap) and spline joint (28 mm thick and 180 mm wide LVL). STS of 8×80 mm and 8×140 mm were used for the shear connector tests in wall-to-wall and floor-to-floor assembly, respectively. The test results showed a ductile performance of the shear connectors if the end/edge distances are satisfied in the connections. Overall, the half-lap joints showed a better performance compared to the spline joints in terms of stiffness, strength and ductility. To meet the seismic design provisions, Gavric et al. (2015b) proposed an overstrength factor of 1.6 for the screws connections.

Hossain et al. (2016) evaluated the performance of STS's shear resistance on 3-layered CLT panels. They conducted monotonic and cyclic tests on double-angled butt joints where the screws were installed at an angle of 45° between two panels with an inclination of 32.5° to the face of the panels resulting in an angle of 53.4° between the screw axis and the wood fiber direction. Results showed that the double-angled butt joints were moderate to highly ductile with an average ductility ratio of 4.1 and 7.7, respectively under monotonic and cyclic tests. The high ductility ratios of this kind of connections could be efficiently used for the lateral load resisting systems in high seismic zones. However, it is unclear how these type of complex-angled (53.4°) connectors can be accurately assembled in an actual construction project.

1.5.2 CLT Shear Walls in Platform-type Construction

Understanding the actual behaviour of CLT shear walls under lateral loads is important for a reliable design of CLT buildings. Researchers have recently shown increased attention to predicting the behaviour of CLT walls under cyclic loading (Ceccotti et al. 2006a, Popovski et al. 2010, Gavric et al. 2015c).

Popovski et al. (2010) performed a series of quasi-static monotonic tests on CLT shear walls. A total of 32 walls were tested with 12 different configurations of wall-to-floor, wall-to-wall and storey-to-storey connections. The walls were made of 3-ply boards with a thickness of 94 mm. Several types of connectors (hold-downs and steel brackets) and fasteners (annular ring nails, spiral nails, screws and timber rivets) were used for the connections. Both single walls and coupled walls with different aspect ratios were tested. Test results showed that the seismic performance of the CLT walls with the connections of brackets with nails or screws was adequate where the wall deflection occurred mostly was due to the deformation in the connections and step joints. Placing hold-downs on each end of the wall further improved the seismic performance by improving stiffness of 81% with relatively high ductility capacity compared to the walls without hold-downs. Introduction of half-lap (step) joints was an efficient solution for coupled walls to improve ductility. Nonlinear behaviour of the walls was localized at the connections only, where the panels remained undamaged and well connected to the floor even after a “near collapse” state.

Gavric et al. (2015c) performed an extensive study to predict the behaviour of CLT walls under seismic loads. At first, cyclic tests were conducted on CLT wall connections such as hold-downs, angle brackets and self-tapping screws: wall-to-foundation, wall-to-floor, wall-to-wall, and floor-to-floor connections (Gavric et al. 2015a and Gavric et al. 2015b). It was observed that the hold-downs exhibited high strength and stiffness in uplift while they did not have significant stiffness and resistance in shear. The angle brackets showed high strength and stiffness both in uplift and shear. Non-linear numerical models of the connections were developed by calibrating against test results. The connections (angle bracket, hold-down and self-tapping screws) were modeled using non-linear springs which characterized the hysteretic behaviour. Trilinear models defined by nine parameters were developed to represent the hysteretic behaviour of the non-linear springs. Gavric

(2015c) performed cyclic tests on both single and coupled CLT walls with three different wall configurations: a) single wall panels (2.95 m x 2.95 m); b) coupled wall panels (two panels-1.48 m x 2.95 m) with over-lapped screwed joint; and c) coupled wall panels (two panels-1.48 m x 2.95 m) with LVL spline joint. The walls were constructed from 5-ply CLT panels of 85 mm thick made of European Spruce. Angle brackets (BMF 90×48×3×116 mm) and hold-downs (HTT22) were used to connect the wall to the foundation using annular ring nails (12-4X60 mm). Self-tapping screws (Φ 8 x 100 mm) were used for the wall-to-wall vertical joints. It was observed that the failure of the systems was located mostly at the connections, while the CLT wall panels were subjected to negligible in-plane deformations. The coupled wall exhibited the behaviour of “single wall behaviour” and act like a rigid body. The vertical joints resisted the shear forces between two adjacent walls. Analytical models for the CLT wall systems were proposed to calculate the total displacement, δ_{ot} which is a summation of displacement due to rocking δ_r , bending δ_b , shear δ_{sh} and slip δ_s . The CLT wall deformation mostly depended on rocking and sliding, while deformation due to bending and shear was found to be negligible.

Gavric and Popovski (2014) evaluated five different design models (D1 to D5) determining the resistance of CLT shear walls under lateral in-plane loads based on connection properties (Figure 1.6). Model D1 assumed that the resistance is equal to the shear resistance of the brackets only. Model D2 assumed that the resistance was based on the shear resistance of the brackets, and the overturning from the hold-downs. These two models represent the current design practice in Europe and North America, while the other three models (D3-D5) were newly proposed ones. Model D3 assumed that the wall undergoes pure rocking behaviour so the resistance was determined by taking into account the uplift contribution of the connectors only. Model D4 and D5 assumed that both sliding and rocking of the brackets contribute to the resistance of the shear

walls under different interaction equations. Model D4 assumed circular interaction formula, while the model D5 assumed interaction under linear domain, as summarized in Figure 1.6.

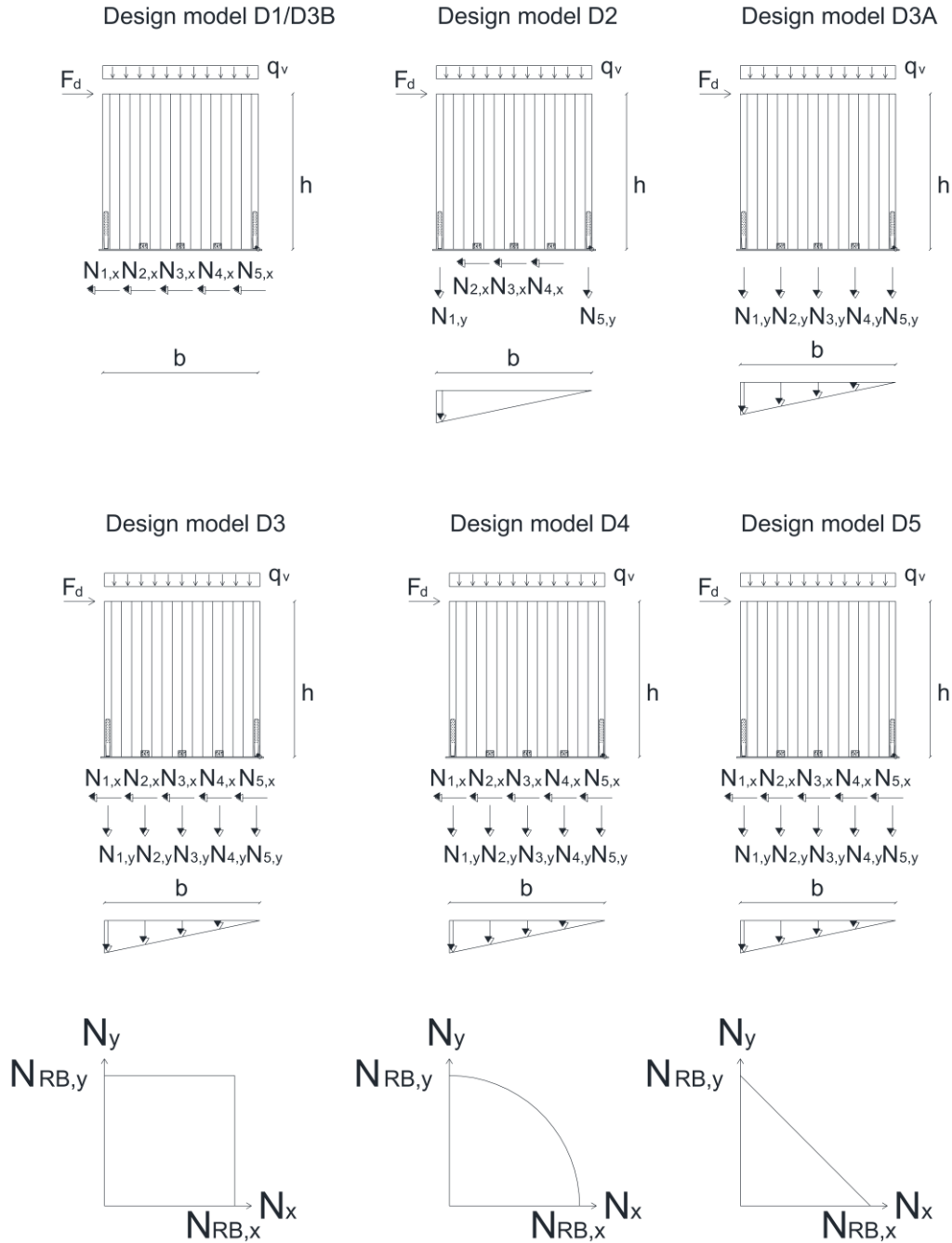


Figure 1.6 Lateral resistance of CLT shear wall from Gavric and Popovski (2014): model D1 to D5 (with permission)

In all five models, Gavric and Popovski (2014) considered the CLT panels as linear elastic and also the connections to be as linear elastic since the models deal with forces that are at or below the factored resistance of the shear walls. The lateral design resistance was calculated using Johansen's yield model with the embedment properties modified for CLT. The numbers of nails in hold-downs and brackets were selected such that the yielding occurs in the nails and not in the connectors (brackets or hold-downs). The strength of brackets in uplift and shear was assumed to be equal while it was assumed that hold-downs only resist uplift forces. The design resistance of a CLT shear wall under lateral loads was assumed to be reached when the first bracket or hold-down at the bottom reached its design lateral resistance. The resistance of the CLT coupled wall due to shear and overturning moments can be calculated based on the equilibrium of forces:

$$F_d^* = \min \begin{cases} F_{d,S}^* = 4 N_{RB,x} \\ F_{d,M}^* = \frac{q_v b^2}{4h} + \frac{N_{RH} x_1}{h} + \frac{N_{RB}}{h x_1} (x_2^2 + x_3^2 + x_4^2 + x_5^2) + N_{RS} \frac{b}{2h} \end{cases} \quad (1.8)$$

where F_d^* is the design lateral resistance of coupled shear wall, $F_{d,S}^*$ is the resistance due to sliding, $F_{d,M}^*$ is the resistance due to overturning moment, q_v is the vertical force, b and h are the width and height of the wall, respectively; N_{RB} , N_{RH} and N_{RS} are the resistance of brackets, hold-downs and vertical joints, respectively; x_i are distances of connectors as described in Figure 1.7.

The design values from the analytical models were then compared to the results from CLT wall tests (Popovski et al. 2010). The safety margin of the models was defined as the ratio of the ultimate capacity of the tested walls ($F_{ult, exp}$) to the design capacity (F_d) predicted from the models. The ratio between experimental resistance and the analytical design value of a CLT wall when using a specific model represents the “safety margin” of that model. The average ratios of $F_{ult, exp}/F_d$ using D1-D5 of 1.2, 2.7, 2.0, 2.2 and 2.6, respectively, indicate how conservative the design models are.

The models that account for sliding-uplift interaction in the brackets (models D3-D5) showed higher consistency compared to models D1 and D2. Model D4 that accounts for sliding-uplift interaction according to a circular domain, proved to be the most suitable candidate for future development of design procedures for determining the resistance of CLT walls under lateral loads. By comparing the model's predictions to the experimental results, it was found that the perpendicular walls affect the strength of the structure and should be included in the analyses.

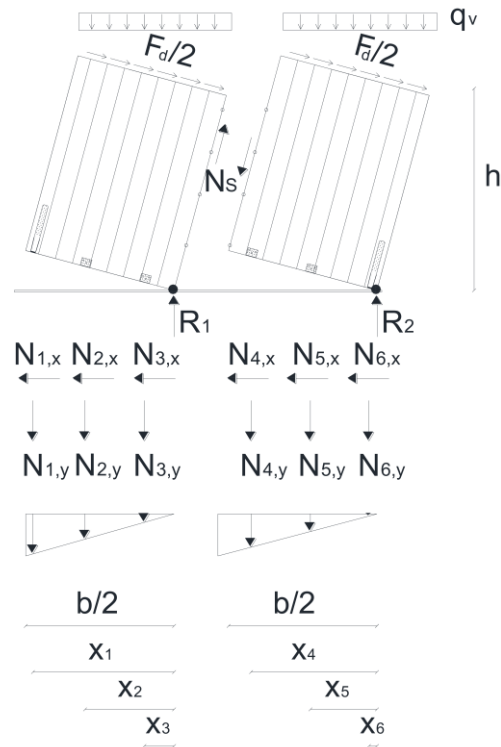


Figure 1.7 Lateral resistance of coupled CLT shear wall from Gavric and Popovski (2014) (with permission)

Reynolds et al. (2017) investigated the deformation and load resistance of CLT shear walls for platform construction. CLT two-story shear walls were tested under vertical and lateral loads. At ultimate loading, the movement of the shear walls was governed by rigid body movement of the panels. The authors reported that the design methods currently used by structural engineers

underestimate the resistance of the shear walls. More accurate design methods for CLT shear walls assume the panel to rotate about the compression edge of the wall. However, the best-captured behaviour near the maximum resistance of the CLT walls is when the length of contact along the base of the wall is not a single point as assumed by Gavric and Popovski (2014). The length of contact in their proposed method was determined by equilibrium with the forces in the connections and the forces applied to the shear wall. The sliding resistance and overturning resistance of the shear wall can be estimated as:

$$S_u = \sum_j F_s + \mu \left(\sum_i F_u + V \right) \quad (1.9)$$

$$M_u = \sum_i F_u \left(d_i - \frac{x}{2} \right) + V \left(d_v - \frac{x}{2} \right) \quad (1.10)$$

where S_u and M_u are the sliding and overturning resistance of shear wall, respectively; F_u and F_s are the capacity and sliding resistance of the connectors, respectively; d_i is the distance of the connectors from the compression edge; and V is the vertical load on wall at distance d_v from the compression edge.

Tamagnone et al. (2017) proposed a non-linear procedure for seismic design of CLT wall systems. The panels were assumed as rigid elastic brittle material and the metal connections as elasto-plastic material. At the wall-to-support interface the compressive force was considered as triangular force distribution where the neutral axis can be calculated from an iterative procedure. The displacement of the wall during rocking can happen in the negative Z-direction (e.g. hypothetically the wall corner can penetrate into the foundation/floor below) which is quite unrealistic. Furthermore, the proposed method considered the behaviour of wood to be a uniaxial elastic material similar to steel or concrete; this is a substantial simplification compared to wood's actual orthotropic behaviour.

Tamagnone et al. (2017) then carried out FEA of 2D CLT walls and 3D CLT building using SAP2000 (Computers and Structures Inc. 2013) and ABAQUS (ABAQUS 2012) to validate the proposed method. The 3D 3-storey CLT building schematized the shake table building from the SOFIE project (Ceccotti et al. 2013). The FE analyses of the 2D CLT wall's models showed acceptable accuracy. However, the 3D model of the building produced large errors due to the fact that the FEA model could not capture the box effect of the CLT building, i.e. the actual in-plane stiffness of the building was higher than in the models. However, after considering a tri-linear model for the angle bracket connections, the errors in the 3D model were found acceptable. Although the authors claimed that the proposed method is a simplified design method for CLT shear wall systems, the iterative procedure to find the neutral axis at the wall-to-support interface involves rigorous calculation and may be impractical for the design purposes.

1.6 CLT Buildings under Lateral Loading

1.6.1 CLT Structural Systems

CLT buildings can be constructed in several ways with the most common CLT construction methods being platform type construction (Figure 1.8a) and balloon type construction (Figure 1.8b).

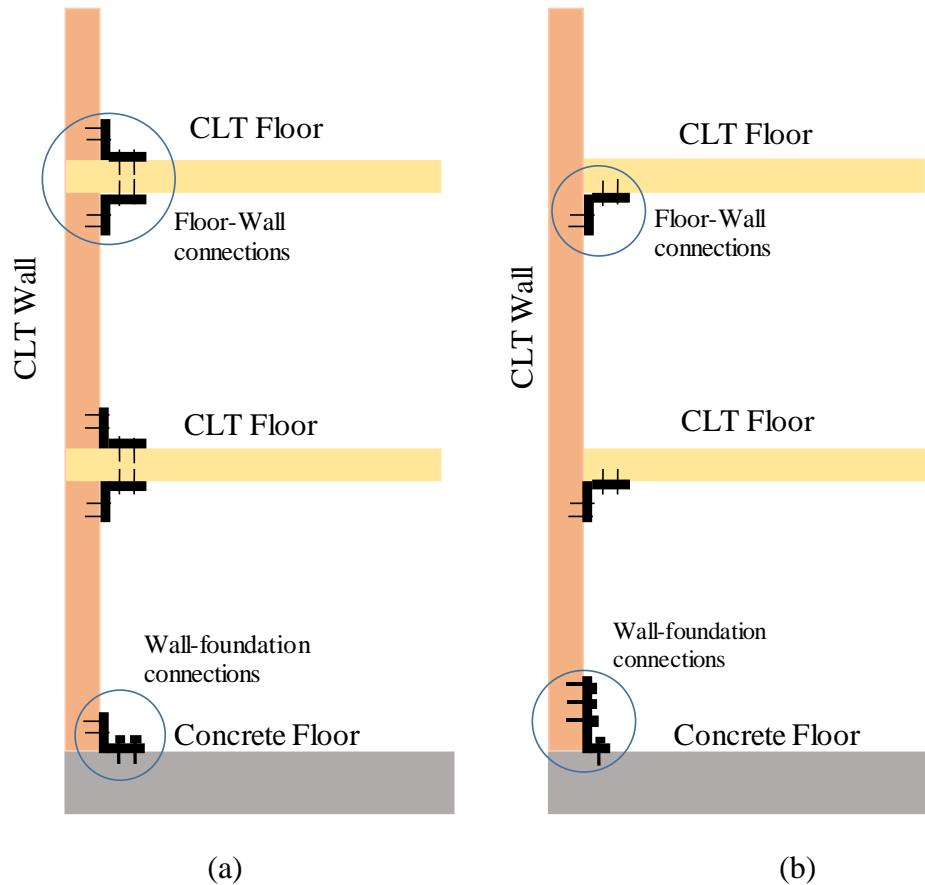


Figure 1.8 CLT structural system: (a) platform-type and (b) balloon-type construction

Platform construction is the most common approach used for low to mid-rise CLT buildings, where each floor acts as a platform for the floor above. The CLT building is either directly connected to a reinforced concrete (RC) foundation or sits a top of an RC podium. The walls are connected to foundations or RC podium by steel brackets and hold-downs using metal fasteners like screws and nails. The walls are connected to the floors in the upper storeys by brackets and/or hold-downs. The panels in between floors and walls are connected by STSs using either half-lap or spline joints. In a platform construction, the CLT shear walls can rock or slide under lateral loading. Hold-downs are designed to resist rocking forces and the brackets to resist the sliding forces. A disadvantage of this construction system is the accumulation of the compression perpendicular to grain stresses on the CLT floor panels which limits the number of storeys of this construction type.

In balloon construction, the walls are continuous for several storeys and the floor panels are attached to the walls at each storey. There is no compression perpendicular to grain issue when using balloon CLT construction. As CLT panels can be manufactured in length up to 19.5 m (Nordic Structures 2013), for tall structures, the wall panels must be connected along the height. Since each shear wall takes all the loads along the building height and transfers them to the foundation, the connections are usually more complex in this type of construction.

1.6.2 European Studies on CLT Buildings

The most comprehensive study to quantify the seismic behaviour of CLT buildings was the SOFIE project (Ceccotti et al. 2006a, 2006b, 2008, and 2013), undertaken by the National Research Council of Italy (CNR-IVALSA) in collaboration with the National Institute for Earth Science and Disaster Prevention (NIED) and the Building Research Institute (BRI), Japan. An extensive reversed cyclic tests were conducted on CLT walls loading in-plane with 4-different configurations of connections and openings (Ceccotti et al. 2006a). The walls were representative of the structural components of a 3-storey building which was later tested on a shake table (Ceccotti and Follessa 2006). The walls consisted of 2.95 m \times 2.95 m CLT panels with 5-layers and a thickness of 85 mm. The 3-storey building was 10m in height and 7 m \times 7 m in plan, and was designed using Eurocode 8 (CEN 2004). Hold-downs and steel angles were used as connections.

The building was tested in three different configurations (two symmetric and one asymmetric) and under 3-earthquakes (Kobe, El Centro and Nocera Umbra). Test results indicated that CLT construction was strong enough to survive 15 consecutive destructive earthquakes without severe damage. The collapse state of the building was defined as the failure of one or more hold-down anchors (uplift greater than 25 mm). The “collapse” was observed during the test with the Nocera Umbra earthquake record with PGA of 1.2g. It was observed that the overall behaviour of the CLT

structure was mostly influenced by the performance of the connections. The connections dissipated the seismic energy whereas the CLT panels behaved as rigid bodies. The load-deformation curves showed that the CLT walls had high stiffness, yet still maintained good energy dissipating performance.

A numerical model of the structure was developed to simulate the behaviour during the shake table tests (Ceccotti 2008). Non-linear time history analyses were performed using different earthquake records. The analyses showed good agreement with the test results. The q -factor for seismic design according to Eurocode 8 (CEN 2004) was evaluated according to the acceleration based approach. The average q -factor of 3.4 was obtained from the analyses.

In 2007, another series of shake table tests were conducted on a 7-storey CLT building (Ceccotti et al. 2013). The building was 23.5 m tall and 7.5 m \times 13.5 m in plan. The walls were built from CLT panels with a thickness of 85 to 142 mm made of European spruce. Hold-downs (Simpson HTT22) and steel angles (BMF07116 and BMF07105) with self-tapping screws, annular ring shank nails, lag screws and steel bolts were used as connectors to connect wall-to-wall and wall-to-floor. The building was designed with a q -factor of 3 and an importance factor of 1.5 according to Eurocode 8 (CEN 2004). Three earthquake records were chosen for the shake table tests: JMA Kobe, the Italian earthquake of Nocera Umbra, and Kashiwazaki R1. The structure withstood all earthquakes excitations without any significant damage. The structure also demonstrated self-centering capabilities along with high stiffness.

Rinaldin and Fragiaco (2016) analyzed CLT buildings which were originally tested as part of the SOFIE project (Ceccotti et al. 2013). They developed FEA models of three and 7-storey CLT buildings and validated their models against shake table test results. The CLT panels were modelled using elastic shell elements and the metal connectors modelled using nonlinear springs.

The nonlinear springs were calibrated against test results on metal connectors under cyclic loading. They observed that the frictional coefficient provides additional resistance to CLT shear walls against lateral loading which was never been estimated from any experimental tests. Therefore, they conducted a parametric study and calculated the frictional coefficient to be of 0.6. This was estimated by minimizing the difference between experimental versus numerical results. They performed the nonlinear dynamic analyses on CLT buildings and results showed a strong agreement with the shake table test results. The numerical models captured the seismic response of the buildings with errors of up to 20% in terms of relative acceleration and up to 7% in terms of roof displacement.

Sustersic et al. (2015) investigated the seismic performance of a 4-storey case study CLT building. They developed an FEA model of the building in SAP2000 (Computers and Structures Inc. 2013) and performed nonlinear dynamic analyses. The building was on a 8.5 m \times 6.5 m footprint with 140 mm thick of 5-layer CLT wall on the perimeter. Two posts and one beam located inside the building supported the 5-layer CLT slab. The walls were the main lateral load-resisting system (LFRS) in the building that were connected to the floors through bracket connections. The analyses results showed that smaller wall segments connected by vertical joints dissipated higher energy and increased the seismic performance by showing ductile behaviour. The estimated seismic force reduction factor (q -factor according to Eurocode 8 (CEN 2004) and R factor according to ASCE 7-10 (ASCE 2010) for the single and coupled CLT wall were 2.1 and 2.9, respectively. The nonlinear analyses also considered the contribution of the frictional resistance of the wall in the CLT building. It was observed that the overall base shear and top displacement decreased after considering the frictional resistance. However, they recommended ignoring its contribution to the design until further detailed experimental tests can be completed.

Traditional steel connectors (brackets and hold-downs) for CLT buildings dissipate limited energy under seismic event. Therefore, it may not be suitable to use them in high seismic zones (Latour and Rizzano 2017). Latour and Rizzano (2017) investigated the seismic behaviour of CLT buildings equipped with both traditional and innovative connections. As an innovative connector for CLT buildings, they tested steel bracket known as “XL-Stub”. The new innovative connector XL-Stub was primarily tested and applied for steel beam-column connections (Latour et al. 2011). The authors performed monotonic and cyclic tests on XL-Stub connectors as an alternative to hold-downs for CLT wall systems. It was found that the connectors had higher energy dissipation and displacement capacity compared to traditional hold-downs.

An FEA model of 3-storey CLT building was developed using traditional hold-downs in SeismoStruct (Seismosoft 2013) program. The case study building was adopted from SOFIE project (Ceccotti et al. 2013). The building was modelled using link elements where the link properties were calibrated against CLT connectors’ experimental results. The FEA model was verified with full-scale shake table test results. Another FEA model of the same CLT building was developed equipped with XL-Stub connectors. Similar to traditional connectors, the XL-Stub connectors were modelled using link elements calibrated against test results. The dynamic analyses showed that the CLT building equipped with XL-Stub showed significant improvement in terms of seismic modification factor (q -factor according to Eurocode 8 (CEN 2004)). The q -factor for CLT buildings with the XL-Stub and traditional connectors were found as 4.7 and 2.5, respectively.

1.6.3 North American Studies on CLT Buildings

FPInnovations investigated the performance of a 2-storey CLT house under lateral loads (Popovski and Gavric 2015). The house was 6.0 m x 4.8 m in plan and had a total height of 4.9 m. The walls

were constructed using 3-ply CLT panels of 94 mm thick made of European Spruce. Steel brackets and hold-downs with spiral nails were used for the connections with the assumption that the shear loads were transferred by the brackets only. The building was designed for the location of Vancouver, BC in which the seismic demand was calculated following the equivalent static procedure of NBCC (2010) with $R_d = 2.0$ and $R_0 = 1.5$. The house was tested under quasi-static monotonic and cyclic loading in two directions, one direction at a time. The failure mode of the house was similar in both loading directions: the lateral resistance decreased once the bracket connections reached their shear capacity with slight damage in wood crushing and fastener yielding. The overall failure was due to combined sliding and rocking at the bottom of the first storey. However, no global instabilities were detected and the relative slip between CLT floor panels was negligible. The rocking of the wall panels was not fully restricted, despite the rigid connection of the CLT floors and walls. The maximum storey drift was observed in the bottom storey and was 3.2% of the storey height.

Pei et al. (2013) estimated the seismic modification factor (R -factor) for multi-storey CLT buildings. To do so, they designed a 6-storey CLT shear wall building following direct displacement design (DDD) approach and performed dynamic time-history analysis (THA) using SAPWood (Pei and & van de Lindt 2011) program. Results showed that an approximate R -factor of 4.5 can be assigned to CLT wall components when the building is designed following ASCE 7–10 (ASCE 2010) equivalent lateral force procedure (ELFP) method.

Pei et al. (2017) proposed a new seismic design approach for tall CLT platform building. In their design methods, they considered the CLT floors as the coupling elements that transfer shear forces along the building's width (Figure 1.9). This process eliminates the need for an anchor tie-down system for walls within the floor plan. They illustrated the proposed method by designing a 12-

storey CLT platform building in a high seismic area located in Los Angeles, California, USA. The building was designed with an R factor of 3.0. A FEA model of the building was developed and a nonlinear static analysis was conducted. The results showed that the load transferring mechanism in the proposed method has a good potential as the simplified design methodology for CLT platform buildings. However, it should be noted that the dynamic response of the building needs to be evaluated. Furthermore, the design methods of the CLT building also requires validating against experimental results.

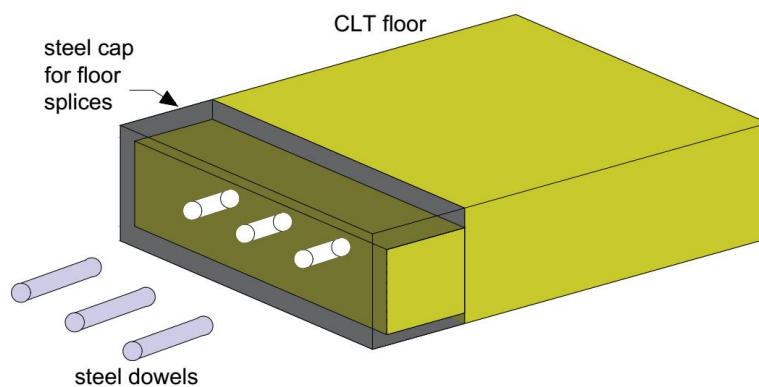


Figure 1.9 Connection detail of CLT floor as a coupling beam (Reproduced from Pei et al. 2017)

1.6.4 Asian Studies on CLT Buildings

Yasumura et al. (2015) investigated a low-rise 2-storey CLT structure under reverse cyclic loading. The structure contained two types of walls of $6\text{ m} \times 2.7\text{ m}$ and $1\text{ m} \times 2.7\text{ m}$ with openings. The CLT panels were 90 mm thick. The structure was designed by elastic calculation with a base shear co-efficient of 1.0. The test results showed that the structures' capacity was found to be up to 80% higher than the design load. The stiffness of the large wall was found to be more than twice the stiffness of the small wall. An FEA model of the structure was developed in SAP2000 (Computers and Structures Inc. 2013). The CLT panels were modelled using elastic shell elements, whereas

the connections were modelled with inelastic springs that dissipated the seismic energy. The results showed that the elastic design procedure resulted in a conservative design. Therefore, nonlinear FEA could be a useful tool for an optimized design of CLT structures.

In 2011, the Japanese national research initiated a project to investigate structural design method for CLT buildings in Japan. Full-scale shake table tests were conducted on 3- and 5-storey CLT buildings (Kawai et al. 2016). The 5-storey building was tested under three-dimensional input wave of 100% Kobe ground motion, whereas the three storey building was tested under 140% of Kobe ground motion. The five storey building showed some slight damage such as yielding of anchor bolts and compressive rupture at the corner of CLT wall panels. At the 140% ground motions level, the three storey building was severely damaged however did not collapse. The damage to the building included vertical cracks at the corners of the CLT wall's openings, the fracture of an anchor bolt and the compressive rupture at the corners of CLT wall panels. It was observed the CLT panels also failed in shear in one location and by splitting due to compressive force at the bottom. Additionally, failure was observed in steel plates and screw joints -i.e. withdrawal of screws was observed.

Based on the knowledge gained from the shake table tests (Kawai et al. 2016), the structural design of the mid-rise CLT buildings were examined by Miyake et al. (2016). The capacity and the required shear wall length (L_{req}) were estimated based on the buildings' seismic performance in accordance with the Japanese building standard (The Building Standard Law of Japan 2013). FEA models using elastic shell elements for CLT panels and inelastic springs for connections were verified against shake table test results. The FEA results showed that the required-wall quantity for the 5-storey CLT building was approximately two times larger than the 3-storey building.

1.7 Code Provision for CLT Platform Building Design

1.7.1 CSA O86

The 2016-supplement of CSA O86 (CSA O86-16 2016.) provides seismic design guidelines for CLT platform buildings. The following provisions shall be satisfied according:

- The CLT platform-type of buildings shall not exceed 30 m in height. For high seismic zone, the height shall be limited to 20 m.
- Type 4 (in-plane discontinuity of the walls along the height of the building) and Type 5 (out-of-plane offsets of the walls along the height of the building) irregularities as defined in the NBCC (2015) shall not be allowed.
- In a CLT shear walls the CLT panels must act as a rigid body, while the factored resistance of the shear walls shall be governed by connections.
- Allowable kinematic behaviours of the shear walls are rocking or combination of rocking and sliding.
- The force reduction factors of $R_d \leq 2.0$ and $R_o = 1.5$ shall apply to platform CLT buildings.
- All energy dissipation shall occur in a) brackets and hold-downs between CLT shear walls and foundations or floors below and b) vertical joints between the CLT panels in shear walls.
- CLT shear walls shall have an aspect ratio (height/length) of 1.0 to 4.0. In case of the aspect ratio of less than 1.0, the wall segments shall be divided into sub-segments that allows preventing the failure of the walls under sliding only.
- CLT buildings with panel's aspect ratios of less than 1.0 shall be designed with $R_d R_o = 1.3$.
- Net section effects and openings shall be accounted for in the design.

1.7.2 Capacity-based design approached considered in CSA O86

Capacity design procedures allow for designing a structure that can sustain relatively large deformations under earthquake loading, thus dissipating the seismic input energy. The method ensures that all inelastic deformations occur in selected ductile components, while the brittle components are designed to have the capacity to remain intact. Because of timber's brittle characteristics when loaded in tension or shear, any failure in a wood component is undesirable. Unlike with other structural systems that use concrete or steel, the design guidelines for CLT platform buildings are still limited.

CSA-O86 is one of the first standards worldwide to introduce specific provisions, providing guidelines for the capacity design of CLT platform buildings. It requires that the energy dissipation mechanism shall occur in (a) shear connectors in the vertical joints in a coupled wall, (b) shear connectors between walls and the floors or foundations underneath and (c) hold-down connections (with the exception of continuous steel rods). Although CSA-O86 covers basic capacity design provisions, this research identified some additional recommendations for the connection and component design of CLT platform-type buildings:

Energy Dissipating Components:

- Bracket and hold-down connections that connect CLT walls to floor or foundations panels underneath.
- The vertical joints in-between wall panels -they must yield first before the bracket and hold-down connections are subjected to rocking or a combined rocking-sliding. This will allow the individual panel in a coupled wall to undergo rigid body motion.
- Discrete hold-downs at both ends of the wall and at both sides of the vertical joints for the coupled wall. However, no energy dissipation is allowed in continuous hold-downs.

Elastic Components:

- CLT panels that are components of any wall or diaphragm i.e. no wood failure;
- The joints between floor panels in a diaphragm to have sufficient stiffness and over strength in order to remain elastic and to allow the diaphragm to act as a single unit;
- Connections between floors to the walls below;
- Connections between the perpendicular walls;
- Continuous hold-downs (rods), if used, that run through several storeys or the entire height of the building.

1.7.3 IBC 2015 & NDS 2015

The International Building Code (IBC 2015) allows CLT for Type IV (heavy timber) construction where the following criteria are met:

- CLT shall be permitted within exterior walls assemblies with two hours of fire rating or less provided that the CLT is protected by fire retardant treated wood sheathing not less than 15/32 inch or by gypsum board not less than 0.5 inch thick or by a noncombustible material. The thickness of the walls shall not less than 6 inches.
- CLT floors shall not be less than 4 inches thick and shall be continuous from support to support.
- CLT roofs shall be without concealed spaces. CLT roofs shall be not less than 3 inches thick and shall be continuous from support to support.

The 2015 National Design Specification (NDS 2015) provides design values for CLT elements.

The provisions can be summarized as:

- The NDS design values provided apply only to performance-rated CLT produced in accordance with ANSI/APA PRG-320.
- The reference design values shall be used from the CLT manufacturer's specifications.
- The net thickness of all layers shall not be less than 5/8 inch or more than 2 inches. The total thickness of the CLT panels shall not exceed 20 inches.

Currently, there are no codes or standards available in the US for the seismic design of CLT buildings. As an alternative, the designers can choose performance-based design procedures where the CLT platform building needs to demonstrate an equivalent performance to that of an existing system in ASCE 7 (2010).

1.8 Research Need

While accurate quantification of the in-plane stiffness of CLT wall panels is required to design a CLT structure subjected to lateral loads, there is currently no universally accepted guideline available. Also, no general procedure is available to estimate the in-plane stiffness of CLT panels with openings. Therefore, the proposed guidelines and formulas to estimate in-plane stiffness of CLT wall panels with various types of openings will be a useful tool for the design of CLT shear walls for platform-type construction.

The resistance of CLT shear walls are amongst the key properties for the design of CLT buildings under lateral loading. However, the stiffness and resistance properties of CLT walls reported in some technical approvals vary significantly (Flaig and Blass 2013). Currently, there are no procedures for determining the stiffness and resistance of CLT shear walls in the North American wood design standards (CAS O86 in Canada, NDS in USA). Therefore, a methodology and equations to estimate the resistance and stiffness of CLT shear walls with various types and

assembly of connections would help engineers and practitioners to successfully design CLT platform-type buildings.

The deflection of CLT shear walls is one of the main parameters which is required to quantify accurately to design CLT buildings for the serviceability limit state. Current standards, however, do not provide guidance to estimate the deflection of CLT shear walls. Models to estimate the total in-plane deflection based on the actual kinematic behaviour of CLT shear walls and under consideration of the influence of perpendicular walls and floors on top would help establish an acceptable serviceability limit state design for CLT platform buildings under lateral loading.

1.9 Objectives

The objectives of this research are to develop:

- Analytical models to estimate the in-plane stiffness of CLT panels with openings.
- Analytical models to estimate the in-plane stiffness and strength of CLT shear walls.
- Formulas to estimate the deflection of CLT shear walls for platform construction.
- Formulas to estimate the resistance of CLT shear walls for platform construction.

1.10 Thesis Outline

Chapter 1 provides a literature review of the research on CLT and its application for a platform-type of construction.

Chapter 2 presents a proposal to estimate the in-plane stiffness of CLT panels with openings including detailed experimental, numerical and analytical investigations with the consideration of wall aspect ratio and size, shape and location of openings.

Chapter 3 describes a methodology to estimate the stiffness and strength of CLT shear walls in platform-type construction. Both single and coupled shear walls are investigated numerically with models validated using full-scale test results. Finally, a parametric study is conducted with the variation of types and number of connectors on various CLT shear walls.

Chapter 4 describes a methodology to estimate the deflection of CLT shear walls for platform-type construction. Analytical models are developed for the deflection of both single and coupled shear walls. The influence of perpendicular walls and floors above are also considered while calculating the in-plane deflection of CLT shear walls under lateral loading.

Chapter 5 proposes new formulas to estimate the resistance of both single and coupled CLT shear walls based on their kinematic behaviour (rocking, or a combination of rocking and sliding). Additionally, a capacity-based design procedure is proposed that provides engineers with guidance for designing platform-framed CLT buildings.

Chapter 6 summarizes the findings from this research with recommendations for future research.

Chapter 2: In-Plane Stiffness of CLT Panels with Openings²

2.1 Introduction

To design CLT shear walls, understanding of the mechanical properties of CLT panels is needed. Several previous studies aimed to predict the properties of CLT panels loaded in-plane. Blass and Fellmoser (2004) developed a method based on the composite theory and proposed k-factors to account for the strength and stiffness of CLT panels, based on single layer properties. Moosbrugger et al. (2006) proposed analytical models to estimate the shear stiffness of CLT panels. Their models are based on the regular periodic internal geometry of CLT wall elements, considering uniform shear loading on the boundaries. Flaig and Blass (2013) developed analytical equations for shear stiffness of CLT beams and verified them with test results.

Openings are very common in CLT walls (Figure 2.1) to accommodate doors and windows. The areas around an opening experience stress concentrations that can reduce in-plane stiffness and load bearing capacity of the panel.

²The material from this chapter has been published in the following journal and conferences:

Shahnewaz, M., Tannert, T., Alam, M. S. & Popovski, M. (2017). In-Plane Stiffness of Cross Laminated Timber Panels with Openings. *Structural Engineering International*, IABSE, DOI: 10.2749/101686617X14881932436131.

Shahnewaz, M., Tannert, T., Alam, M. S. & Popovski, M. (2017). Sensitivity analysis of in-plane stiffness of CLT Walls with Openings. *16th World Conference on Earthquake Conference*, WCEE 2017, 9-13th January 2017, Santiago, Chile.

Shahnewaz, M., Tannert, T., Alam, M. S. & Popovski, M. In-plane stiffness of CLT walls with and without opening. *World Conference on Timber Engineering*, WCTE 2016, 22-25th August, Vienna, Austria.

Shahnewaz, M., Tannert, T., Alam, M. S. & Popovski, M. (2016). CLT walls with openings: in-plane stiffness using finite element and its sensitivity analysis. *5th International Structural Specialty Conference*, CSCE 2016, 1-4th June 2016, London, ON, Canada.

Shahnewaz, M., Tannert, T., Alam, M. S. & Popovski, M. (2015). Experimental and finite element analysis of cross laminated timber (CLT) Panels. In *First International Conference on Advances in Civil Infrastructure and Construction Materials* 2015, 14-15th December 2015, Dhaka, Bangladesh.

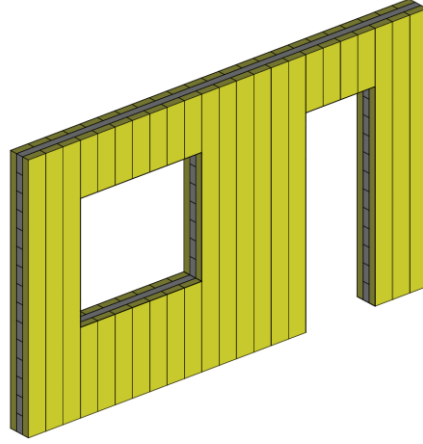


Figure 2.1 Three-ply CLT panel with door and window

In the case of light-frame wood shear walls, often only the full wall segments are taken into consideration when determining the wall resistance. While this approach may be appropriate for light-frame wood shear walls, it can lead to significant underestimation of the stiffness and resistance of CLT walls (Dujic et al. 2007). Another approach is the coupled-beam analogy where the panel above and below the opening is considered as coupled-beams (Diekmann 1995). The concept is based on rigorous mechanics concepts which may not be practical for design purposes. Moosbrugger et al. (2006) performed FEA to quantify the stiffness of a CLT panel with a quadratic opening at the centre and proposed an equation to estimate the reduced stiffness of a CLT panel:

$$\frac{G_{\text{wall}}}{G^*} = \exp^{-6(b/B)^{2.5}} \quad (2.1)$$

where G_{wall} is the shear stiffness of the wall and G^* is the equivalent shear modulus for the panel, B is the half of wall width, and b is the half of the opening width.

Dujic et al. (2007) experimentally investigated CLT wall panels with different opening locations and observed that for walls with an opening up to 30% of the wall area, the wall strength did not change. The stiffness, however, was reduced by about 50%.

While accurate quantification of the in-plane stiffness of CLT wall panels is required to design a CLT structure subjected to lateral loads, there is currently no general approach available. The strength and the stiffness properties reported in technical approvals for verification of in-plane stiffness of CLT walls vary significantly (Flaig and Blass 2013). The objective of this research is to propose an analytical expression to estimate the in-plane stiffness of CLT walls with the consideration of wall aspect ratio and size, shape and location of openings.

2.2 Finite Element Analysis for CLT panels with openings

2.2.1 Model Development

A 3D FEA model was developed in the commercial finite-element package ANSYS (ANSYS APDL 16.0) (Figure 2.2). The CLT panel was modelled using 20-node solid elements (SOLID186). Elastic material properties (as listed in Table 2.1) were assigned in each orthogonal direction of the individual lamellas as provided by manufacturer specifications. The inelastic behaviour was out of scope for the present study. The glue-line between layers of lamellas was modelled using contact elements (Conta_174 and Targe_170), where the edges were considered to be non-glued. A frictional co-efficient of 1.0 was used for the glue-line to account for its rigidity. The connection between the CLT wall and floor was modelled using linear spring elements (COMBIN14). The stiffness properties for the connections taken from previous research (Schneider et al. 2015). Schneider et al. (2015) performed connection tests on 3-ply CLT panels (30+34+30 mm). Steel bracket connections (Simpson Strong-Tie: $90 \times 48 \times 116$ mm) with 18 spiral nails (16d 3.9×89 mm) were tested under quasi-static monotonic tension and shear loading. The spring elements in the FEA utilize the average tension and shear stiffness from the connection

tests of 8710 N/mm and 5040 N/mm, respectively. Similar connections were used for full-scale CLT wall tests at FPInnovations (Popovski et al. 2010).

Table 2.1 CLT material properties

Species	Elastic Modulus (MPa)			Shear Modulus (MPa)			Poisson's Ratio		
	E_x	E_y	E_z	G_{xy}	G_{yz}	G_{zx}	ν_{xy}	ν_{yz}	ν_{zx}
Canadian S-P-F	12400	900	900	700	700	50	0.35	0.35	0.04
European Spruce	12000	370	370	690	690	50	0.35	0.35	0.04

2.3 Model Validation

Two sets of experiments were used for model validation. The first set consisted of four-point bending tests on CLT panels at FPInnovations, Quebec, Canada. Three series of 5-ply (each layer of 35 mm) CLT panels were tested with a span of 3.5 m, 5.9 m and 8.4 m (two replicates of each type), as shown in Figure 2.2a. The specimens were 1.2 m high and laterally supported on both sides at a spacing of one-fifth of the beam span. The boards with a thickness of 175 mm were from Canadian S-P-F. The deformation under quasi-static monotonic loading was measured at mid-span by LVDT allowing the in-plane stiffness to be calculated.

The second set consisted of one quasi-static monotonic test on a CLT wall at FPInnovations, Vancouver, Canada (Popovski et al. 2010). The CLT panel was 3-ply with 2.3 m x 2.3 m panel size and thickness of 94 mm (30+34+30 mm) made of European spruce. The CLT wall was connected to the concrete foundation using 4-steel brackets (Simpson Strong-Tie: $90 \times 48 \times 116$ mm with spiral nails 18-16d 3.9×89 mm). The FEA model was validated using the load-deformation curves from the test results, as shown in Figure 2.3 where the load-deformation plots

for CLT beams are the average curves of the two tests. The numerical results closely matched with the elastic part of the experimental curves.

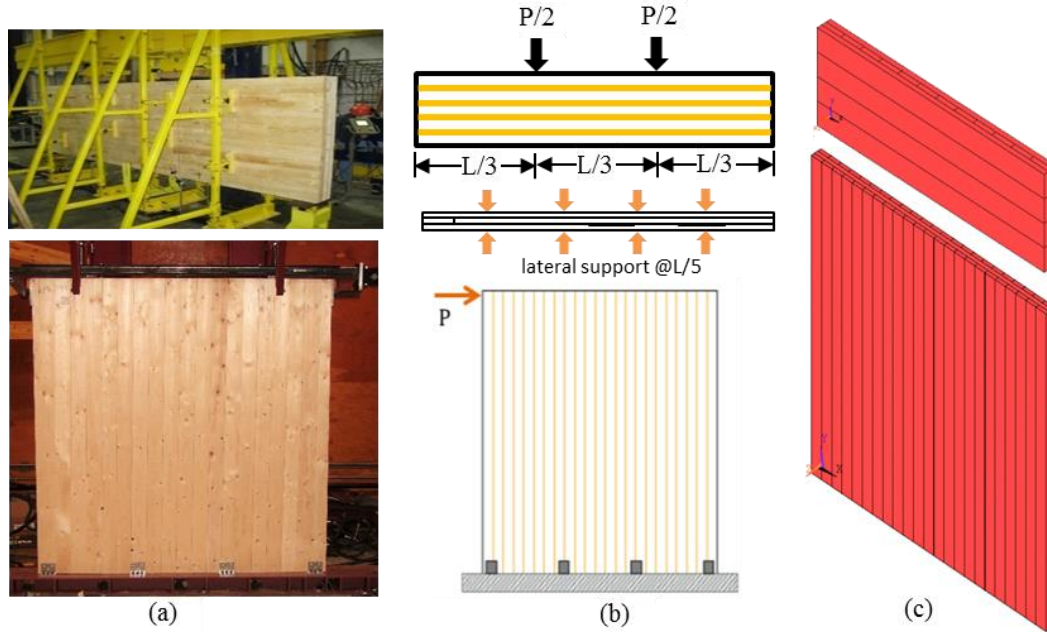


Figure 2.2 (a) Experimental and (b) schematic test setup for CLT beams and walls, (c) FE models, and (d) experimental versus FEA load-deflection curves

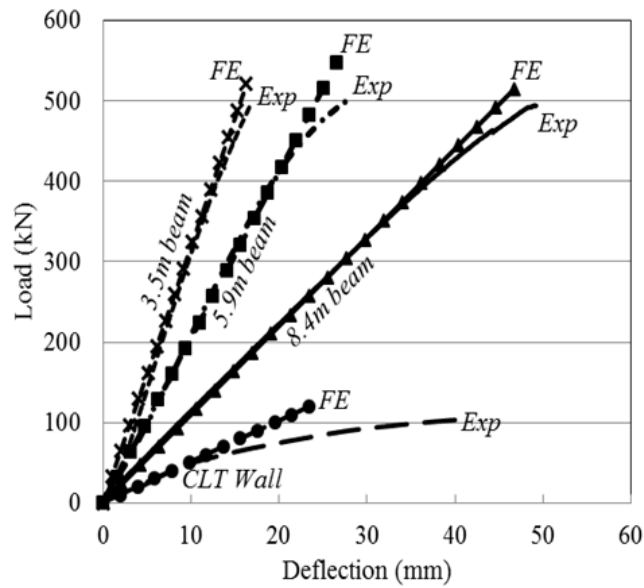


Figure 2.3 Experimental versus FEA load-deflection curves

2.4 Parametric Study on 3-ply CLT Wall Panels with Openings

A parametric study was performed to investigate the stiffness reduction of CLT panels with the variation of aspect ratios, and the size, shape and location of openings. The size of the openings were varied from 20-80% of the length and height of the wall. The openings' area and aspect ratios were varied from 5-54% of the total area of the wall and 0.4-1.0 (smaller to larger dimension), respectively. Openings offsets of up to 32% were considered in the parametric study. Furthermore, the study also investigated the effect of wall aspect ratios (L/H), varied from 0.3 to 2.0.

2.4.1 Effect of opening size

Typical openings, like a window and a door as shown in Figure 2.4, were considered in the parametric study. A maximum of 54% of the total wall area was removed in the FEA. It was found that with a removal of half of the wall area the stiffness of the wall reduced up to 86. As Figure 2.5 illustrates, the stiffness reduction has a non-linear relationship to wall area reduction. From FEA, it was found that the ratio of opening to wall area A_o/A_w , the aspect ratio of opening r_o (smaller to larger dimension) and the aspect ratio of opening to wall $r_{o/w}$ (max of l_o/L or h_o/H) affect reduction in wall stiffness (Figure 2.5). Parameters A_o/A_w and r_o showed a linear relationship and parameter $r_{o/w}$ showed a non-linear relationship with the wall stiffness. Considering the database from the parametric study (as shown in Figure 2.5), Eq. (2.2) was proposed to calculate the in-plane stiffness of CLT wall panels with openings based on symbolic regression. Symbolic regression searches simple and accurate expressions that fit a given dataset. It utilizes genetic programming to obtain mathematical models from building blocks such as functions, operators, variables and constants. The solution is selected on the basis of the assigned fitness functions. In order to search for the best-fitted model the fitness function checks the mean-square error to determine the accuracy of the mathematical model against the given database.

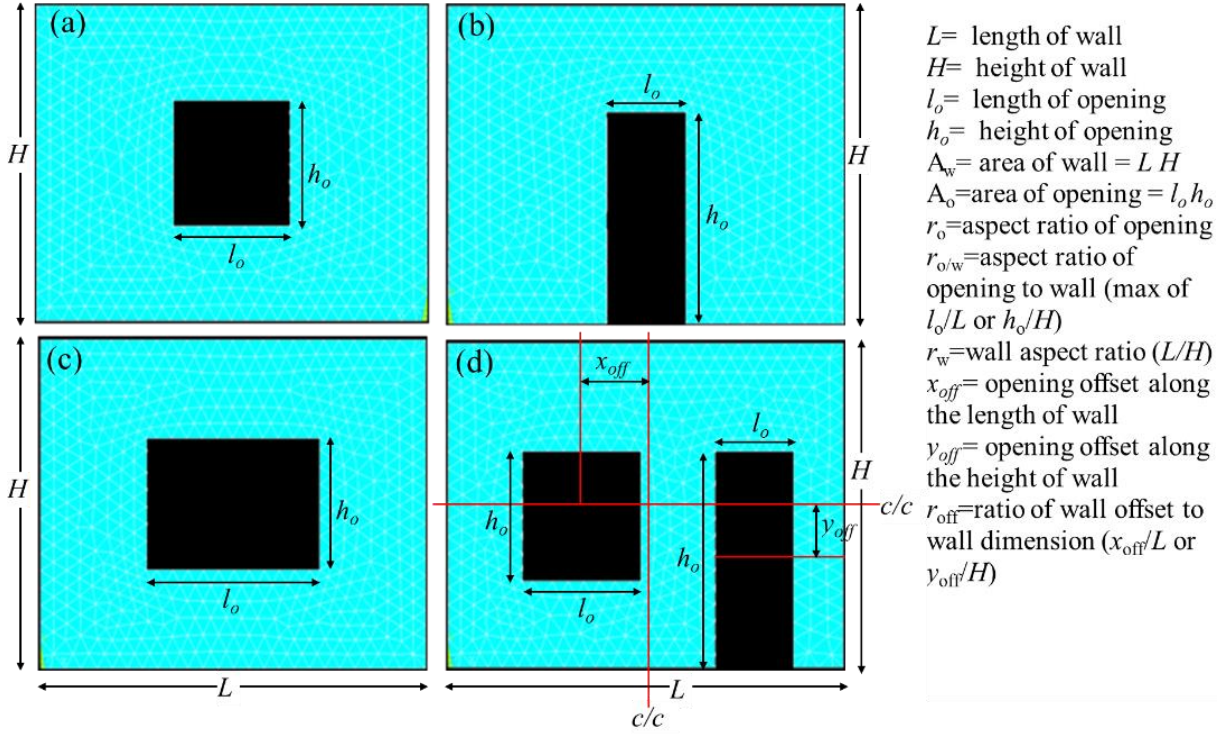


Figure 2.4 Typical openings in CLT Walls and description of parameters

$$K_{opening} = K_{full} \left[1 - \frac{r_{o/w} \left(\frac{A_o}{A_w} \right)}{\sqrt{r_{o/w} + r_o \left(\frac{A_o}{A_w} \right)}} \right] \quad (2.2)$$

where $K_{opening}$ and K_{full} are the stiffness of walls with and without opening, respectively; A_o and A_w are the areas of walls with and without opening, respectively; r_o is the aspect ratio of the opening (smaller to larger dimension); and $r_{o/w}$ is the maximum aspect ratio of opening to wall dimension (max of l_o/L or h_o/H , where L and H are the wall length and height, respectively, and l_o and h_o are the opening length and height, respectively).

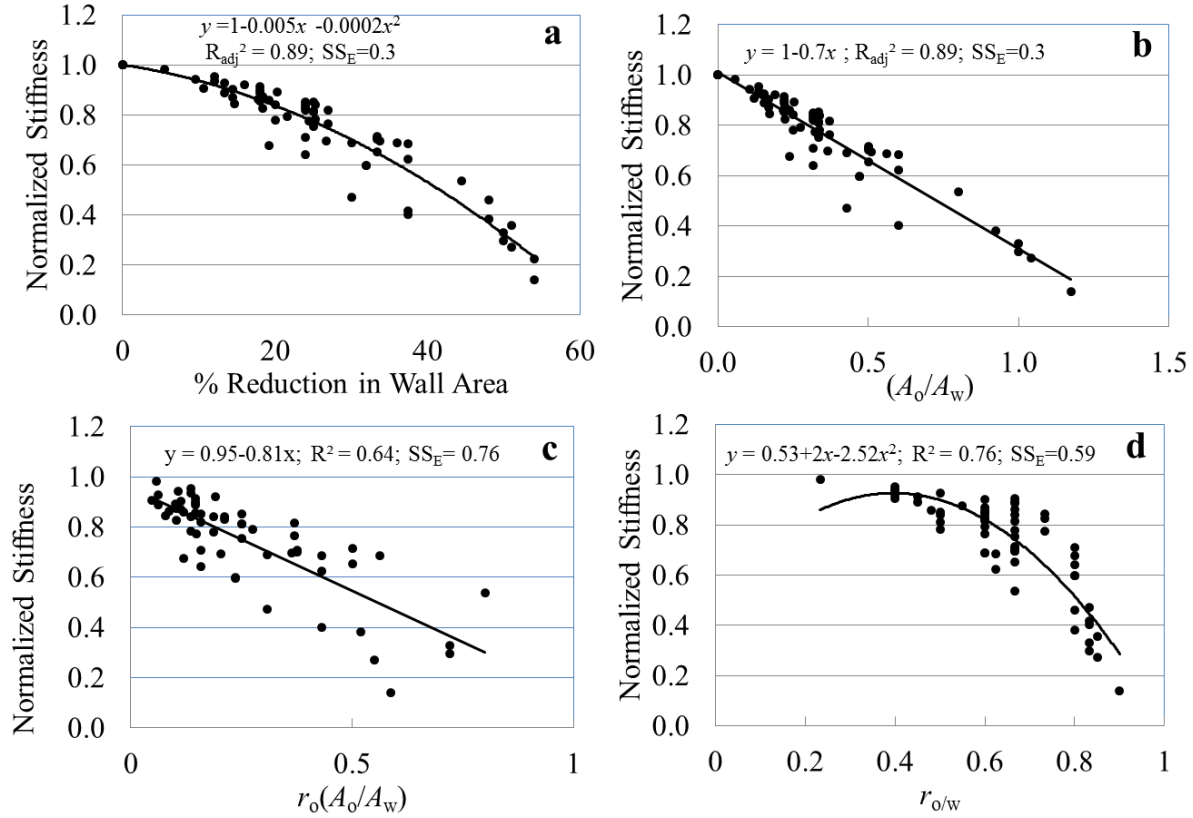


Figure 2.5 Effect of opening on CLT wall stiffness; normalized stiffness versus a) % reduction in wall area; b) ratio of opening to wall area (A_o/A_w); c) product of opening aspect ratio (r_o) and opening to wall area (A_o/A_w); and d) aspect ratio of opening to wall ($r_{o/w}$)

The proposed equation is more accurate in predicting stiffness of CLT walls with openings when compared to a previously proposed model by Dujic et al. (2007), as shown in Figure 2.6. The average ratio of the wall stiffness to the predicted stiffness (as in Eq. 2.2) was found close to 1.0. On the other hand, the previously proposed model from Dujic et al. (2007) was found highly conservative with average wall stiffness to the predicted stiffness of 1.5.

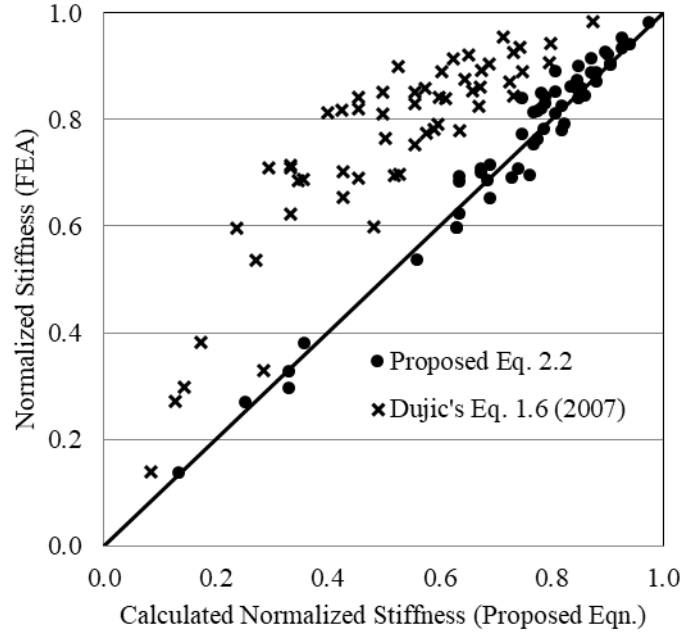


Figure 2.6 FEA vs. calculated stiffness of CLT walls from this study compared to previous studies

2.4.2 Effect of opening-to-wall height ratio

The reduction in wall stiffness was found to increase for ratios $h_o/H > 0.8$. Therefore, Eq. (2.2) was adjusted using the same symbolic regression procedure as described for Eq. (2.2):

$$K_{opening} = K_{full} \left[1 - \frac{r_{o/w} \left(\frac{A_o}{A_w} \right) e^{\delta(r_w - 1)}}{\sqrt{r_{o/w} + r_o \left(\frac{A_o}{A_w} \right)}} \right] \quad (2.3)$$

$$\delta = \begin{cases} 0 & \text{if } h_o / H < 0.8 \\ 1 & \text{if } h_o / H \geq 0.8 \end{cases}$$

where r_w is the wall aspect ratio (L/H) and all other parameters are the same as in Eq. (2.2).

2.4.3 Effect of opening offset

The offset of the opening from the centre of the panel further reduced wall stiffness up to 30%, see Figure 2.8a. Therefore, to account the opening offset, another modification to Eq. (2.2) is proposed:

$$K_{opening} = K_{full} \left[1 - \frac{r_{o/w} \left(\frac{A_o}{A_w} \right)}{\sqrt{r_{o/w} + r_o \left(\frac{A_o}{A_w} \right)} - 2(r_{off} / r_w)} \right] \quad (2.4)$$

where r_{off} is the ratio of wall offset to wall dimension (x_{off}/L or y_{off}/H) and all other parameters are as in Eq.(2.2). Combining the previous equations, the reduced stiffness of CLT walls with openings can be estimated as:

$$K_{opening} = K_{full} \left[1 - \frac{r_{o/w} \left(\frac{A_o}{A_w} \right) e^{\delta(r_w-1)}}{\sqrt{r_{o/w} + r_o \left(\frac{A_o}{A_w} \right)} - 2(r_{off} / r_w)} \right] \quad (2.5)$$

$$\delta = \begin{cases} 0 & \text{if } h_o / H < 0.8 \\ 1 & \text{if } h_o / H \geq 0.8 \end{cases}$$

The stiffness of CLT wall without opening, K_{full} can be calculated by adding the reciprocal of wall bending, K_b and shear, K_s stiffness as in Eq. (2.6).

$$\frac{1}{K_{full}} = \frac{1}{K_b} + \frac{1}{K_s} \quad (2.6)$$

where the bending stiffness, K_b of the wall panel can be estimates as Eq. (2.7):

$$K_b = \frac{3EI_{eff}}{h^3} = \frac{3}{h^3} \left[\frac{E_{90}}{E_0} + \left(1 - \frac{E_{90}}{E_0} \right) \frac{t_{m-2} - t_{m-4} + \dots \pm t_1}{t_m} \right] E_0 I \quad (2.7)$$

Here the effective bending stiffness, $(EI)_{eff}$ for a CLT panel loaded in-plane can be calculated from the equation by Blass and Fellmoser (2004) where E_o and E_{90} are the modulus of elasticity in parallel and perpendicular to grain directions, t_m is the total thickness of the CLT panel. The parameters, t_1 to t_m are described in Figure 4.83.

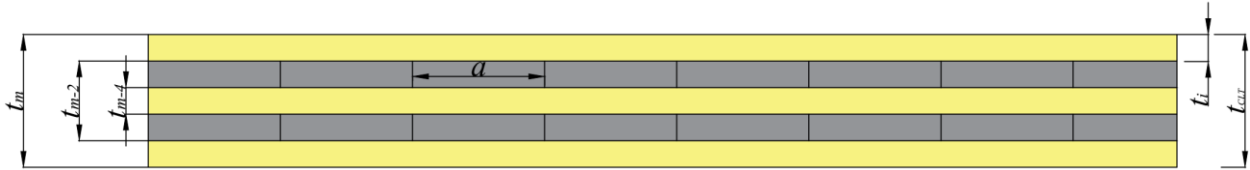


Figure 2.7 Bending stiffness calculation from the cross section of m-ply CLT panel

The shear stiffness, K_s of the wall panel can be estimates as Eq. (2.8):

$$K_s = \frac{G_{CLT} t_{CLT} b}{h} \quad (2.8)$$

The shear modulus of the CLT panel, G_{CLT} is also referred to as equivalent shear modulus of the CLT panel which is measured parallel to the grain of outer lamella can be estimated using formula proposed by Moosbrugger et al. (2006):

$$G_{CLT} = \frac{G_{||}}{1 + 6 \left(\frac{G_{||}}{G_{\perp} + G_{||}} \right) (t_i / a)^2} \quad (2.9)$$

where G_{\perp} is the shear moduli perpendicular to the grain, $G_{||}$ is the shear moduli parallel to the grain and t_i/a is the board thickness-to-width ratio (Figure 2.7).

2.4.4 Effect of panel aspect ratio

The effect of panel aspect ratios (L/H) on the in-plane stiffness was investigated for the range of aspect ratios from 0.3 to 2.0. It was observed that the in-plane stiffness increased linearly with aspect ratio (Figure 2.8b). It should be noted that the stiffness of the rectangular wall was calculated with respect to the square wall (as shown in Figure 2.8b). The stiffness of a rectangular wall can be calculated as in Eq. (2.6):

$$K_{\text{rectangular}} = K_{\text{square}} \left[\left(\frac{L}{H} \right)^2 \left(1.31 - \frac{1}{3} \left(\frac{L}{H} \right) \right) \right] \quad (2.10)$$

where $K_{\text{rectangular}}$ and K_{square} is the stiffness of rectangular and square walls, respectively; L and H is the wall length and height, respectively.

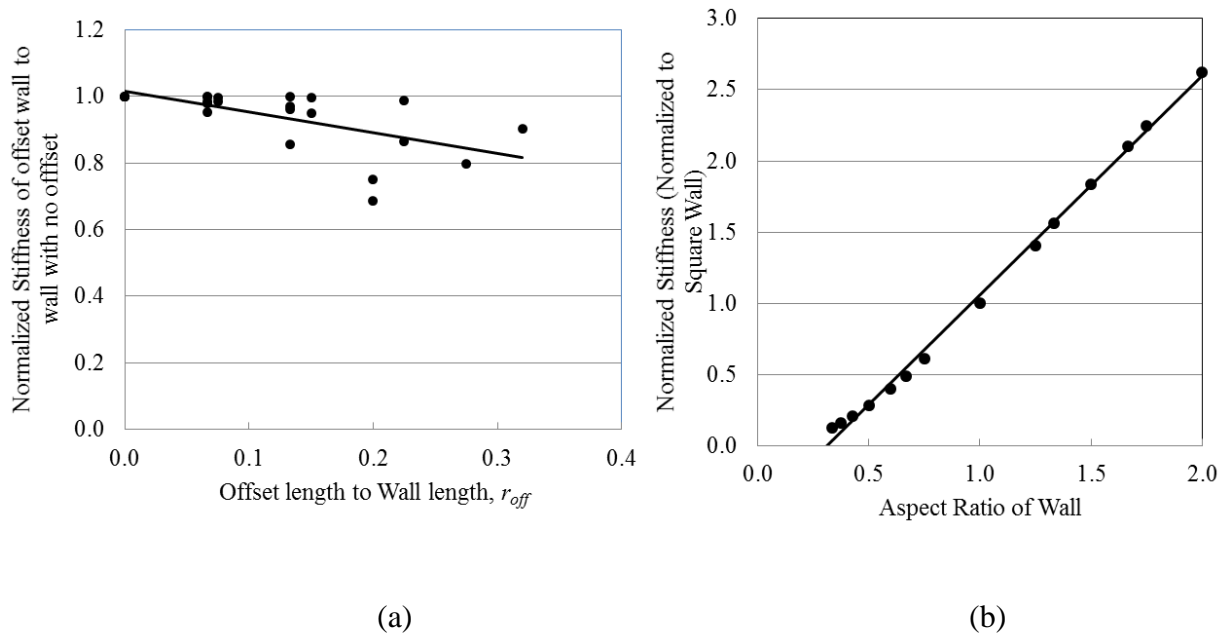


Figure 2.8 Effect of opening offset (a) and aspect ratio (b) on CLT wall stiffness

2.5 Sensitivity Analysis on 3-ply CLT Wall Panels with Openings

2.5.1 Methods

The proposed equations (Eq. 2.3 to Eq. 2.5) contain six parameters that contributed the overall stiffness of the CLT walls. However, their contributions need to be assessed from sensitivity analyses that quantify the contribution of each input variable to the model response.

In this research, a sensitivity analysis was performed using the commercial software package optiSLang (Most and Will 2008). Advanced Latin Hypercube Sampling (ALHS) was used for random sampling of input parameters. ALHS is effective in representing the non-linearity of the model in a reduced space. Meta-models were used to represent the model responses of surrogate functions in terms of the model inputs. A surrogate model is often advantageous due to the inherent complexity of many engineering problems (Sacks et al. 1989, Simpson et al. 2001). To overcome the limitations of common Meta-models such as Moving Least Square approximation or Neural Networks that require a high number of samples to represent high-dimensional problems with sufficient accuracy, the Meta-model of Optimal Prognosis (MOP) approach was developed (Most and Will 2008). MOP uses the generalized coefficient of determination (*CoD*) which results for the special case of pure polynomial regression. The *CoD* assesses the approximation quality of a polynomial regression by measuring the relative amount of variation:

$$R^2 = \frac{SS_R}{SS_T} = 1 - \frac{SS_E}{SS_T}; \quad 0 \leq R^2 \leq 1 \quad (2.11)$$

where SS_T is the total variance, SS_R the variation due to the regression and SS_E the unexplained variation:

$$SS_T = \sum_{i=1}^N (y_i - \mu_Y)^2, SS_R = \sum_{i=1}^N (\hat{y}_i - \mu_{\hat{Y}})^2, SS_E = \sum_{i=1}^N (y_i - \hat{y}_i)^2 \quad (2.12)$$

To penalize for over-fitting, the adjusted Coefficient of Determination (Montgomery and Runger 2003) is used:

$$R_{adj}^2 = 1 - \frac{N-1}{N-p} (1 - R^2) \quad (2.13)$$

where N is the number of sample points and p is the number of regression co-efficients. The quality of an approximation was evaluated in terms of the prognosis quality by using an additional data set. The agreement between this real test data and the meta-model estimates is measured by the coefficient of prognosis *CoP* (Most and Will 2008):

$$CoP = \left(\frac{\mathbf{E} \left[Y_{Test} \hat{Y}_{Test} \right]}{\sigma_{Y_{Test}} \sigma_{\hat{Y}_{Test}}} \right)^2 ; \quad 0 \leq CoP \leq 1 \quad (2.14)$$

An optimal meta-model can be searched with a defined *CoP*. A polynomial regression is developed thereafter and the coefficients of importance (*CoI*) are calculated for each variable:

$$CoI_{Y, X_i} = R_{Y, X}^2 - R_{Y, X-i}^2 \quad (2.15)$$

where $R_{Y, X}^2$ is the CoD of the full model including all terms of the variables in X and $R_{Y, X-i}^2$ is the *CoD* of the reduced model where all linear, quadratic and interactions terms belonging to X_i are removed.

The sensitivity analysis for the proposed CLT wall stiffness equation (Eq. 2.5) involved six steps:

- A solver chain was created in optiSLang for the sensitivity analysis.
- The range of the input parameters and their types were defined as summarized in Table 2.2.

- ALHS was used to randomly create 1,000 samples within the defined input parameters range.
- An input file was created for the proposed equation which links to the ALHS.
- A Python script was run 1,000 times to generate all output.
- The MOP was created to quantify the contribution of each parameter on the proposed model.

The algorithm for the sensitivity analysis is presented in Figure 2.9. The parameters for the sensitivity analysis are given in Table 2.2.

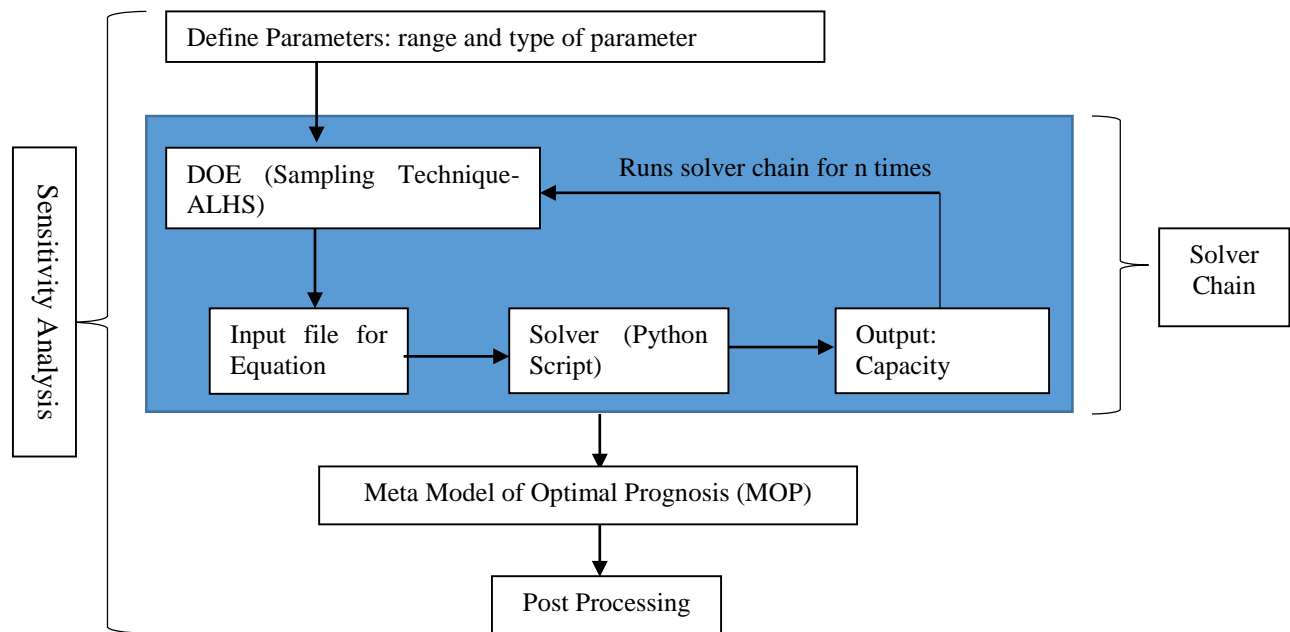


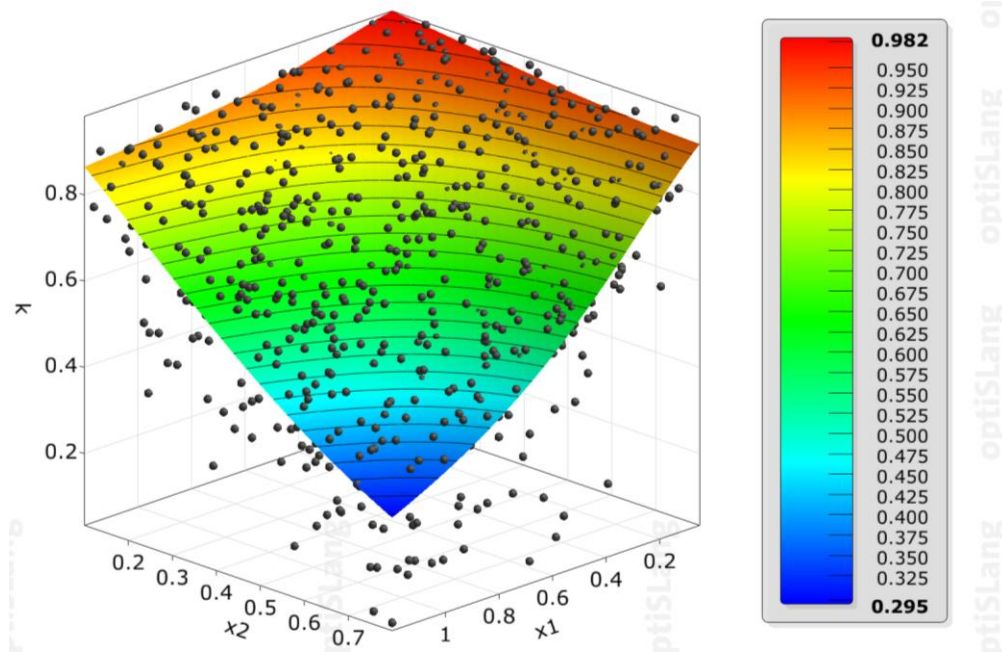
Figure 2.9 Algorithm for sensitivity Analysis in optiSLang

2.5.2 Results of Sensitivity Analyses

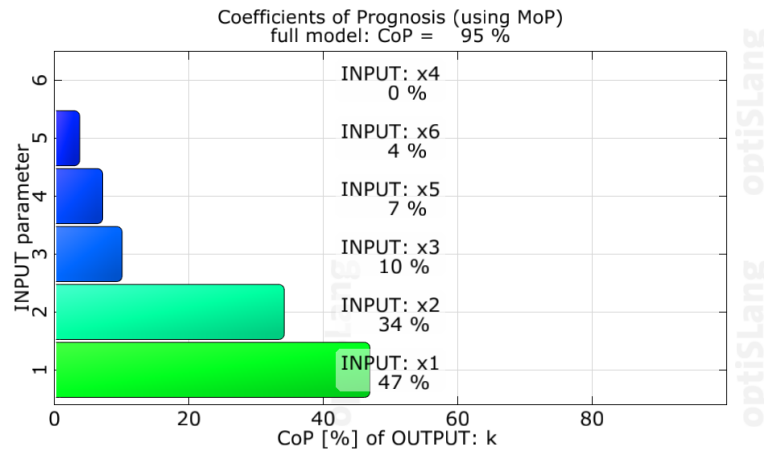
The stiffness of the CLT wall with openings was described as a function of the six parameters. From the sensitivity analysis using the 1,000 samples, the approximation of the stiffness with respect to each parameter was established and the total model *CoP* was calculated as 95% which indicated a very good approximation. The impact of two input parameters on the output is

illustrated in a 3D space as shown in Figure 2.10. It shows the MLS approximation of the CLT wall stiffness with opening with respect to input parameters $A_o/A_w(x_1)$ and $r_{o/w}(x_2)$. The individual *CoP* values of each parameter, see Table 2.2 showed that parameters x_1 (A_o/A_w) and x_2 ($r_{o/w}$) have the highest influence on the reduced CLT wall stiffness. Parameters x_5 (h_o/H) and x_6 (r_w) have little influence on the CLT wall stiffness with *CoP* values less than 5%. Therefore, these two parameters -i.e. the influence of opening-to-wall height ratio and the wall aspect ratio -can be ignored and Eq. (2.16) is proposed to estimate the reduced stiffness of CLT walls with openings. The ratio of stiffness from FEA vs stiffness calculated using Eq. (2.16) was close to 1.0 with a 7% standard deviation. The R_{adj}^2 and SS_E of the proposed equation were 0.91 and 0.19, respectively.

$$K_{opening} = K_{full} \left[1 - \frac{r_{o/w} \left(\frac{A_o}{A_w} \right)}{\sqrt{r_{o/w} + r_o \left(\frac{A_o}{A_w} \right)} - 2(r_{off} / r_w)} \right] \quad (2.16)$$



(a)



(b)

Figure 2.10 (a) MLS approximation of the CLT wall stiffness, k with respect to the two input parameters, $A_o/A_w(x_1)$ and $r_{o/w}(x_2)$; (b) and CoP values of each parameter

Table 2.2 Parameter ranges and importance for sensitivity analysis

Parameters		Range	CoP
ratio of opening to wall area	$A_o/A_w (x_1)$	0.05 – 1.20	46%
maximum aspect ratio of opening-to-wall	$r_{o/w} (x_2)$	0.10 – 0.80	33%
aspect ratio of opening	$r_o (x_3)$	0.30 – 2.00	10%
ratio of wall offset to wall dimension	$r_{off} (x_4)$	0.00 – 0.32	7%
ratio of opening-to-wall height	$h_o/H (x_5)$	0.20 – 0.90	4%
wall aspect ratio	$r_w (x_6)$	1.00 – 2.00	0%

2.6 In-plane Stiffness of 5-ply and 7-ply CLT Wall Panels with Openings

The before proposed equations to estimate the reduced stiffness of CLT wall panels with openings are limited to 3-ply panels. Commonly however, CLT shear walls in a building can also be thicker. In general, the in-plane stiffness of CLT walls will increase with the increase of the number of plies. Therefore, it is important to estimate whether the reduction in the in-plane stiffness of CLT walls with openings in panels other than 3-ply will follow the same trend as 3-ply CLT. In this section, the study was extended towards 5-ply and 7-ply CLT panels with equal layer thickness where the boards are placed in orthogonally alternating orientation to the neighboring layer. The CLT panels investigated in this chapter are suitable for the CLT shear wall assemblies in a platform construction where the orientation of the outer layers is in the upright direction.

2.6.1 Numerical Study on 5-ply and 7-ply CLT Walls

To calculate the reduced stiffness of 5-ply and 7-ply CLT walls with openings, 3D FEA models were developed where the CLT panels were modelled using solid elements and the connections were modelled using linear spring elements (Figure 2.11). The elastic material properties listed in

Table 2.1 were assigned in each orthogonal direction of the individual lamellas as provided by manufacturer specifications. The glue-line between layers of lamellas was modelled using contact elements whereas the edges were considered to be non-glued.

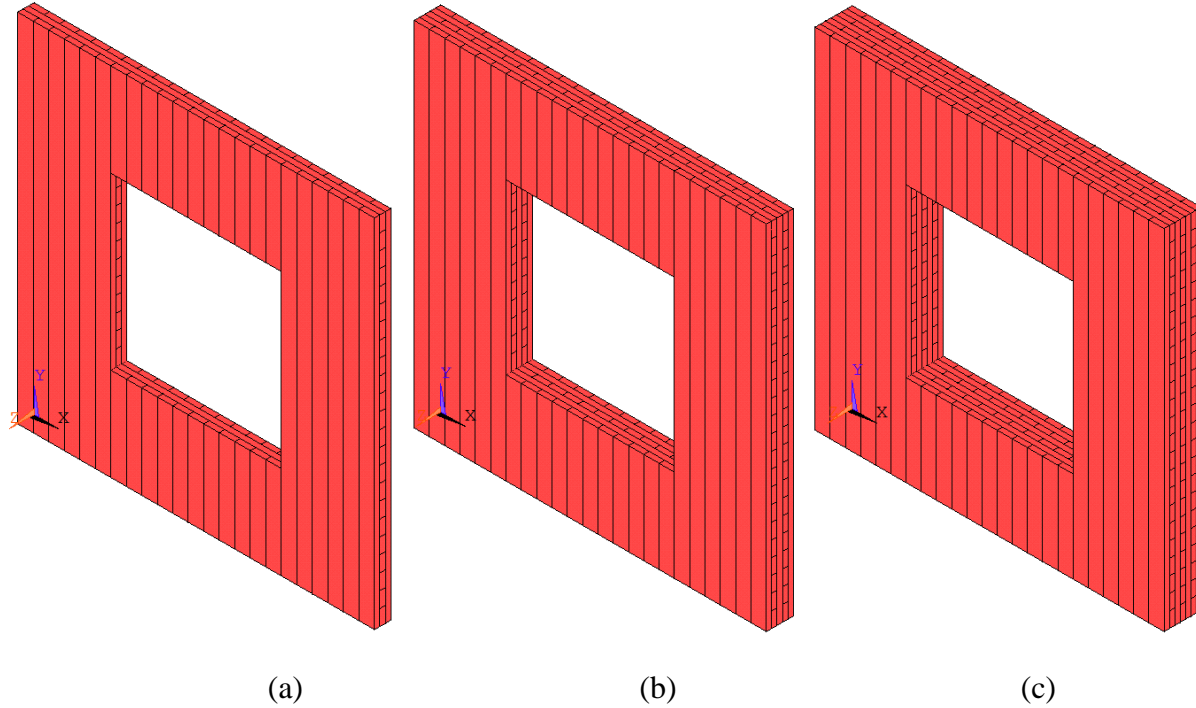


Figure 2.11 CLT panels with openings: (a) 3-layer, (b) 5-layer, and (c) 7-layer

2.6.2 Parametric Study on 5-ply and 7-ply CLT Wall Panels with Openings

Similar to 3-ply CLT walls, a parametric study was performed to investigate the stiffness reduction of CLT wall panels with the variation the size, shape and location of openings. The size, i.e. the length and height of the openings, were varied from 20-80% of the length and height of the wall. The openings' area was varied from 5-54% of the total area of the wall and the aspect ratio was varied from 0.4-1.0 (smaller to larger dimension), respectively. A maximum of 54% of the total wall area was removed in the FEA. Previous analysis on 3-ply panels showed that with a removal of half of the wall area the stiffness of the wall was reduced by up to 86% (Figure 2.12). A

reduction of up to 83% and 81% was observed on 5-ply and 7-ply CLT walls, respectively (Figure 2.12). Therefore, with an increase in the number of lamellas the reduction in CLT wall stiffness with openings decreases. This is because the CLT walls with higher number of lamellas are stiffer and less sensitive to reduction in stiffness in presence of openings.

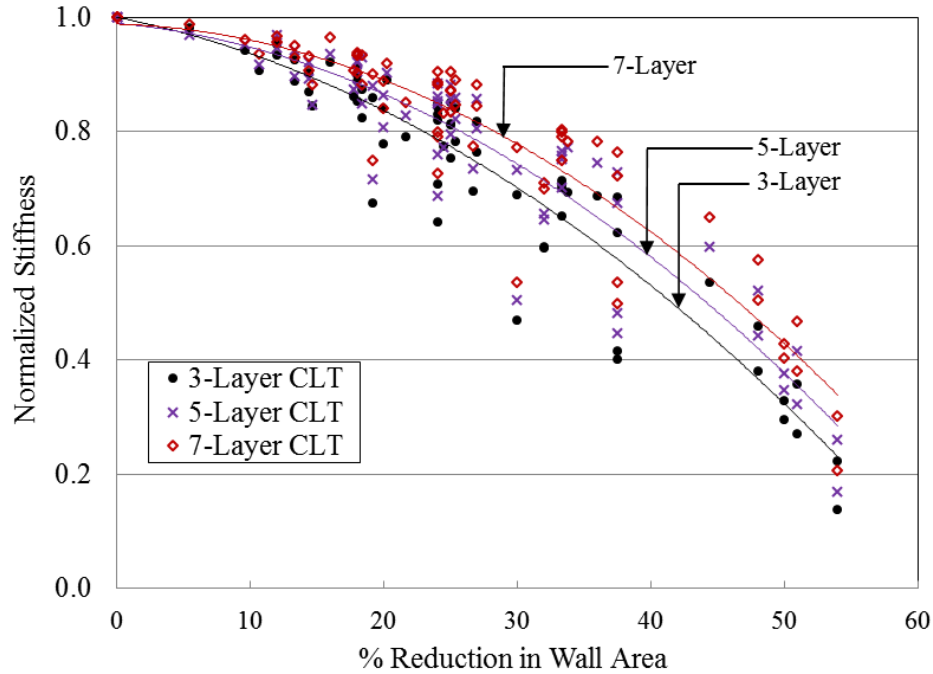


Figure 2.12 Effect of opening on the reduction of 3, 5, and 7-ply CLT walls stiffness

2.6.3 Results and Discussion

The stiffness reduction in 5-ply and 7-ply CLT walls follow the same trend as 3-ply wall (Figure 2.12). The average reduction in 5-ply and 7-ply walls was 3% and 6% less, respectively, compared to 3-ply walls. Both 5-ply and 7-ply walls are stiffer than the 3-ply panels, therefore, with the presence of the same size of openings they had less reduction compared to 3-ply walls. Therefore, the estimated stiffness for 5-ply and 7-ply walls using Eq. (2.2) provides a conservative estimate

that follows the bottom trend line as shown in Figure 2.12. The difference or error can be considered as acceptable considering current timber design practice in the codes.

2.7 Summary

FEA were conducted to calculate the in-plane stiffness of CLT wall panels with openings. The model was used for parametric studies on the impact of opening size, shape and location as well as the wall aspect ratio on the wall stiffness. Subsequently, equations were developed to estimate the in-plane stiffness of CLT walls with openings. Finally, a sensitivity analyses allowed reducing the number of model parameters to those that have a significant impact on the stiffness reduction of CLT walls with openings. The investigations allow drawing the following conclusions:

- FEA accurately described the in-plane load-deformation behaviour of CLT beams and walls. The panel stiffness as computed by FEA closely matched the experimental results.
- The proposed equations better predicted the stiffness of the CLT walls compared to a previously proposed equation from the literature.
- The sensitivity analysis showed that the ratio of opening to wall area and the maximum aspect ratio of opening to wall have a significant impact on the stiffness reduction of CLT walls with openings.
- The opening-to-wall height have little impact on the stiffness reduction of CLT walls with openings, therefore, can be ignored.
- The FEA was extended on 5-ply and 7-ply walls with openings. The stiffness reduction in CLT walls with higher number of lamellas was less compared to 3-ply walls with openings, i.e. walls with higher number of lamellas, are stiffer and less sensitive to stiffness reduction with the presence of openings. Therefore, the proposed equations for 3-ply wall with

openings can be conservatively used to estimate the stiffness reduction of CLT wall with openings having more than 3-ply lamellas.

The study does not consider CLT panels of unequal board thickness. In the more common cases, where the cross layers have smaller thickness, the stiffness reduction of the CLT panels with openings is smaller than predicted herein. Therefore it is postulated, that the proposed equations of this chapter can be used conservatively to estimate the stiffness reduction of CLT panels with unequal board thickness.

Chapter 3: Strength and Stiffness of Single and Coupled CLT Shear Walls³

3.1 Introduction

The research presented in this chapter investigated CLT shearwalls with different connections for platform-framed construction with the objective to quantify the stiffness and strength of CLT shear walls under in-plane loading. The use of CLT in residential and non-residential buildings is becoming increasingly popular in North America. While the 2016 supplement to the Canadian Standard for Engineering Design in Wood, CSAO86, provides provisions for CLT structures used in platform-type applications, it does not provide guidance for the in-plane stiffness and strength of CLT shear walls.

Up until now platform-type construction, where each floor act as a platform for the floor above, is the most common structural system used for low to mid-rise CLT buildings. The building is either directly connected to a RC foundation or sits a top of an RC podium. The CLT shear walls, both single and coupled walls (Figure 3.1a, b and c) are connected to foundations or a RC podium by steel brackets and hold-downs using metal fasteners like screws and nails (Figure 3.1d and e). The CLT walls to the floors in the upper storeys are connected by brackets and/ hold-downs or by long STS. The panels in between floors and walls are connected by screws using either lap or spline joints (Figure 3.1f and g).

³ A version of this chapter has been published in the 6th International Conference on Engineering Mechanics and Materials, CSCE, Vancouver, Canada.

Shahnewaz, M., Tannert, T., Alam, M. S. & Popovski, M. (2017). Performance of Cross Laminated Timber Shear walls under Cyclic Loading. 6th International Conference on Engineering Mechanics and Materials, CSCE, May 31 - June 3 2017, Vancouver, BC, Canada.

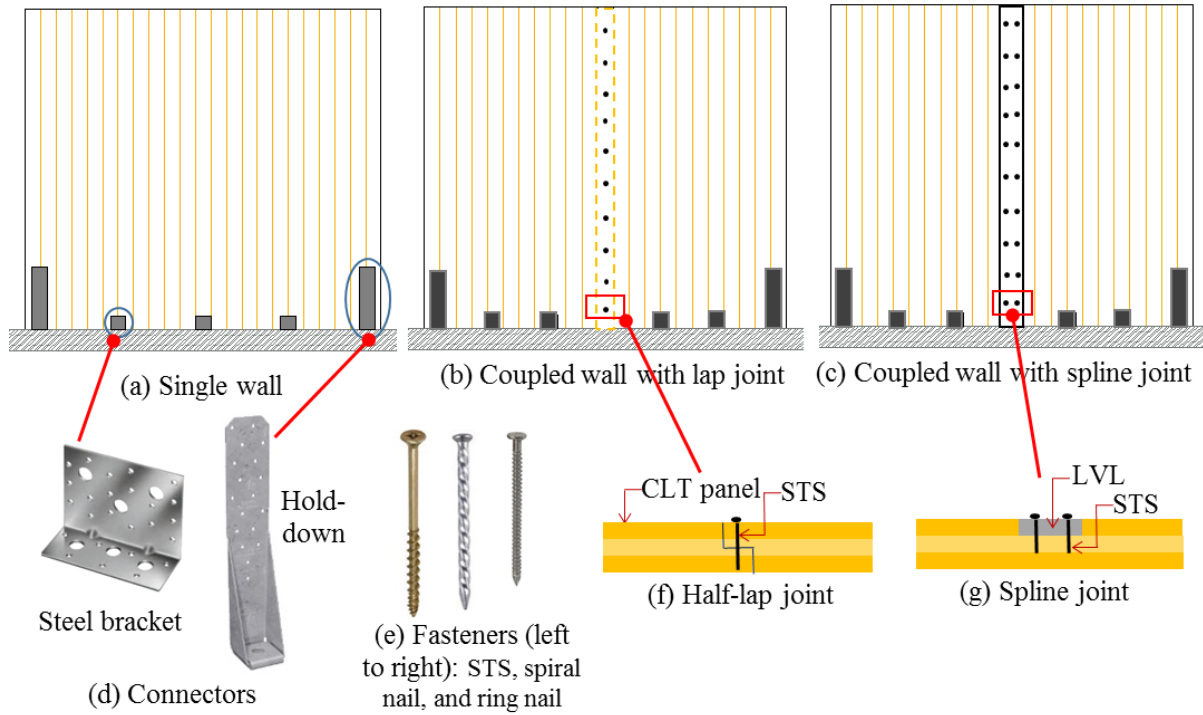


Figure 3.1 CLT shear walls: (a) single, (b) coupled with lap joint, (c) coupled with spline joint, (d) bracket and hold-down connectors, (e) fasteners, (f) half-lap joint, (g) spline joint

For an efficient design of CLT shear walls in CLT platform construction, it is important to evaluate the actual behaviour of different CLT walls and connectors. Previous research investigated the mechanical behaviour of brackets, hold-downs and screws' shear connectors (Tomasi and Smith 2014, Gavric et al. 2015a, Gavric et al. 2015b, Schneider et al. 2015, Hossain et al. 2016) for the application of CLT wall-to-floor/foundation and wall-to-wall connections. Other work specifically investigated the behaviour of CLT walls under monotonic and cyclic loading (Ceccotti et al. 2006, Popovski et al. 2010, Gavric et al. 2015c, Reynolds et al. 2017). The results demonstrated that the failure was located mostly at the connections, while the CLT wall panels were subjected to negligible in-plane deformations.

3.2 Finite Element Analysis of CLT Connections

3.2.1 Tests on CLT Connections

The present research utilizes the results from previous research (Gavric et al. 2015a and Schneider et al. 2015) to develop an FEA model for different types of connectors connecting CLT wall-to-floor, wall-to-foundation, and wall-to-wall. Gavric and Schneider tested 3-ply CLT panels, 85 mm and 94 mm thick, respectively. A wall configuration with steel brackets, hold-downs, and STS connections is shown in Figure 3.1.

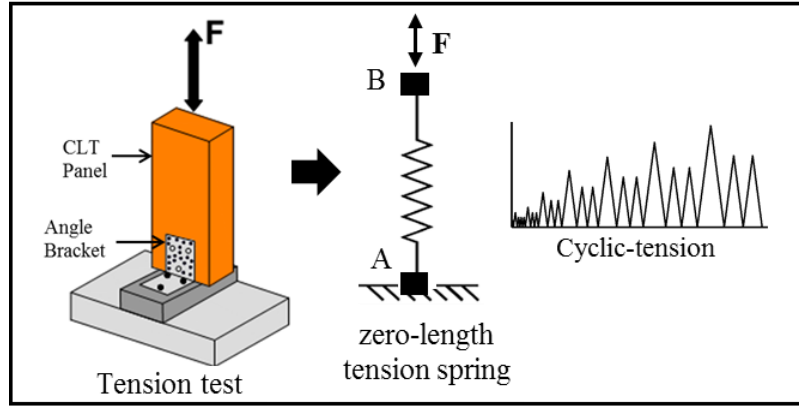
Two types of Simpson Strong-Tie steel brackets (Bracket A: 90×48×116 mm and Bracket B: 90×105×105 mm) with different fasteners were used; their properties are listed in Table 3.1. Gavric et al. (2015a) also performed tests on two types of Simpson Strong-Tie hold-downs e.g., HTT16 and HTT22 using ring nails fasteners. Additionally, double plane shear tests on CLT wall-to-wall half-lap and spline joints using a different number of STSs (Gavric et al. 2015b) were performed. The connections are designated as B₁ to B₅ for brackets, HD₁ to HD₂ for hold-downs, and WW₁ to WW₂ for shear connectors throughout this article as shown in Table 3.1. Gavric's brackets, hold-downs, and STSs shear connectors were tested following EN 12512 (2001) loading protocol and Schneider's brackets were tested following CUREE (ASTM E2126 2011) loading protocol.

Table 3.1 CLT connection Types and IDs

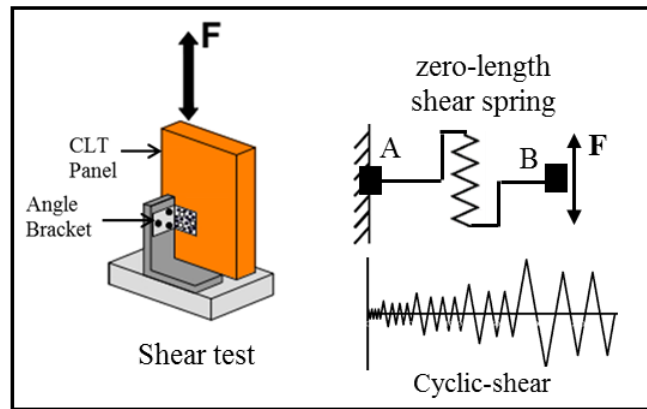
Connection Type	Connection ID	Fasteners
Bracket A: 90×48×116 mm	B ₁	18-16d SN 3.9×89 mm
	B ₂	18-SFS screw 4×70 mm
	B ₃	10-SFS screw 5×90 mm
	B ₄	12- RN 3.4×76 mm
	B ₅	11- RN 4×60 mm
Hold-down: HTT22	HD ₁	12- RN 4×60 mm
Hold-down: HTT16	HD ₂	18-16d SN 3.9×89 mm
Half-lap joint	WW ₁	STS Φ8×80 mm
Spline joint	WW ₂	STS Φ8×80 mm

3.2.2 FEA Model for Connections

FEA models of CLT connections were developed in OpenSees (McKenna et al. 2000). Both tension and shear connections were modelled using zero-length spring element as shown in Figure 3.2. It is defined by two nodes at the same location where the nodes are connected by uniaxial material model “Pinching4” (Figure 3.3) to represent the force-deformation relationship for the element. The least-square method was employed to estimate the parameters of the Pinching4 model from the backbone of the tested connections.



(a)



(b)

Figure 3.2 CLT connection's tests configuration: (a) cyclic tension test and FE model, and (b) shear test and FE model

3.2.3 Hysteresis Pinching4 Model

The hysteresis behaviour of the springs was modelled using the Pinching4 model (Mitra 2012). Pinching4 is a piecewise linear model with a “pinched” load-deformation response that accounts for strength and stiffness degradation under seismic loading (Figure 3.3). The model includes 16 parameters -i.e. 4-positive and 4-negative points to define the backbone curve. Unload-reload paths along with pinching behaviour are defined by 6-parameters. Both symmetric and non-symmetric hysteresis can be modelled by Pinching4.

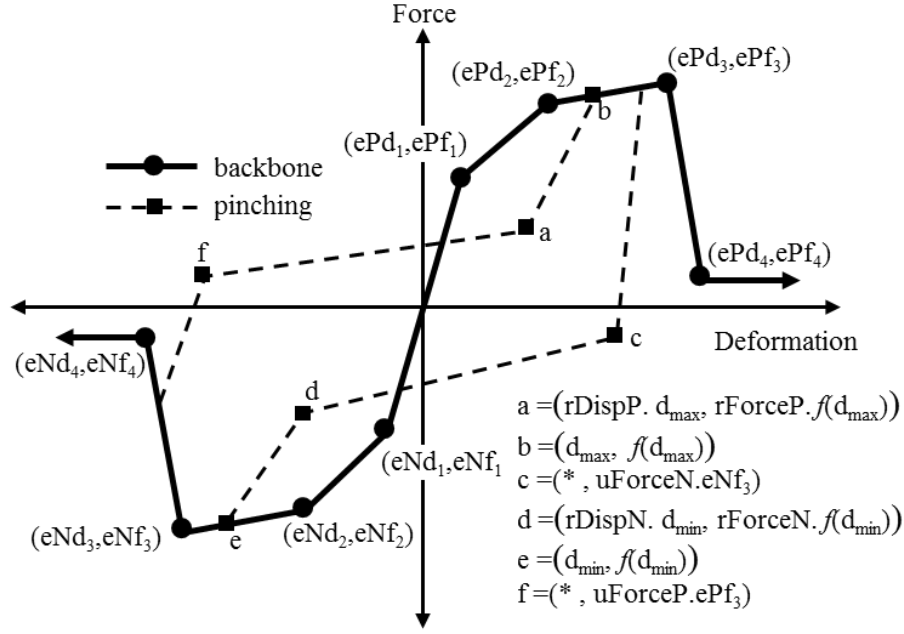


Figure 3.3 Pinching4 Model

3.2.4 Model Validation for CLT Connections

The models were validated by test results presented by Gavric et al. (2015a and 2015b) and Schneider et al. (2015). The comparisons between FEA and tests are plotted in Figure 3.4. Specifically, Figure 3.4a and Figure 3.4b show the hysteresis of bracket B_1 under cyclic shear and tension, respectively. Figure 3.4c shows the hysteresis of hold-down HD_1 under cyclic tension and Figure 3.4d shows the hysteresis of STS half-lap joint WW_1 under cyclic shear. Comparing FEA vs test results, it can be concluded that Pinching4 accurately captured the load-deformation hysteresis behaviour including the backbone curves of CLT connections. From the FE analyses, the connections' stiffness, ductility, yield and ultimate load, and yield and ultimate displacement were calculated.

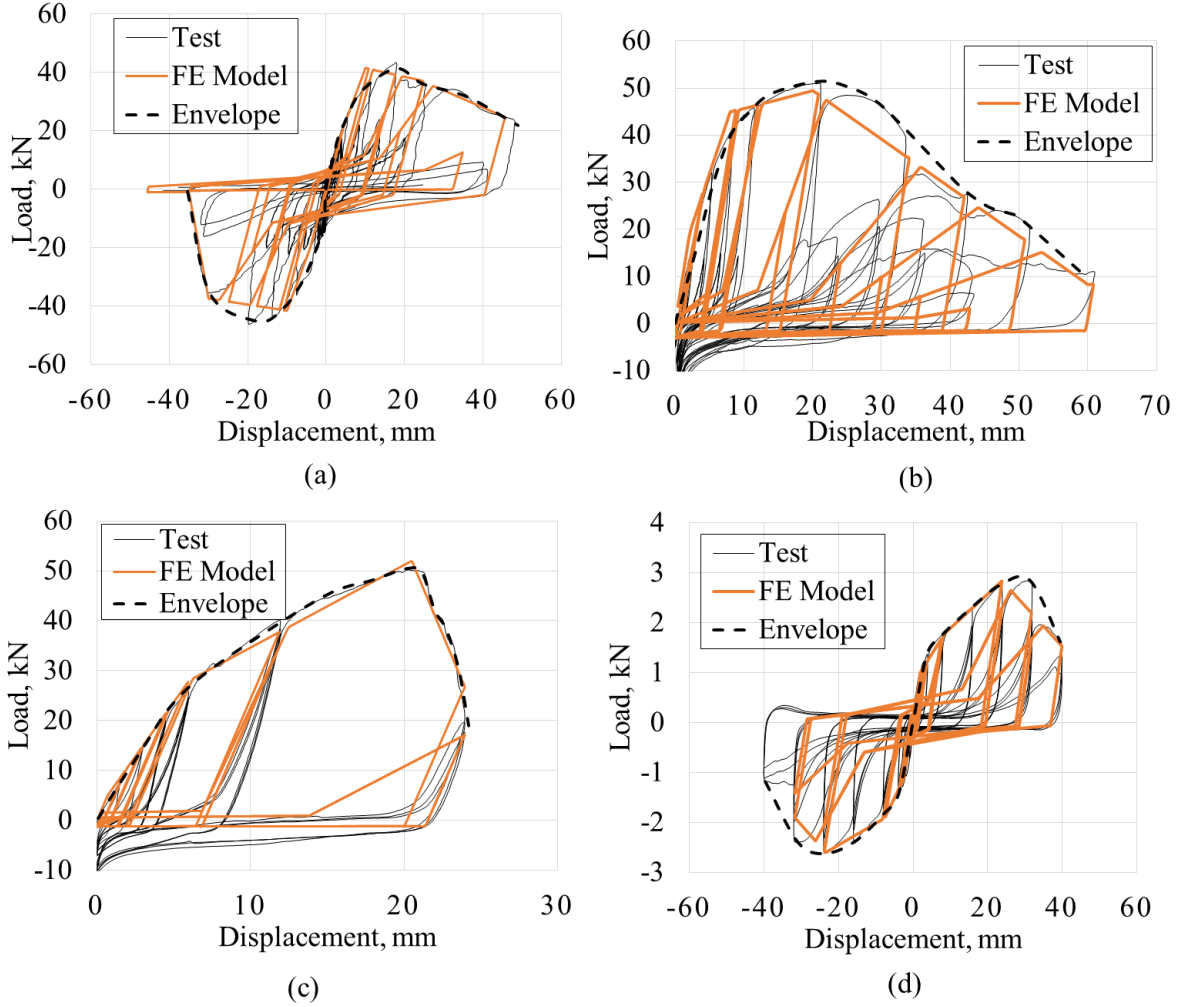


Figure 3.4 CLT Connection's test vs FEA model: (a) bracket B_1 - shear, (b) bracket B_1 - tension, (c) hold-down HD_1 -tension, and (d) STS connector WW_1 -shear (one connector)

All parameters as listed in Table 3.2 were computed based on equivalent energy elastic plastic (EEEP) curves (ASTM E2126 2011). An EEEP curve is a perfectly elastic plastic representation of the actual response of the specimen which encompasses the same area of the actual backbone curve from the origin to the ultimate displacement. Table 3.2 shows that the brackets have similar strength, stiffness and ductility under tension and shear tests; therefore, they can be utilized for designing for both shear and tension resistance.

Table 3.2 CLT Connection's FEA results and estimated parameters from EEEP curve

ID	d_{peak} mm	P_u kN	d_u mm	P_y kN	d_y mm	D -	K_e kN/mm
Tension test							
B ₁	20.0	39.5	29.6	45.4	6.9	4.3	6.6
B ₂	16.0	43.0	27.9	48.0	8.1	3.4	5.9
B ₃	17.6	35.0	23.4	37.3	7.8	3.0	4.8
B ₄	17.9	31.6	22.8	35.2	4.6	5.0	7.7
B ₅	21.8	20.2	23.1	20.2	8.1	2.9	2.5
HD ₁	20.5	40.8	22.0	41.8	8.5	2.6	4.9
Shear Test							
B ₁	10.0	33.7	33.2	38.1	7.7	4.3	5.0
B ₂	23.2	42.1	32.4	50.0	9.4	3.5	5.9
B ₃	24.0	41.6	33.7	43.0	10.7	3.2	4.2
B ₄	23.8	34.6	29.5	37.3	6.9	4.4	5.6
B ₅	30.9	20.9	35.4	23.9	11.2	3.2	2.2
¹ WW ₁	23.5	2.2	31.1	2.2	6.4	4.9	0.4
¹ WW ₂	39.2	1.6	47.9	1.7	9.7	5.0	0.2

Note: ¹calculations are based on single connector/shear plane

The peak loads (P_{peak}) and the energy dissipation capacity (E) from the hysteresis loops are shown in Table 3.3. The differences between FE analyses and tests results were found up to 7% and 12% for peak loads and energy dissipation, respectively. These differences can be considered as acceptable for the validation purposes.

Table 3.3 Comparison of CLT Connection's FEA vs test results

ID	P_{peak} (kN)			E (kN-m)		
	FE	test	% Δ	FE	test	% Δ
Tension test						
B ₁	51.9	51.0	1.8	6.2	6.0	3.3
B ₂	52.1	53.9	3.4	4.4	4.1	7.9
B ₃	44.3	44.3	0.0	2.5	2.7	6.5
B ₄	39.9	42.2	5.5	2.8	2.5	10.8
B ₅	25.8	24.2	6.6	0.9	1.0	1.9
HD ₁	51.9	50.2	3.3	1.3	1.4	8.5
Shear Test						
B ₁	41.5	44.8	7.4	6.5	7.2	10.6
B ₂	53.4	54.8	2.5	8.5	8.3	2.8
B ₃	51.9	50.6	2.7	8.6	8.2	5.5
B ₄	43.3	42.1	2.9	6.6	5.9	11.7
B ₅	26.0	27.8	6.6	4.8	5.2	7.7
¹ WW ₁	2.7	2.7	0.9	0.5	0.5	7.5
¹ WW ₂	2.0	2.0	0.1	0.6	0.5	5.2

Note: ¹calculations are based on single connector/shear plane

3.3 Finite Element Analysis of CLT Shear Walls

3.3.1 Experimental Tests on CLT Shear Walls

Full-scale tests on CLT walls were conducted at FPInnovations, Vancouver, Canada (Popovski et al. 2010). CLT panels were 3-ply with a thickness of 94 mm made of European spruce (Figure 3.1a). Steel brackets and hold-downs connectors with various fasteners (annular ring nails, spiral nails, screws, and timber rivets) were used for the wall-to-foundation connections. The test setup for single and coupled CLT shear wall is shown in Figure 3.5a and Figure 3.5b.

In addition to FPInnovations' tests, the present analysis also utilizes single and coupled CLT shear walls tests from Gavric et al. (2015c). They performed cyclic tests on three different wall configurations: a) single shear walls (panel of 3m x 3m), b) coupled shear walls (two panels of each 1.5m x 3m) with half-lap joint, and c) coupled shear wall (two panels of each 1.5m x 3m) with LVL spline joint. Brackets and hold-downs with annular ring nails were used for wall-to-foundation connections and STSs were used for wall-to-wall vertical shear connections.

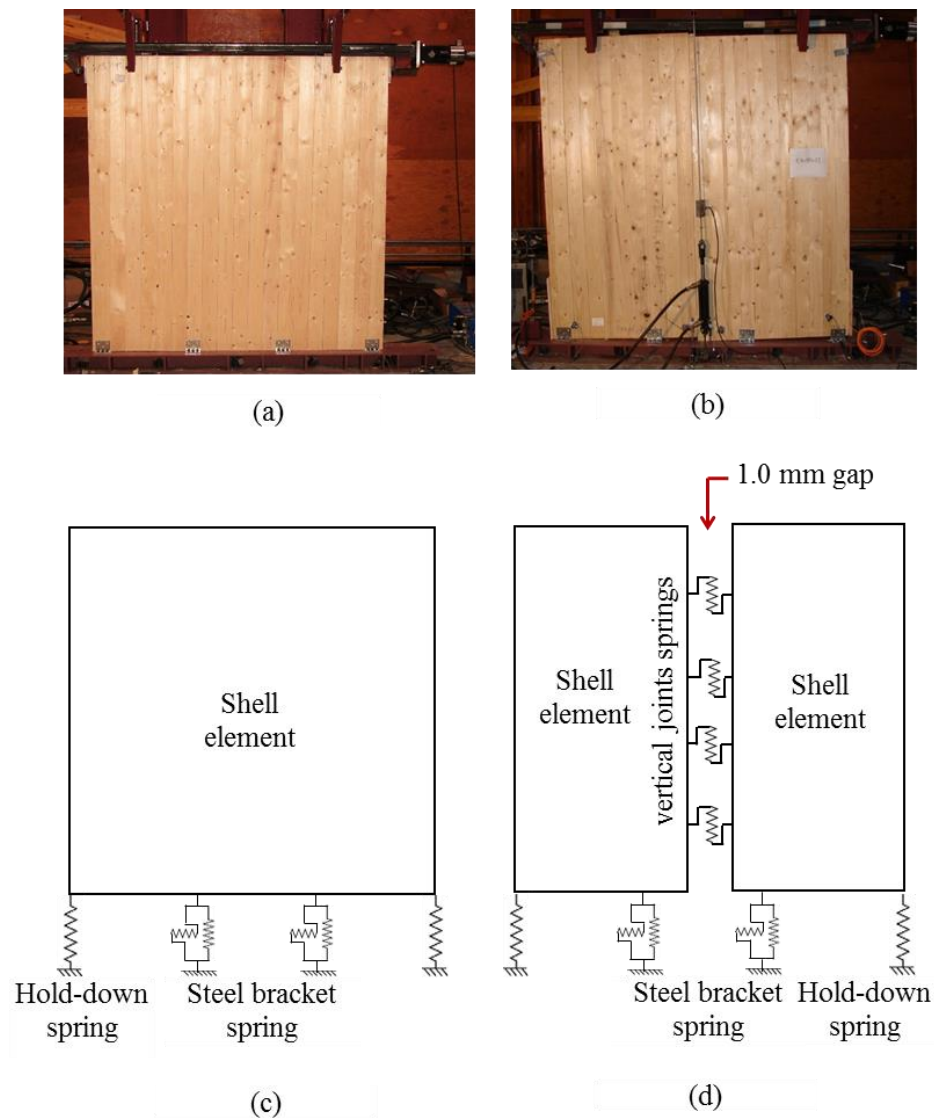


Figure 3.5 CLT shear wall's test setup: (a) single wall and (b) coupled wall; and Schematic of FE models: (c) single wall and (d) coupled wall

3.3.2 Shear Wall Model Formulation

FEA models of CLT single and coupled shear walls were developed in OpenSees (McKenna et al. 2000) (Figure 3.5c and Figure 3.5d). Test results on CLT shear walls showed that CLT panel acted as a rigid body and all the non-linear deformation occurred at connections (Popovski et al. 2010). To represent the actual kinematic behaviour of CLT shear walls, the CLT panels were modelled using plane-stress shell elements with elastic material properties and the metal connectors were modelled using non-linear zero-length springs with “pinching4” hysteresis properties as shown in Figure 3.3.

Both Gavric’s and Schneider’s tests (Gavric et al. 2015a and Schneider et al. 2015) showed that the bracket connections have similar resistance to cyclic shear and tension (Table 3.2), therefore, each bracket connectors in the FEA were modelled with two-orthogonal zero-length springs at the same location calibrated from connection tests as described in the previous section. The orthogonal zero-length springs simulate the sliding and rocking of the shear walls.

In contrast, the hold-downs were modelled using only a single zero-length springs to resist rocking by neglecting their shear resistance as observed in hold-downs tests (Gavric et al. 2015a). In the case of coupled shear walls FEA model (Figure 3.5d), the vertical shear connectors for both half-lap and spline joint were modelled using two-node non-linear spring elements with “pinching4” material model. A small physical gap of 1 mm was kept in between two CLT panel connected by screws in the FEA model which allowed each wall to rock under lateral loading. The calibrated models for connections (brackets, hold-downs and STSs screw connections) were incorporated in the CLT shear wall model.

3.3.3 CLT Walls Model Validation

The FEA models were validated with full-scale CLT shear walls tests (Popovski et al. 2010 and Gavric et al. 2015c), as described in section 3.3.1. As listed in Table 3.4, 8-single CLT shear walls tests from Popovski et al. (2010) and, 2-single and 6-coupled shear wall tests from Gavric et al. (2015c) were used. The hysteresis loops along with their backbone curves indicate a strong agreement between tests and FEA (Figure 3.6). From the backbone curves, the parameters representing the seismic performance of the CLT shear walls (stiffness, strength and ductility) were calculated (Table 3.5). All parameters were computed based on EEEP curves according to ASTM E2126 (2011). As seen in Table 3.6, the average differences between FEA and tests on single CLT walls tests' (Popovski et al. 2010) in the peak loads, peak displacements and energy dissipation capacities were 5%, 10% and 6%, respectively. Similarly, by comparing FEA to tests on coupled CLT walls, the average differences in the peak loads, peak displacements and energy dissipation capacities were found to be 4%, 7% and 11%, respectively. The differences were small and can be considered as acceptable.

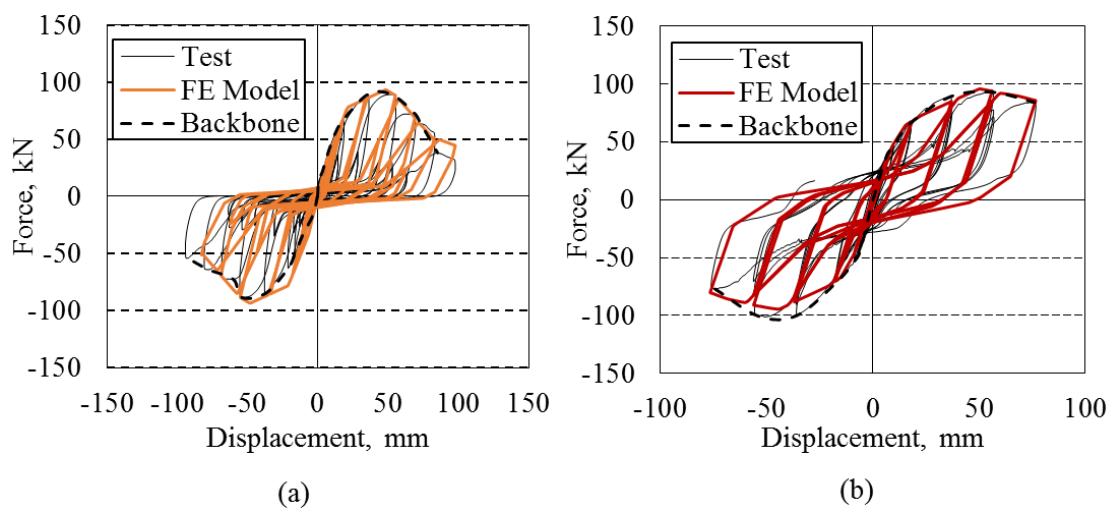


Figure 3.6 CLT shear wall's FEA vs Test: (a) single shear wall-CA-SN-00 (Popovski et al. 2010), (b) coupled shear wall-II.1 (Gavric et al. 2015)

Table 3.4 Experimental data set for single and coupled CLT shear walls

Test Wall ID	No. of brackets (Type)	No. of hold- downs (Type)	No. of screw in vertical joints (Type)	Vertical Load kN/m
Single Shear Wall				
¹ CA-SN-00	4 (B ₁)	-	-	0.0
¹ CA-SN-02	4 (B ₁)	-	-	10.0
¹ CA-SN-03	4 (B ₁)	-	-	20.0
¹ CA-S1-05	4 (B ₂)	-	-	20.0
¹ CA-S2-06	4 (B ₃)	-	-	20.0
¹ CA-RN-04	4 (B ₄)	-	-	20.0
¹ CA-SN-20	7 (B ₁)	-	-	20.0
¹ CA-SNH-08	3 (B ₁)	2 (HD ₂)	-	20.0
² I.1	2 (B ₅)	2 (HD ₁)	-	18.5
² I.2	4 (B ₅)	2 (HD ₁)	-	18.5
Coupled Shear Wall				
² II.1	4 (B ₅)	2 (HD ₁)	20 (WW ₁)	18.5
² II.3	4 (B ₅)	2 (HD ₁)	10 (WW ₁)	18.5
² II.4	4 (B ₅)	4 (HD ₁)	5 (WW ₁)	18.5
² III.1	4 (B ₅)	2 (HD ₁)	2×20 (WW ₂)	18.5
² III.2	4 (B ₅)	2 (HD ₁)	2×10 (WW ₂)	18.5
² III.3	4 (B ₅)	4 (HD ₁)	2×5 (WW ₂)	18.5

Note: ¹Popovski et al. (2010), ²Gavric et al. (2015)

Table 3.5 CLT single and coupled shear walls parameters from EEEP curve

Test Wall ID	P_{peak} kN	d_{peak} kN	E kN-m	P_u kN	d_u mm	P_y kN	d_y mm	D -	K_e kN/mm
Single Shear Wall									
¹ CA-SN-00	93.3	48.3	26.4	73.2	66.3	82.3	19.0	3.5	4.4
¹ CA-SN-02	96.4	40.2	28.8	74.9	68.9	83.8	17.8	3.9	4.7
¹ CA-SN-03	99.6	46.2	29.9	78.9	80.0	87.3	17.8	4.5	4.9
¹ CA-S1-05	97.8	31.8	25.6	79.7	61.4	90.7	18.6	3.3	4.9
¹ CA-S2-06	92.9	34.8	25.0	76.4	63.7	87.9	19.2	3.3	4.6
¹ CA-RN-04	99.3	35.7	25.6	79.6	56.4	88.9	16.6	3.4	5.4
¹ CA-SN-20	153.9	47.4	44.3	124.9	82.2	140.8	19.4	4.2	7.2
¹ CA-SNH-08	126.2	49.8	36.4	99.5	54.6	103.4	14.3	3.9	7.3
² I.1	75.0	34.7	12.6	59.7	37.4	62.0	12.6	3.0	5.0
² I.2	106.7	51.5	21.9	86.2	56.6	94.6	16.2	3.5	5.9
Coupled Shear Wall									
² II.1	95.1	47.9	30.0	74.9	79.9	83.4	15.7	5.1	5.3
² II.3	84.1	50.5	26.9	66.2	83.4	74.3	14.9	5.6	5.0
² II.4	100.8	57.8	21.1	80.1	79.3	88.7	21.3	3.7	4.2
² III.1	94.6	70.0	30.8	75.4	83.1	85.2	18.5	4.5	4.6
² III.2	88.2	68.6	27.3	68.6	82.5	75.2	19.5	4.3	3.9
² III.3	101.7	56.1	21.1	81.0	80.9	90.1	22.3	3.6	4.0

Note: ¹Popovski et al. (2010), ²Gavric et al. (2015)

Table 3.6 Comparison of CLT shear walls FEA vs test results

Test Wall ID	P_{peak} (kN)			d_{peak} (mm)			E (kN-m)		
	FE	test	% Δ	FE	test	% Δ	FE	test	% Δ
Single Shear Wall									
¹ CA-SN-00	93.3	88.9	5.0	48.3	44.9	7.6	26.4	27.8	5.1
¹ CA-SN-02	96.4	90.3	6.8	40.2	41.7	3.6	28.8	30.5	5.8
¹ CA-SN-03	99.6	98.1	1.5	46.2	44.1	4.8	29.9	31.0	3.5
¹ CA-S1-05	97.8	102.7	4.8	31.8	35.3	9.9	25.6	28.1	8.9
¹ CA-S2-06	92.9	100.1	7.2	34.8	42.2	17.5	25.0	26.9	7.1
¹ CA-RN-04	99.3	102.3	2.9	35.7	39.2	8.9	25.6	26.8	4.8
¹ CA-SN-20	153.9	152.1	1.2	47.4	40.9	15.9	44.3	45.5	2.7
¹ CA-SNH-08	126.2	118.2	6.8	49.8	53.1	6.3	36.4	37.7	3.3
² I.1	75.0	70.7	6.1	34.7	38.7	10.5	12.6	13.1	4.4
² I.2	106.7	104.2	2.4	51.5	57.3	10.2	21.9	24.1	9.1
Coupled Shear Wall									
² II.1	95.1	97.2	2.2	47.9	53.4	10.4	30.0	32.0	6.3
² II.3	84.1	84.4	0.4	50.5	46.6	8.3	26.9	28.4	5.1
² II.4	100.8	93.1	8.3	57.8	53.8	7.3	21.1	24.5	13.7
² III.1	94.6	102.5	7.7	70.0	66.0	6.0	30.8	33.1	6.7
² III.2	88.2	91.8	3.9	68.6	65.4	5.0	27.3	25.5	7.0
² III.3	101.7	102.9	1.1	56.1	54.3	3.3	21.1	28.0	24.6

Note: ¹Popovski et al. (2010), ²Gavric et al. (2015)

3.4 Parametric Study for Single and Coupled CLT Walls

3.4.1 Single CLT Shear Walls

A parametric study was performed on single CLT shear walls with variation in the number and types of brackets and hold-downs used. Two types of shear walls were considered: Case A - CLT shear wall with brackets only; and Case B - CLT shear walls with brackets and hold-downs.

The CLT panels were 2.3 m×2.3 m with 3-ply of 94 mm thick. The shear walls with brackets were analyzed with five different types of fasteners (B_1 to B_5 , see Table 3.1). The number of brackets were varied from 4 to 7. Where walls were connected by brackets and hold-downs (Case B), two types of hold-downs (HD_1 or HD_2) were considered at the end of wall-to-floor interfaces. The number of brackets was varied from 2 to 5; therefore, the total number of connectors remained the same as in Case A type walls. The shear walls were analyzed under CUREE loading protocol and the parameters of the shear wall, i.e. stiffness, strength, ductility and energy dissipation capacity, were calculated from EEEP curves. All individual EEEP are presented in Appendix A.

The change in single CLT shear wall's performance is shown in Figure 3.7. The capacity, stiffness and energy dissipation increases with an increase in the number of connectors. By increasing the connectors from 4 to 7, the average capacity, stiffness and energy dissipation in single shear walls with brackets increased by 57%, 39%, and 30%, respectively (Figure 3.7a, Figure 3.7b and Figure 3.7d). Similarly, the average capacity, stiffness and energy dissipation increase in the shear walls with brackets and hold-downs was 53%, 33%, and 39%, respectively (Figure 3.7e, Figure 3.7f and Figure 3.7h). However, the change in ductility with the increase in the number of connectors was found to be insignificant, although the overall trend was a negative one (Figure 3.7c and Figure 3.7g). The average ductility of the single shear walls was found to be 3.9.

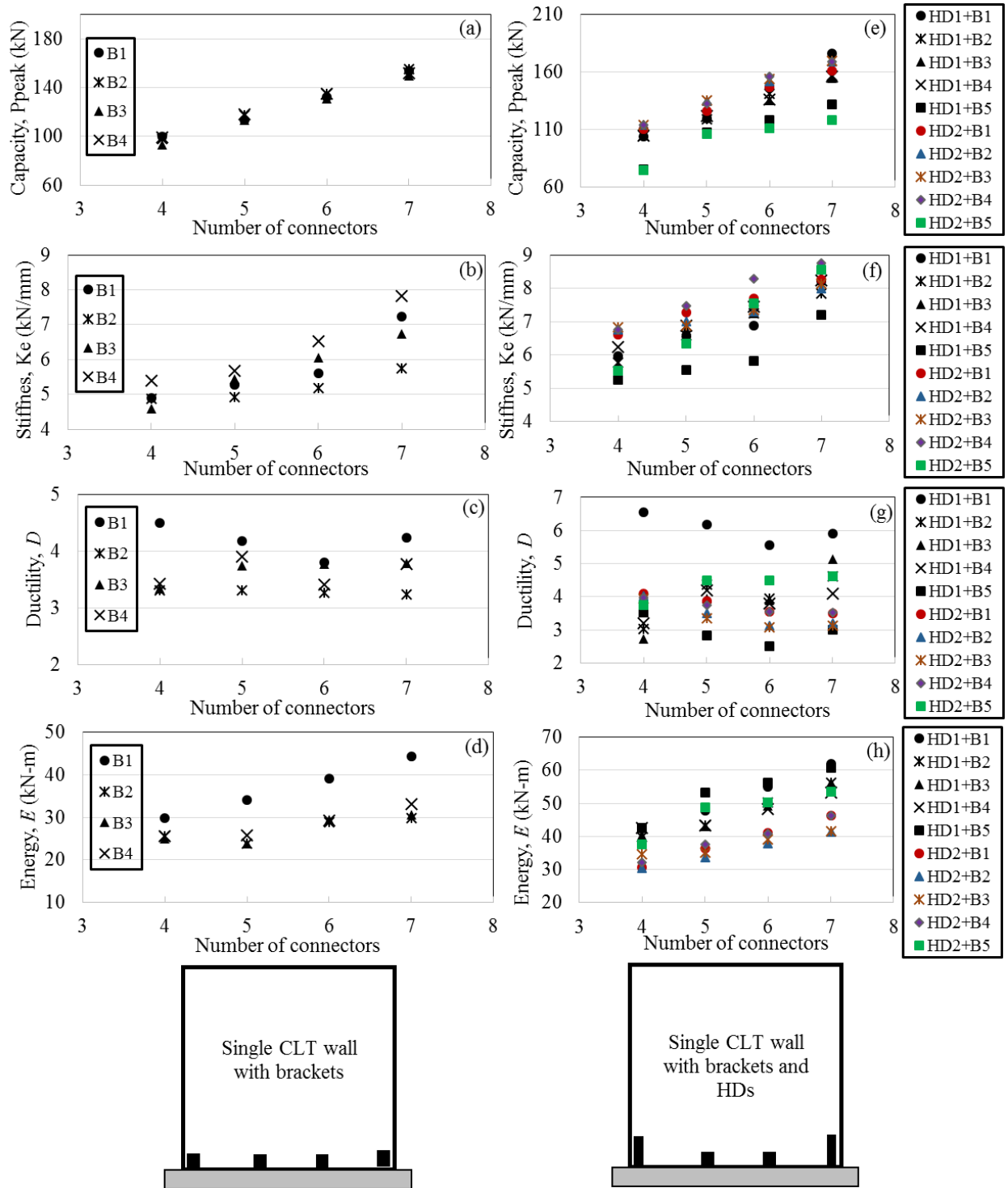


Figure 3.7 Single walls with brackets: (a) capacity, (b) stiffness, (c) ductility, and (d) energy; Single walls with brackets and HDs: (e) capacity, (f) stiffness, (g) ductility, and (h) energy

3.4.2 Coupled CLT Shear Walls

A similar parametric study was performed on coupled CLT shear walls with variation in the number and types of brackets (B_1 to B_5), hold-downs (HD_1 to HD_2) and vertical joints (WW_1 to WW_2). The FEA was conducted on 3-ply CLT panels of 94 mm thick. Two $1.15 \text{ m} \times 2.3 \text{ m}$ panels (total wall size same as single wall: $2.3 \text{ m} \times 2.3 \text{ m}$) were connected by vertical joints as shown in Figure 3.1b and Figure 3.1c. Two types of coupled shear walls were considered in the parametric study: Case C - CLT coupled shear wall with 2 hold-downs (2HDs) at the outer edges of each panel; and Case D - CLT coupled shear walls with 4 hold-downs (4HDs) both at the outer and inner edges of each panel. Each wall had a total of 4 brackets (2 on each side of the panel) connected with half-lap joints (WW_1 : 20 screws in one row) or spline joints (WW_2 : 20 screws in two rows: 2×10). The shear walls were analyzed under CUREE loading protocol. The parameters of the shear wall's stiffness, strength, ductility and energy dissipation capacity were calculated from EEEP curves (Appendix B).

A comparison of coupled CLT shear wall's capacity, stiffness, ductility and energy dissipation utilizing the variation in types of brackets, hold-downs and shear connectors is plotted in Figure 3.8. The average capacity, stiffness, ductility and energy dissipation in the coupled shear walls with half-lap joints was found to be higher 16%, 32%, 10%, and 18%, respectively, when compared to walls with spline joints (Figure 3.8a, Figure 3.8b and Figure 3.8d). Furthermore, the coupled shear walls with 4-HDs showed higher capacity, stiffness and energy dissipation -i.e. 43%, 25%, and 14% higher, respectively, when compared to the coupled shear walls with 2-HDs (Figure 3.8e, Figure 3.8f and Figure 3.8h). By contrast, the ductility decreases with an increase in the number of HDs by 20%. However, the average ductility of the coupled shear walls found to be 5.1, some 31% higher than the single CLT shear walls' average of 3.9.

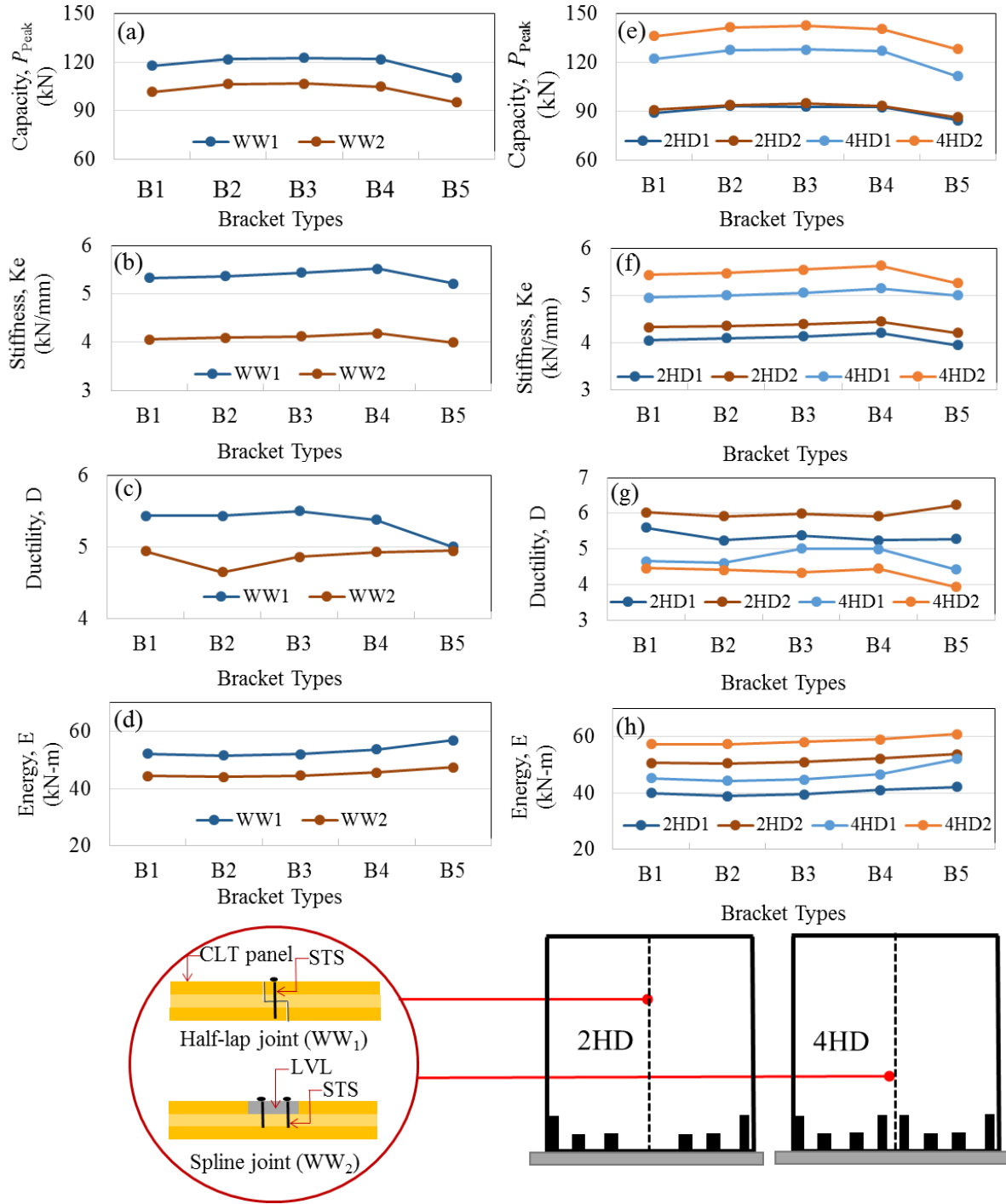


Figure 3.8 Coupled CLT shear walls with half-lap vs spline joints: (a) capacity, (b) stiffness, (c) ductility, and (d) energy; coupled CLT shear walls with 2-HDs vs 4-HDs: (e) capacity, (f) stiffness, (g) ductility, and (h) energy

3.5 Summary

The present study evaluated the behaviour of single and coupled CLT shear walls under lateral loading. FEA models of CLT connections were developed using nonlinear springs which were calibrated against test results. The calibrated Pinching4 model of the connections was utilized to model full-scale single and coupled CLT shear walls under reversed cyclic loading. The FEA models of the CLT shear walls were compared to and verified against test results on single and coupled shear walls. A parametric study was conducted with variation in the number and type of connectors. The capacity, stiffness, ductility and energy dissipation for both single and coupled CLT shear walls were calculated. The investigations allow drawing the following conclusions:

- The FEA models accurately predicted the hysteresis behaviour of CLT connectors, e.g. brackets, hold-downs and shear screws.
- The FEA models of CLT shear walls closely predicted the load-deformation curves and the energy dissipation capacities of the shear walls when compared to test results.
- It has been observed that the strength, stiffness and energy dissipation of the single and coupled CLT shear walls increases with the increase in the number of connectors.
- Ductility in the coupled shear walls was found to be 31% higher than in single shear walls. The decrease in ductility with an increase in the number of connectors was not significant.
- Single shear walls with hold-downs and brackets performed better under seismic loading compared to walls with brackets only (23% higher stiffness, 49% more energy dissipation).
- Coupled shear walls with 4-HDs performed better compared to coupled shear walls with 2-HDs -e.g. 43%, 25%, and 14% higher capacity, stiffness and energy dissipation observed.
- Coupled shear walls with half-lap performed better under seismic loading compared to walls with spline joints.

Chapter 4: Deflection of Cross-Laminated Timber Shear Walls⁴

4.1 Introduction

Accurate quantification of the deflection of CLT shear walls is required to design CLT buildings for the serviceability limit state. The 2016 supplement to the Canadian Standard for Engineering Design in Wood CSAO86 (2016) provides provisions for CLT structures used in platform-type applications. The standard, however, does not provide guidance to estimate the deflection of CLT shear walls. The present study proposes a simple linear model to estimate the total in-plane deflection of CLT shear walls that experience sliding or rocking or a combination of sliding and rocking under consideration of the influence of perpendicular walls and floors on top.

CLT shear walls in a platform-type of construction consist of two parts: connections and CLT panels (Figure 4.1). The CLT shear walls, both single and coupled walls are connected to foundations or podium and to the floors in the upper storeys by steel brackets and hold-downs using metal fasteners such as screws and nails. The individual wall panels are most often connected by screws using either lap or spline joints. In order to account for the total lateral deflection at the top of the wall the contributions from the connections and the CLT panels need to be considered.

⁴ A version of this chapter has been submitted for publication in the World Conference on Timber Engineering, Seoul, Republic of Korea.

Shahnewaz, M., Tannert, T., Alam, M. S. & Popovski, M. Deflection of Cross Laminated Timber Shear Walls in Platform Construction. *World Conference on Timber Engineering*, WCTE 2018, 20-23rd August, Seoul, Republic of Korea (Submitted).

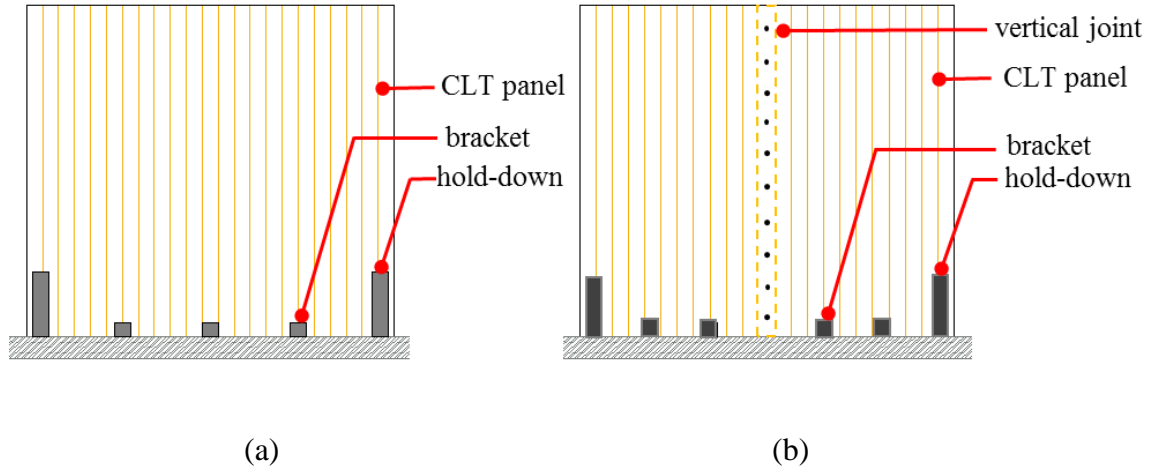


Figure 4.1 Components of (a) single and (b) coupled CLT shear wall

To date, a limited number of studies have reported on the deflection of CLT shear walls under lateral loading. Gavric et al. (2015) proposed models to estimate the total wall displacement δ_{tot} based on its kinematic behaviour, as a summation of deflection due to slip (δ_s), rocking (δ_r), bending (δ_b), and shear (δ_{sh}). They considered five different models that accounted for the force-deflection relation of CLT shear walls. Each model considered different combinations of the brackets' and hold-downs' resistance where they resist shear and/or tension forces. In the model, the lateral load on top of the wall is increased in increments from where the increment of deflection can be calculated in each load step. This iterative procedure requires much computational effort and seems impractical for design engineers. Furthermore, the influence from the perpendicular walls and the floors above on the in-plane deflection of CLT shear walls was not accounted for by Gavric et al. (2015).

4.2 Single and Coupled Shear Walls and their Connections

A fictitious floor plan of a shear wall building is shown in Figure 4.2. The CLT shear walls, labeled A and B are single and coupled shear walls, respectively. The walls A and B are not connected to

any wall, i.e. they do not have influence of perpendicular walls. Whereas, single walls labeled C and coupled walls labeled D, are influenced by perpendicular walls when they are loaded in-plane laterally in the direction of the global Y-axis.

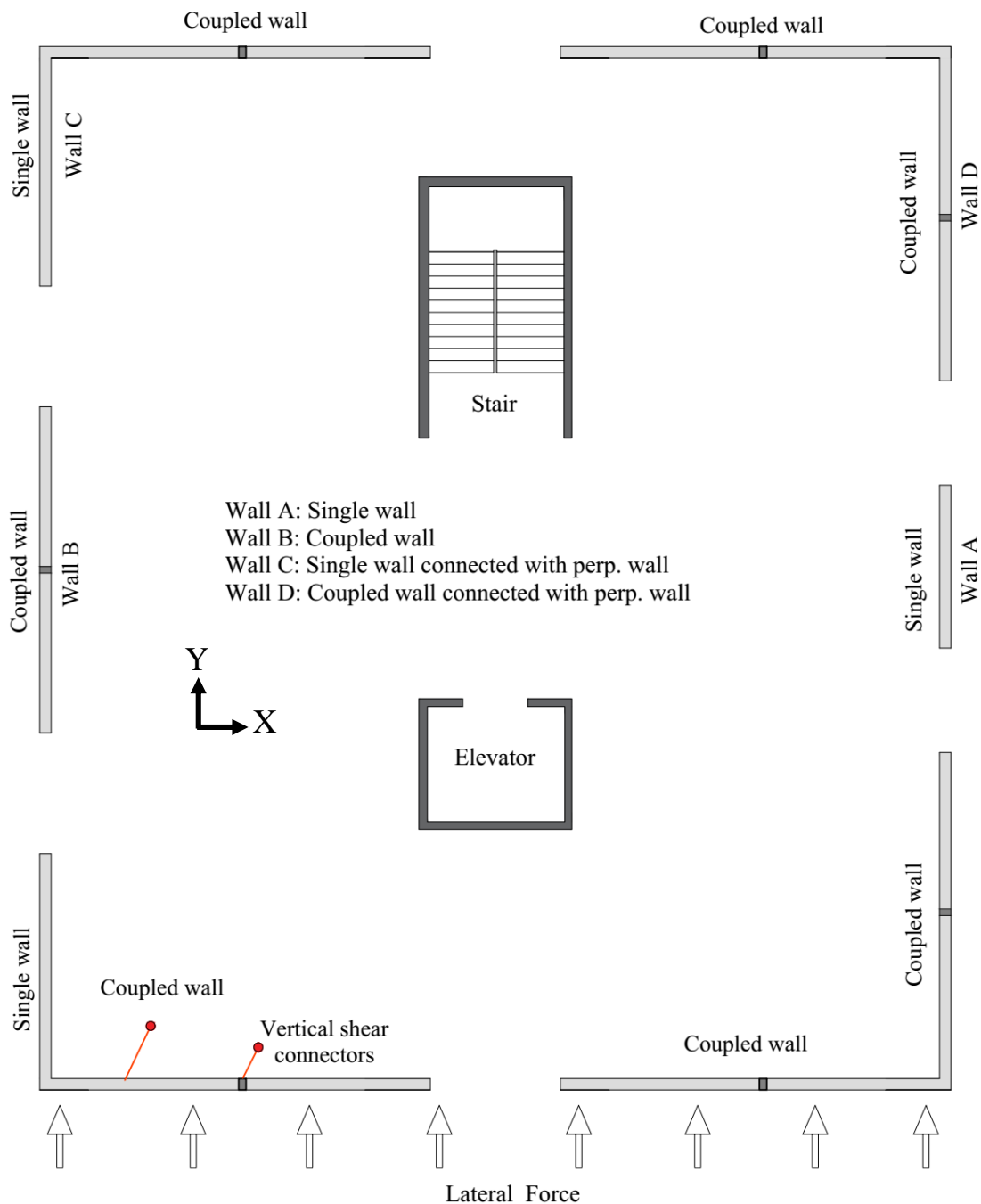


Figure 4.2 CLT shear walls in a typical floor plan

Typical connection details between CLT shear walls to perpendicular walls are shown in Figure 4.3. The perpendicular walls are usually connected to the in-plane CLT shear walls using STSs (Figure 4.3a and Figure 4.3c) or brackets (Figure 4.3b and d). Two types of wall configurations between in-plane walls and perpendicular walls are possible. In configuration 1, the in-plane shear wall's movement due to sliding and rocking is prevented by the STSs and screws in the brackets along with the frictional resistance of the perpendicular walls (Figure 4.3a and Figure 4.3b). Whereas in configuration 2, the perpendicular wall panel itself prevents the in-plane deflection (Figure 4.3c and Figure 4.3d).

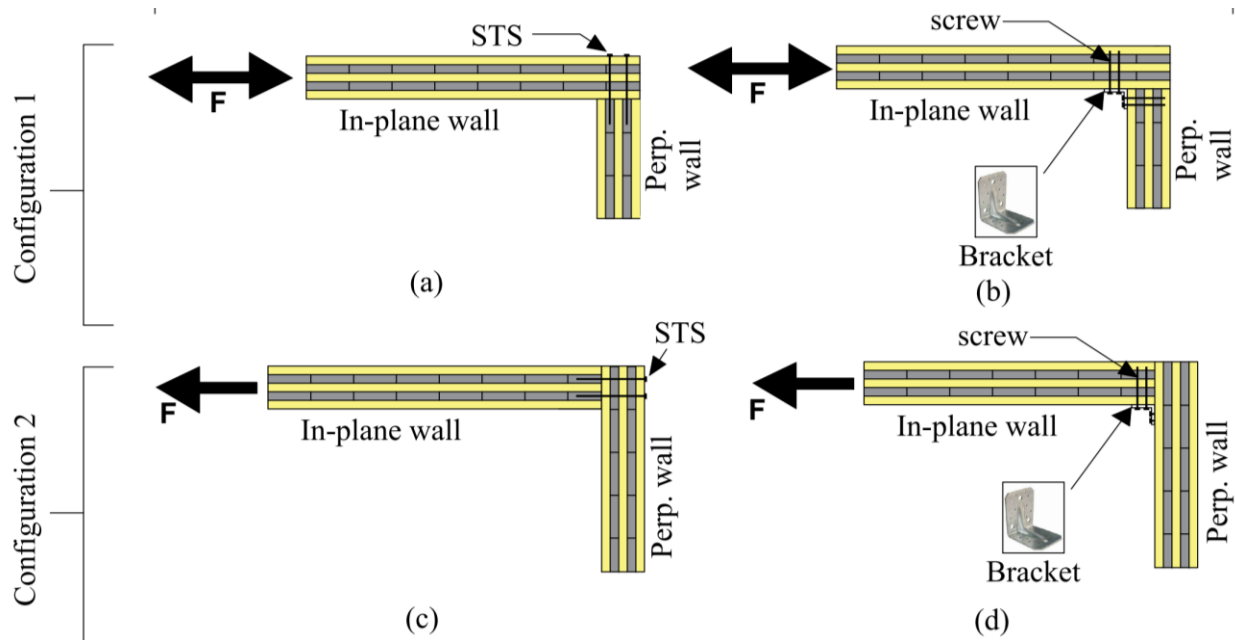


Figure 4.3 Top view of in-plane connections to perpendicular walls: Configuration 1 (a) STSs connection, (b) bracket; Configuration 2 by (c) STSs connection, (d) bracket

As seen in configuration 1, the kinematic behaviour of the in-plane wall will be the same irrespective of the loading directions (Figure 4.3a and Figure 4.3b). By contrast, the kinematic behaviour of the in-plane wall in configuration 2 is quite different and depends on the loading

directions. Both the sliding and rocking deflection of the in-plane shear wall in configuration 2 are completely prevented by the perpendicular wall when the in-plane wall is loaded laterally towards the right direction. However, when the in-plane wall is loaded toward the left direction, as seen in Figure 4.3c and Figure 4.3d, it pulls the perpendicular wall during any rocking and/or sliding movement. The brackets at the bottom in between perpendicular wall to floor underneath will be activated and that will prevent the in-plane deflection of the shear wall.

Apart from the perpendicular walls, the floors above also contribute to the total deflection of the in-plane shear wall. The deflections of CLT shear walls are also influenced by the floor above, shown in the isometric view in Figure 4.4.

Similarly, the in-plane shear wall usually connected by STSs or by brackets (Figure 4.5a and Figure 4.5b) with the floor above. Therefore, the connections are influencing the lateral in-plane deflection of CLT shear walls along with the frictional resistance of the floors.

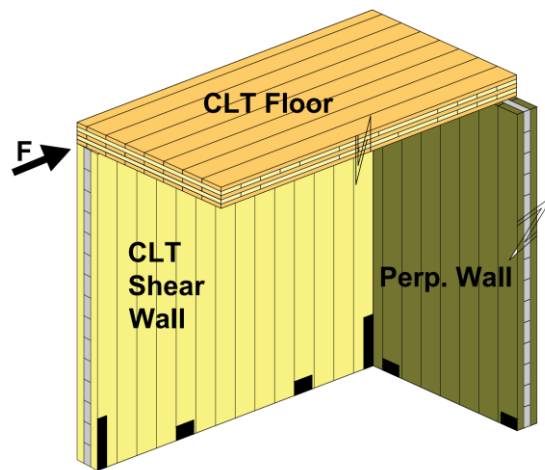


Figure 4.4 Influence of perpendicular wall and floor on CLT shear wall's deflection

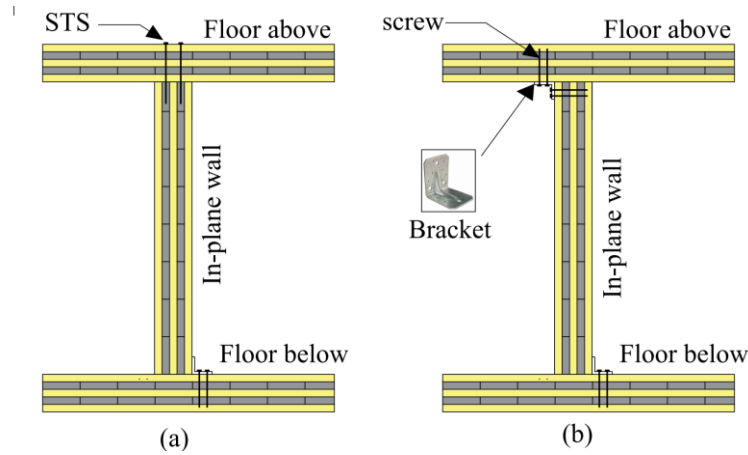


Figure 4.5 Cross section of in-plane connections floor to in-plane walls: (a) STSs connection and (b) bracket connection

The following assumptions were made to account for the impact of perpendicular wall and the floor above on the deflection of CLT shear walls:

- Only the connections between CLT wall to the floor panel above and to the perpendicular wall are considered. The connections between perpendicular wall-to-floors below and above are ignored, except in the case in configuration 2 (Figure 4.3c and Figure 4.3d) when the connections between perpendicular wall-to-floor below directly influence the kinematic behaviour of the shear wall. These connections will remain elastic.
- The perpendicular walls and the floor above influence sliding and rocking of the in-plane wall. However, their influence on CLT panel's bending and shear deformations is assumed to be small and negligible.
- The frictional resistance generates at the interface between CLT shear wall-to-floor below due to gravity loading is included in this study.
- The friction at the interfaces between CLT shear wall to perpendicular wall and floor above is not considered in this study.

4.3 Deflection of Single CLT Shear Walls without Perpendicular Walls

The total deflection of a CLT single shear wall δ can be calculated as the summation of deflection due to panel bending (δ_b) and shear (δ_s) and wall sliding (δ_{sl}) and rocking (δ_r):

$$\delta = \delta_b + \delta_s + \delta_{sl} + \delta_r \quad (4.1)$$

Figure 4.6 illustrated these four components. The procedure to estimate each part of the deflection components are discussed in the following sections.

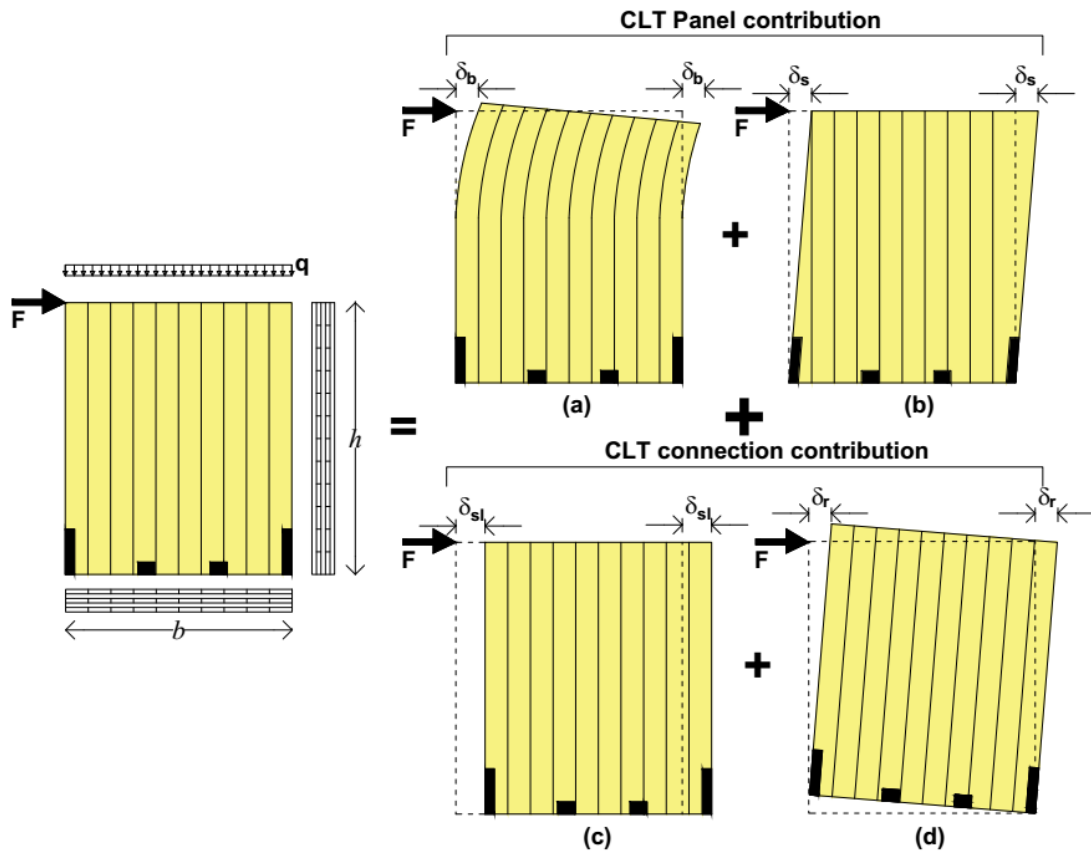


Figure 4.6 The deflection calculation of the CLT shear wall under lateral loading

4.3.1 Bending Deflection

Previous experimental and analytical investigations showed that the CLT panels have high in-plane stiffness and remain elastic under in-plane loading (Ceccotti et al. 2006, Popovski et al. 2010, Shahnewaz et al. 2016a, Shahnewaz et al. 2016b). Therefore, under lateral loading the elastic bending deflection, δ_b (as shown in Figure 4.7) of the CLT panel can be calculated as:

$$\delta_b = \frac{Fh^3}{3EI_{eff}} \quad (4.2)$$

where F is the lateral force on the wall, h is the height of the wall, and EI_{eff} is the effective bending stiffness of the CLT panel.

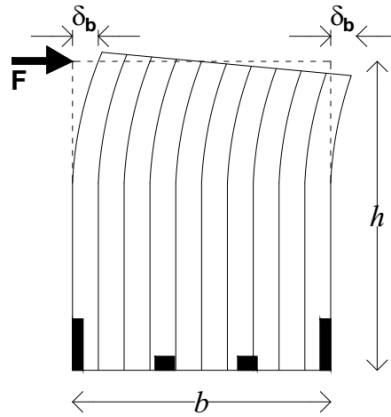


Figure 4.7 Deflection due to bending of CLT panel

According to Blass and Fellmoser (2004), the effective bending stiffness for a CLT panel loaded in-plane can be calculated as:

$$(EI)_{eff} = k_4 (E_0 I) \quad (4.3)$$

where the constant, k_4 can be calculated using Eq. (4.4).

$$k_4 = \frac{E_{90}}{E_0} + \left(1 - \frac{E_{90}}{E_0}\right) \frac{a_{m-2} - a_{m-4} + \dots \pm a_1}{a_m} \quad (4.4)$$

where E_o and E_{90} are the modulus of elasticity in parallel and perpendicular to grain directions, a_m is the total thickness of the CLT panel. The parameters, a_1 to a_m are described in Figure 4.8.

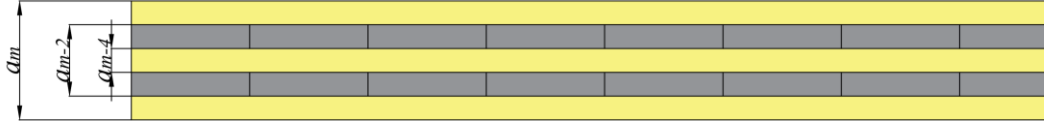


Figure 4.8 Cross section of m -ply CLT panel

4.3.2 Shear Deflection

The deflection of the CLT panels due to shear can be evaluated as shown in Figure 4.9 and calculated as:

$$\delta_s = \frac{Fh}{G_{CLT} t_{CLT} b} \quad (4.5)$$

where F is the lateral force on the wall, h is the height of the wall, b is the width of the wall, G_{CLT} is the shear modulus of CLT panel and t_{CLT} is the total thickness of CLT panel.

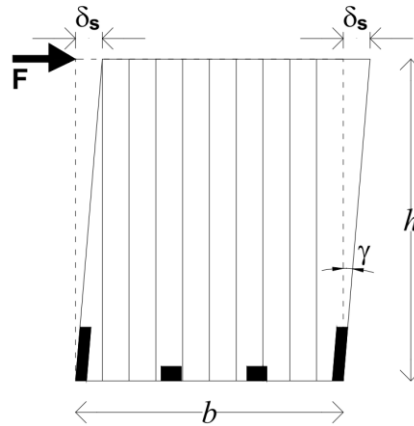


Figure 4.9 Deflection due to shear deformation of CLT panel

The shear modulus of the CLT panel, G_{CLT} is also referred to as equivalent shear modulus of the CLT panel and is measured parallel to the grain of outer lamella. The shear modulus of the CLT panel can be estimated using Eqs. (4.6) and (4.7):

$$\frac{G^*}{G} = \frac{1}{1 + 3(G / G_{\text{eff}})(t_i / a)^2} \quad (4.6)$$

$$\frac{G^*}{G} = \left(1 + (u / a) \left(1 + 2(G / G_Q) \right) + 2(G / E)(u / a)^3 + 3(G / G_{\text{eff}})(1 + u / a)^2 (t_i / a)^2 \right)^{-1} \quad (4.7)$$

where $G_{\text{eff}} = (G_{\perp} + G_{\parallel}) / 2$, is the effective shear modulus, G_{\perp} is the shear moduli perpendicular to the grain, G_{\parallel} or G is the shear moduli parallel to the grain, G^* is the equivalent shear modulus, G_Q is the transverse shear modulus, t_i/a is the board thickness-to-width ratio and u/a is the board-spacing to board-width ratio.

4.3.3 Sliding Deflection

Hold-downs and angle brackets (Figure 4.10) provide sliding resistance to CLT shear walls. Gravity loading also contributes to the sliding resistance through friction.

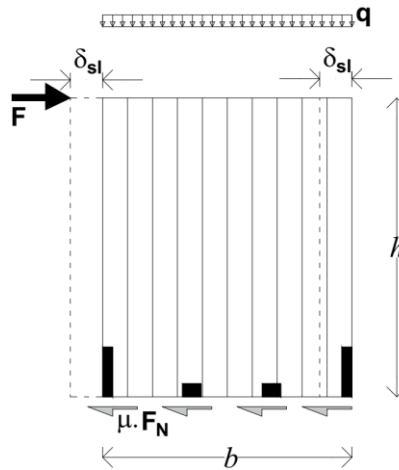


Figure 4.10 deflection due to sliding of CLT shear wall

The sliding deflection of the CLT shear wall can be estimated as:

$$\delta_{sl} = \frac{F'}{n_B k_B} = \frac{F - \mu F_N}{n_B k_B} = \frac{F - \mu(qb)}{n_B k_B} \quad (4.8)$$

where F' is the resultant force on shear walls, i.e. the difference between the lateral force F and the frictional force (μF_N) between CLT panel and floor or foundation, q is the vertical load (herein assumed as a uniformly distributed load) on the shear wall, b is the width of the wall, n_B is the number of brackets and k_B is the stiffness of the bracket connections. Under certain loading conditions, there is no guarantee that the friction will act; therefore, it should be ignored and Eq. (4.8) can be simplified to:

$$\delta_{sl} = \frac{F}{n_B k_B} \quad (4.9)$$

4.3.4 Rocking Deflection

The rocking or overturning of the CLT shear wall is resisted by the corner connectors, i.e. hold-downs, as shown in Figure 4.11.

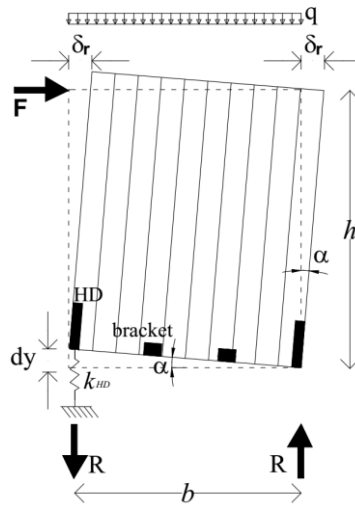


Figure 4.11 Deflection due to rocking of CLT shear wall

The reaction force of the corner connectors, R , can be calculated from the equilibrium of the forces:

$$R = \frac{1}{b} \left(F h - \frac{q b^2}{2} \right) \quad (4.10)$$

where q is the vertical force on shear walls, b is the length of the wall.

The rotation of the shear wall due to lateral force can be calculated as:

$$\tan \alpha \approx \alpha = \frac{dy}{b} = \frac{\delta_r}{h} \quad (4.11)$$

where α is the rotation of the CLT shear wall and dy is the vertical deformation of the corner connection which can be calculated as the ratio of reaction force and connection stiffness as:

$$dy = \frac{R}{k_{HD}} \quad (4.12)$$

where k_{HD} is the stiffness of the hold-down.

Replacing Eqs. (4.10) and (4.11) into Eq. (4.12), the deflection due to rocking can be calculated as:

$$\delta_r = \left(\frac{F h^2}{b^2} - \frac{qh}{2} \right) \frac{1}{k_{HD}} \quad (4.13)$$

4.3.5 Total Deflection of Single CLT Shear Wall without perpendicular walls

The total deflection of the CLT shear walls can be estimated by adding the deflections due to bending, shear, sliding and rocking of the shear wall. Therefore, by substituting Eqs. (4.2), (4.5), (4.9), and (4.13) into Eq. (4.1), the total deflection of the single CLT shear wall can be estimated as:

$$\delta = \frac{Fh^3}{3EI_{eff}} + \frac{Fh}{G_{CLT}t_{CLT}b} + \frac{F}{n_Bk_B} + \left(\frac{Fh^2}{b^2} - \frac{qh}{2} \right) \frac{1}{k_{HD}} \quad (4.14)$$

4.4 Deflection of Single CLT Shear Walls with Perp. Walls and Floors above

In a platform-type of building, the CLT shear walls are connected to perpendicular walls and to the floors above which influence the total deflection under lateral loading. Two types of configuration are possible in case of an in-plane wall to perpendicular wall connection (Figure 4.4). The deflection equations for the two configurations are discussed in the following.

4.4.1 Perpendicular Wall Configuration 1

4.4.1.1 *Rocking Deflection*

The kinematic behaviour of the CLT shear wall due to a lateral force F in case of perpendicular wall configuration 1 is shown in Figure 4.12.

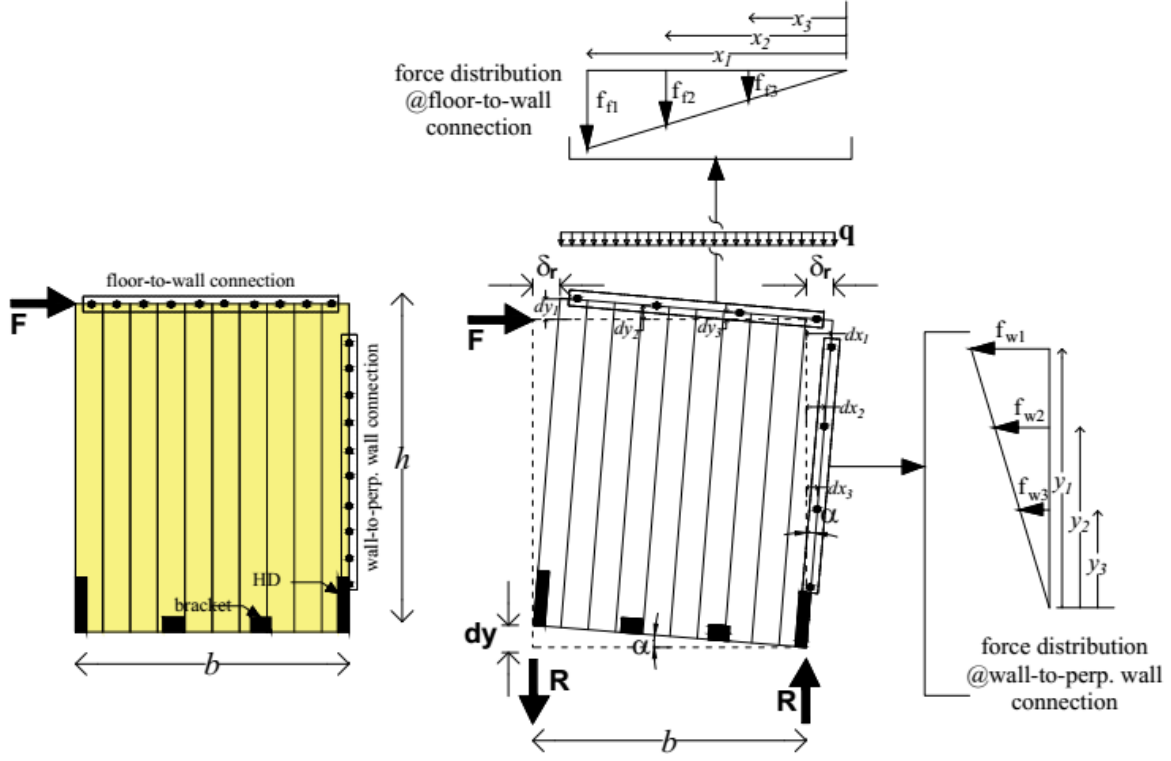


Figure 4.12 Force distribution due to CLT wall's rocking in presence of perpendicular wall and floor above

It is assumed that the connections between wall to the perpendicular wall and to the floor above will remain elastic. Therefore, the reaction forces will follow a triangular distribution. The overturning force is resisted by: i) the hold-downs; ii) the connections between the wall-to-perpendicular wall; and iii) the connections to the floor above. The reaction force of the corner connectors, R , can be calculated by taking the summation of the moment at the lower right corner:

$$Rb + \sum_{i=1}^{n_f} x_i f_{fi} + \sum_{i=1}^{n_w} y_i f_{wi} - Fh + \frac{qb^2}{2} = 0 \quad (4.15)$$

$$R = \frac{1}{b} \left[Fh - \frac{qb^2}{2} \right] - \frac{1}{b} \left[\sum_{i=1}^{n_f} x_i f_{fi} + \sum_{i=1}^{n_w} y_i f_{wi} \right] \quad (4.16)$$

where q is the vertical force on shear walls, b is the length of the wall, h is the height of the wall, f_{fi} and f_{wi} are the reaction forces of wall-to-floor and wall-to-perpendicular wall connections, respectively, x_{fi} and y_{wi} are the distance of the wall-to-floor and wall-to-perpendicular wall connectors from lower right corner of the wall, respectively, and n_f and n_w are the total number of wall-to-floor and wall-to-perpendicular wall connections, respectively.

The rotation of the shear walls due to lateral force can be calculated as:

$$\tan \alpha \simeq \alpha = \frac{dy}{b} = \frac{\delta_r}{h} \quad (4.17)$$

where α is the rotation of the CLT shear wall and dy is the vertical deformation of the corner connection which can be calculated as the ratio of reaction force and connection stiffness as:

$$dy = \frac{R}{k_{HD}} \quad (4.18)$$

where k_{HD} is the stiffness of the hold-down.

Substituting Eqs. (4.16) and (4.17) into Eq. (4.18), the modified deflection due to rocking is:

$$\delta_r = \left(\frac{F \cdot h^2}{b^2} - \frac{qh}{2} \right) \frac{1}{k_{HD}} - \frac{h}{b^2} \left(\sum_{i=1}^{n_f} x_i f_{fi} + \sum_{i=1}^{n_w} y_i f_{wi} \right) \frac{1}{k_{HD}} \quad (4.19)$$

Now, the reaction forces of the wall-to-floor connectors, f_{fi} can be calculated as:

$$f_{fi} = k_{fi} dy_i \quad (4.20)$$

where k_{fi} is the stiffness of the i^{th} wall-to-floor connectors and dy_i is the vertical deformation of the i^{th} wall-to-floor connectors (Figure 4.12). Using similar triangle formula, dy_i can be calculated:

$$dy_i = \frac{dy}{b} x_i \quad (4.21)$$

By substituting Eq. (4.17) into Eq. (4.21):

$$dy_i = \frac{\delta_r}{h} x_i \quad (4.22)$$

The reaction forces of the wall-to-floor connectors, f_{fi} can be rewritten using Eq. (4.22) as:

$$f_{fi} = k_{fi} \left(\frac{\delta_r}{h} x_i \right) \quad (4.23)$$

Similarly, the reaction forces of the wall-to-perpendicular wall connectors, f_{wi} can be expressed as:

$$f_{wi} = k_{wi} \left(\frac{\delta_r}{h} y_i \right) \quad (4.24)$$

where k_{wi} is the stiffness of the i^{th} wall-to-perpendicular wall connectors.

By substituting Eqs. (4.23) and (4.24) into Eq. (4.19), the modified deflection of the CLT shear wall due to rocking can be estimated as:

$$\delta_r = \left[\left(\frac{F \cdot h^2}{b^2} - \frac{qh}{2} \right) \frac{1}{k_{HD}} \right] \left[1 + \frac{1}{b^2} \left(\sum_{i=1}^{n_f} x_i^2 k_{fi} + \sum_{i=1}^{n_w} y_i^2 k_{wi} \right) \frac{1}{k_{HD}} \right]^{-1} \quad (4.25)$$

4.4.1.2 Sliding Deflection

The lateral resistance of the connections between the shear wall to perpendicular wall and floor above provide additional resistance against sliding deformation (Figure 4.13).

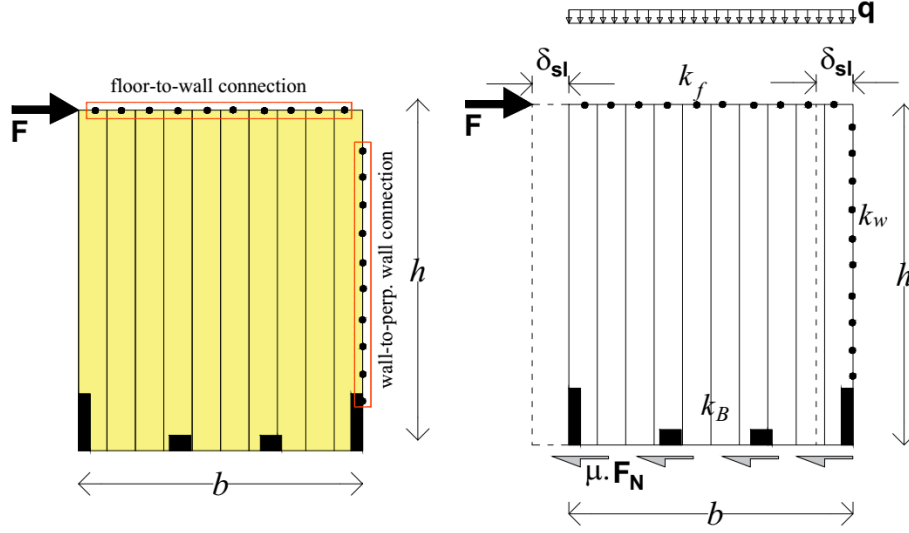


Figure 4.13 Modified sliding deflection of CLT shear wall

The modified sliding deflection the CLT shear wall can be estimated as:

$$\delta_{sl} = \frac{F'}{n_B k_B + n_w k_w + n_f k_f} = \frac{F - \mu \cdot F_N}{n_B k_B + n_w k_w + n_f k_f} = \frac{F - \mu \cdot (qb)}{n_B k_B + n_w k_w + n_f k_f} \quad (4.26)$$

where F' is the resultant force on shear walls, i.e. the difference between the lateral force F and the frictional force (μF_N) between CLT panel and floor or foundation, q is the vertical load on the shear walls, b is the width of the wall, n_B , n_w and n_f are the total number of brackets/connections in wall-to-foundation or floor below, wall-to-perpendicular wall and wall-to-floor above, respectively; k_B , k_w and k_f are the stiffness of the brackets/connections in wall-to-foundation or floor below, wall-to-perpendicular wall and wall-to-floor above, respectively. By ignoring the frictional resistance, Eq. (4.26) can be simplified to:

$$\delta_{sl} = \frac{F}{n_B k_B + n_w k_w + n_f k_f} \quad (4.27)$$

Here, the stiffness of the brackets/connections in wall-to-foundation or floor below, wall-to-perpendicular wall, and wall-to-floor above (k_B , k_w and k_f) are considered as acting in a series.

4.4.1.3 Total Deflection

By replacing Eqs. (4.2), (4.5), (4.25), and (4.27) into Eq. (4.1), the total deflection of the single CLT shear wall with perpendicular wall configuration 1 and floor can be estimated as:

$$\delta = \left(\frac{Fh^3}{3EI_{eff}} + \frac{F \cdot h}{G_{CLT} \cdot t_{CLT} \cdot b} + \frac{F}{n_B k_B + n_w k_w + n_f k_f} + \left(\frac{F \cdot h^2}{b^2} - \frac{qh}{2} \right) \frac{1}{k_{HD}} \left[1 + \frac{1}{b^2} \left(\sum_{i=1}^{n_f} x_i^2 k_{fi} + \sum_{i=1}^{n_w} y_i^2 k_{wi} \right) \frac{1}{k_{HD}} \right]^{-1} \right) \quad (4.28)$$

Eq. (4.28) can be simplified to Eq. (4.14) if there is no there is no perpendicular walls or floors above:

$$\delta = \frac{Fh^3}{3EI_{eff}} + \frac{F \cdot h}{G_{CLT} \cdot t_{CLT} \cdot b} + \frac{F}{n_B k_B} + \left(\frac{F \cdot h^2}{b^2} - \frac{qh}{2} \right) \frac{1}{k_{HD}} \quad (4.29)$$

4.4.2 Perpendicular Wall Configuration 2

In configuration 2, under lateral loading, the in-plane shear wall will pull the perpendicular wall (Figure 4.14a). Therefore, the bracket connections underneath the perpendicular wall resist the lateral load, i.e. prevent lateral deflection of the in-plane shear wall. Based on the assumption that the in-plane wall will likely move laterally along with the perpendicular wall, the deflection under rocking and sliding is calculated in the following sub-sections.

4.4.2.1 Rocking Deflection

The rocking behaviour of the CLT shear wall due to a lateral force F in case of configuration 2 is shown in Figure 4.14b.

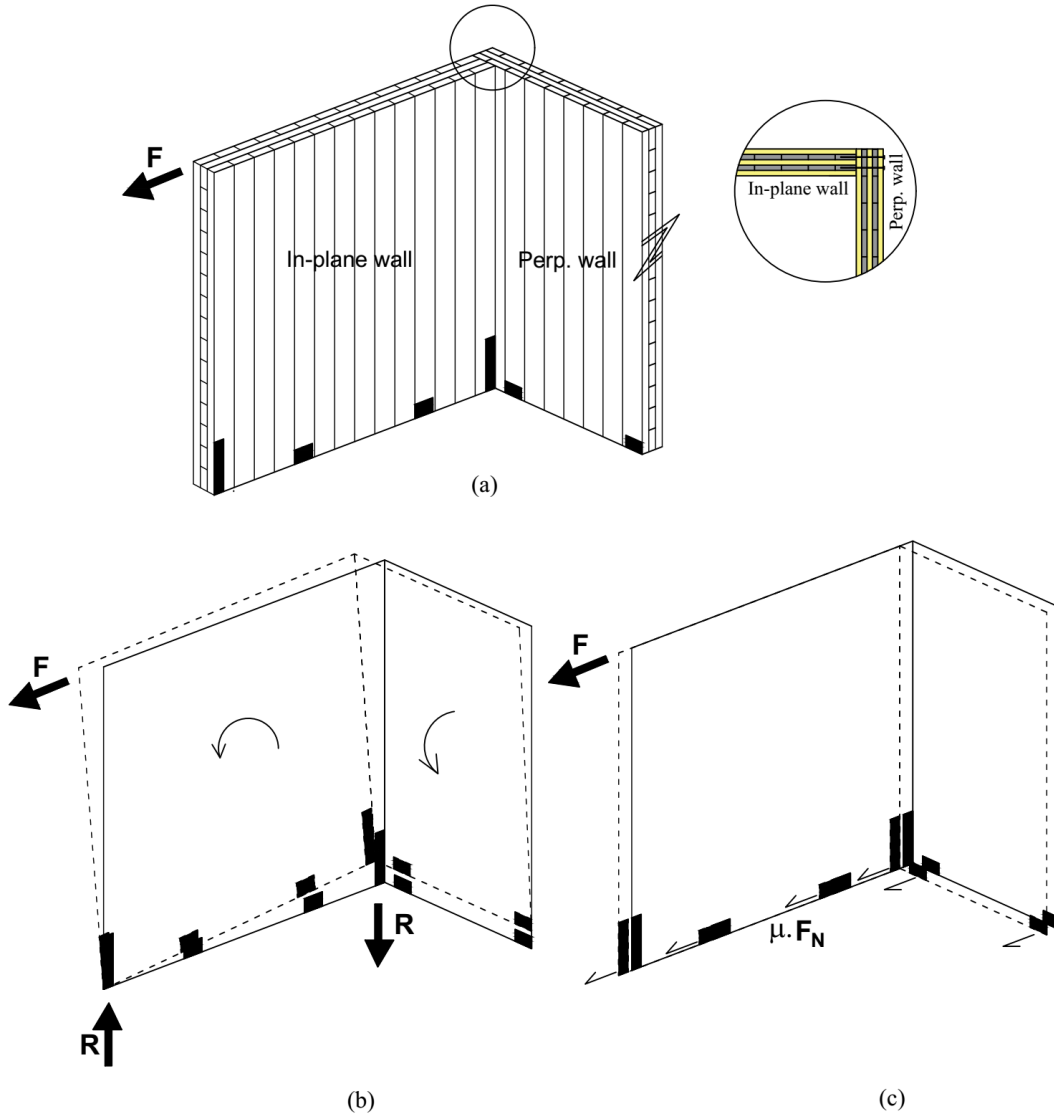


Figure 4.14 (a) CLT shear wall with perpendicular wall in configuration 2, (b) walls under rocking, and (c) walls under sliding

It is assumed that the connections between wall to the perpendicular wall and to the floor above will remain elastic. The brackets underneath the perpendicular wall will resist the tension force R , on the right side of the in-plane wall along with the hold-down at that location. Therefore, after adding the brackets stiffness of the perpendicular wall in Eq. (4.25), the rocking deflection, δ_r of the in-plane wall in presence of perpendicular wall can be calculated as:

$$\delta_r = \left(\frac{F h^2}{b^2} - \frac{qh}{2} \right) \frac{1}{k_{HD} + n_p k_{t,p}} \left[1 + \frac{1}{b^2} \left(\sum_{i=1}^{n_f} x_i^2 k_{fi} \right) \frac{1}{k_{HD} + n_p k_{t,p}} \right]^{-1} \quad (4.30)$$

where q is the vertical force on shear walls, b is the length of the wall, h is the height of the wall, k_{HD} is the stiffness of the hold-down, n_p and $k_{t,p}$ are the number of brackets and tensile stiffness of the brackets in perpendicular wall.

The withdrawal resistance of the in-plane wall-to-perpendicular wall connections does influence the deflection in the case of configuration 2; however, this influence is difficult to quantify without experimental investigations; therefore, as a conservative approach, the contribution of these connections has been ignored in Eq. (4.30).

4.4.2.2 Sliding Deflection

The brackets underneath the perpendicular wall will provide additional resistance against sliding deflection of the in-plane shear wall (Figure 4.14c). Therefore, the modified sliding deflection of the CLT shear wall can be estimated as:

$$\delta_{sl} = \frac{F'}{n_B k_B + n_f k_f + n_p k_{s,p}} = \frac{F - \mu F_N}{n_B k_B + n_f k_f + n_p k_{s,p}} = \frac{F - \mu(qb)}{n_B k_B + n_p k_{s,p}} \quad (4.31)$$

where F' is the resultant force on shear walls, the difference between the lateral force F and the frictional force (μF_N) between CLT panel and floor or foundation, q is the vertical load on the shear walls, b is the width of the wall, n_B and k_B are the total number of brackets and the stiffness of the brackets in wall-to-foundation or floor below, respectively, and n_p and $k_{s,p}$ are the total number of brackets and the shear stiffness of the brackets in perpendicular wall-to-foundation or floor below, respectively. However, by ignoring the frictional resistance, Eq. (4.31) can be simplified to:

$$\delta_{sl} = \frac{F}{n_B k_B + n_f k_f + n_p k_{s,p}} \quad (4.32)$$

4.4.2.3 Total Deflection

By substituting Eqs. (4.2), (4.5), (4.30), and (4.32) into Eq. (4.1), the total deflection of the CLT shear wall in presence of perpendicular walls (configuration 2) and floors can be estimated as:

$$\delta = \left(\frac{Fh^3}{3EI_{eff}} + \frac{F \cdot h}{G_{CLT} \cdot t_{CLT} \cdot b} + \frac{F}{n_B k_B + n_f k_f + n_p k_{sl,p}} + \left(\frac{F \cdot h^2}{b^2} - \frac{qh}{2} \right) \frac{1}{k_{HD} + n_p k_{t,P}} \left[1 + \frac{1}{b^2} \left(\sum_{i=1}^{n_f} x_i^2 k_{fi} \right) \frac{1}{k_{HD} + n_p k_{t,P}} \right]^{-1} \right) \quad (4.33)$$

Eq. (4.33) can be simplified to Eq. (4.14) if there are no perpendicular walls or floors above:

$$\delta = \frac{Fh^3}{3EI_{eff}} + \frac{F \cdot h}{G_{CLT} \cdot t_{CLT} \cdot b} + \frac{F}{n_B k_B} + \left(\frac{F \cdot h^2}{b^2} - \frac{qh}{2} \right) \frac{1}{k_{HD}} \quad (4.34)$$

4.5 Deflection of Coupled CLT Shear Walls

Coupled CLT shear walls formed by connecting two or more panels vertically are common in a CLT platform building since there is a limitation for transporting large panels to the construction site. Also in Canada, CSA O86 imposes a restriction on the maximum aspect ratio of shear walls (length-to-height) of 1.0. Therefore, commonly two or more panels are connected vertically to form a coupled wall. Typical vertical joints in coupled walls are half-lap and spline joints (Figure 4.15d and e) connected by STS. The deflection of a typical coupled shear wall can be described in terms of its kinematic response under lateral loading as shown in Figure 4.16 and Figure 4.17.

The following assumptions are made to estimate the total deflection of the coupled shear wall:

- The connectors used for the vertical joints in a coupled wall with 4-HDs are flexible enough so that each wall can facilitate wall rocking.
- By contrast, the vertical joints in a coupled wall with 2-HDs are stiff enough so that the coupled wall can rock like a single rigid body.
- Both parts of the coupled wall will undergo the same horizontal deformation at the top.
- The horizontal forces acting on each wall segment are proportional to their stiffness.

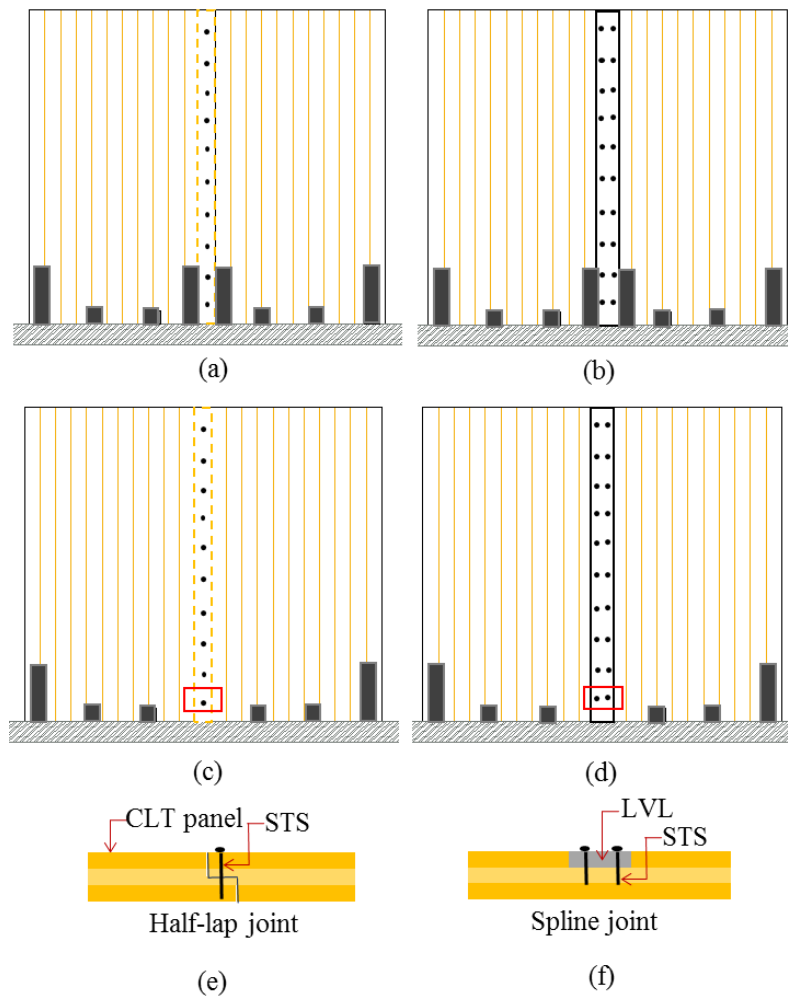


Figure 4.15 Coupled shear wall with: (a) 4-HDs and half-lap, (b) 4-HDs and spline joints, (c) 2-HDs and half-lap, (d) 2-HDs and spline joint, (e) half-lap schematic, (f) spline joint schematic

4.5.1 Deflection of Coupled Shear Walls (4 HDs) without Perp. Walls

In this case, two additional hold-downs are placed on both sides of the vertical joints. Under rocking action, each panel rocks separately, and those two hold-downs will resist tension forces. However, it should be noted that the vertical joints have to be designed flexible enough so as to allow each panel to rock.

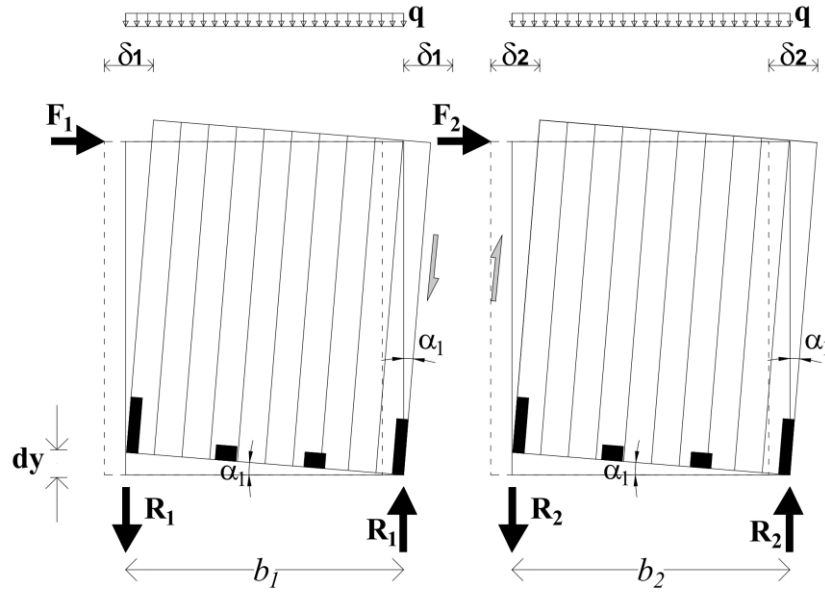


Figure 4.16 Deflection of coupled CLT shear wall with 4-HDs

Since each panel rocks individually, the deflection equation of single CLT shear walls can be utilized to estimate the deflection of each panel in a coupled CLT shear wall. After rearranging Eq. (4.14), the deflection of each panel in a coupled wall with 4-HDs as shown in Figure 4.16 can be estimated as:

$$\delta_i = \frac{F_i}{\left(\frac{3EI_{eff}}{h^3}\right)} + \frac{F_i}{\left(\frac{G_{CLT} \cdot t_{CLT} \cdot b_i}{h}\right)} + \frac{F_i}{(n_B k_B)} + \frac{F_i}{\left(\frac{b_i^2 k_{HD}}{h^2}\right)} - \left(\frac{qh}{2k_{HD}}\right) \quad (4.35)$$

where F_i is the lateral force on each panel, EI_{eff} is the effective bending stiffness of the CLT shear walls, b_i is the width of each panel in the coupled wall, h is the height of the wall, G_{CLT} is the shear modulus of the panel, t_{CLT} is the thickness of the panel, q is the vertical force on shear walls, n_B is the number of brackets, k_B is the stiffness of the bracket, and k_{HD} is the stiffness of the hold-down. Eq. (4.35) can be rewritten in terms of the bending K_b , shear K_s , sliding K_{sl} and rocking K_r stiffness of each panel in the coupled wall:

$$\delta_i = F_i \left(\frac{1}{K_{b,i}} + \frac{1}{K_{s,i}} + \frac{1}{K_{sl,i}} + \frac{1}{K_{r,i}} \right) - \frac{qh}{2k_{HD}} \quad (4.36)$$

where the bending $K_{b,i}$, shear $K_{s,i}$, sliding $K_{sl,i}$ and rocking $K_{r,i}$ stiffness of each wall segment can be calculated as:

$$K_{b,i} = \frac{3(EI_{eff})_i}{h^3} \quad (4.37)$$

$$K_{s,i} = \frac{G_{CLT} \cdot t_{CLT} \cdot b_i}{h} \quad (4.38)$$

$$K_{sl,i} = n_{B,i} k_{B,i} \quad (4.39)$$

$$K_{r,i} = \frac{b^2 k_{HD,i}}{h^2} \quad (4.40)$$

The total stiffness of each panel in the CLT coupled wall, K_i can be expressed as the summation of the reciprocal stiffness of each panel in the coupled wall:

$$\frac{1}{K_i} = \frac{1}{K_{b,i}} + \frac{1}{K_{s,i}} + \frac{1}{K_{sl,i}} + \frac{1}{K_{r,i}} \quad (4.41)$$

Eq. (4.35) can be simplified by replacing Eq. (4.41):

$$\delta_i = \frac{F_i}{K_i} - \frac{qh}{2k_{HD}} \quad (4.42)$$

where the deflection of each panel can be written as:

$$\delta_1 = \frac{F_1}{K_1} - \frac{qh}{2k_{HD}} \quad (4.43)$$

$$\delta_2 = \frac{F_2}{K_2} - \frac{qh}{2k_{HD}} \quad (4.44)$$

where $F_1, F_2, \delta_1, \delta_2$ and K_1, K_2 are the lateral force, the deflection and stiffness on the left and right panels of the coupled wall, respectively. The summation of the forces F_1 and F_2 shall be equal to the total lateral force, F :

$$F = F_1 + F_2 \quad (4.45)$$

where the forces F_1 and F_2 are proportional to the stiffness of each segment of the coupled wall:

$$F_i \propto K_i \quad (4.46)$$

Since it is assumed that the deflection at the top of each coupled wall's segment are equal ($\delta_1 = \delta_2 = \delta$), substituting Eqs. (4.43) and (4.44) into Eq. (4.45), the deflection of a coupled CLT shear wall with two or more panels can be calculated as:

$$\delta = \frac{F}{\sum K_i} - \frac{qh}{2k_{HD}} \quad (4.47)$$

4.5.2 Deflection of Coupled Shear Walls (4 HDs) with Perp. Walls and Floor Above

Similar to single CLT shear walls, the total deflection of the coupled CLT shear walls is also influenced by the presence of perpendicular walls and floors above. As seen in Figure 4.3, two

types of configuration are possible in case of an in-plane wall to perpendicular wall connection. The deflection equations for the two configurations in CLT coupled shear walls with 4-HDs are discussed in the following sub-sections.

4.5.2.1 Perpendicular wall configuration 1

For the perpendicular wall configuration 1 (Figure 4.3a), the total deflection of a coupled CLT shear wall in presence of perpendicular walls and floors above can be estimated as:

$$\delta = \frac{F}{\sum K_i} - \frac{qh}{2k_{HD}} \frac{1}{r} \quad (4.48)$$

where the stiffness of each wall segment, K_i can be calculated using Eq. (4.41):

$$\frac{1}{K_i} = \frac{1}{K_{b,i}} + \frac{1}{K_{s,i}} + \frac{1}{K_{sl,i}} + \frac{1}{K_{r,i}} \quad (4.49)$$

where the bending $K_{b,i}$, shear $K_{s,i}$ and sliding $K_{sl,i}$ stiffness of each wall segment can be estimated as:

$$K_{b,i} = \frac{3(EI_{eff})_i}{h^3} \quad (4.50)$$

$$K_{s,i} = \frac{G_{CLT} \cdot t_{CLT} \cdot b_i}{h} \quad (4.51)$$

$$K_{sl,i} = n_{B,i} k_{B,i} + n_{w,i} k_{w,i} + n_{f,i} k_{f,i} \quad (4.52)$$

The rocking stiffness, $K_{r,i}$ of the left and right wall panels can be calculated as:

$$K_{r,i} = \left(\frac{b_{i,l}^2 k_{HD,i}}{h^2} \right) \frac{1}{r} \quad (4.53)$$

$$K_{r,r} = \left(\frac{b_{i,r}^2 k_{HD,i}}{h^2} \right) \frac{1}{r} \quad (4.54)$$

The factors r and r' account for the reduction of rocking deflection in a coupled shear wall due to perpendicular walls and floors can be estimated as:

$$r = \left[1 + \frac{1}{b_{i,r}^2} \left(\sum_{i=1}^{n_f} x_i^2 k_{fi} + \sum_{i=1}^{n_w} y_i^2 k_{wi} \right) \frac{1}{k_{HD}} \right]^{-1} \quad (4.55)$$

$$r' = \left[1 + \frac{1}{b_{i,l}^2} \left(\sum_{i=1}^{n_f} x_i^2 k_{fi} \right) \frac{1}{k_{HD}} \right]^{-1} \quad (4.56)$$

4.5.2.2 Perpendicular wall configuration 2

For the perpendicular wall configuration 2 (Figure 4.3b), the total deflection of a coupled CLT shear wall in presence of perpendicular walls and floors above can be estimated as:

$$\delta = \frac{F}{\sum K_i} - \frac{qh}{2k_{HD}'} \frac{1}{r'} \quad (4.57)$$

where k_{HD}' is the modified stiffness of the HDs and can be calculated as:

$$k_{HD}' = k_{HD} + n_p k_{t,p} \quad (4.58)$$

where n_p and $k_{t,p}$ are the number of brackets and tensile stiffness of the brackets in the perpendicular wall.

The stiffness of each wall segment, K_i can be calculated using Eq. (4.49):

$$\frac{1}{K_i} = \frac{1}{K_{b,i}} + \frac{1}{K_{s,i}} + \frac{1}{K_{sl,i}} + \frac{1}{K_{r,i}} \quad (4.59)$$

where the bending $K_{b,i}$, shear $K_{s,i}$, sliding $K_{sl,i}$ and rocking, $K_{r,i}$ stiffness of each wall segment can be estimated as:

$$K_{b,i} = \frac{3(EI_{eff})_i}{h^3} \quad (4.60)$$

$$K_{s,i} = \frac{G_{CLT} \cdot t_{CLT} \cdot b_i}{h} \quad (4.61)$$

$$K_{sl,i} = n_{B,i} k_{B,i} + n_{f,i} k_{f,i} + n_p k_{s,p} \quad (4.62)$$

The rocking stiffness, $K_{r,i}$ of the left and right wall panels can be calculated as:

$$K_{r,l} = \left(\frac{b_i^2 k_{HD,i}}{h^2} \right) \frac{1}{r'} \quad (4.63)$$

$$K_{r,r} = \left(\frac{b_i^2 k'_{HD,i}}{h^2} \right) \frac{1}{r'} \quad (4.64)$$

The factor r' accounts for the reduction of rocking deflection in a coupled shear wall due to perpendicular walls and floors can be estimated as:

$$r' = \left[1 + \frac{1}{b_i^2} \left(\sum_{i=1}^{n_f} x_i^2 k_{fi} \right) \frac{1}{k_{HD}} \right]^{-1} \quad (4.65)$$

4.5.3 Deflection of Coupled CLT Shear Walls with 2-HDs

In this case of a coupled shear wall with stiff vertical joints, the wall panels move like a single rigid body. Two hold-downs at the outer edges of the wall are sufficient to resist tension forces (Figure 4.16). In this case, the total deflection of the coupled shear wall can be calculated using the proposed equations for single CLT shear wall. Therefore, the deflection of coupled CLT shear

wall with 2-HDs without any influence of perpendicular wall and floor can be estimated using Eq. (4.66):

$$\delta = \frac{Fh^3}{3EI_{eff}} + \frac{Fh}{G_{CLT}t_{CLT}b} + \frac{F}{n_Bk_B} + \left(\frac{Fh^2}{b^2} - \frac{qh}{2} \right) \frac{1}{k_{HD}} \quad (4.66)$$

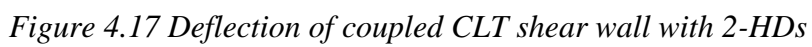
Similarly, the deflection of coupled CLT shear wall with 2-HDs with perpendicular wall and floor can be estimated using Eqs. (4.67) and (4.68).

For perpendicular wall configuration 1 (Figure 4.3a):

$$\delta = \left(\frac{Fh^3}{3EI_{eff}} + \frac{Fh}{G_{CLT}t_{CLT}b} + \frac{F}{n_Bk_B + n_wk_w + n_fk_f} + \left(\frac{Fh^2}{b^2} - \frac{qh}{2} \right) \frac{1}{k_{HD}} \left[1 + \frac{1}{b^2} \left(\sum_{i=1}^{n_f} x_i^2 k_{fi} + \sum_{i=1}^{n_w} y_i^2 k_{wi} \right) \frac{1}{k_{HD}} \right]^{-1} \right) \quad (4.67)$$

For perpendicular wall configuration 2 (Figure 4.3b):

$$\delta = \left(\frac{Fh^3}{3EI_{eff}} + \frac{Fh}{G_{CLT}t_{CLT}b} + \frac{F}{n_Bk_B + n_fk_f + n_pk_{sl,p}} + \left(\frac{Fh^2}{b^2} - \frac{qh}{2} \right) \frac{1}{k_{HD} + n_pk_{t,p}} \left[1 + \frac{1}{b^2} \left(\sum_{i=1}^{n_f} x_i^2 k_{fi} \right) \frac{1}{k_{HD} + n_pk_{t,p}} \right]^{-1} \right) \quad (4.68)$$



4.6 Overview of Equations to Estimate the Deflection of CLT Shear Walls

The formulas to estimate the deflection of single and coupled CLT shear walls proposed in this chapter are summarized in Table 4.1, Table 4.2 and Table 4.3.

Table 4.1 Deflection formulas for Single CLT walls

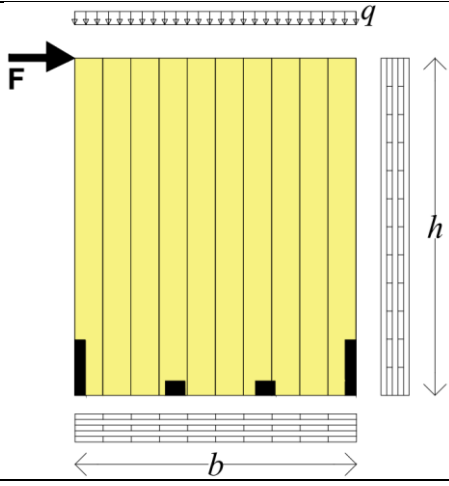
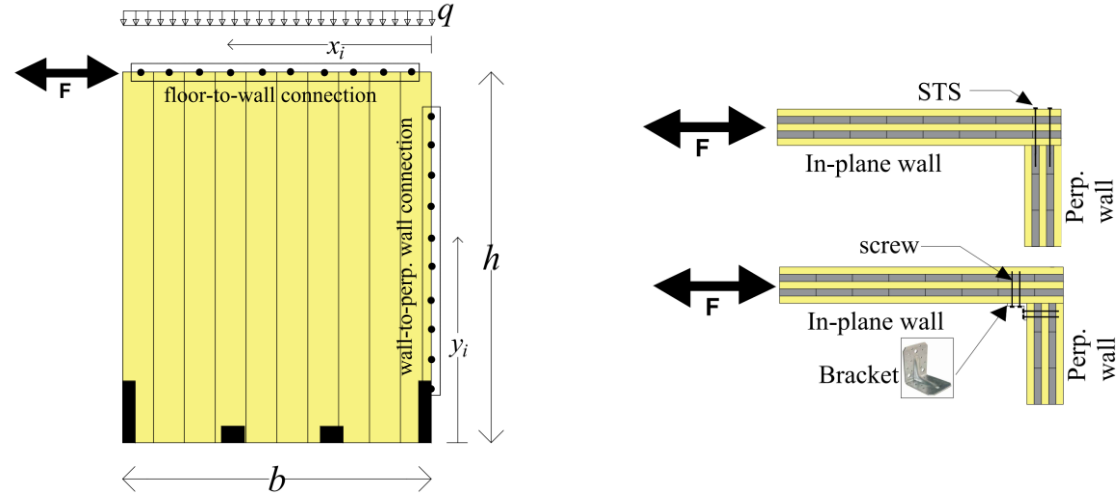
Single CLT shear wall without perpendicular wall and floor above	
	$\delta = \frac{Fh^3}{3EI_{eff}} + \frac{Fh}{G_{CLT}t_{CLT}b} + \frac{F}{n_Bk_B} + \left(\frac{Fh^2}{b^2} - \frac{qh}{2} \right) \frac{1}{k_{HD}}$
Single CLT shear wall with perpendicular wall (configuration 1) and floor above	
	$\delta = \left[\frac{Fh^3}{3EI_{eff}} + \frac{F.h}{G_{CLT}.t_{CLT}.b} + \frac{F}{n_Bk_B + n_wk_w + n_fk_f} + \left(\frac{F.h^2}{b^2} - \frac{qh}{2} \right) \frac{1}{k_{HD}} \left[1 + \frac{1}{b^2} \left(\sum_{i=1}^{n_f} x_i^2 k_{fi} + \sum_{i=1}^{n_w} y_i^2 k_{wi} \right) \frac{1}{k_{HD}} \right]^{-1} \right]$

Table 4.1 (Contd.)

Single CLT shear wall with perpendicular wall (configuration 2) and floor above	
$\delta = \left(\frac{Fh^3}{3EI_{eff}} + \frac{F \cdot h}{G_{CLT} \cdot t_{CLT} \cdot b} + \frac{F}{n_B k_B + n_f k_f + n_p k_{sl,p}} + \left(\frac{F \cdot h^2}{b^2} - \frac{qh}{2} \right) \frac{1}{k_{HD} + n_p k_{t,p}} \left[1 + \frac{1}{b^2} \left(\sum_{i=1}^{n_f} x_i^2 k_{fi} \right) \frac{1}{k_{HD} + n_p k_{t,p}} \right]^{-1} \right)$	
<p>Note: ¹Configuration 2 works when the force, F is applied in the leftward direction. It has been assumed that the deflection is completely prevented by the perpendicular wall when F is applied in the rightward direction.</p>	
<p>δ = deflection of wall F = lateral force on wall; q = vertical load; h = height of the wall; b = width of the wall G_{CLT} = shear modulus of CLT panel; EI_{eff} = effective bending stiffness of the CLT panel t_{CLT} = total thickness of CLT panel k_B, k_{HD}, k_w, k_f = stiffness of the brackets, hold-downs, wall-to-perpendicular wall and wall-to-floor above, respectively n_B, n_w, n_f = total number of brackets/connections in wall-to-foundation or floor below, wall-to-perpendicular wall and wall-to-floor above, respectively k_{fi}, k_{wi} = stiffness of the i^{th} wall-to-floor and wall-to-perp. wall connectors, respectively $k_{t,p}$ = tensile stiffness of the brackets in the perpendicular wall n_p = number of brackets in the perpendicular wall x_{fi}, y_{wi} = distance of the wall-to-floor and wall-to-perpendicular wall connectors from lower right corner of the wall, respectively</p>	

Table 4.2 Deflection formulas for Coupled CLT walls with 4-HDs

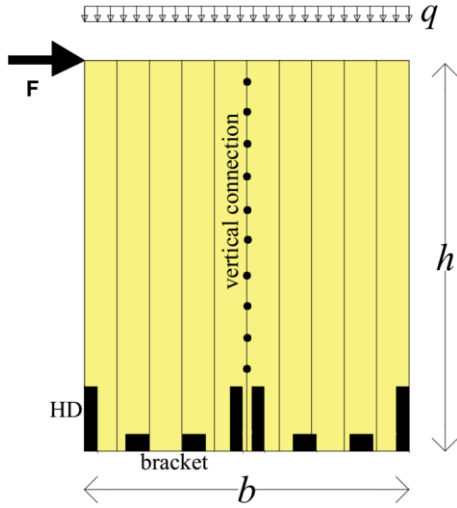
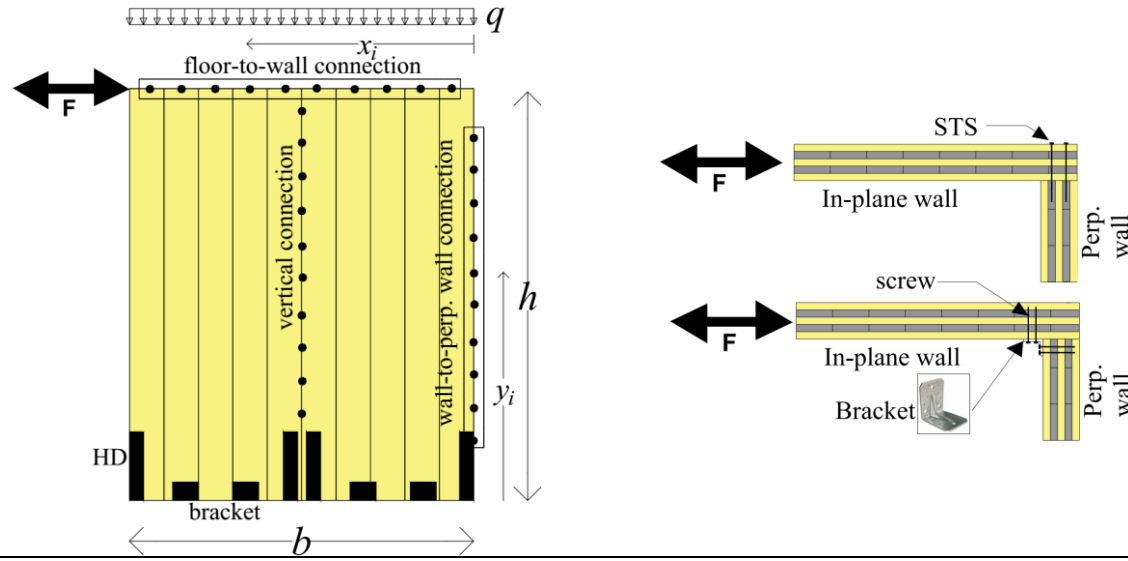
Coupled CLT shear wall without perpendicular wall and floor above	
	$\delta = \frac{F}{\sum K_i} - \frac{qh}{2k_{HD}}$ $\frac{1}{K_i} = \frac{1}{K_{b,i}} + \frac{1}{K_{s,i}} + \frac{1}{K_{sl,i}} + \frac{1}{K_{r,i}}$ $K_{b,i} = \frac{3(EI_{eff})_i}{h^3}; K_{s,i} = \frac{G_{CLT} \cdot t_{CLT} \cdot b_i}{h}$ $K_{sl,i} = n_{B,i} k_{B,i}; K_{r,i} = \frac{b^2 k_{HD,i}}{h^2}$
Coupled CLT shear wall with perpendicular wall (configuration 1) and floor above	
	
$\delta = \frac{F}{\sum K_i} - \frac{qh}{2k_{HD}} \frac{1}{r}$ $\frac{1}{K_i} = \frac{1}{K_{b,i}} + \frac{1}{K_{s,i}} + \frac{1}{K_{sl,i}} + \frac{1}{K_{r,i}}; K_{b,i} = \frac{3(EI_{eff})_i}{h^3}; K_{s,i} = \frac{G_{CLT} \cdot t_{CLT} \cdot b_i}{h};$ $K_{sl,i} = n_{B,i} k_{B,i} + n_{w,i} k_{w,i} + n_{f,i} k_{f,i}; K_{r,i} = \left(\frac{b_{i,l}^2 k_{HD,i}}{h^2} \right) \frac{1}{r}; K_{r,r} = \left(\frac{b_{i,r}^2 k_{HD,i}}{h^2} \right) \frac{1}{r}$ $r = \left[1 + \frac{1}{b_{i,r}^2} \left(\sum_{i=1}^{n_f} x_i^2 k_{fi} + \sum_{i=1}^{n_w} y_i^2 k_{wi} \right) \frac{1}{k_{HD}} \right]^{-1}; r' = \left[1 + \frac{1}{b_{i,l}^2} \left(\sum_{i=1}^{n_f} x_i^2 k_{fi} \right) \frac{1}{k_{HD}} \right]^{-1}$	

Table 4.2 (Contd.)

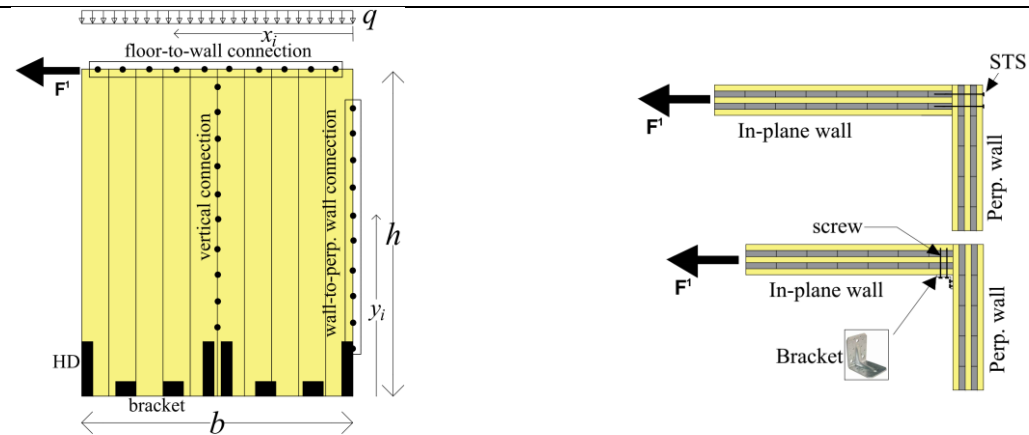
Coupled CLT shear wall with perpendicular wall (configuration 2) and floor above	
	
$\delta = \frac{F}{\sum K_i} - \frac{qh}{2k'_{HD}} \frac{1}{r'}; k'_{HD} = k_{HD} + n_p k_{t,p}; \frac{1}{K_i} = \frac{1}{K_{b,i}} + \frac{1}{K_{s,i}} + \frac{1}{K_{sl,i}} + \frac{1}{K_{r,i}}$ $K_{b,i} = \frac{3(EI_{eff})_i}{h^3}; K_{s,i} = \frac{G_{CLT} \cdot t_{CLT} \cdot b_i}{h}; K_{sl,i} = n_{B,i} k_{B,i} + n_{f,i} k_{f,i} + n_p k_{s,p}$ $K_{r,l} = \left(\frac{b_i^2 k_{HD,i}}{h^2} \right) \frac{1}{r'}; K_{r,r} = \left(\frac{b_i^2 k'_{HD,i}}{h^2} \right) \frac{1}{r'}; r' = \left[1 + \frac{1}{b_i^2} \left(\sum_{i=1}^{n_f} x_i^2 k_{fi} \right) \frac{1}{k_{HD}} \right]^{-1}$	
<p>Note: ¹Configuration 2 works when the force, F is applied in the leftward direction. It has been assumed that the deflection is completely prevented by the perpendicular wall when F is applied in the rightward direction.</p>	
<p>δ = deflection of wall</p> <p>$K_{b,i}, K_{s,i}, K_{sl,i}, K_{r,i}$ = bending, shear, sliding and rocking stiffness of each wall segment, respectively</p> <p>$K_{r,l}, K_{r,r}$ = rocking resistance of the left and right panel, respectively</p> <p>F = lateral force on wall; q = vertical load; h = height of the wall; b = width of the wall</p> <p>G_{CLT} = shear modulus of CLT panel; EI_{eff} = effective bending stiffness of the CLT panel</p> <p>t_{CLT} = total thickness of CLT panel</p> <p>k_B, k_{HD}, k_w, k_f = stiffness of the brackets, hold-downs, wall-to-perpendicular wall and wall-to-floor above, respectively</p> <p>n_B, n_w, n_f = total number of brackets/connections in wall-to-foundation or floor below, wall-to-perpendicular wall and wall-to-floor above, respectively</p> <p>k_{fi}, k_{wi} = stiffness of the i^{th} wall-to-floor and wall-to-perp. wall connectors, respectively</p> <p>$k_{t,p}$ = tensile stiffness of the brackets in the perpendicular wall</p> <p>n_p = number of brackets in the perpendicular wall</p> <p>x_{fi}, y_{wi} = distance of the wall-to-floor and wall-to-perpendicular wall connectors from lower right corner of the wall, respectively</p>	

Table 4.3 Deflection formulas for Coupled CLT walls with 2-HDs

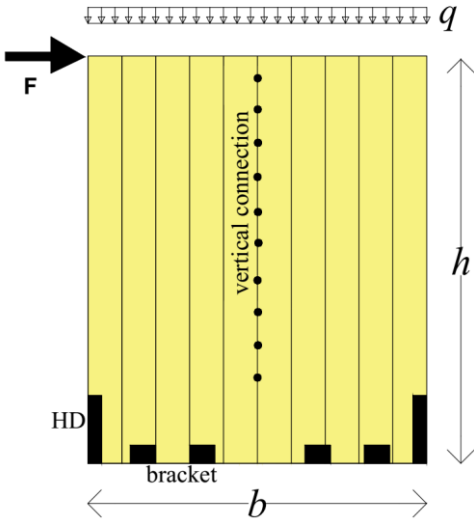
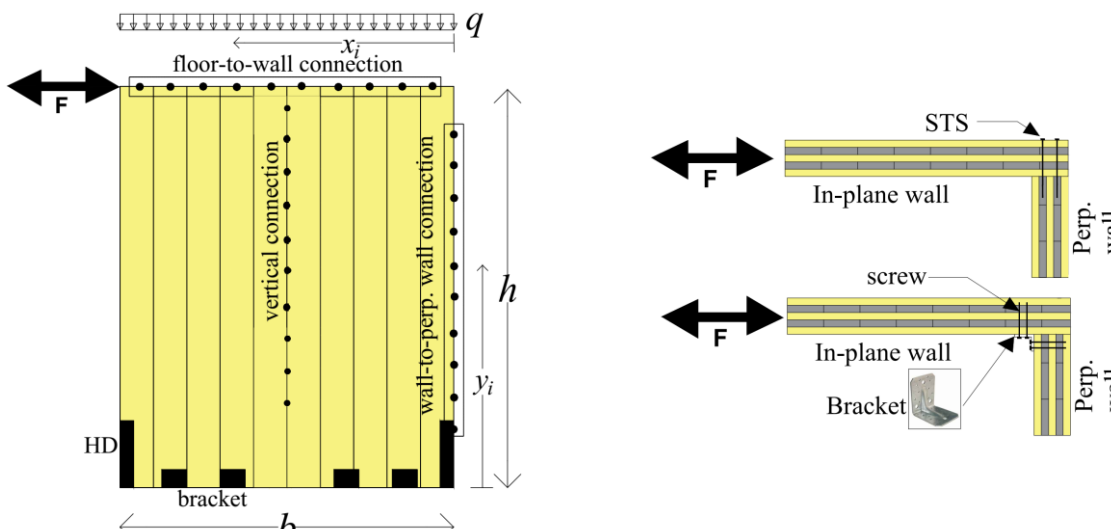
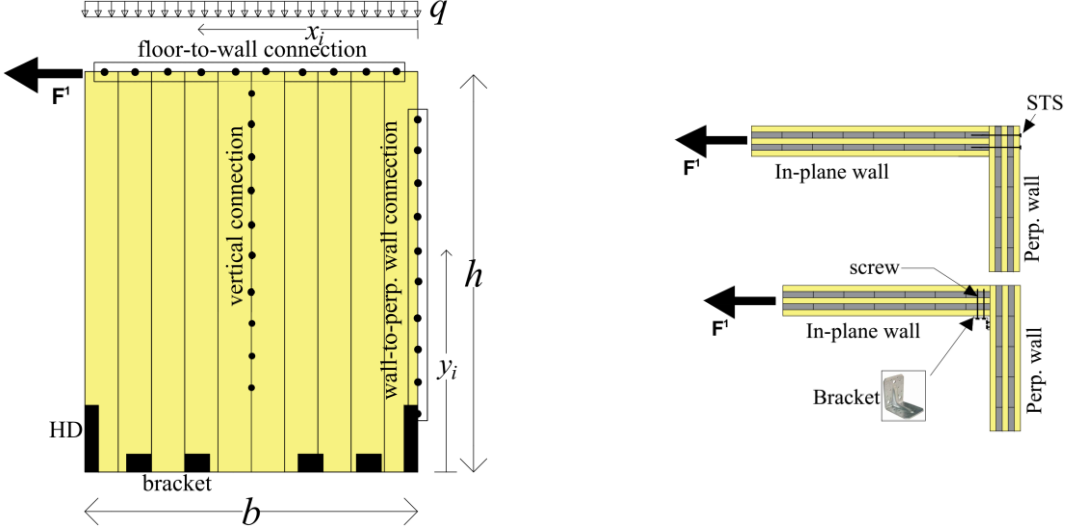
Coupled CLT shear wall without perpendicular wall and floor above	
	$\delta = \frac{Fh^3}{3EI_{eff}} + \frac{Fh}{G_{CLT}t_{CLT}b} + \frac{F}{n_Bk_B} + \left(\frac{Fh^2}{b^2} - \frac{qh}{2} \right) \frac{1}{k_{HD}}$
Coupled CLT shear wall with perpendicular wall (configuration 1) and floor above	
	$\delta = \left(\frac{Fh^3}{3EI_{eff}} + \frac{F.h}{G_{CLT}.t_{CLT}.b} + \frac{F}{n_Bk_B + n_wk_w + n_fk_f} + \left(\frac{F.h^2}{b^2} - \frac{qh}{2} \right) \frac{1}{k_{HD}} \left[1 + \frac{1}{b^2} \left(\sum_{i=1}^{n_f} x_i^2 k_{fi} + \sum_{i=1}^{n_w} y_i^2 k_{wi} \right) \frac{1}{k_{HD}} \right]^{-1} \right)$

Table 4.3 (Contd.)

Coupled CLT shear wall with perpendicular wall (configuration 2) and floor above	
	
$\delta = \left(\frac{Fh^3}{3EI_{eff}} + \frac{F \cdot h}{G_{CLT} \cdot t_{CLT} \cdot b} + \frac{F}{n_B k_B + n_f k_f + n_p k_{sl,p}} \right. \\ \left. + \left(\frac{F \cdot h^2}{b^2} - \frac{qh}{2} \right) \frac{1}{k_{HD} + n_p k_{t,p}} \left[1 + \frac{1}{b^2} \left(\sum_{i=1}^{n_f} x_i^2 k_{fi} \right) \frac{1}{k_{HD} + n_p k_{t,p}} \right]^{-1} \right)$	
<p>Note: ¹Configuration 2 works when the force, F is applied in the leftward direction. It has been assumed that the deflection is completely prevented by the perpendicular wall when F is applied in the rightward direction.</p>	
<p>δ = deflection of wall F = lateral force on wall; q = vertical load; h = height of the wall; b = width of the wall G_{CLT} = shear modulus of CLT panel; EI_{eff} = effective bending stiffness of the CLT panel t_{CLT} = total thickness of CLT panel k_B, k_{HD}, k_w, k_f = stiffness of the brackets, hold-downs, wall-to-perpendicular wall and wall-to-floor above, respectively n_B, n_w, n_f = total number of brackets/connections in wall-to-foundation or floor below, wall-to-perpendicular wall and wall-to-floor above, respectively k_{fi}, k_{wi} = stiffness of the i^{th} wall-to-floor and wall-to-perp. wall connectors, respectively $k_{t,p}$ = tensile stiffness of the brackets in the perpendicular wall n_p = number of brackets in the perpendicular wall x_{fi}, y_{wi} = distance of the wall-to-floor and wall-to-perpendicular wall connectors from lower right corner of the wall, respectively</p>	

4.7 Summary

This chapter proposed equations to calculate the deflection of single and coupled shear walls under lateral loading. These equations consider the influence of the perpendicular walls and the floors above. The following conclusions can be drawn from this investigation:

- The total deflection of the CLT shear walls was calculated from the contribution of the wall panels i.e. bending and shear deflection of the panels and the contribution of the connectors accounted by sliding and rocking deflection of the walls.
- It was observed that perpendicular walls and the floor above significantly affect the deflection of the in-plane wall. Therefore, their contributions were accounted for in the proposed deflection formulas.
- Two perpendicular wall configurations that affect the in-plane wall deflection were investigated. In configuration 1, the in-plane wall is continuous and the perpendicular wall is connected by STSs or brackets. By contrast, in configuration 2, the in-plane wall ends where it connects with the perpendicular wall which is continuous.
- The modified deflection formulas were proposed when the in-plane wall is connected to the perpendicular wall and floor above. However, it was assumed that the influence of the perpendicular walls and the floors above is not significant on the bending and shear deflection of the CLT shear walls.

A step by step procedure to estimate the deflection of single and coupled CLT shear walls has been highlighted in Appendix B. The procedure to estimate the deflection of two single and three coupled CLT shear walls without and with perpendicular walls and floors above have been discussed.

Chapter 5: Lateral Resistance of CLT Single and Coupled Shear Walls⁵

5.1 Introduction

CLT shear walls can be used as the main lateral force resisting system (LFRS) for a platform-type of construction. In a platform building, the CLT shear walls are connected to the floors diaphragms by hold-downs and brackets. The shear force at each storey is resisted by the CLT shear walls at that level and eventually transferred to the level below.

As described in Chapter 3, the resistance of single and coupled walls will be different depending upon their assembly -i.e. the number of connectors, the type of connectors and the aspect ratio of wall. The shear wall's resistance can be estimated from the strength and deformation capacity of the connections connecting wall-to-floor and wall-to-wall. Additionally, frictional resistance due to vertical loading on the shear wall also provides lateral resistance. However, the contribution of the frictional resistance can be largely ignored because the vertical component of the ground motion may nullify it (Pei et al. 2017). In order to evaluate the resistance of CLT shear walls, extensive research was conducted under monotonic and cyclic loading (Ceccotti et al. 2006a, Popovski et al. 2010, Gavric et al. 2015c, Reynolds et al. 2017, Tamagnone et al. 2017). Their test results illustrated that the CLT panels behave like a rigid body and the connections undergo nonlinear deformation that dissipates energy. Other research estimated the lateral resistance of

⁵The first part of this chapter has been submitted for presentation at the 2018 World Conference on Timber Engineering. The second part of this chapter has been published at the 2017 Structures Congress.

Shahnewaz, M., Tannert, T., Alam, M. S. & Popovski, M. (2017). Capacity-Based Design for Platform-Framed Cross-Laminated Timber Buildings. *Structures Congress 2017*, ASCE, April 6-8 2017, Denver, CO, USA.

Shahnewaz, M., Tannert, T., Alam, M. S. & Popovski, M. (2018). Strength and Stiffness of Cross Laminated Timber Shear Walls in Platform Construction. *World Conference on Timber Engineering*, WCTE 2018, August 20-23, Seoul, Republic of Korea.

CLT shear walls. Specifically, Gavric and Popovski (2014) proposed five design models (D1 to D5). The following is a brief summary of the five models:

- D1 assumed pure sliding and that the resistance was equal to the shear resistance of the brackets only.
- D2 assumed sliding and rocking and calculated the resistance based upon the shear resistance of the brackets and the overturning resistance of the hold-downs.
- D3 assumed that the wall undergoes pure rocking behaviour so the resistance was determined by taking into account the uplift contribution of the connectors only.
- D4 assumed sliding and rocking and that the brackets contributed to the shear and uplift resistance following a quadratic interaction formula.
- D5 also assumed sliding and rocking and that the brackets contributed to the shear and uplift resistance, however, followed a linear interaction.

However, model D1 produced inconsistent results -i.e. the design resistance from model was found to be lower than the experimental capacity of the CLT shear wall -while models D4 and D5 are iterative procedures without a close-form solution to estimate the resistance. Furthermore, none of their models considered the combined sliding-rocking behaviour of the shear wall which may be a realistic scenario under seismic loading.

Tamagnone et al. (2017) proposed a non-linear procedure for seismic design of CLT wall systems whereupon a triangular compressive force at the wall-to-support interface was considered and the neutral axis had to be calculated from an iterative procedure. Although wood is an orthotropic material, this model assumed wood to be a uniaxial elastic material. Furthermore, the model assumed that the displacement of the wall during rocking can happen in the negative Z-direction (e.g. whereby the wall corner can penetrate into the foundation) which is not a realistic scenario.

This chapter describes a procedure to calculate the resistance of CLT shear walls for a platform-type of construction. Both single and coupled shear walls with traditional brackets and hold-downs connections are considered. The proposed formulas are based on the parametric study conducted in chapter 3 that evaluated the change of strength, stiffness, ductility and energy dissipation capacity of the CLT single and coupled shear walls with variation in the type and number of connectors.

5.2 Assumptions

The following assumptions were made to estimate the resistance of CLT shear walls:

- Deformations in a CLT shear wall occurs with a rigid body movement of the panel due to a combination of sliding and rocking or rocking alone.
- The fasteners of brackets and hold-downs (HD) are assumed to yield, whereas the steel-part of the brackets and hold-downs and the anchoring bolts themselves will remain elastic.
- The brackets are able to carry forces from both sliding (shear) and rocking (tension), but the hold-downs carry only forces from rocking (tension). Gavric et al. (2015a) showed that the shear (sliding) capacity of the hold-downs is only one-fifth of its tension (rocking) capacity.
- The brackets are assumed to have equal sliding and rocking resistance.
- Friction forces in the interfaces wall-to-floor and wall-to-foundation are ignored. Including friction for the lateral resistance of a shear wall is unreliable for seismic design simply because the vertical component of the ground motion could nullify or negatively affect frictional resistance (Pei et al. 2017). Ignoring the frictional forces results in a conservative estimation of the resistance of the shear wall and is acceptable in terms of design.

- For coupled shear walls the connection (i.e. screws) in the vertical joints will yield first before the screws at the hold-downs and brackets.
- Sliding and rocking reactions of the brackets are proportional to the shear wall's sliding and rocking deformation.

5.3 Resistance of Single CLT Shear Walls

5.3.1 Overview

As shown in Figure 5.1, two configurations have been considered: single CLT shear walls with brackets (Figure 5.1a) and single CLT shear walls with brackets and hold-downs (Figure 5.1b).

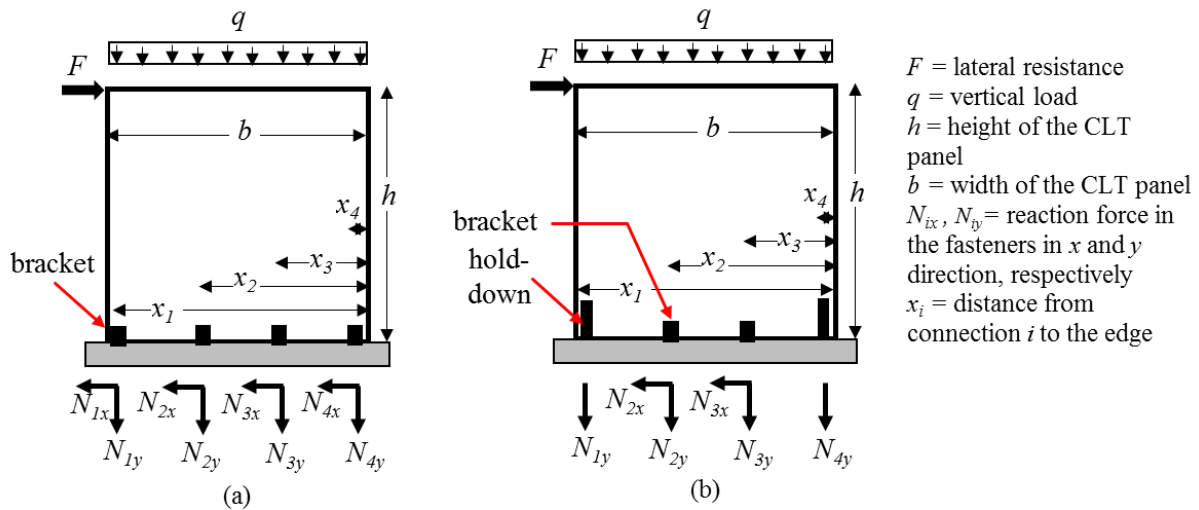


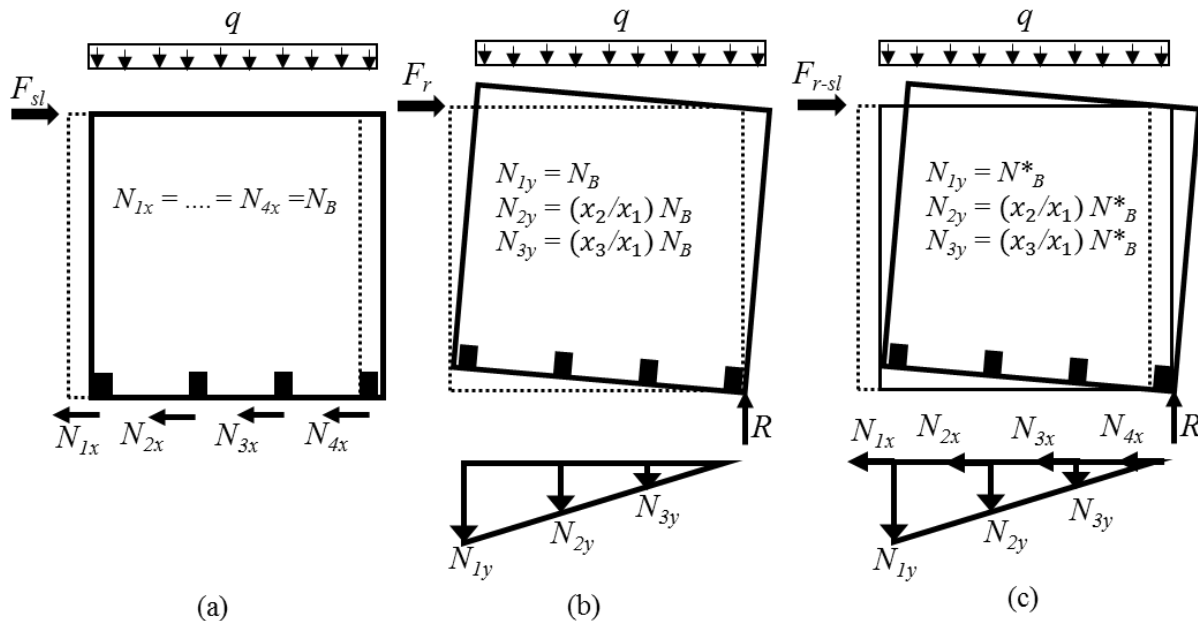
Figure 5.1 Typical configuration of single CLT shear walls with: (a) configuration 1-brackets only and (b) configuration 2 -hold-downs and brackets

The brackets resist both shear and tension forces, whereas the shear resistance of the HD is ignored in configuration 2. The forces on each connector under lateral loading depend on their stiffness and the location of the connectors measured from right side of panel as shown in Figure 5.1.

5.3.2 CLT shear wall with brackets only

CLT shear walls under lateral loading can experience one of three types of kinematic behaviour:

i) sliding of the wall as shown in Figure 5.2a; ii) rocking of the wall as illustrated in Figure 5.2b; and iii) a combination of sliding and rocking of the wall (Figure 5.2c). The procedure to determine the resistance of CLT shear walls under different kinematic behaviour is discussed in the following sub-sections.



F_{sl} , F_r , F_{r-sl} = sliding, rocking, and sliding-rocking resistance, respectively

q = vertical load

h = height of the CLT panel

b = width of the CLT panel

N_{ix} , N_{iy} = reaction force in the fasteners in x and y direction, respectively

x_i = distance from connection i to the edge

Figure 5.2 Kinematic behaviour of single shear walls with brackets subjected to: (a) sliding, (b) rocking and (c) combined rocking-sliding

5.3.2.1 CLT shear wall subjected to sliding

The horizontal forces in a CLT shear wall under lateral loading are resisted by the brackets and the frictional resistance of the wall-to-floor/foundation interface. As discussed in section 5.2, the frictional contribution is ignored because, during an earthquake event, the vertical component of the ground motion can nullify its influence.

The brackets in a CLT shear wall usually have an equal number of fasteners and hence each bracket is expected to resist the same magnitude of horizontal force. In case of a CLT wall where brackets have an unequal number of fasteners, the brackets are expected to share the total sliding forces proportional to their stiffness (number of fasteners). The procedure herein assumes that the CLT shear walls have brackets with equal number of fasteners, i.e. each bracket resists equal sliding force. Therefore, the CLT shear wall resistance F_{sl} , is reached when all brackets reach their ultimate sliding resistance N_{xB} . It has been assumed that both the sliding (N_{xB}) and uplifting (N_{yB}) capacity (or ultimate resistance) of the brackets are equal –i.e. $N_{xB} = N_{yB} = N_B$.

Considering the summation of forces in the x -direction in Figure 5.2a,

$$F_{sl} = N_{1x} + N_{2x} + N_{3x} + N_{4x} = \sum_{i=1}^{i=n_B} N_{ix} \quad (5.1)$$

where N_{ix} is the sliding resistance (the maximum horizontal reaction force) of the connections. It can be assumed that the sliding resistance of the CLT shear wall is reached when all brackets have reached their ultimate resistance -i.e. $N_{ix} = N_B$. Therefore, Eq. (5.1) can be rewritten as:

$$F_{sl} = n_B N_B \quad (5.2)$$

where n_B is the number of brackets.

5.3.2.2 CLT shear wall subjected to rocking

The rocking behaviour of a single CLT shear wall is shown in Figure 5.2b. This procedure assumed that the wall rotates about a single point under lateral loading. The reaction forces of the connectors shall follow a triangular distribution. The rocking resistance of the CLT shear wall can be calculated by taking summation of the moment at the lower right corner of the wall in Figure 5.2b:

$$F_r h = N_{1y}x_1 + N_{2y}x_2 + N_{3y}x_3 + N_{4y}x_4 + q \frac{b^2}{2} \quad (5.3)$$

where N_{iy} is the rocking reaction of each connection, x_i is the distance of each connector from the right corner, b is the width of the CLT panel, q is the vertical load on top of the panel. The rocking resistance of the CLT shear wall is reached when the first bracket (left corner) has reached its ultimate resistance -i.e. $N_{1y} = N_B$. As seen in Eq. (5.3), the first bracket carries the maximum moment due to the rocking of the wall since it has the highest lever arm -i.e. it locates at a maximum distance from the right side of the wall, x_1 . Therefore, when it reaches its ultimate resistance (i.e. fails) the rocking resistance of the wall will reduce immediately with the subsequent failure of the rest of the brackets. Therefore, using the triangular distribution of the bracket's forces in Figure 5.2b, the reaction forces of the brackets can be written as:

$$\begin{aligned} N_{1y} &= N_B \\ N_{2y} &= (x_2 / x_1) N_B \\ N_{3y} &= (x_3 / x_1) N_B \\ N_{4y} &= (x_4 / x_1) N_B \end{aligned} \quad (5.4)$$

Substituting Eq. (5.4) into Eq. (5.3), the rocking resistance of the wall can be estimated as:

$$F_r h = N_B x_1 + N_B \left(\frac{x_2}{x_1} \right) x_2 + N_B \left(\frac{x_3}{x_1} \right) x_3 + N_B \left(\frac{x_4}{x_1} \right) x_4 + q \frac{b^2}{2} \quad (5.5)$$

$$F_r = \frac{N_B}{h x_1} \left(\sum_1^{n_B} x_i^2 \right) + q \frac{b^2}{2h} \quad (5.6)$$

where b and h are the width and height of CLT panel, q is the vertical load on top of the panel, N_B is the rocking resistance of brackets and x_i is the distance of the connectors (i to n_B) from the left to the right end of the shear wall.

In order to avoid sliding failure of the shear walls, the sliding resistance of the wall must be higher than the rocking resistance. For this, a minimum number of brackets is required:

$$n_B > \frac{F_r}{N_B} \quad (5.7)$$

5.3.2.3 CLT shear wall subjected to combined rocking & sliding

The combined rocking and sliding behaviour of a single CLT shear wall is shown in Figure 5.2c. In this case, the resistance of the CLT shear wall could be lower than the resistance of the wall under sliding and rocking only. As seen in Eqs. (5.2) and (5.6), both the sliding and rocking resistances are a function of the ultimate resistance of the bracket N_B which is measured in a uniaxial direction –i.e. shear or tension. In the case of a combined rocking-sliding action, the brackets experience both shear and tension forces as seen in Figure 5.2c. Therefore, the corner left bracket's capacity under combined rocking-sliding will reach at a value lower than its uniaxial ultimate resistance, N_B . The combined rocking-sliding reaction of the bracket can be calculated using the following linear interaction formula (ETA-06/0106, 2016):

$$\frac{N_{B,sl}}{N_B} + \frac{N_{B,r}}{N_B} \leq 1.0 \quad (5.8)$$

where $N_{B,sl}$ and $N_{B,r}$ are the sliding and rocking reaction of the brackets, respectively and N_B is the factored lateral resistance of the brackets. The bracket connections subjected to a combined rocking-sliding loading shall follow the inequalities as described in Eq. (5.8). The interaction diagram for the bracket connection is shown in Figure 5.3a. The equation is adopted from “*Guideline for European Technical Approval (ETAG)- Three Dimensional Nailing Plates*”. The document illustrates the technical assessment of angle brackets for timber-to-timber or timber-to-concrete connections. The technical report also shows that by using a quadratic interaction formula, a close-formed formula to determine the ultimate resistance of the bracket is not possible—i.e. it requires iteration which is not desirable for the design purposes. Therefore, the current procedure utilizes the linear interaction formula as described in Eq. (5.8).

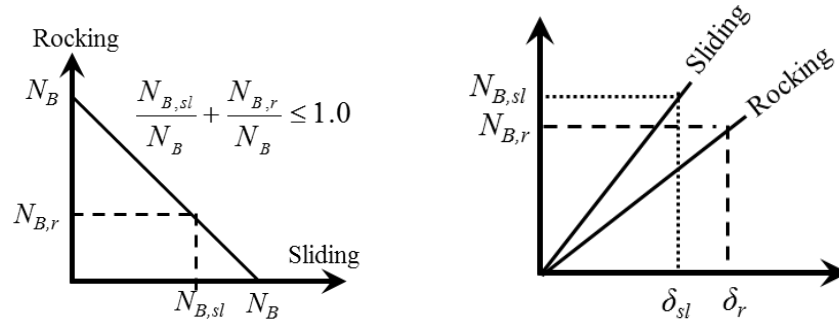


Figure 5.3 (a) Interaction diagram for bracket connection and (b) force-deformation relation for brackets under sliding and rocking

By taking the summation of the moment at the lower right corner of the wall in Figure 5.2c, the rocking-sliding capacity can be calculated as:

$$F_{r-sl} h = N_{1y}x_1 + N_{2y}x_2 + N_{3y}x_3 + N_{4y}x_4 + q \frac{b^2}{2} \quad (5.9)$$

The corner bracket will reach their resistance at a lower value -i.e. $N_{ly} = N_{B,r}$ due to the combined motion of the wall. The modified bracket resistance (i.e. rocking resistance) under rocking-sliding $N_{B,r}$, can be calculated using the interaction Eq. (5.8) as:

$$N_{B,r} = N_B - N_{B,sl} \quad (5.10)$$

The remainder of the brackets will follow the triangular load distribution as shown in Figure 5.2c which can be represented as:

$$\begin{aligned} N_{1y} &= N_B - N_{B,sl} \\ N_{2y} &= (x_2 / x_1)(N_B - N_{B,sl}) \\ N_{3y} &= (x_3 / x_1)(N_B - N_{B,sl}) \end{aligned} \quad (5.11)$$

where N_{iy} is the vertical reaction of the i^{th} brackets located at a distance x_i from the right side of the wall. Substituting Eq. (5.11) with Eq. (5.9):

$$\begin{aligned} F_{r-sl} h &= (N_B - N_{B,sl})x_1 + (N_B - N_{B,sl})\left(\frac{x_2}{x_1}\right)x_2 + (N_B - N_{B,sl})\left(\frac{x_3}{x_1}\right)x_3 \\ &+ (N_B - N_{B,sl})\left(\frac{x_4}{x_1}\right)x_4 + q \frac{b^2}{2} \end{aligned} \quad (5.12)$$

The lateral resistance of the CLT shear wall under combined rocking-sliding can be summarized as:

$$F_{r-sl} = \frac{N_B - N_{B,sl}}{h x_1} \left(\sum_1^{n_B} x_i^2 \right) + q \frac{b^2}{2h} \quad (5.13)$$

The sliding and rocking reaction of the brackets -i.e. $N_{B,sl}$ and $N_{B,r}$ -are assumed to be proportional to the shear wall's sliding (δ_{sl}) and rocking deformation (δ_r) as shown in Figure 5.3b. The ratio of the sliding to rocking deformations, δ_{sl} / δ_r , can be calculated using Eqs. (4.10) and (4.14):

$$\frac{N_{B,sl}}{N_{B,r}} = \frac{\delta_{sl}}{\delta_r} = \frac{\frac{F}{n_B k_B}}{\left(\frac{F \cdot h^2}{b^2} - \frac{qh}{2} \right) \frac{1}{k_B}} \quad (5.14)$$

where k_B is the stiffness of the brackets, n_B is the number of brackets, q is the vertical force on the wall, b and h are the width and the height of the wall, respectively.

Therefore, using Eqs. (5.8) and (5.14), the sliding and rocking reactions of the brackets, $N_{B,sl}$ and $N_{B,r}$ respectively, under combined rocking-sliding behaviour can be calculated in terms of the factored resistance of the brackets, N_B . As seen in Eq. (5.14), at a constant lateral force F , the ratio of $N_{B,sl} / N_{B,r}$ depends on the aspect ratio of the wall. Figure 5.4 shows some examples where the ratio of the sliding to rocking deformation is calculated in CLT shear walls with brackets. The wall aspect ratio, b/h are varied from 0.5 to 2.0. Figure 5.4 illustrates that with the increase in the aspect ratio from 0.5 to 2.0, the dominant kinematic behaviour of the wall has been shifted from a rocking to a sliding movement.

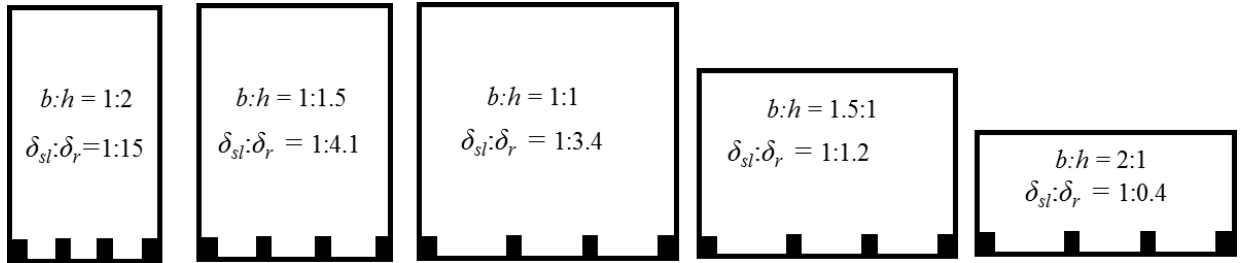


Figure 5.4 Ratio of sliding to rocking deformation with variation of aspect ratio in CLT shear walls with brackets

5.3.3 Single CLT shear wall with brackets and hold-downs

The kinematic behaviour of the CLT shear walls with brackets and hold-downs is plotted in Figure 5.5. The procedure to estimate the resistance of the single CLT shear wall due to sliding (Figure

5.5a), rocking (Figure 5.5b) and combined rocking-sliding (Figure 5.5c) is described in the following sections.

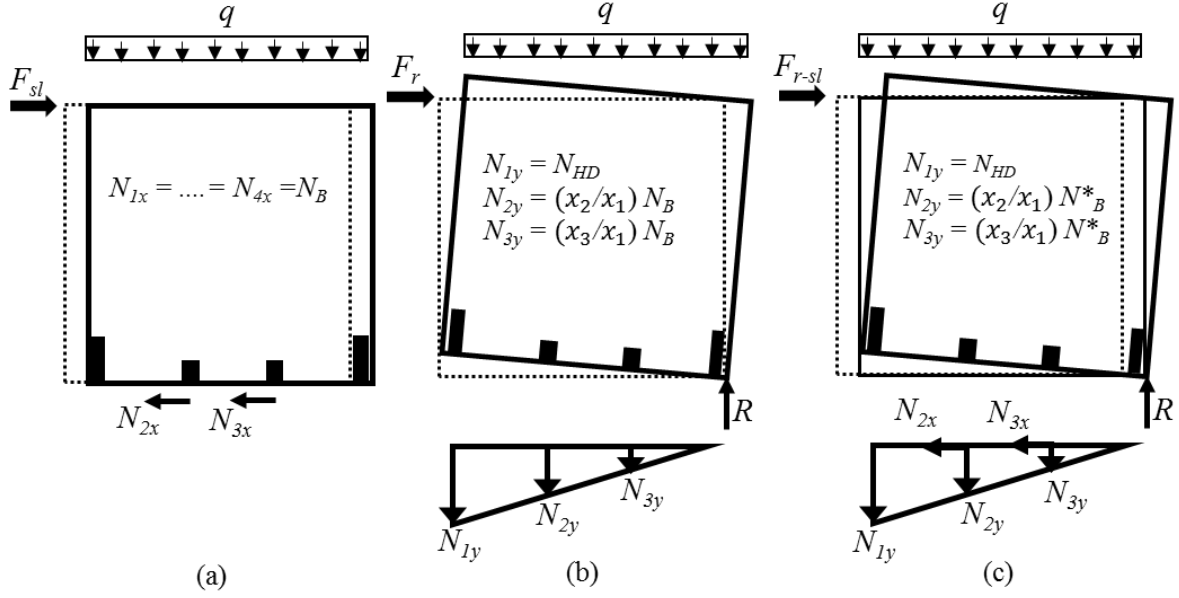
5.3.3.1 *CLT shear wall subjected to sliding*

The procedure assumed that the shear resistance of HDs and the frictional resistance at the wall-to-floor/foundation interface are negligible. Therefore, under sliding action, the brackets are the only connections which resist the horizontal forces. By adding the forces in x -direction as illustrated in Figure 5.5a:

$$F_{sl} = N_{2x} + N_{3x} = \sum^{n_B} N_{ix} \quad (5.15)$$

where N_{ix} is the sliding reaction of the bracket connections and n_B is the number of brackets. As discussed in section 5.3.2.2, the sliding resistance of the CLT shear wall will be reached only when all brackets have reached their ultimate resistance -i.e. $N_{ix} = N_B$. Therefore, Eq. (5.15) can be rewritten as:

$$F_{sl} = n_B N_B \quad (5.16)$$



F_{sl} , F_r , F_{r-sl} = sliding, rocking, and sliding-rocking resistance, respectively
 N_{ix} , N_{iy} = reaction force in the fasteners in x and y direction, respectively
 N_B = bracket's resistance
 N_{HD} = hold-down's resistance
 N_B^* = modified bracket's resistance
 x_i = distance from connection i to the edge
 q = vertical load
 h = height of the CLT panel
 b = width of the CLT panel

Figure 5.5 Kinematic behaviour of shear walls with brackets and HDs subjected to: (a) sliding, (b) rocking and (c) combined rocking-sliding

5.3.3.2 CLT shear wall subjected to rocking

The rocking resistance of the CLT shear wall's hold-down and bracket connections can be calculated by taking a summation of the moment at the lower right corner of the CLT shear wall (Figure 5.5b):

$$F_r h = N_{1y}x_1 + N_{2y}x_2 + N_{3y}x_3 + N_{4y}x_4 + q \frac{b^2}{2} \quad (5.17)$$

The rocking resistance of the CLT shear wall will be reached when the left hold-down has reached its ultimate resistance -i.e. $N_{1y} = N_{HD}$. The rocking reaction for the remainder of the brackets will follow the triangular load distribution as shown in Figure 5.5b. The brackets have lower stiffness and resistance under tension as discussed in Chapter 3 if they have same number of fasteners (Figure 5.6). The procedure assumed that when a bracket is placed at the location of the left corner hold-down it will reach its ultimate rocking resistance at the yield displacement of the hold-down v_y (Figure 5.6). The resistance of the two intermediate brackets can be calculated following the triangular distribution as:

$$\begin{aligned} N_{1y} &= N_{HD} \\ N_{2y} &= (x_2 / x_1) N_B \\ N_{3y} &= (x_3 / x_1) N_B \\ N_{4y} &= (x_4 / x_1) N_{HD} \end{aligned} \quad (5.18)$$

Substituting Eq. (5.18) into Eq. (5.17), the equilibrium equation of the wall under rocking can be written as:

$$F_r h = N_{HD} x_1 + N_B \left(\frac{x_2}{x_1} \right) x_2 + N_B \left(\frac{x_3}{x_1} \right) x_3 + N_{HD} \left(\frac{x_4}{x_1} \right) x_4 + q \frac{b^2}{2} \quad (5.19)$$

The contribution of the right hold-down is negligible since its distance from the right edge of the CLT panel x_4 (Figure 5.1) is close to zero. However, it should be noted that the resistance of the right hold-downs should be included if the hold-downs are not situated near the panel edges. For cases where the hold-down is close to the edge the rocking resistance can be represented by:

$$F_r = \frac{N_{HD} x_1}{h} + \frac{N_B}{x_1 h} \left(\sum_{i=1}^{n_B} x_i^2 \right) + q \frac{b^2}{2h} \quad (5.20)$$

As discussed before, the sliding resistance of the wall must be higher than the rocking resistance.

For this, the minimum number of brackets required can be estimated as:

$$n_B > \frac{F_r}{N_B} \quad (5.21)$$

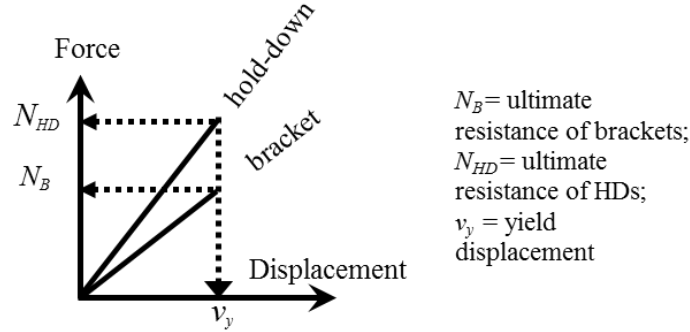


Figure 5.6 Elastic force-displacement relation among hold-down and bracket

5.3.3.3 CLT shear wall subjected to combined rocking & sliding

The combined rocking and sliding behaviour of a single CLT shear wall with brackets and hold-downs is shown in Figure 5.5c. As discussed in the previous section, due to the combined rocking-sliding behaviour, the actual resistance of the CLT shear wall could be lower than the predicted resistance under sliding or rocking only. A step by step procedure to determine the resistance of the CLT wall with brackets due to combined rocking-sliding is discussed in section 5.3.2.3. Similarly, the resistance of the wall with brackets and hold-downs can be estimated as:

$$F_{r-sl} h = N_{HD} x_1 + (N_B - N_{B,sl}) \left(\frac{x_2}{x_1} \right) x_2 + (N_B - N_{B,sl}) \left(\frac{x_3}{x_1} \right) x_3 + q \frac{b^2}{2} \quad (5.22)$$

Here, the intermediate brackets will follow a triangular load distribution as shown in Eq. (5.11).

The modified factored resistance of the brackets under combined rocking-sliding $N_{B,r}$, can be

calculated using Eq. (5.10). Therefore, the lateral resistance of the CLT shear wall with hold-downs under a combined rocking-sliding can be calculated as:

$$F_{r-sl} = \frac{N_{HD}x_1}{h} + \frac{N_B - N_{B,sl}}{x_1h} \left(\sum_{i=1}^{n_B} x_i^2 \right) + q \frac{b^2}{2h} \quad (5.23)$$

As seen in Eq. (5.23), the sliding reaction of the brackets $N_{B,sl}$, under a combined rocking-sliding action can be estimated from the linear interaction formula (Eq. 5.8) and the ratio of the sliding to rocking deformations δ_{sl} / δ_r as:

$$\frac{N_{B,sl}}{N_{B,r}} = \frac{\delta_{sl}}{\delta_r} = \frac{\frac{F}{n_B k_B}}{\left(\frac{F \cdot h^2}{b^2} - \frac{qh}{2} \right) \frac{1}{k_{HD}}} \quad (5.24)$$

where k_B and k_{HD} is the stiffness of the bracket and hold-down, respectively, n_B is the number of brackets, q is the vertical force on the wall and b and h are the width and the height of the wall, respectively.

The ratio $N_{B,sl} / N_{B,r}$ depends on the aspect ratio of the wall. Figure 5.7 shows some examples where the ratio of the sliding to rocking deformation is calculated in CLT shear walls with both brackets and hold-downs. The wall aspect ratio b/h is varied from 0.5 to 2.0. Figure 5.7 shows that with the increase in the aspect ratio from 0.5 to 2.0, the dominant kinematic behaviour of the wall has been shifted from a rocking to a sliding movement.

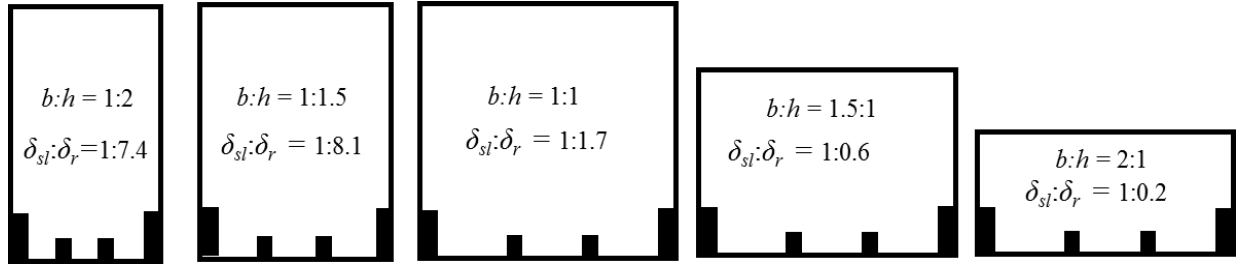
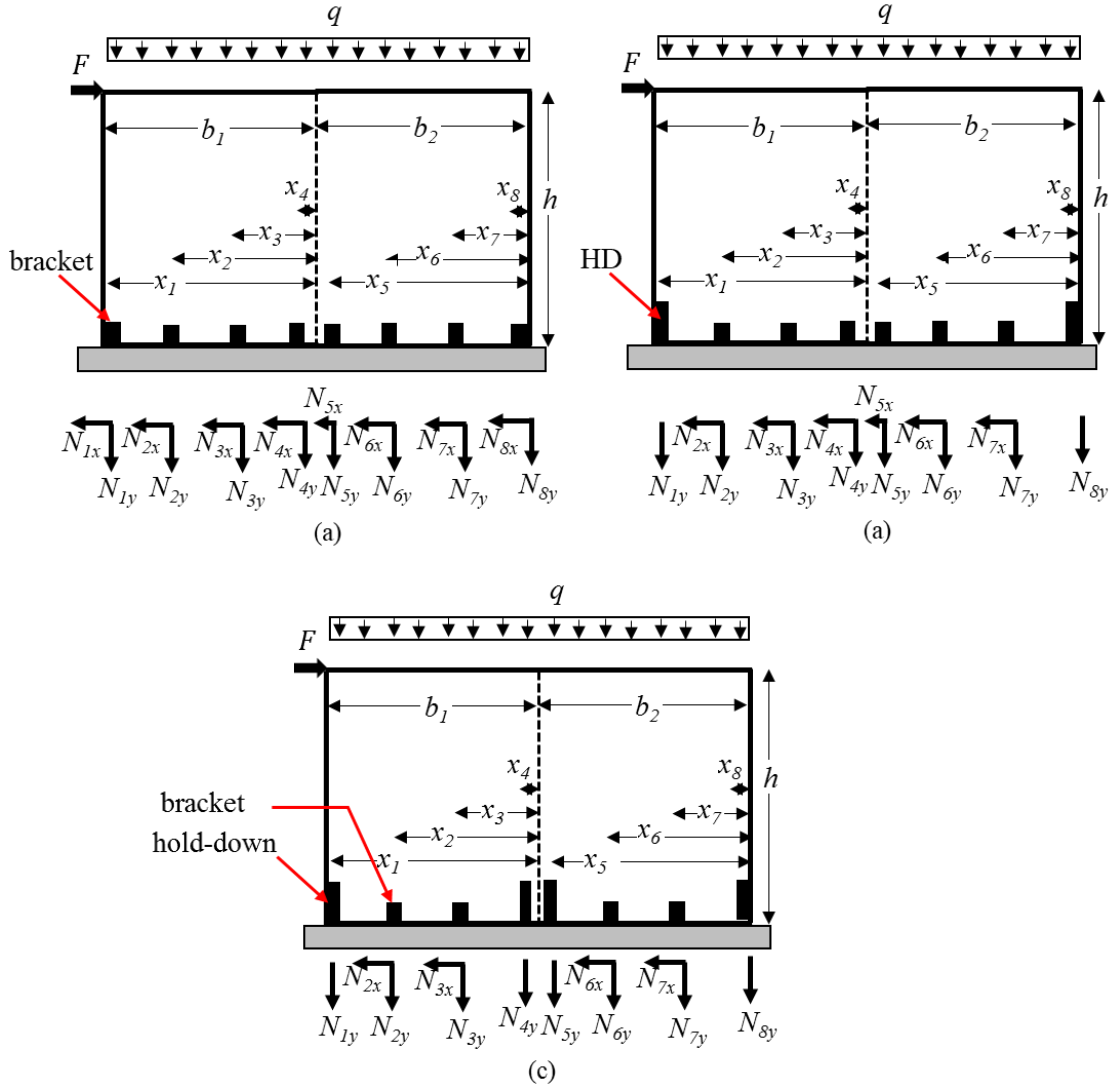


Figure 5.7 Ratio of sliding to rocking deformation with variation of aspect ratio in CLT shear walls with brackets and HDs

5.4 Resistance of Coupled CLT Shear Walls

The kinematic behaviour of coupled CLT shear walls with brackets and hold-downs is plotted in Figure 5.8. A step by step detailed procedure is described in the following sections to estimate the resistance of coupled shear walls under sliding (Figure 5.8a), rocking (Figure 5.8b) and combined rocking-sliding (Figure 5.8c). Three types of configurations have been considered: (a) a coupled wall with brackets, (b) a coupled wall with 2-HDs and brackets and (c) a coupled wall with 4-HDs and brackets. The proposed equations were derived based on the kinematic behaviour of coupled shear with two panels. However, the equations can be expanded for coupled shear walls with more than two panels.



F = lateral force; q = vertical load; h = height of the CLT panel; b = width of the CLT panel
 N_{ix} , N_{iy} = reaction force in the fasteners in x and y direction, respectively;
 x_i = distance from connection i to the edge

Figure 5.8 Resistance of coupled CLT shear walls: (a) with brackets only, (b) with 2-HDs and brackets, and (c) with 4-HDs and brackets

5.4.1 Coupled CLT shear wall with brackets only

5.4.1.1 CLT coupled shear wall subjected to sliding

It is assumed that all brackets have an equal fastener sliding resistance at the point of yielding. The lateral resistance of the CLT shear wall F_{sl} , is reached when all the brackets have reached their

designed lateral resistance N_B . The sliding resistance of the wall can be estimated from the equilibrium of the forces in the x -direction in Figure 5.9a:

$$F_{sl} = N_{1x} + N_{2x} + \dots + N_{8x} = \sum_{i=1}^{i=n_B} N_{ix} \quad (5.25)$$

where N_{ix} is the sliding reaction of the connections. We can now assume that the sliding resistance of the CLT shear wall is reached only when all brackets have reached their factored resistance, i.e. $N_{ix} = N_B$. Therefore, Eq. (5.25) can be rewritten as:

$$F_{sl} = n_B N_B \quad (5.26)$$

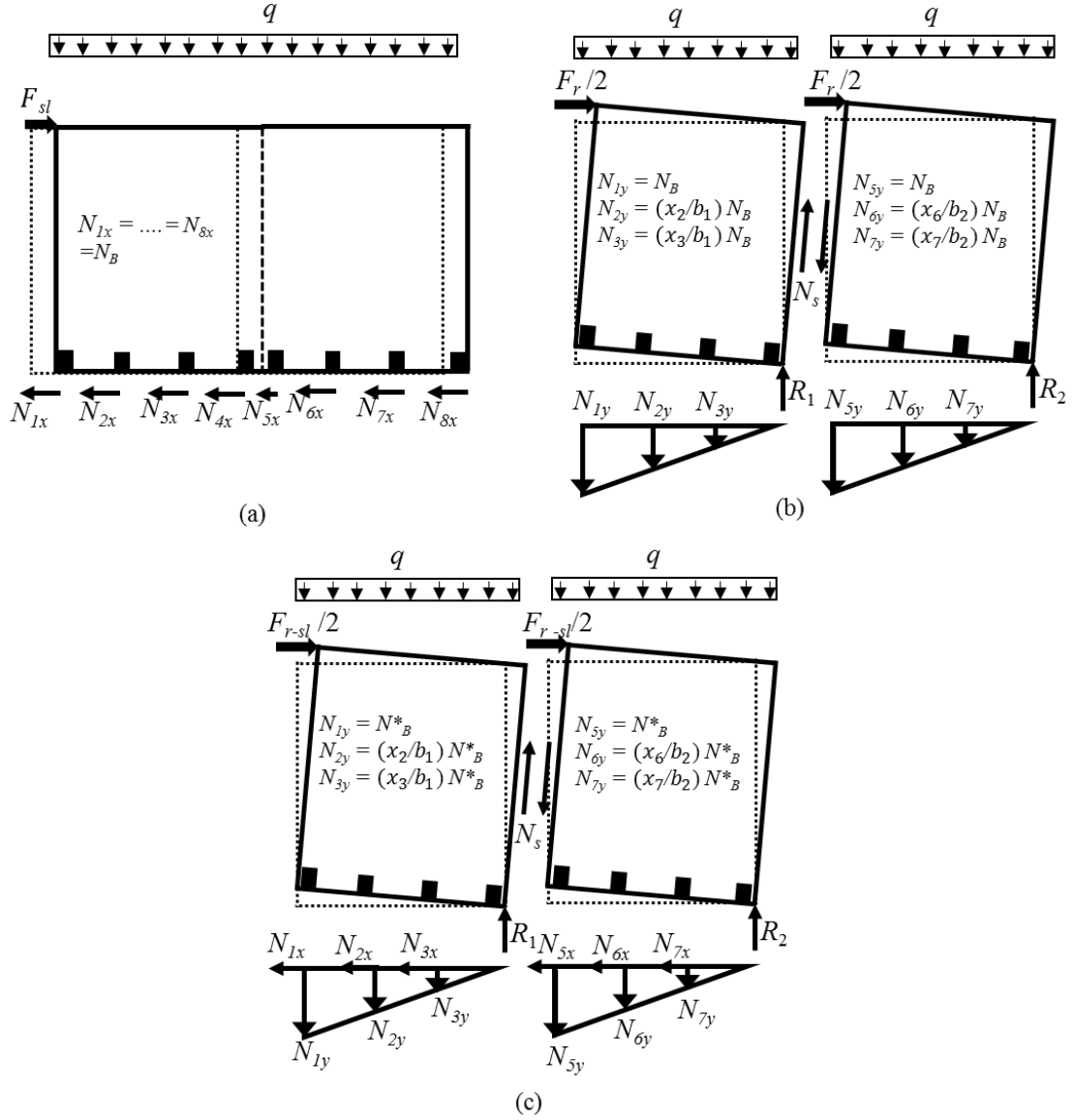
5.4.1.2 CLT coupled wall shear wall subjected to rocking

The rocking resistance of the CLT shear wall's hold-down and bracket connections can be calculated by taking the moment at the lower right corner of the CLT shear wall (Figure 5.9b):

$$F_r h + R_l b_2 = N_{1y}(x_1 + b_2) + N_{2y}(x_2 + b_2) + N_{3y}(x_3 + b_2) + N_{5y}x_5 + N_{6y}x_6 + N_{7y}x_7 + q \frac{b^2}{2} \quad (5.27)$$

where N_{iy} is the rocking reaction of each of the connections, x_i is the distance of each connector from the right corner of the panel, b_1 and b_2 are the widths of the left and right panels, b is the total width of the CLT shear wall ($b = b_1 + b_2$) and q is the vertical load on top of the wall.

The rocking resistance of the CLT shear wall will be reached when the left corner bracket has reached its factored resistance -i.e. $N_{1y} = N_B$. The rocking reaction for the remainder of the brackets will follow a triangular load distribution as shown in Figure 5.9b.



F_{sl} , F_r , F_{r-sl} = sliding, rocking, and sliding-rocking resistance, respectively; N_{ix} , N_{iy} = reaction force in the fasteners in x and y direction, respectively; N_B = bracket's resistance; N_{HD} = hold-down's resistance; N_B^* = modified bracket's resistance; x_i = distance from connection i to the edge; q = vertical load; h = height of the CLT panel; b = width of the CLT panel

Figure 5.9 Kinematic behaviour of coupled shear wall with brackets subjected to: (a) sliding, (b) rocking, and (c) combined rocking-sliding

Therefore, the reaction forces of the brackets can be written as:

$$\begin{aligned}
N_{1y} &= N_B \\
N_{2y} &= (x_2 / b_1) N_B \\
N_{3y} &= (x_3 / b_1) N_B \\
N_{5y} &= (x_5 / b_2) N_B \\
N_{6y} &= (x_6 / b_2) N_B \\
N_{7y} &= (x_7 / b_2) N_B
\end{aligned} \tag{5.28}$$

where N_{iy} is the vertical reaction of the i^{th} bracket located at a distance x_i from the right side of each segment of the wall and b_1 and b_2 are the widths of the left and right panels of the coupled wall, respectively.

The reaction force R_l can be calculated from the equilibrium of the forces in the y-direction for the left panel only:

$$N_{1y} + N_{2y} + N_{3y} + qb_1 = N_s + R_l \tag{5.29}$$

The screws in the vertical joints will yield first and will reach their shear resistance N_s , which can be calculated using Eq. (5.29). Substituting the vertical reaction forces from Eq. (5.28) with Eq. (5.29), the equation can be rewritten as:

$$R_l = N_B + N_B \left(\frac{x_2}{b_1} \right) + N_B \left(\frac{x_3}{b_1} \right) + qb_1 - N_s \tag{5.30}$$

The contribution of the right hold-downs from each panel can be ignored as their edge distances are negligible. Therefore, by substituting R_l from Eq. (5.30), the rocking resistance for a CLT coupled shear wall can be estimated as:

$$F_r = \frac{1}{h} \left[N_B x_1 + \frac{N_B}{b_1} (x_2^2 + x_3^2) + \frac{N_B}{b_2} (x_5^2 + x_6^2 + x_7^2) + q \frac{b^2}{2} - qb_1 b_2 + N_s b_2 \right] \tag{5.31}$$

Eq. (5.31) can be simplified as Eq. (5.32) if we consider equal panel length -i.e. $b_1 = b_2 = b / 2$,

$$F_r = \frac{1}{h} \left[\frac{2N_B}{b} \left(\sum_{i=1}^{n_B} x_i^2 \right) + q \frac{b^2}{4} + \frac{N_S b}{2} \right] \quad (5.32)$$

The failure of the coupled shear walls is avoided by providing a minimum number of brackets as:

$$n_B > \frac{F_r}{N_B} \quad (5.33)$$

5.4.1.3 CLT coupled wall subjected to combined rocking-sliding

Similar to a single shear wall, the resistance of a coupled CLT shear wall could be lower under combined rocking-sliding when compared to a wall subjected to sliding or rocking only. By taking the moment at the lower right corner of the CLT shear wall (Figure 5.9c):

$$F_{r-sl} h + R_1 b_2 = N_{1y}(x_1 + b_2) + N_{2y}(x_2 + b_2) + N_{3y}(x_3 + b_2) + N_{5y}x_5 + N_{6y}x_6 + N_{7y}x_7 + q \frac{b^2}{2} \quad (5.34)$$

The reaction of the brackets will follow a triangular load distribution as shown in Figure 5.9c, where it is assumed, the bracket will reach its factored rocking resistance at the yield displacement of v_y (Figure 5.6). Therefore, the reaction forces of the brackets determined as described in section 5.3.2.3 and calculated as:

$$\begin{aligned} N_{1y} &= N_{B,r} \\ N_{2y} &= (x_2 / b_1) N_{B,r} \\ N_{3y} &= (x_3 / b_1) N_{B,r} \\ N_{5y} &= (x_5 / b_2) N_{B,r} \\ N_{6y} &= (x_6 / b_2) N_{B,r} \\ N_{7y} &= (x_7 / b_2) N_{B,r} \end{aligned} \quad (5.35)$$

where N_{iy} is the vertical reaction of the i^{th} brackets located at a distance x_i from the right side of each wall segment in the coupled wall as shown in Figure 5.9c.

The reaction force R_l in Figure 5.9c can be calculated by taking a summation of forces in the y -direction on the left panel:

$$N_{1y} + N_{2y} + N_{3y} + qb_1 = N_s + R_l \quad (5.36)$$

The modified factored resistance of the brackets can be calculated from Eq. (5.37):

$$N_{B,r} = N_B - \max \{ N_{B,sl,i} \} \quad (5.37)$$

where N_B is the factored resistance of the bracket, $N_{B,r}$ is the modified factored resistance of the bracket under combined rocking-sliding, and $N_{B,sl,i}$ is the sliding reaction of the bracket of each wall segment in the coupled wall. The sliding and rocking reaction of the brackets can be calculated using the linear interaction formula in Eq. (5.38) and the ratio of sliding to rocking reaction $N_{B,sl,i} / N_{B,r,i}$ in Eq. (5.39):

$$\frac{N_{B,sl,i}}{N_B} + \frac{N_{B,r,i}}{N_B} \leq 1.0 \quad (5.38)$$

$$\frac{N_{B,sl,i}}{N_{B,r,i}} = \frac{\frac{F_i}{n_{B,i} k_{B,i}}}{\left(\frac{F_i \cdot h^2}{b_i^2} - \frac{qh}{2} \right) \frac{1}{k_B}} \quad (5.39)$$

Substituting Eqs. (5.35) and (5.36) into Eq. (5.34), the combined rocking-sliding capacity of the coupled shear wall with brackets can be expressed as:

$$F_{r-sl} = \frac{1}{h} \left[N_{B,r} x_1 + \frac{N_{B,r}}{b_1} (x_2^2 + x_3^2) + \frac{N_{B,r}}{b_2} (x_5^2 + x_6^2 + x_7^2) + q \frac{b^2}{2} - qb_1 b_2 + N_s b_2 \right] \quad (5.40)$$

For an equal panel length -i.e. $b_1 = b_2 = b/2$, Eq. (5.37) can be simplified as:

$$F_{r-sl} = \frac{1}{h} \left[\frac{2(N_B - \max\{N_{B,sl,i}\})}{b} \left(\sum_{i=1}^{n_B} x_i^2 \right) + q \frac{b^2}{4} + \frac{N_S b}{2} \right] \quad (5.41)$$

5.4.2 CLT coupled shear wall with brackets and 2-hold-downs

This section describes a procedure to estimate the capacity of coupled CLT shear walls with brackets and 2-hold-downs, where the hold-downs are placed at the outer edge of the panels only as seen in Figure 5.8b.

5.4.2.1 CLT coupled shear wall subjected to sliding

By ignoring the sliding resistance of the 2-hold-downs (as seen in Figure 5.10a) the total resistance of the coupled shear wall subjected to sliding only can be calculated using Eq. (5.42):

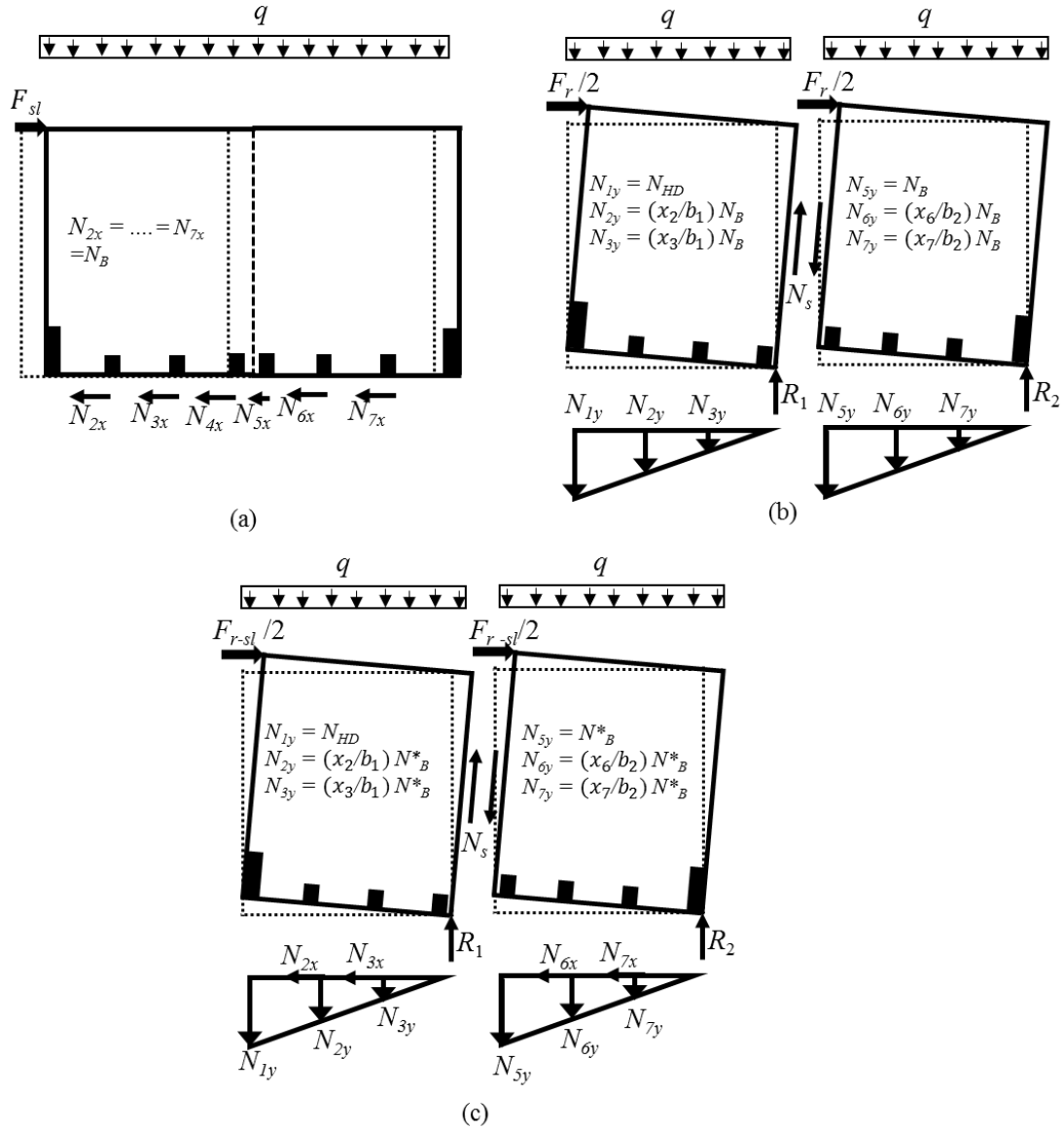
$$F_{sl} = n_B N_B \quad (5.42)$$

5.4.2.2 CLT coupled wall shear wall subjected to rocking

The rocking resistance of the CLT shear wall hold-down and bracket connections can be calculated by taking the moment at the lower right corner of the CLT shear wall (Figure 5.10b):

$$F_r h + R_1 b_2 = N_{1y}(x_1 + b_2) + N_{2y}(x_2 + b_2) + N_{3y}(x_3 + b_2) + N_{5y}x_5 + N_{6y}x_6 + N_{7y}x_7 + q \frac{b^2}{2} \quad (5.43)$$

where N_{iy} is the rocking reaction of each of the connections, x_i is the distance of each connector from the right corner of the panel, b_1 and b_2 are the widths of left and right panels, b is the total width of the CLT shear wall ($b = b_1 + b_2$) and q is the vertical load on top of the panel.



F_{sl} , F_r , F_{r-sl} = sliding, rocking, and sliding-rocking resistance, respectively; N_{ix} , N_{iy} = reaction force in the fasteners in x and y direction, respectively; N_B = bracket's resistance; N_{HD} = hold-down's resistance; N_B^* = modified bracket's resistance; x_i = distance from connection i to the edge; q = vertical load; h = height of the CLT panel; b = width of the CLT panel

Figure 5.10 Kinematic behaviour of coupled shear wall with brackets and 2-hold-downs subjected to: (a) sliding, (b) rocking and (c) combined rocking-sliding

The rocking resistance of the CLT coupled wall is reached when the hold-down in the left panel has reached its factored resistance -i.e. $N_{1y} = N_{HD}$. The rocking reaction for the intermediate brackets

in the wall will follow a triangular load distribution which follows Eq. (5.44) as shown in Figure 5.10b.

$$\begin{aligned}
N_{1y} &= N_{HD} \\
N_{2y} &= (x_2 / b_1) N_B \\
N_{3y} &= (x_3 / b_1) N_B \\
N_{5y} &= (x_5 / b_2) N_B \\
N_{6y} &= (x_6 / b_2) N_B \\
N_{7y} &= (x_7 / b_2) N_B
\end{aligned} \tag{5.44}$$

where N_{iy} is the vertical reaction of the i^{th} brackets located at a distance x_i from the right side of each segment of the wall and b_1 and b_2 are the widths of the coupled wall's left and right panels, respectively.

The reaction forces R_l can be calculated from the equilibrium of the forces in the y-direction for the left panel only:

$$N_{1y} + N_{2y} + N_{3y} + qb_1 = N_s + R_l \tag{5.45}$$

Substituting the vertical reaction forces from Eq. (5.44) into Eq. (5.45), the equation can then be rewritten as:

$$R_l = N_{HD} + N_B \left(\frac{x_2}{b_1} \right) + N_B \left(\frac{x_3}{b_1} \right) + qb_1 - N_s \tag{5.46}$$

Rearranging Eq. (5.43), the rocking resistance of CLT coupled shear wall with brackets and 2-HDs can be estimated as:

$$F_r = \frac{1}{h} \left[N_{HD} x_1 + \frac{N_B}{b_1} (x_2^2 + x_3^2) + \frac{N_B}{b_2} (x_5^2 + x_6^2 + x_7^2) + q \frac{b^2}{2} - qb_1 b_2 + N_s b_2 \right] \tag{5.47}$$

Eq. (5.44) can be simplified considering equal panel length -i.e. $b_1 = b_2 = b / 2$:

$$F_r = \frac{1}{h} \left[\frac{N_{HD} b}{2} + \frac{2N_B}{b} \left(\sum^{n_B} x_i^2 \right) + q \frac{b^2}{4} + \frac{N_S b}{2} \right] \quad (5.48)$$

Failure of the coupled shear walls can be avoided by providing a minimum number of brackets:

$$n_B > \frac{F_r}{N_B} \quad (5.49)$$

5.4.2.3 CLT coupled wall subjected to combined rocking-sliding

The resistance of the coupled CLT shear wall could be lower under combined rocking-sliding when compared to a wall subjected to sliding or rocking only. By taking the moment at the lower right corner of the CLT shear wall (Figure 5.10c):

$$F_{r-sl} h + R_l b_2 = N_{1y}(x_1 + b_2) + N_{2y}(x_2 + b_2) + N_{3y}(x_3 + b_2) + N_{5y}x_5 + N_{6y}x_6 + N_{7y}x_7 + q \frac{b^2}{2} \quad (5.50)$$

The rocking resistance of the CLT coupled wall is reached when the hold-down in the left panel reaches its factored resistance i.e. $N_{1y} = N_{HD}$. The rocking reaction for the remainder of the brackets will follow a triangular load distribution as shown in Figure 5.10c. Therefore, the reaction forces of the brackets can be written as:

$$\begin{aligned} N_{1y} &= N_{HD} \\ N_{2y} &= (x_2 / b_1) N_{B,r} \\ N_{3y} &= (x_3 / b_1) N_{B,r} \\ N_{5y} &= (x_5 / b_2) N_{B,r} \\ N_{6y} &= (x_6 / b_2) N_{B,r} \\ N_{7y} &= (x_7 / b_2) N_{B,r} \end{aligned} \quad (5.51)$$

The reaction forces R_l , in Figure 5.10c can be calculated by taking a summation of the forces in the y-direction for the left panel only:

$$N_{1y} + N_{2y} + N_{3y} + qb_1 = N_s + R_1 \quad (5.52)$$

The modified factored resistance of the brackets can be calculated as:

$$N_{B,r} = N_B - \max \{ N_{B,sl,i} \} \quad (5.53)$$

where N_B is the factored resistance of the bracket, $N_{B,r}$ is the modified factored resistance of the bracket under combined rocking-sliding, and $N_{B,sl,i}$ is the sliding reaction of the bracket of each wall segment in the coupled wall. The sliding and rocking reaction of the brackets can be calculated using the linear interaction formula in Eq. (5.54) and from the ratio of sliding to rocking reaction

$N_{B,sl,i} / N_{B,r,i}$ as:

$$\frac{N_{B,sl,i}}{N_B} + \frac{N_{B,r,i}}{N_B} \leq 1.0 \quad (5.54)$$

$$\frac{N_{B,sl,i}}{N_{B,r,i}} = \frac{\frac{F_i}{n_{B,i} k_{B,i}}}{\left(\frac{F_i \cdot h^2}{b_i^2} - \frac{qh}{2} \right) \frac{1}{k_{HD}}} \quad (5.55)$$

The combined rocking-sliding resistance of the coupled shear wall with brackets and 2-HDs from Eq. (5.50) can thus be rewritten as:

$$F_{r-sl} = \frac{1}{h} \left[N_{HD} x_1 + \frac{N_{B,r}}{b_1} (x_2^2 + x_3^2) + \frac{N_{B,r}}{b_2} (x_5^2 + x_6^2 + x_7^2) + q \frac{b^2}{2} - qb_1 b_2 + N_s b_2 \right] \quad (5.56)$$

For an equal panel length -i.e. $b_1 = b_2 = b/2$, Eq. (5.56) can be simplified as:

$$F_{r-sl} = \frac{1}{h} \left[\frac{b N_{HD}}{2} + \frac{2(N_B - \max \{ N_{B,sl,i} \})}{b} \left(\sum x_i^2 \right) + q \frac{b^2}{4} + \frac{N_s b}{2} \right] \quad (5.57)$$

5.4.3 CLT coupled shear wall with brackets and 4-hold-downs

The procedure to estimate the resistance of coupled CLT shear walls with brackets and 4-hold-downs is discussed in this section. Each panel in the shear wall contains two hold-downs placed at both the outer and inner edges of the panel as seen in Figure 5.8c.

5.4.3.1 CLT coupled shear wall subjected to sliding

The sliding resistance of the coupled shear wall with brackets and 4-hold-downs (Figure 5.11a) would be the same as described in Eq. (5.58):

$$F_{sl} = n_B N_B \quad (5.58)$$

5.4.3.2 CLT coupled wall shear wall subjected to rocking

The rocking resistance of the CLT shear wall's hold-down and bracket connections can be calculated by taking the moment at the lower right corner of the CLT shear wall (Figure 5.11b):

$$F_r h + R_1 b_2 = N_{1y}(x_1 + b_2) + N_{2y}(x_2 + b_2) + N_{3y}(x_3 + b_2) + N_{5y}x_5 + N_{6y}x_6 + N_{7y}x_7 + q \frac{b^2}{2} \quad (5.59)$$

where N_{iy} is the rocking reaction of each of the connections, x_i is the distance of each connector from the right corner of the panel, b_1 and b_2 are the respective widths of the left and right panels, b is the total width of the CLT shear wall ($b = b_1 + b_2$) and q is the vertical load on top of the panel.

The rocking resistance of the CLT coupled wall is reached when the hold-down in the left panel reaches its factored resistance -i.e. $N_{1y} = N_{HD}$. The rocking reaction for the remainder of the brackets will follow the triangular load distribution as shown in Figure 5.11b:

$$\begin{aligned}
N_{1y} &= N_{HD} \\
N_{2y} &= (x_2 / b_1) N_B \\
N_{3y} &= (x_3 / b_1) N_B \\
N_{5y} &= (x_5 / b_2) N_B \\
N_{6y} &= (x_6 / b_2) N_B \\
N_{7y} &= (x_7 / b_2) N_B
\end{aligned} \tag{5.60}$$

where N_{iy} is the vertical reaction of the i^{th} brackets located at a distance x_i from the right side of each segment of the wall and b_1 and b_2 are the widths of the coupled wall's left and right panels, respectively.

The reaction force R_l can be calculated by taking a summation of forces in the y-direction for the left panel only:

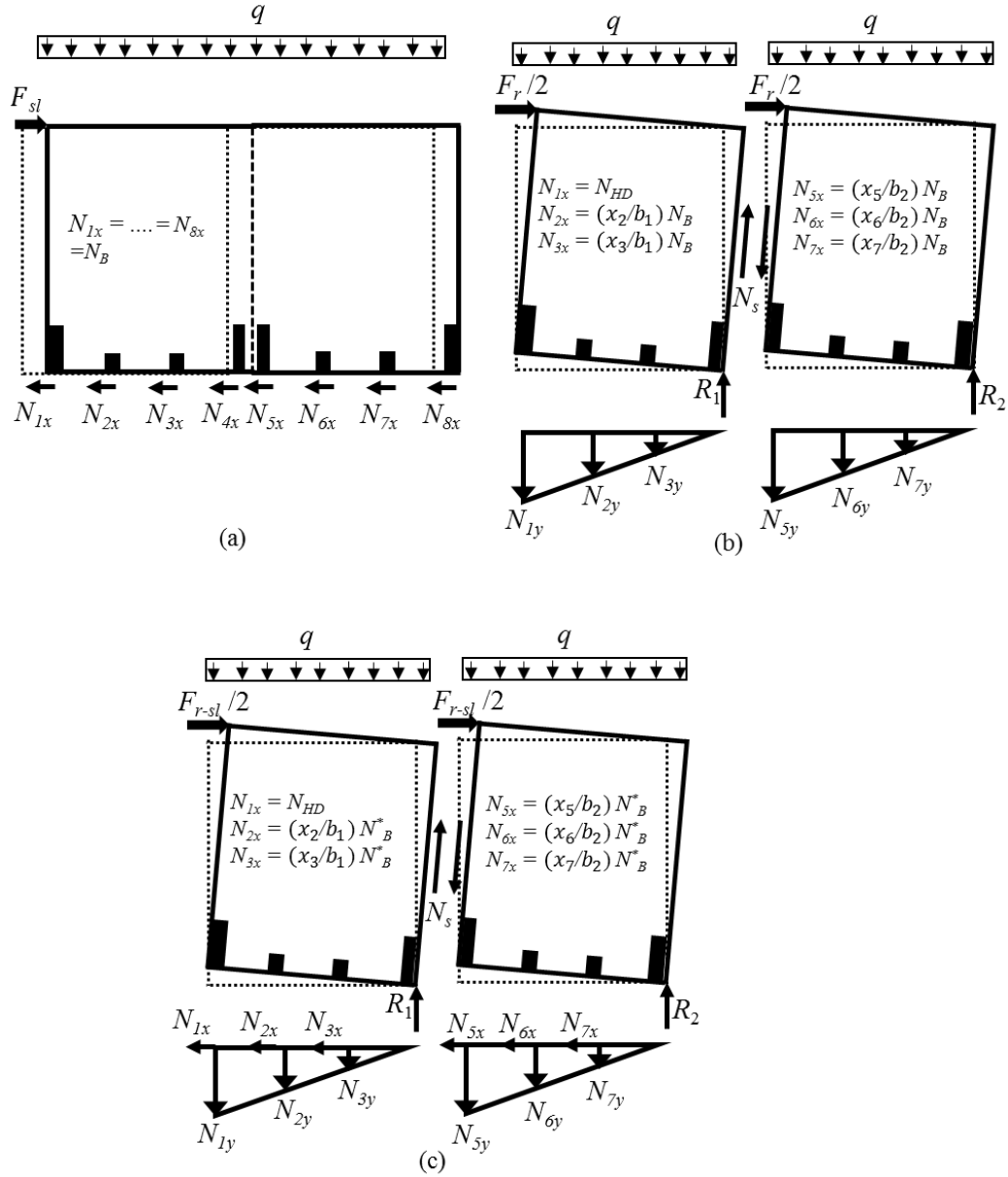
$$N_{1y} + N_{2y} + N_{3y} + qb_1 = N_s + R_l \tag{5.61}$$

By substituting Eqs. (5.60) and (5.61) with Eq. (5.59), the rocking resistance for a CLT coupled shear wall with brackets and four hold-downs can be determined as:

$$F_r = \frac{1}{h} \left[N_{HD}(x_1 + x_5) + \frac{N_B}{b_1}(x_2^2 + x_3^2) + \frac{N_B}{b_2}(x_6^2 + x_7^2) + q \frac{b^2}{2} - qb_1b_2 + N_sb_2 \right] \tag{5.62}$$

Eq. (5.62) can be simplified considering equal panel length -i.e. $b_1 = b_2 = b / 2$:

$$F_r = \frac{1}{h} \left[N_{HD}b + \frac{2N_B}{b} \left(\sum_{i=1}^{n_B} x_i^2 \right) + q \frac{b^2}{4} + \frac{N_sb}{2} \right] \tag{5.63}$$



F_{sl} , F_r , F_{r-sl} = sliding, rocking, and sliding-rocking resistance, respectively; N_{ix} , N_{iy} = reaction force in the fasteners in x and y direction, respectively; N_B = bracket's resistance; N_{HD} = hold-down's resistance; N_B^* = modified bracket's resistance; x_i = distance from connection i to the edge; q_v = vertical load; h = height of the CLT panel; b = width of the CLT panel

Figure 5.11 Kinematic behaviour of coupled shear wall with brackets and 4-hold-downs subjected to: (a) sliding, (b) rocking, and (c) combined rocking-sliding

5.4.3.3 CLT coupled wall subjected to combined rocking-sliding

The combined rocking-sliding resistance of the coupled shear wall with brackets and 4-HDs can be estimated by taking the moment at the lower right corner of the CLT shear wall (Figure 5.11c):

$$F_{r-sl} h + R_1 b_2 = N_{1y}(x_1 + b_2) + N_{2y}(x_2 + b_2) + N_{3y}(x_3 + b_2) + N_{5y}x_5 + N_{6y}x_6 + N_{7y}x_7 + q \frac{b^2}{2} \quad (5.64)$$

The rocking resistance of the CLT coupled wall is reached when the hold-down in the left panel reaches its factored resistance, i.e. $N_{1y} = N_{HD}$. The rocking reaction for the remainder of the brackets will follow the triangular load distribution as shown in Figure 5.11c. Therefore, the reaction forces of the brackets can be written as:

$$\begin{aligned} N_{1y} &= N_{HD} \\ N_{2y} &= (x_2 / b_1) N_{B,r} \\ N_{3y} &= (x_3 / b_1) N_{B,r} \\ N_{5y} &= (x_5 / b_2) N_{B,r} \\ N_{6y} &= (x_6 / b_2) N_{B,r} \\ N_{7y} &= (x_7 / b_2) N_{B,r} \end{aligned} \quad (5.65)$$

where the modified factored resistance of the brackets can be calculated from Eq. (5.66):

$$N_{B,r} = N_B - \max \{ N_{B,sl,i} \} \quad (5.66)$$

where N_B is the factored resistance of the bracket, $N_{B,r}$ is the modified factored resistance of the bracket under combined rocking-sliding, and $N_{B,sl,i}$ is the sliding reaction of each wall segment in the coupled wall. The sliding and rocking reaction of the brackets can be calculated using Eq. (5.54) and the ratio of sliding to rocking reaction $N_{B,sl,i} / N_{B,r,i}$ as described in Eq. (5.55).

The combined rocking-sliding resistance of the coupled shear wall with brackets and 4-HDs from Eq. (5.67) can be rewritten as:

$$F_{r-sl} = \frac{1}{h} \left[N_{HD}(x_1 + x_5) + \frac{N_{B,r}}{b_1}(x_2^2 + x_3^2) + \frac{N_{B,r}}{b_2}(x_6^2 + x_7^2) + q \frac{b^2}{2} - qb_1b_2 + N_sb_2 \right] \quad (5.67)$$

For an equal panel length, i.e. $b_1 = b_2 = b/2$, Eq. (5.67) can be simplified as:

$$F_{r-sl} = \frac{1}{h} \left[N_{HD}b + \frac{2(N_B - \max\{N_{B,sl,i}\})}{b} \left(\sum_{i=1}^{n_B} x_i^2 \right) + q \frac{b^2}{4} + \frac{N_sb}{2} \right] \quad (5.68)$$

5.5 Yielding of Vertical Shear Connectors in Coupled CLT Shear Wall

In the case of a coupled shear wall it has been assumed that the vertical joints in between two panels should yield first before the brackets and hold-downs. Here, the ultimate resistance of the vertical shear connectors must follow the criteria in Eqs. (5.69) and (5.70).

Coupled shear wall with brackets only:

$$N_s < \frac{N_B}{b_1} \left(\sum_{i=1}^{n_{Bl}} x_i \right) + qb_1 \quad (5.69)$$

Coupled shear wall with brackets and hold-downs:

$$N_s < N_{HD} + \frac{N_B}{b_1} \left(\sum_{i=1}^{n_{Bl}} x_i \right) + qb_1 \quad (5.70)$$

where n_{Bl} is the number of brackets in the left panel only.

5.6 Overview of equations to estimate the resistance of CLT shear walls

The formulas to estimate the resistance of single and coupled CLT shear walls proposed in this chapter and summarized in Figure 5.12 and Figure 5.13, respectively, are based on the kinematic behaviour of the shear wall when subjected to sliding, rocking and combined rocking-sliding.

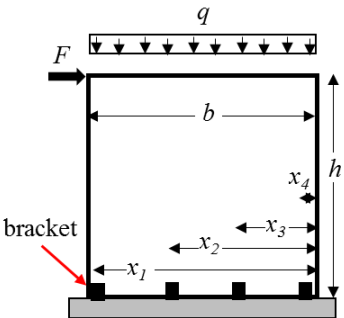
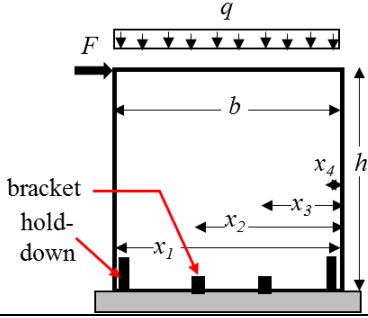
Single CLT shear wall with brackets	
	<p>Rocking:</p> $F_r = \frac{N_B}{h x_1} \left(\sum_1^{n_B} x_i^2 \right) + q \frac{b^2}{2h}$ <p>Combined rocking-sliding:</p> $F_{r-sl} = \frac{N_B - N_{B,sl}}{h x_1} \left(\sum_1^{n_B} x_i^2 \right) + q \frac{b^2}{2h}$
Single CLT shear wall with brackets and HDs	
	<p>Rocking:</p> $F_r = \frac{N_{HD} x_1}{h} + \frac{N_B}{x_1 h} \left(\sum_1^{n_B} x_i^2 \right) + q \frac{b^2}{2h}$ <p>Combined rocking-sliding:</p> $F_{r-sl} = \frac{N_{HD} x_1}{h} + \frac{N_B - N_{B,sl}}{x_1 h} \left(\sum_1^{n_B} x_i^2 \right) + q \frac{b^2}{2h}$
<p>F_r, F_{r-sl} = rocking and combined sliding-rocking resistances, respectively q = vertical load h = height of the CLT panel b = width of the CLT panel x_i = distance from connection i to the edge N_B = bracket's resistance N_{HD} = hold-down's resistance N_B^* = modified bracket's resistance $N_{B,sl}$ = sliding reaction of the brackets under a combined rocking-sliding</p>	

Figure 5.12 Equations for resistance of single CLT shear walls

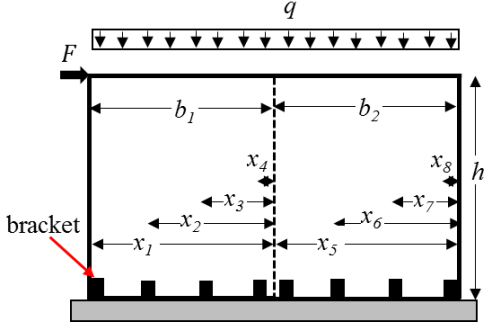
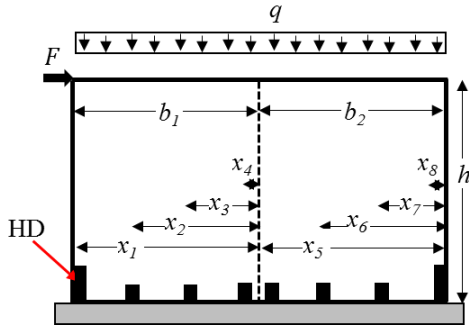
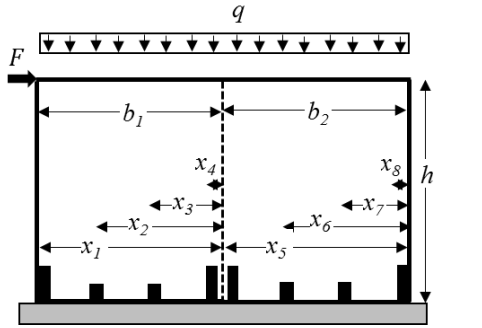
Coupled CLT shear wall with brackets	
	<p>Rocking:</p> $F_r = \frac{1}{h} \left[\frac{2N_B}{b} \left(\sum_{i=1}^{n_B} x_i^2 \right) + q \frac{b^2}{4} + \frac{N_S b}{2} \right]$ <p>Combined rocking-sliding:</p> $F_{r-sl} = \frac{1}{h} \left[\frac{2(N_B - \max \{N_{B,sl,i}\})}{b} \left(\sum_{i=1}^{n_B} x_i^2 \right) + q \frac{b^2}{4} + \frac{N_S b}{2} \right]$
Coupled CLT shear wall with brackets and 2-HDs	
	<p>Rocking:</p> $F_r = \frac{1}{h} \left[\frac{N_{HD} b}{2} + \frac{2N_B}{b} \left(\sum_{i=1}^{n_B} x_i^2 \right) + q \frac{b^2}{4} + \frac{N_S b}{2} \right]$ <p>Combined rocking-sliding:</p> $F_{r-sl} = \frac{1}{h} \left[\frac{bN_{HD}}{2} + \frac{2(N_B - \max \{N_{B,sl,i}\})}{b} \left(\sum_{i=1}^{n_B} x_i^2 \right) + q \frac{b^2}{4} + \frac{N_S b}{2} \right]$
Coupled CLT shear wall with brackets and 4-HDs	
	<p>Rocking:</p> $F_r = \frac{1}{h} \left[N_{HD} b + \frac{2N_B}{b} \left(\sum_{i=1}^{n_B} x_i^2 \right) + q \frac{b^2}{4} + \frac{N_S b}{2} \right]$ <p>Combined rocking-sliding:</p> $F_{r-sl} = \frac{1}{h} \left[N_{HD} b + \frac{2(N_B - \max \{N_{B,sl,i}\})}{b} \left(\sum_{i=1}^{n_B} x_i^2 \right) + q \frac{b^2}{4} + \frac{N_S b}{2} \right]$
<p>F_r, F_{r-sl} = rocking and combined sliding-rocking resistances, respectively q = vertical load h = height of the CLT panel b = width of the CLT panel x_i = distance from connection i to the edge N_B = bracket's resistance N_{HD} = hold-down's resistance N_B^* = modified bracket's resistance $N_{B,sl,i}$ = sliding reaction of panels under a combined rocking-sliding N_S = resistance of the vertical shear connectors</p>	

Figure 5.13 Equations for resistance of coupled CLT shear walls

5.7 Parametric study

A parametric study was conducted on both single and coupled CLT shear walls. Total 56 single CLT shear walls and 40 coupled CLT shear walls were analyzed using the FEA procedure as discussed in Chapter 3. The hysteresis load-deformations of the walls were computed and the backbone curves of the shear wall's load-deformation curves were developed using the EEEP procedure. The peak loads or capacities of the shear walls were calculated from an average of the positive and negative part of the EEEP curves. The results from the parametric study are reported in Appendix A and are discussed in the following sub-sections.

5.7.1 Parametric study on single CLT shear walls

Two types of single CLT shear walls were considered in the parametric study: Case A - CLT shear wall with brackets only; and Case B - CLT shear walls with brackets and hold-downs. The wall panels were 2.3 m×2.3 m with 3-ply of 94 mm thick. The shear walls with brackets were analyzed with five different types of fasteners (B_1 to B_5 , see Table 3.1). The number of brackets were varied from 4 to 7. Where CLT shear walls were connected by brackets and hold-downs (i.e. Case B), two types of hold-downs (HD_1 or HD_2) were considered. The number of brackets in the Case B type of walls was varied from 2 to 5; therefore, the total number of connectors remained the same as in Case A type walls.

The resistances of the 56 single CLT shear walls, F_d as listed in Appendix D1 were calculated using the proposed formulas. The results from the FEA and the proposed formulas are compared in Figure 5.14 and Figure 5.15 for single and coupled shear walls, respectively. The ratio of the peak load to calculated resistance (P_{peak}/F_d) -i.e. a factor of safety was estimated.

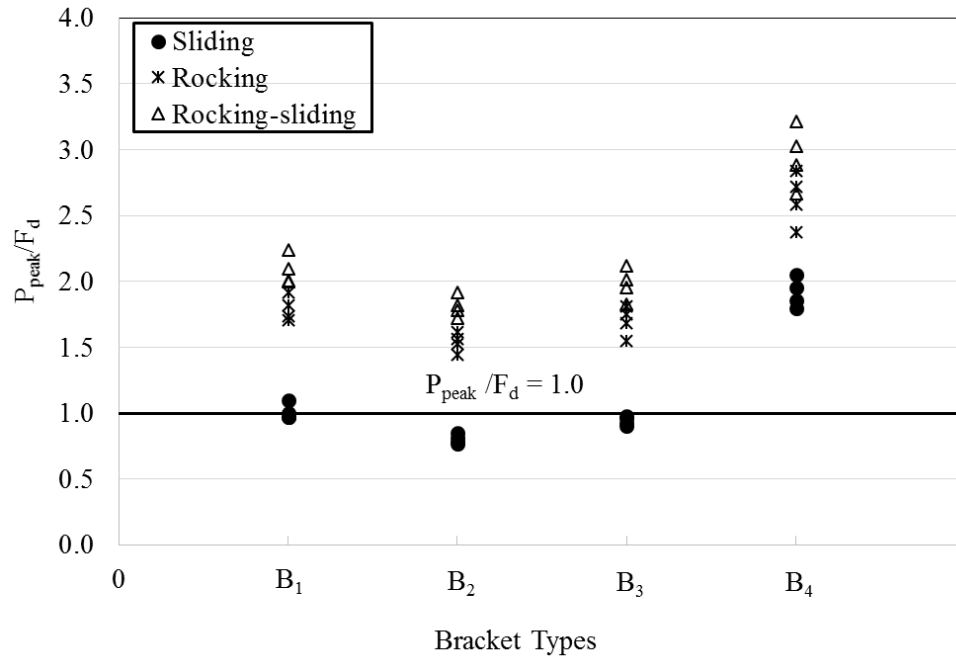


Figure 5.14 Peak vs resistance of single CLT shear wall with brackets only

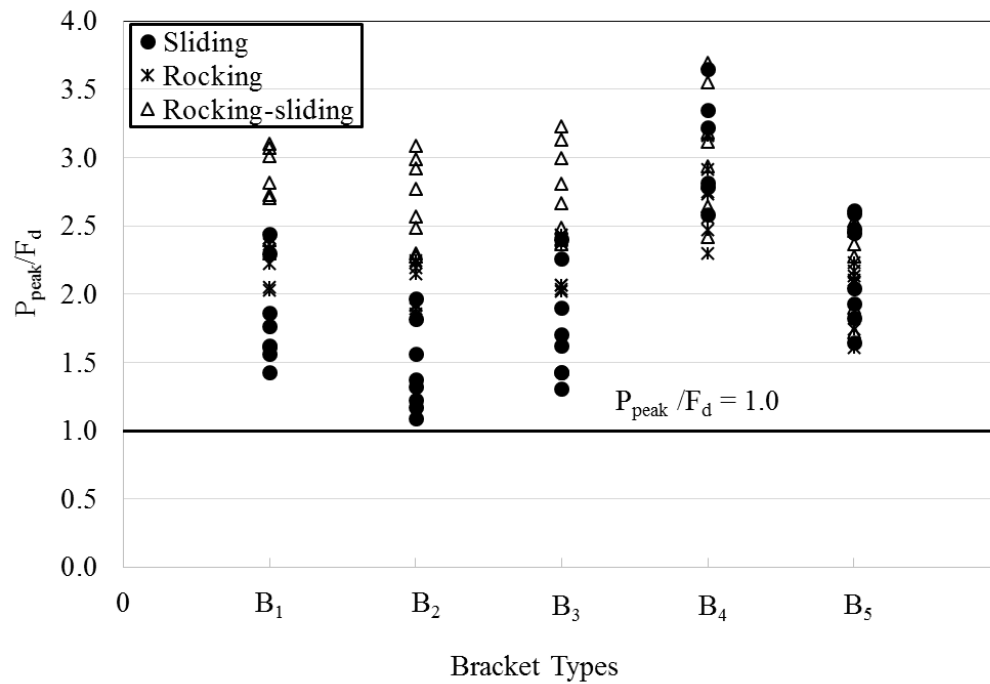


Figure 5.15 Peak vs resistance of single CLT shear wall (with brackets and hold-downs)

The figures clearly illustrates that the safety margin when using the sliding formulas to estimate the shear walls resistance is none –i.e. the calculated sliding resistance and the peak loads from the FEA were very close. Therefore, a smaller value of reduction factor shall require to determine in order to use the sliding formulas for the design purposes. By contrast, the rocking and the combined rocking-sliding kinematic motion produced conservative results compared to the estimated resistance under sliding. Additionally, in single shear walls (Figure 5.15) the shear walls with hold-downs estimated a higher factor of safety when compared to the shear walls with brackets only. The average P_{peak}/F_d for single shear walls with brackets and hold-downs was found to be higher (i.e. rocking = 2.3 and combined rocking-sliding = 2.7) when compared to the average capacity of walls with brackets only (i.e. rocking = 1.9 and combined rocking-sliding = 2.2).

5.7.2 Parametric study on coupled CLT shear walls

A similar parametric study was performed on coupled CLT shear walls with variation in the number and types of brackets (B_1 to B_5), hold-downs (HD_1 to HD_2) and vertical joints (WW_1 to WW_2). The FEA was conducted on 3-ply CLT panels of 94 mm thick. Two 1.15 m × 2.3 m panels (total wall size same as single wall: 2.3 m × 2.3 m) were connected by vertical joints. Two types of coupled shear walls were considered in the parametric study: Case C - CLT coupled shear wall with 2 hold-downs (2HDs) at the outer edges of each panel; and Case D - CLT coupled shear walls with 4 hold-downs (4HDs) both at the outer and inner edges of each panel. The wall panels were connected with half-lap joints (WW_1 : 20 screws in one row) or spline joints (WW_2 : 20 screws in two rows: 2×10). The shear walls were analyzed under CUREE loading protocol. The capacities of the walls were calculated using EEEP procedure and are listed in Appendix D2. The results from the FEA and the proposed formulas were compared. The ratio of the peak load to calculated resistance (P_{peak}/F_d) -i.e. a factor of safety was estimated, see Figure 5.16 and Figure 5.17 .

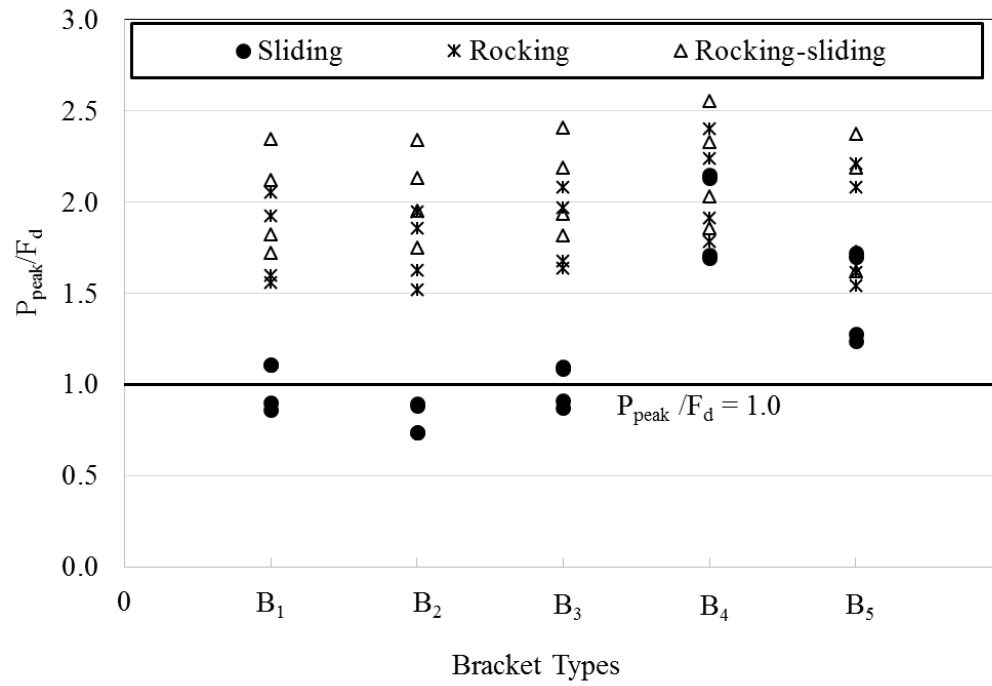


Figure 5.16 Peak vs resistance of coupled CLT shear wall with brackets and two hold-downs

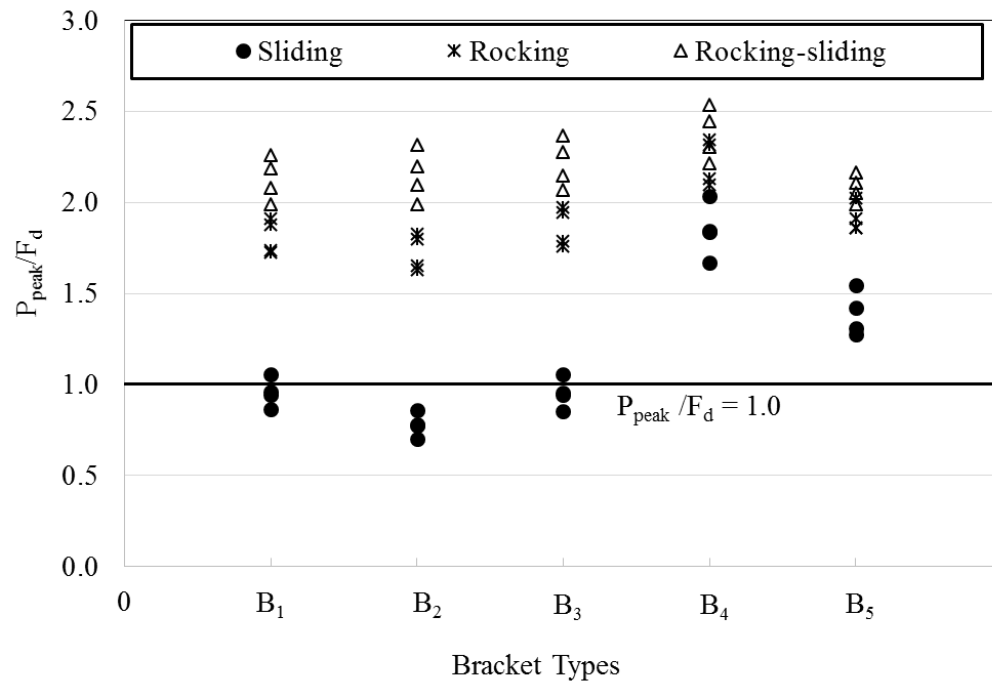


Figure 5.17 Peak vs resistance of coupled CLT shear wall with brackets and four hold-downs

Similar to single shear walls, the estimated resistance of the coupled shear walls under sliding motion clearly overestimated compared to peak loads found from FEA. The factor of safety under sliding motion was found close to 1.0. On the contrary, under both rocking and combined rocking-sliding action of the coupled shear walls, the proposed formulas produced a higher margin of safety when compared to walls under sliding only. The average P_{peak}/F_d for coupled shear walls with brackets and 4-hold-downs under rocking and combined rocking-sliding was found to be 1.9 and 2.2, respectively compared to be 1.2 under sliding only.

5.8 Summary

The study presented in this chapter proposed a methodology and formulas to estimate the resistance of CLT shear walls under lateral loading. The kinematic behaviours of single and coupled CLT shear walls due to sliding, rocking and a combination of rocking and skidding were evaluated. Both single and coupled CLT shear walls with connectors such as brackets, hold-downs and vertical joints were considered. Resistance formulas were proposed for two types of single walls: Case A - CLT shear wall with brackets only; and Case B - CLT shear walls with brackets and hold-downs. Furthermore, resistance formulas were proposed for three types of coupled CLT shear walls: Case C - CLT shear wall with brackets only; Case D - CLT shear walls with brackets and 2-HDs; and Case E - CLT shear walls with brackets and 4-HDs. A parametric study was conducted with variation on the number and types of connectors. The estimated resistances using the proposed formulas were compared against FEA results. The investigations allow drawing the following conclusions:

- The sliding resistance of the single shear walls calculated using the proposed formula were found very close to the peak values found from FEA.

- Both the rocking and the combined sliding-rocking behaviour of the single walls produced a higher factor of safety when compared to FEA results. The safety margin from these behaviour of the wall was found to be higher compared to walls under sliding only.
- Similar to single walls, the estimated sliding resistance of the coupled walls found close to peak values from the FEA; the factor of safety was 1.2. By contrast, the rocking and combined rocking-sliding produced higher factor of safety when compared to sliding only.
- The P_{peak}/F_d –i.e. factor of safety for both coupled walls with 2-HDs and 4-HDs were found to be similar. The coupled walls with 4-HDs produced slightly higher factor of safety of ($P_{peak}/F_d=2.2$) when compared to the coupled walls with 2-HDs ($P_{peak}/F_d=2.1$).

The proposed formulas to estimate the resistance of CLT shear walls could be a useful tool for engineers in future designing of CLT platform buildings.

Chapter 6: Conclusion

6.1 Key Contributions

The research presented in this thesis investigated CLT shear walls under lateral loading for a platform-type of construction. The main objective of this research was to develop lateral design guidelines for CLT shear walls. The specific objectives were to develop i) analytical models to estimate the in-plane stiffness of CLT panels with openings; ii) analytical models to estimate the in-plane stiffness and resistance of CLT shear walls; iii) formulas to estimate the deflection of CLT shear walls for platform construction; and iv) formulas to estimate the resistance of CLT shear walls for platform construction. Several significant milestones have been reached that have led to achieving this research's objectives. For this, extensive numerical and analytical investigations have been conducted on CLT connections and shear walls.

- The first part of this research estimated the in-plane stiffness of CLT wall panels with openings. The accurate estimation of the in-plane stiffness of CLT panels with openings is one of the main requirement for the design of CLT shear walls in a platform buildings. FEA were conducted on CLT shear walls and beams loaded in-plane. The FEA models were developed in ANSYS and verified against full-scale test results on CLT beams and walls. A parametric study was conducted to evaluate the impact of opening size, shape and location as well as the wall's aspect ratio on the in-plane stiffness of CLT walls. Simplified analytical equations were proposed to calculate the reduction of the in-plane stiffness of CLT panels with various types of openings.

- The second part of this research evaluated the behaviour of single and coupled shear walls under lateral loading. The calculation for in-plane strength and stiffness of CLT shear walls under lateral loading is required for the seismic design of a CLT platform building where the CLT shear

walls are the primary LFRS. The shear walls were connected to the foundations or floors by traditional brackets and hold-downs. In coupled shear walls the panels were connected vertically by half-lap or spline joints using self-tapping screws. FEA models of CLT connections –i.e. brackets, hold-downs and screws –were developed in OpenSees (McKenna et al. 2000) using nonlinear springs. The parameters for the springs were determined by calibrating the models against tests. The calibrated springs were integrated into the full-scale FEA models of the CLT shear walls. The FEA models of the full-scale CLT shear walls were compared with tests and the errors were found acceptable. A parametric study was conducted with the variation of the number and types of connectors. The strength, stiffness, ductility and energy dissipation of the CLT shear walls were estimated from the parametric study.

- The third part of this research estimated the in-plane deflection of CLT shear walls and proposed deflection formulas for single and coupled shear walls. The contribution of CLT panels –i.e. shear and bending and the contribution of the connections under sliding and rocking – were considered in the proposed equations. The calculation of total deflection with perpendicular walls and floors above is one of the major challenges currently ignored by engineers and practitioners. Herein, the influence of perpendicular walls and floors above were also accounted for.
- The fourth part of this research developed a procedure for determining the lateral resistance of the CLT shear walls. The kinematic behaviour of CLT shear walls due to sliding, rocking and combined rocking-sliding was evaluated separately. Analytical equations to estimate the resistance of CLT shear walls were proposed based on the kinematic behaviour of the walls. The resistance of single CLT shear walls was estimated in two separate cases: a) with brackets only and b) with brackets and two hold-downs located at the outer corners of the wall. Three different cases were analyzed and equations were proposed for coupled shear walls: a) with brackets only, b) brackets

and 2-hold-downs located at the outer corners of the wall and c) brackets and 4-hold-downs –i.e. two at the outer corners and two at the inner edges of the vertical joints connecting two panels. The combined sliding and rocking behaviour could prove to be the governing factor in designing CLT shear walls under lateral loads, something which has never been accounted for in any previous studies. This procedure, to estimate the resistance of CLT shear walls under lateral loads, can be efficiently applied to the seismic design of CLT platform buildings.

6.2 Future Research

This research addressed lateral design aspects of CLT shear walls for platform buildings. Additional research is recommended to further improve the proposed models and equations:

- The proposed equations to estimate the in-plane stiffness of CLT wall panels with openings were based on 3, 5 and 7-ply CLT panels with equal board thickness. The proposed equations for 3-ply CLT panels produced acceptable results when used for 5 and 7-ply panels. Therefore, these equations can be used conservatively for CLT panels with more than 3-ply for both equal and unequal board thicknesses. However, a future study could focus on CLT panels with unequal board thickness to propose a generalized equation that covers panels with any number of layers with equal or unequal board thickness.
- The procedure described in Chapter 3 to estimate the stiffness and strength of CLT shear walls covered only traditional connections –i.e. brackets and hold-downs for wall-to-foundation/floor and screws for wall-to-wall connections. Other innovative connections with higher capacity and ductility should be investigated for the application in tall buildings.
- The contribution of friction was ignored in the proposed equations to estimate the resistance and deflection of CLT shear walls because under seismic loading its contribution to the

overall resistance could be nullified or have a negative effect. However, an experimental investigation is required to validate this assumption.

- For ultimate limit state design, it is required to determine the reduction factors (ϕ) for the proposed resistance formulas of CLT shear walls. For this, reliability analyses need to be conducted considering all parameters such as types of shear walls, types of connectors and their properties, number of lay-ups and CLT material properties and their uncertainties.
- Building codes are moving towards performance-based design procedures. Therefore, future research should extend the findings reported in this thesis to establish procedures for a performance-based design of CLT platform buildings.
- CLT balloon-type construction also becoming popular. Future research should follow the methodologies reported in this thesis to determine the key parameters (e.g. stiffness, strength and deflection) of CLT balloon-type shear walls.
- Future research should develop efficient and smart connections which are easy to assemble and can effectively dissipate high seismic energy.
- The present study focused only the structural issues to design the CLT platform buildings under lateral loading. Other important issues such as fire safety, envelope and acoustic performance, construction sequence, and life-cycle assessment require further research.

Bibliography

- ASCE (2010). "Minimum design loads for buildings and other structures." American Society of Civil Engineers/Structural Engineering Institute (SEI) 7-10, Reston, Virginia, USA.
- ANSI/APA PRG 320. (2017). "Standard for Performance-Rated Cross-Laminated Timber." American National Standards Institute. New York, NY, USA.
- ANSYS 16.0. (2015). "ANSYS Mechanical APDL." [Software]
- Ashtari, S. (2012). "In-plane Stiffness of Cross-laminated Timber Floors." MSc Thesis, UBC Vancouver, Canada.
- ASTM E2126-11. (2011). "Standard test methods for cyclic (reversed) load test for shear resistance of walls for buildings." West Conshohocken: ASTM International.
- Bill 169. (2017). "Ontario Forestry Revitalization Act (14 Storey Wood Frame Buildings): An Act to amend the Building Code Act, 1992 with respect to the height of wood frame buildings." Available at:
http://www.ontla.on.ca/web/bills/bills_detail.do?locale=en&Intranet=&BillID=5197
[Accessed Oct 31, 2017].
- Blass, H.J. & Fellmoser P. (2004). "Design of solid wood panels with cross layers." *In Proceedings of 8th World Conference on Timber Engineering*, Lahti, Finland.
- Bogensperger, T., Moosbrugger, T., Schickhofer, G. (2007). "New Test Configuration for CLT-Wall-Elements under Shear Load." *In Proceedings of CIB W18*, Bled, Slovenia.
- Bogensperger, T., Moosbrugger, T., Silly, G. (2010). "Verification of CLT-plates under loads in plane." *In Proceedings of World Conference on Timber Engineering*, Riva del Garda, Italy.
- Brandner, R., Bogensperger, T., Schickhofer, G. (2013). "In plane Shear Strength of Cross Laminated Timber (CLT): Test Configuration, Quantification and influencing Parameters." *In Proceedings of CIB W18*, Vancouver, Canada.

- Brandner, R., Dietsch, P., Dröscher, J., Schulte-Wrede, M., Kreuzinger, H., & Sieder, M. (2017). “Cross laminated timber (CLT) diaphragms under shear: Test configuration, properties and design.” *Construction and Building Materials*, 147 (2017), 312-327.
- Building Code of British Columbia, BCBC. (2012). Office of Housing and Construction Standards. National Research Council Canada, Victoria, BC, CA.
- Ceccotti A., and M. Follesa. (2006). “Seismic behaviour of multi-storey XLAM buildings.” *Proceedings of COST E29: International Workshop on Earthquake Engineering on Timber Structures*, November 9-10, 2006, Coimbra, Portugal.
- Ceccotti, A. (2008). “New technologies for construction of medium-rise buildings in seismic regions: The XLAM case.” *Structural Engineering International* (SEI), 18(2):156-165.
- Ceccotti, A., Lauriola, M., Pinna, M., Sandhaas C. (2006a). “SOFIE Project- Cyclic Tests on Cross-Laminated Wooden Panels.” *Proceedings of the 9th World conference on timber engineering*, Portland, Oregon, USA.
- Ceccotti, A., Follesa, M., Lauriola, M.P., Sandhaas C. (2006b). “SOFIE Project –Test Results on the Lateral Resistance of Cross-Laminated Wooden Panels.” *Proceedings of the First European Conference on Earthquake Engineering and Seismicity*, Geneva, Switzerland.
- Ceccotti, A., Sandhaas, C., Okabe, M., Yasumura, M., Minowa, C., and Kawai, N. (2013). “SOFIE project–3D shaking table test on a seven-storey full-scale cross-laminated timber building.” *Earthquake Engineering & Structural Dynamics*, 42(13), 2003-2021.
- Computers and Structures Inc. (2013). “CSI analysis reference manual for SAP2000.” Berkeley, CA, USA.
- CSA O86-16 (2016). “Engineering design in wood.” Canadian standards association, Mississauga, ON.
- CUAP Common Understanding of Assessment Procedure (2005). Solid wood slab element to be used as a structural element in buildings, ETA request No 03.04/06, OIB Österreichisches Institut für Bautechnik”, Schenkenstraße 4, 1010 Wien, Austria.

- Diekmann, E.F. (1995). “Diaphragms and Shearwalls.” Wood Engineering and Construction Handbook, Faherty, K.F., Williamson, T.G.
- Dujic, B., Klobcar, S., Zarnic, S.R. (2007). “Influence of Openings on Shear Capacity of Wooden Walls.” *In Proceedings CIB W18*, Bled, Slovenia.
- EN 12512 (2001). “Timber structures—test methods—cyclic testing of joints made with mechanical fasteners”. CEN, Brussels, Belgium.
- European Committee for Standardization (CEN). (2004). “Design of structures for earthquake resistance—Part 1: General rules, seismic actions and rules for buildings.” Eurocode 8, European Standard EN 1998-1, Brussels, Belgium
- EN 384. (2004). “Structural timber. Determination of characteristic values of mechanical properties and density.” The British Standards Institution, BSI, London.
- ETA-06/0106 (2016). “Guideline for European Technical Approval (ETAG)- Three Dimensional Nailing Plates.” European Technical Assessment, Copenhagen, Denmark.
- Flaig, M., Blass, H.J. (2013). “Shear strength and shear stiffness of CLT-beams loaded in plane.” *In Proceedings of CIB W18*, Vancouver, Canada.
- Gagnon, S., Pirvu, C. (2011). “Cross laminated timber (CLT) Handbook.” FPInnovations, Vancouver, Canada.
- Gavric, I., and Popovski, M. (2014). “Design models for CLT shearwalls and assemblies based on connection properties.” *Proceedings of the International Network on Timber Engineering Research*, Bath, UK.
- Gavric, I., Fragiocomo, M., & Ceccotti, A. (2015a). “Cyclic behaviour of typical metal connectors for cross-laminated (CLT) structures.” *Materials and Structures*, 48(6), 1841-1857.
- Gavric, I., Fragiocomo, M., & Ceccotti, A. (2015b). “Cyclic behaviour of typical screwed connections for cross-laminated (CLT) structures.” *European Journal of Wood and Wood Products*, 73(2), 179-191.

- Gavric, I., Fragiaco, M., and Cecotti, A. (2015c). "Cyclic Behaviour of CLT Wall Systems: Experimental Tests and Analytical Prediction Model." *J. Struct. Eng.*, ASCE, 10.1061/(ASCE)ST.1943-541X.0001246, 04015034.
- GCWood. (2017). "Green Construction through Wood Program." Available at: <http://www.nrcan.gc.ca/forests/federal-programs/gcwood/20046> [Accessed Oct 31, 2017].
- Veilleux, L., Gagnon, S., & Dagenais, C. (2015). "Mass Timber Buildings up to 12 Storeys: Directives and Explanatory Guide." Available at: <http://collections.banq.qc.ca/ark:/52327/bs2553717> [Accessed Oct 31, 2017].
- Hossain, A., Danzig, I., & Tannert, T. (2016). Cross-Laminated Timber Shear Connections with Double-Angled Self-Tapping Screw Assemblies. *Journal of Structural Engineering*, 142(11), 04016099.
- IBC (International Building Code). (2015). "International building code." International Code Council, Falls Church, VA.
- Jobstl, R. A., Bogensperger, T., Schickhofer, G. (2008). "In-plane Shear Strength of Cross Laminated Timber." *In Proceedings of CIB W18*, St. Andrews, Canada.
- Kawai, N., Miyake, T., Yasumura, M., Isoda, H., Koshihara, M., Nakajima, S., Araki, Y., Nakagawa, T., & Sato, M. (2016). "Full scale shake table tests on five story and three story CLT building structures." *World Conference on Timber Engineering, WCTE 2016*, 22-25th August, Vienna, Austria.
- Kraetzig W, Meyer I, & Meskouris K. (1989). "Damage evolution in reinforced concrete members under cyclic loading." *5th international conference on structural safety and reliability*, San Francisco, CA, 795–802.
- Latour, M., & Rizzano, G. (2017). "Seismic behaviour of cross-laminated timber panel buildings equipped with traditional and innovative connectors." *Archives of Civil and Mechanical Engineering*, 17(2), 382-399.

- Latour, M., Piluso, V., & Rizzano, G. (2011b). “Experimental analysis of innovative dissipative bolted double split tee beam-to-column connections.” *Steel Construction*, 4 (2), 53–64.
- McKenna F, Fenves GL, Jeremic B, Scott MH. (2000). “Open system for earthquake engineering simulation.” <<http://opensees.berkeley.edu>>.
- Mitra N. (2012). “Pinching4 model.” OpenSees User Documetation.
<http://opensees.berkeley.edu/wiki/index.php/Pinching4_Material>
- Miyake, T., Yasumura, M., Kawai, N., Isoda, H., Koshihara, M., Tsuchimoto, T., Araki, Y., & Nakagawa, T. (2016). “Structural possibility of clt panel constructions in High seismic area.” World Conference on Timber Engineering, WCTE 2016, 22-25th August, Vienna, Austria.
- Montgomery, D.C., Runger, G.C. (2003). “Applied statistics and probability for engineers.” John Wiley & Sons.
- Moosbrugger, T., Guggenberger, W., Bogensperger, T. (2006). “Cross-Laminated Timber Wall Segments under Homogenous Shear - with and without Openings.” *In Proceedings of World Conference on Timber Engineering*, Portland, USA.
- Most, T., Will, J. (2008). “Metamodel of Optimal Prognosis-an automatic approach for variable reduction and optimal metamodel selection.” *Weimar Optimization and Stochastic Days 5.0*, Weimar, Germany.
- NBCC (2010). “National Building Code of Canada 2010, Canadian Commission on Building and Fire Codes.” National Research Council of Canada, Ottawa, ON.
- NBCC (2015). “National Building Code of Canada 2015, Canadian Commission on Building and Fire Codes.” National Research Council of Canada, Ottawa, ON.
- NDS 2015. (2015). “National Design Specification for Wood Construction.” Washington, DC: American Wood Council.

- Nordic Structures. (2013). "NORDIC X-LAM Cross-Laminated Timber (CLT)." Available at: <http://nordic.ca/en/products/nordic-x-lam-cross-laminated-timber-clt> [Accessed Oct 31, 2017].
- Pai, S. G. S., Lam, F., & Haukaas, T. (2016). "Force Transfer around Openings in Cross-Laminated Timber Shear Walls." *Journal of Structural Engineering*, 143(4), 04016215.
- Parliament of British Columbia (2009). "Wood First Act." Available at: https://www.leg.bc.ca/pages/bclass-legacy.aspx#/content/legacy/web/39th1st/1st_read/gov09-1.htm [Accessed Oct 31, 2017].
- Pei, S., & van de Lindt, J. W. (2011). "Seismic numerical modeling of a six-story light-frame wood building: Comparison with experiments." *Journal of Earthquake Engineering*, 15(6), 924-941.
- Pei, S., Lenon, C., Kingsley, G., & Deng, P. (2017). "Seismic Design of Cross-Laminated Timber Platform Buildings Using a Coupled Shearwall Concept." *Journal of Architectural Engineering*, 23(3), 06017001. DOI: 10.1061/(ASCE)AE.1943-5568.0000257
- Pei, S., van de Lindt, J. W., & Popovski, M. (2013). Approximate R-factor for cross-laminated timber walls in multistory buildings. *Journal of Architectural Engineering*, 19(4), 245-255.
- Popovski, M., & Gavric, I. (2015). "Performance of a 2-story CLT house subjected to lateral loads." *Journal of Structural Engineering*, 142(4), E4015006. DOI: 10.1061/(ASCE)ST.1943-541X.0001315.
- Popovski, M., Schneider, J., Schweinsteiger, M. (2010). "Lateral load resistance of cross laminated wood panels." In *Proceedings of World Conference on Timber Engineering*, Riva del Garda, Italy.
- Reynolds, T., Foster, R., Bregulla, J., Chang, W. S., Harris, R., & Ramage, M. (2017). "Lateral-Load Resistance of Cross-Laminated Timber Shear Walls." *Journal of Structural Engineering*, 143(12), 06017006.

- ReNew Canada, The Infrastructure Magazine. (2016). “The Rise of Wood: Evolution of Building Materials and Codes.” Available at: <https://mosesstructures.com/wp-content/uploads/2016/08/ReNew-Canada-The-Rise-of-Wood.pdf?x48167> [Accessed Nov 3, 2017].
- Rinaldin, G., & Fragiacomio, M. (2016). “Non-linear simulation of shaking-table tests on 3-and 7-storey X-Lam timber buildings.” *Engineering Structures*, 113 (2016), 133-148.
- Sacks, J., Welch, W.J., Mitchell, T.J., Wynn, H.P. (1989). “Design and analysis of computer experiments.” *Statistical science*, 4(4), 409-423.
- Schneider, J., Shen, Y., Stiemer, S. F., & Tesfamariam, S. (2015). “Assessment and comparison of experimental and numerical model studies of cross-laminated timber mechanical connections under cyclic loading.” *Construction and Building Materials*, 77(2015), 197-212.
- Seismosoft (2013). “SeismoMatch– A computer program for spectrum matching of earthquake records”, available from <http://www.seismosoft.com>.
- Seismosoft (2016). “SeismoMatch– A computer program for spectrum matching of earthquake records”, available from <http://www.seismosoft.com>.
- Simulia, Dassault Systemes. (2012). “ABAQUS 6.12 documentation.” Providence, Rhode Island, USA.
- Shahnewaz, M., Tannert, T., Alam, M. S. & Popovski, M. (2016a). In-plane stiffness of CLT walls with and without opening. *World Conference on Timber Engineering*, WCTE 2016, 22-25th August, Vienna, Austria.
- Shahnewaz, M., Tannert, T., Alam, M. S. & Popovski, M. (2016b). CLT walls with openings: in-plane stiffness using finite element and its sensitivity analysis. *5th International Structural Specialty Conference*, CSCE 2016, 1-4th June 2016, London, ON, Canada.

- Shahnewaz, M., Tannert, T., Alam, M. S. & Popovski, M. (2017a). In-Plane Stiffness of Cross Laminated Timber Panels with Openings. *Structural Engineering International*, IABSE, 27(2), 217-223. DOI: 10.2749/101686617X14881932436131.
- Shahnewaz, M., Tannert, T., Alam, M. S. & Popovski, M. (2017b). Sensitivity Analysis of In-Plane Stiffness of CLT Walls with Openings. *16th World Conference on Earthquake Conference*, WCEE 2017, 9-13th January 2017, Santiago, Chile.
- Shahnewaz, M., Tannert, T., Alam, M. S. & Popovski, M. (2017c). Performance of Cross Laminated Timber Shear walls under Cyclic Loading. *6th International Conference on Engineering Mechanics and Materials*, CSCE, May 31-June 3 2017, Vancouver, BC, Canada.
- Shahnewaz, M., Tannert, T., Alam, M. S. & Popovski, M. (2017d). Capacity-Based Design for Platform-Framed Cross-Laminated Timber Buildings. *Structures Congress 2017*, ASCE, April 6-8, 2017, Denver, CO, USA.
- Shahnewaz, M., Tannert, T., Alam, M. S. & Popovski, M. (2015). Experimental and Finite Element Analysis of Cross Laminated Timber (CLT) Panels. In *First International Conference on Advances in Civil Infrastructure and Construction Materials 2015*, 14-15th December 2015, Dhaka, Bangladesh.
- Simpson, T.W., Poplinski, J.D., Koch, P.N., Allen, J.K. (2001). "Metamodels for computer-based engineering design: survey and recommendations." *Engineering with computers*, 17(2), 129-150.
- Sustersic, I., Fragiacomio, M., & Dujic, B. (2015). "Seismic analysis of cross-laminated multistory timber buildings using code-prescribed methods: Influence of panel size, connection ductility, and schematization." *Journal of Structural Engineering*, 142(4), E4015012. DOI: 10.1061/(ASCE)ST.1943-541X.0001344.
- Tamagnone, G., Rinaldin, G., & Fragiacomio, M. (2017). "A novel method for non-linear design of CLT wall systems." *Engineering Structures*, In Press.

- Tomasi, R., & Smith, I. (2014). "Experimental characterization of monotonic and cyclic loading responses of CLT panel-to-foundation angle bracket connections." *Journal of Materials in Civil Engineering*, 27(6), 04014189.
- UBC News (2016). "Structure of UBC's tall wood building now complete." Available at: <http://news.ubc.ca/2016/09/15/structure-of-ubcs-tall-wood-building-now-complete/> [Accessed Oct 31, 2017].
- Yasumura, M., Kobayashi, K., Okabe, M., Miyake, T., & Matsumoto, K. (2015). "Full-scale tests and numerical analysis of low-rise CLT structures under lateral loading." *Journal of Structural Engineering*, 142(4), E4015007. DOI: 10.1061/(ASCE)ST.1943-541X.0001348.
- Yawalata, D., Lam, F. (2011). "Development of Technology for Cross Laminated Timber Building Systems." Research report, University of British Columbia, Vancouver, Canada.

Appendix A: Parameter studies

Appendix A1: CLT single shear walls

Wall ID	P_{peak} kN	E kN-m	P_u kN	d_u mm	P_y kN	d_y mm	D -	K_e kN/mm
W.4B ₁	99.6	29.9	78.9	80.0	87.3	17.8	4.5	4.9
W.5B ₁	113.6	34.1	90.8	80.2	101.2	19.2	4.2	5.3
W.6B ₁	132.6	39.2	106.5	80.1	118.0	21.1	3.8	5.6
W.7B ₁	153.9	44.3	124.9	82.2	140.8	19.4	4.2	7.2
W.4B ₂	97.8	25.6	79.7	61.4	90.7	18.6	3.3	4.9
W.5B ₂	117.4	23.8	93.8	71.6	106.4	21.6	3.3	4.9
W.6B ₂	134.9	28.9	107.5	77.2	124.1	23.6	3.3	5.2
W.7B ₂	155.0	29.9	124.1	79.8	141.6	24.7	3.2	5.7
W.4B ₃	92.9	25.0	76.4	63.7	87.9	19.2	3.3	4.6
W.5B ₃	113.7	23.8	90.6	70.3	101.9	18.8	3.7	5.4
W.6B ₃	131.2	29.5	105.4	73.7	118.1	19.6	3.8	6.1
W.7B ₃	150.0	30.6	120.7	76.4	135.7	20.3	3.8	6.7
W.4B ₄	99.3	25.6	79.6	56.4	88.9	16.6	3.4	5.4
W.5B ₄	118.1	25.7	95.0	59.3	87.7	14.9	3.9	5.7
W.6B ₄	134.7	29.2	108.3	63.0	120.5	18.5	3.4	6.5
W.7B ₄	152.1	33.0	121.7	64.8	134.4	17.2	3.8	7.8
W.2HD ₁ .2B ₁	103.9	42.4	74.8	89.8	83.5	14.1	6.6	6.0
W.2HD ₁ .3B ₁	119.9	47.9	94.5	105.1	111.5	17.1	6.2	6.6
W.2HD ₁ .4B ₁	146.1	55.1	111.1	106.9	132.0	19.2	5.6	6.9
W.2HD ₁ .5B ₁	176.4	62.0	134.1	112.6	155.9	19.1	5.9	8.2
W.2HD ₁ .2B ₂	104.6	39.7	82.6	47.4	89.1	15.5	3.0	5.8
W.2HD ₁ .3B ₂	118.8	43.4	95.4	70.7	106.8	16.2	4.4	6.6
W.2HD ₁ .4B ₂	141.2	50.4	114.0	68.2	124.5	17.2	4.0	7.3
W.2HD ₁ .5B ₂	156.7	56.2	124.6	84.7	143.8	18.4	4.6	7.8
W.2HD ₁ .2B ₃	107.2	40.4	86.7	45.0	92.9	16.4	2.7	5.7
W.2HD ₁ .3B ₃	121.1	43.2	97.8	62.1	106.1	15.7	4.0	6.8
W.2HD ₁ .4B ₃	135.6	49.3	109.1	64.5	120.0	16.6	3.9	7.2
W.2HD ₁ .5B ₃	154.7	56.3	123.8	85.4	138.1	16.6	5.2	8.3

Wall ID	P_{peak}	E	P_u	d_u	P_y	d_y	D	K_e
	kN	kN-m	kN	mm	kN	mm	-	kN/mm
W.2HD ₁ .2B ₄	104.3	42.6	84.3	45.6	90.2	14.5	3.2	6.2
W.2HD ₁ .3B ₄	121.7	43.3	96.7	66.7	109.2	15.2	4.2	6.9
W.2HD ₁ .4B ₄	136.2	48.3	111.2	63.6	124.3	16.7	3.8	7.4
W.2HD ₁ .5B ₄	156.3	53.3	124.7	72.0	144.3	17.5	4.1	8.2
W.2HD ₁ .2B ₅	75.2	42.7	59.7	42.5	63.2	12.1	3.5	5.2
W.2HD ₁ .3B ₅	107.2	53.2	85.4	45.8	89.2	16.5	2.8	5.6
W.2HD ₁ .4B ₅	117.8	56.3	96.4	43.3	101.0	17.3	2.5	5.8
W.2HD ₁ .5B ₅	131.7	60.7	104.7	44.7	107.3	14.9	3.0	7.2
W.2HD ₂ .2B ₁	110.3	30.7	86.9	54.2	87.3	13.2	4.1	6.6
W.2HD ₂ .3B ₁	126.2	36.4	99.5	54.6	103.4	14.3	3.9	7.3
W.2HD ₂ .4B ₁	146.6	41.0	115.0	53.1	114.9	15.0	3.6	7.7
W.2HD ₂ .5B ₁	161.4	46.2	130.1	55.3	130.2	15.8	3.5	8.3
W.2HD ₁ .2B ₂	113.5	30.3	90.5	53.8	90.6	13.6	4.0	6.8
W.2HD ₂ .3B ₂	134.9	33.7	106.3	53.0	106.0	15.2	3.5	7.0
W.2HD ₂ .4B ₂	152.2	37.9	121.1	53.1	123.6	16.9	3.1	7.3
W.2HD ₂ .5B ₂	169.2	41.4	135.3	55.5	139.0	17.4	3.2	8.0
W.2HD ₂ .2B ₃	113.8	34.6	90.7	52.4	90.8	12.3	4.0	6.8
W.2HD ₂ .3B ₃	135.2	35.1	107.1	53.0	109.0	15.8	3.4	6.9
W.2HD ₂ .4B ₃	154.0	39.2	123.5	52.9	125.6	17.2	3.1	7.4
W.2HD ₂ .5B ₃	169.5	41.7	136.0	53.5	139.2	17.2	3.1	8.1
W.2HD ₂ .2B ₄	114.0	32.0	89.9	54.1	92.0	13.7	4.0	6.8
W.2HD ₂ .3B ₄	132.4	37.5	106.1	54.4	108.1	14.5	3.8	7.5
W.2HD ₂ .4B ₄	155.9	41.0	123.1	52.7	122.7	14.8	3.6	8.3
W.2HD ₂ .5B ₄	168.8	46.4	135.8	55.5	137.7	15.7	3.5	8.8
W.2HD ₂ .2B ₅	74.6	37.6	60.0	41.5	61.2	11.2	3.7	5.5
W.2HD ₂ .3B ₅	105.7	48.7	85.5	62.0	87.3	13.8	4.5	6.3
W.2HD ₂ .4B ₅	111.1	50.4	88.4	56.1	94.0	12.5	4.5	7.6
W.2HD ₂ .5B ₅	118.3	53.5	95.0	54.1	100.4	11.7	4.6	8.6

Appendix A2: CLT coupled shear walls

Wall ID	P_{peak}	E	P_u	d_u	P_y	d_y	D	K_e
	kN	kN-m	kN	mm	kN	mm	-	kN/mm
W.2HD ₁ .4B ₁ .WW ₁	100.2	45.0	78.6	104.3	89.4	18.3	5.7	4.9
W.2HD ₁ .4B ₂ .WW ₁	101.8	44.1	79.8	106.5	87.5	17.8	6.0	4.9
W.2HD ₁ .4B ₃ .WW ₁	103.0	44.7	80.5	105.6	89.8	18.0	5.9	5.0
W.2HD ₁ .4B ₄ .WW ₁	103.1	46.3	80.7	101.5	92.8	18.3	5.5	5.1
W.2HD ₁ .4B ₅ .WW ₁	97.8	46.9	76.8	92.7	85.7	18.3	5.1	4.7
W.2HD ₁ .4B ₁ .WW ₂	78.0	34.9	60.2	109.3	64.2	20.0	5.5	3.2
W.2HD ₁ .4B ₂ .WW ₂	84.8	33.7	63.0	98.9	71.8	22.0	4.5	3.3
W.2HD ₁ .4B ₃ .WW ₂	82.8	34.2	63.4	108.7	72.6	22.1	4.9	3.3
W.2HD ₁ .4B ₄ .WW ₂	82.1	35.7	63.2	106.9	72.0	21.6	4.9	3.3
W.2HD ₁ .4B ₅ .WW ₂	71.3	37.3	55.5	109.2	63.2	19.8	5.5	3.2
W.2HD ₂ .4B ₁ .WW ₁	100.4	57.2	79.3	116.2	91.1	17.7	6.6	5.2
W.2HD ₂ .4B ₂ .WW ₁	103.4	57.2	80.9	116.2	94.3	18.2	6.4	5.2
W.2HD ₂ .4B ₃ .WW ₁	103.9	57.5	81.6	115.9	94.3	18.0	6.5	5.2
W.2HD ₂ .4B ₄ .WW ₁	104.0	58.7	81.8	113.2	96.2	18.2	6.2	5.3
W.2HD ₂ .4B ₅ .WW ₁	99.2	60.2	78.2	109.7	88.0	17.7	6.2	5.0
W.2HD ₂ .4B ₁ .WW ₂	81.4	44.1	63.8	115.0	73.1	21.0	5.5	3.5
W.2HD ₂ .4B ₂ .WW ₂	84.7	43.9	66.4	120.3	77.9	22.2	5.4	3.5
W.2HD ₂ .4B ₃ .WW ₂	86.4	44.5	63.5	120.5	77.1	21.8	5.5	3.5
W.2HD ₂ .4B ₄ .WW ₂	82.7	45.7	64.1	119.7	76.6	21.4	5.6	3.6
W.2HD ₂ .4B ₅ .WW ₂	73.5	47.2	57.3	122.2	66.9	19.4	6.3	3.4
W.4HD ₁ .4B ₁ .WW ₁	127.6	47.3	100.7	103.1	113.9	21.1	4.9	5.4
W.4HD ₁ .4B ₂ .WW ₁	134.1	45.9	104.6	104.3	116.7	21.4	4.9	5.5
W.4HD ₁ .4B ₃ .WW ₁	134.3	46.3	105.3	112.6	119.7	21.6	5.2	5.5
W.4HD ₁ .4B ₄ .WW ₁	133.3	49.2	104.4	108.5	118.0	20.9	5.2	5.6
W.4HD ₁ .4B ₅ .WW ₁	110.1	57.5	89.1	88.8	98.7	17.7	5.0	5.6
W.4HD ₁ .4B ₁ .WW ₂	117.2	42.9	96.2	104.0	106.4	23.6	4.4	4.5
W.4HD ₁ .4B ₂ .WW ₂	121.4	42.6	96.4	105.6	110.7	24.4	4.3	4.5
W.4HD ₁ .4B ₃ .WW ₂	121.8	43.0	96.0	114.0	108.5	23.7	4.8	4.6
W.4HD ₁ .4B ₄ .WW ₂	121.1	43.9	95.5	111.8	108.2	23.3	4.8	4.7
W.4HD ₁ .4B ₅ .WW ₂	113.1	46.6	94.7	86.6	100.3	22.7	3.8	4.4

Wall ID	P_{peak}	E	P_u	d_u	P_y	d_y	D	K_e
	kN	kN-m	kN	mm	kN	mm	-	kN/mm
W.4HD ₂ .4B ₁ .WW ₁	142.9	59.2	110.0	94.3	121.4	20.7	4.6	5.9
W.4HD ₂ .4B ₂ .WW ₁	148.6	58.9	115.3	95.4	126.2	21.4	4.5	5.9
W.4HD ₂ .4B ₃ .WW ₁	149.8	59.6	113.6	93.2	124.7	20.8	4.5	6.0
W.4HD ₂ .4B ₄ .WW ₁	147.6	60.9	113.3	93.3	125.1	20.5	4.6	6.1
W.4HD ₂ .4B ₅ .WW ₁	133.6	62.9	105.7	74.2	112.7	20.1	3.7	5.6
W.4HD ₂ .4B ₁ .WW ₂	130.1	55.3	102.1	95.3	110.2	22.0	4.4	5.0
W.4HD ₂ .4B ₂ .WW ₂	134.6	55.7	106.1	97.5	114.3	22.7	4.4	5.0
W.4HD ₂ .4B ₃ .WW ₂	136.0	56.4	107.8	94.5	115.0	22.6	4.2	5.1
W.4HD ₂ .4B ₄ .WW ₂	133.7	57.0	105.6	94.7	113.0	21.9	4.4	5.2
W.4HD ₂ .4B ₅ .WW ₂	123.0	58.6	101.3	92.0	107.9	22.1	4.2	4.9

Appendix B: Examples on Deflection of CLT Shear Walls

Appendix B1: Single CLT shear wall

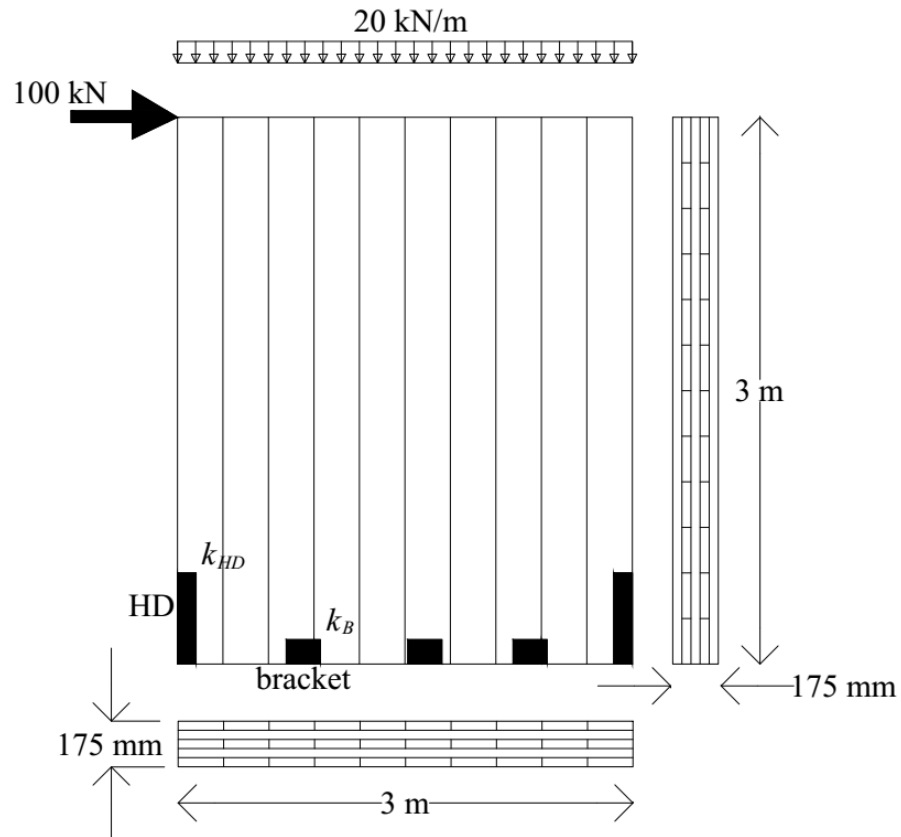


Figure B.1 Deflection calculation in a single CLT shear wall

Table B.1 Properties of CLT shear wall

Parameters	
Length, b [mm]	3000
Height, h [mm]	3000
No. of brackets, n_B	3
Stiffness of bracket, k_B [N/mm]	5000
Stiffness of hold-downs, k_{HD} [N/mm]	6000
Modulus of elasticity parallel to grain, E_o [N/mm ²]	12000
Shear modulus, G_{CLT} [N/mm ²]	250
No of layer in CLT panel, n	5
Total thickness of CLT panel, t_{CLT} [mm]	175
Vertical loading, q [kN/m]	20

The effective bending stiffness for a CLT panel loaded in plane can be calculated using Eqs. (4.3) and (4.4) as:

$$(EI)_{eff} = k_4 (E_o I) = \left(\frac{E_{90}}{E_o} + \left(1 - \frac{E_{90}}{E_o} \right) \frac{a_3 - a_1}{a_5} \right) (E_o I)$$

$$E_{90} = \frac{E_o}{30} = 12000 / 30 = 400 \text{ N/mm}^2$$

$$a_5 = 175 \text{ mm}; a_3 = 105 \text{ mm}; a_1 = 35 \text{ mm}$$

$$k_4 = \frac{400}{12000} + \left(1 - \frac{400}{12000} \right) \frac{105 - 35}{175} = 0.42$$

Therefore, the effective bending stiffness of the CLT panel is:

$$(EI)_{eff} = 0.42 * 12000 * \left(\frac{175 * 3000^3}{12} \right) = 1.98 \times 10^{15} \text{ N-mm}^2$$

The deflection of the CLT single shear wall due to bending, shear, sliding, and rocking can be calculated using Eqs. (4.2), (4.5), (4.7), and (4.11), respectively:

$$\delta_b = \frac{Fh^3}{3EI_{eff}} = \frac{100 \times 10^3 * 3000^3}{3 * 1.98 \times 10^{15}} = 0.45 \text{ mm}$$

$$\delta_s = \frac{F.h}{G_{CLT} t_{CLT} b} = \frac{100 \times 10^3 * 3000}{250 * 175 * 3000} = 2.29 \text{ mm}$$

$$\delta_{sl} = \frac{F}{n_B k_B} = \frac{100 \times 10^3}{3 * 5000} = 6.67 \text{ mm}$$

$$\delta_r = \left(\frac{F.h^2}{b^2} - \frac{qh}{2} \right) \frac{1}{k_{HD}} = \left(\frac{100 \times 10^3 * 3000^2}{3000^2} - \frac{20 * 3000}{2} \right) \frac{1}{6000} = 11.67 \text{ mm}$$

Therefore, the total deflection of the single CLT shear wall due to 100kN lateral loading:

$$\delta = 0.45 + 2.29 + 6.67 + 11.67 = 21.1 \text{ mm}$$

Appendix B2: Single CLT shear wall connected to a perpendicular wall

Deflection of the single CLT shear wall due to 100 kN lateral load with the perpendicular wall and the floor above with self-taping screws is shown in Figure 5.17B.2. The properties of the connectors is described in Table B.2. The properties of the CLT wall and its connections to floor/foundation below is described in Table B.1.

Table B.2 Connection properties of CLT shear wall-to-perp. wall and floor above

Properties	
Stiffness of CLT wall-to-floor above connections, k_{fi} [N/mm]	500
Stiffness of CLT wall-to-perp. wall connections, k_{wi} [N/mm]	500
Tensile stiffness of brackets in perpendicular wall, $k_{t,P}$ [N/mm]	1000
Shear stiffness of brackets in perpendicular wall, $k_{s,P}$ [N/mm]	1000
No. of brackets in the perp. wall, n_p	3
Spacing of STSs in CLT shear wall-to-perp. wall connections [mm]	500
Spacing of STSs in CLT shear wall-to-floor connections [mm]	500

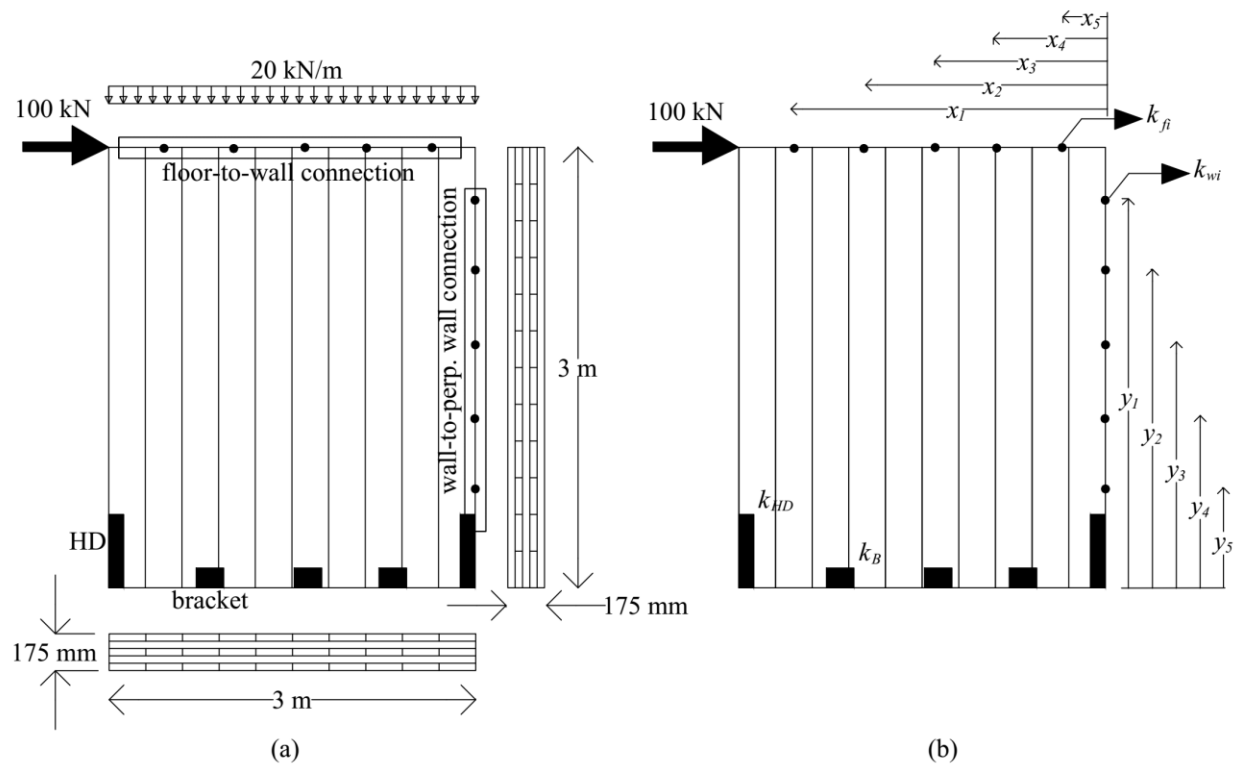


Figure C.2 Deflection calculation in a single CLT shear wall with perp. wall and floor above: (a) schematic of wall with connections; (b) properties of connections

Perpendicular wall configuration 1

The connections of the in-plane wall-to-perpendicular wall (configuration 1) and the floor above are shown in Figure B.3.

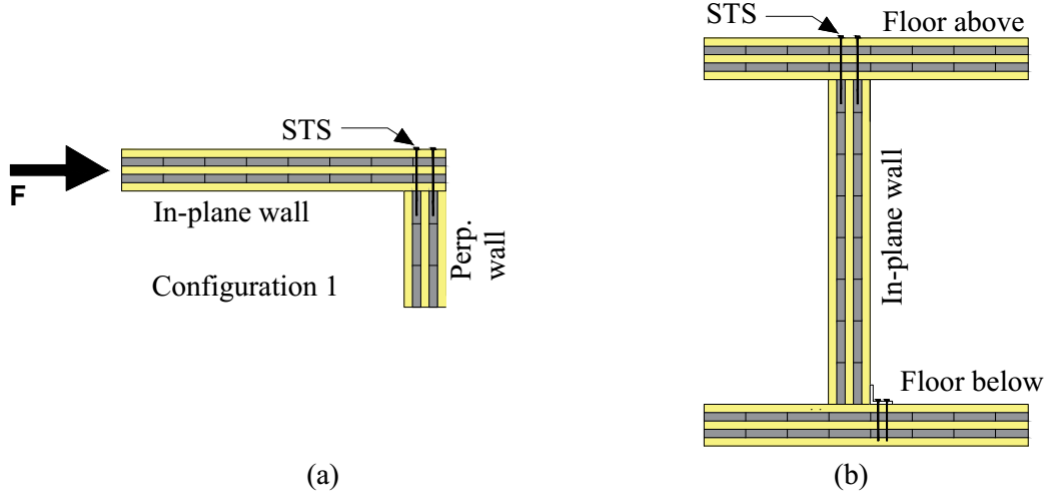


Figure B.3 (a) wall-to-perp. wall connections and (b) in-plane wall-to-floor connections

Using Eq. (4.23), the modified rocking deflection of the CLT shear wall can be calculated as:

$$\begin{aligned}\delta_r &= \left(\frac{F \cdot h^2}{b^2} - \frac{qh}{2} \right) \frac{1}{k_{HD}} \left[1 + \frac{1}{b^2} \left(\sum_{i=1}^{n_f} x_i^2 k_{fi} + \sum_{i=1}^{n_w} y_i^2 k_{wi} \right) \frac{1}{k_{HD}} \right]^{-1} \\ &= \left(\frac{100 \times 10^3 \cdot 3000^2}{3000^2} - \frac{20 \cdot 3000}{2} \right) \frac{1}{6000} \\ &\quad \left[1 + \frac{1}{3000^2} \left(500(500^2 + 1000^2 + 1500^2 + 2000^2 + 2500^2) \right) \frac{1}{6000} \right. \\ &\quad \left. + \frac{1}{3000^2} \left(500(500^2 + 1000^2 + 1500^2 + 2000^2 + 2500^2) \right) \frac{1}{6000} \right]^{-1} \\ &= 9.3 \text{ mm}\end{aligned}$$

Similarly, the modified sliding deflection of the CLT shear wall can be calculated using Eq. (4.25) as:

$$\delta_{sl} = \frac{F}{n_B k_B + n_w k_w + n_f k_f} = \frac{100 \times 10^3}{3 \cdot 5000 + 5 \cdot 500 + 5 \cdot 500} = 5.0 \text{ mm}$$

Therefore, the total deflection of the single CLT shear wall with perpendicular wall configuration 1 and floor above due to 100kN lateral loading:

$$\delta = 0.45 + 2.29 + 5.0 + 9.3 = 17 \text{ mm}$$

Perpendicular wall configuration 2

The connections of the in-plane wall-to-perpendicular wall (configuration 2) and the floor above are shown in Figure C.4.

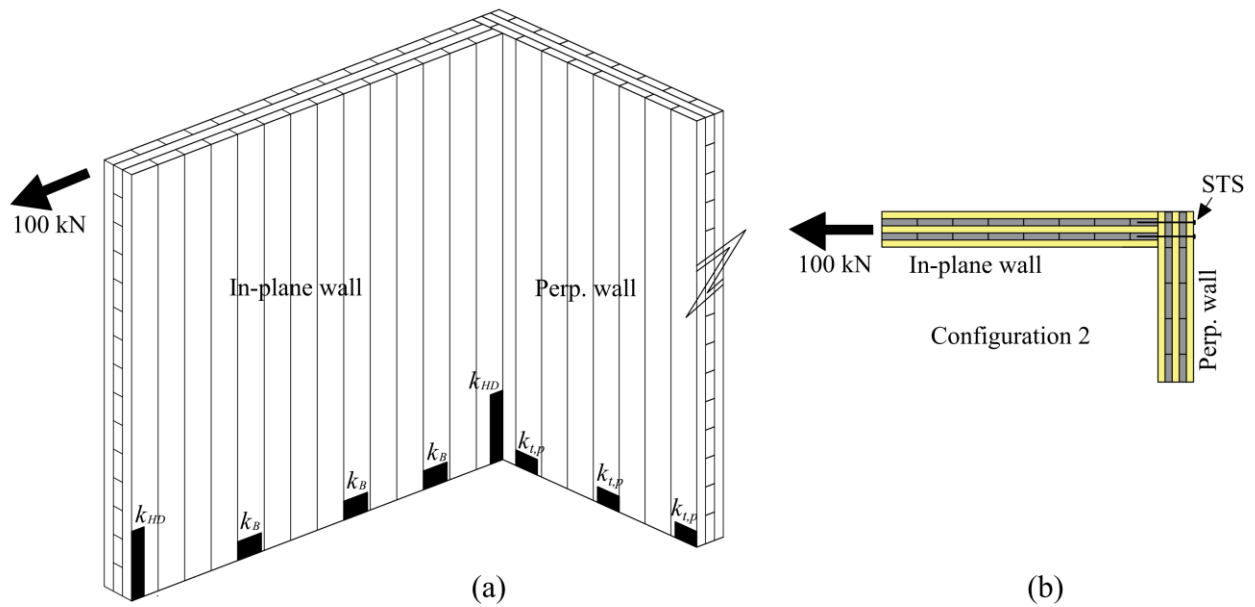


Figure B.4 (a) In-plane wall-to-perp. wall's configuration 2 and (b) connections between in-plane wall-to-perp. wall in configuration 2

Now using Eq. (4.25), the modified rocking deflection of the CLT shear wall can be calculated as:

$$\begin{aligned}
\delta_r &= \left(\frac{F h^2}{b^2} - \frac{qh}{2} \right) \frac{1}{k_{HD} + n_p k_{t,p}} \left[1 + \frac{1}{b^2} \left(\sum_{i=1}^{n_f} x_i^2 k_{fi} \right) \frac{1}{k_{HD} + n_p k_{t,p}} \right]^{-1} \\
&= \left(\frac{100 \times 10^3 * 3000^2}{3000^2} - \frac{20 * 3000}{2} \right) \frac{1}{6000 + 3 * 1000} \\
&\quad \left[1 + \frac{1}{3000^2} (500(500^2 + 1000^2 + 1500^2 + 2000^2 + 2500^2)) \frac{1}{6000 + 3 * 1000} \right]^{-1} \\
&= 7.2 \text{ mm}
\end{aligned}$$

Similarly, the modified sliding deflection of the CLT shear wall can be calculated using Eq. (4.25)

as:

$$\delta_{sl} = \frac{F}{n_B k_B + n_f k_f + n_p k_{s,p}} = \frac{100 \times 10^3}{3 * 5000 + 5 * 500 + 3 * 1000} = 4.88 \text{ mm}$$

Therefore, the total deflection of the single CLT shear wall with perpendicular wall configuration 2 and floor above due to 100kN lateral loading:

$$\delta = 0.45 + 2.29 + 7.2 + 4.48 = 14.8 \text{ mm}$$

Appendix B3: Coupled CLT shear wall with 4-HDs

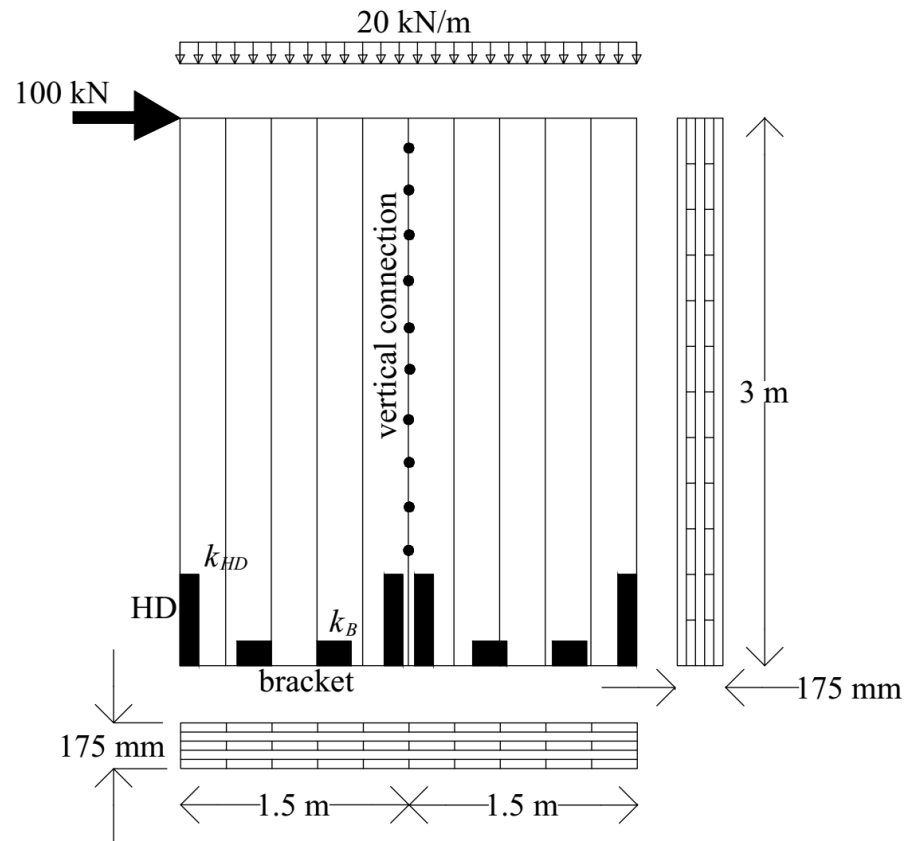


Figure B.5 Geometry and properties of coupled CLT shear walls with 4-HDs

Table C.3: Properties of coupled CLT shear wall

Parameters	
Number of panels	2
Length of left panel, b_l [mm]	1500
Length of right panel, b_r [mm]	1500
Height, h [mm]	3000
No. of brackets in each panel, n_B	2
Stiffness of bracket, k_B [N/mm]	5000
Stiffness of hold-downs, k_{HD} [N/mm]	6000
Modulus of elasticity parallel to grain, E_o [N/mm ²]	12000
Shear modulus, G_{CLT}	250
No of layer for CLT panel, n	5
Thickness of CLT panel, t_{CLT} [mm]	175
Vertical loading, q [kN/m]	20

The deflection of the coupled shear wall can be calculated using Eq. 4.45 as:

$$\delta = \frac{F}{\sum K_i} - \frac{qh}{2k_{HD}}$$

where

$$\frac{1}{K_i} = \frac{1}{K_{b,i}} + \frac{1}{K_{s,i}} + \frac{1}{K_{sl,i}} + \frac{1}{K_{r,i}}$$

Now, the bending, $K_{b,i}$, shear, $K_{s,i}$, sliding, $K_{sl,i}$ and rocking, $K_{r,i}$, stiffness of each wall segment can be calculated as:

$$K_{b,1} = K_{b,2} = \frac{3(EI_{eff})_i}{h^3} = \frac{3 \cdot 1.98 \times 10^{15}}{3000^3} = 220500 \text{ N/mm}$$

$$K_{s,1} = K_{s,2} = \frac{G_{CLT} \cdot t_{CLT} \cdot b_i}{h} = \frac{250 \cdot 175 \cdot 1500}{3000} = 21875 \text{ N/mm}$$

$$K_{sl,1} = K_{sl,2} = n_{B,i} k_{B,i} = 2 \cdot 5000 = 10000 \text{ N/mm}$$

$$K_{r,1} = K_{r,2} = \frac{b^2 k_{HD,i}}{h^2} = \frac{1500^2 \cdot 6000}{3000^2} = 1500 \text{ N/mm}$$

The total stiffness of the coupled shear wall is:

$$\frac{1}{K_{wall}} = \frac{1}{\sum K_i} = \frac{1}{1224 + 1224} \Rightarrow K_{wall} = 2448 \text{ N/mm}$$

Therefore, the deflection of the coupled shear wall is:

$$\delta = \frac{F}{\sum K_i} - \frac{qh}{2k_{HD}} = \frac{100 \times 10^3}{2448} - \frac{20 \cdot 3000}{2 \cdot 6000} = 40.8 \text{ mm}$$

Appendix B4: Coupled CLT shear wall with 4-HDs connected to a perpendicular wall

Deflection of the coupled CLT shear wall due to 100 kN lateral load with the perpendicular wall and the floor above with self-taping screws is shown in Figure 5.17B.6. The properties of the connectors is described in Table B.4. The properties of the CLT coupled wall and its connections to floor/foundation below is described in Table B.3.

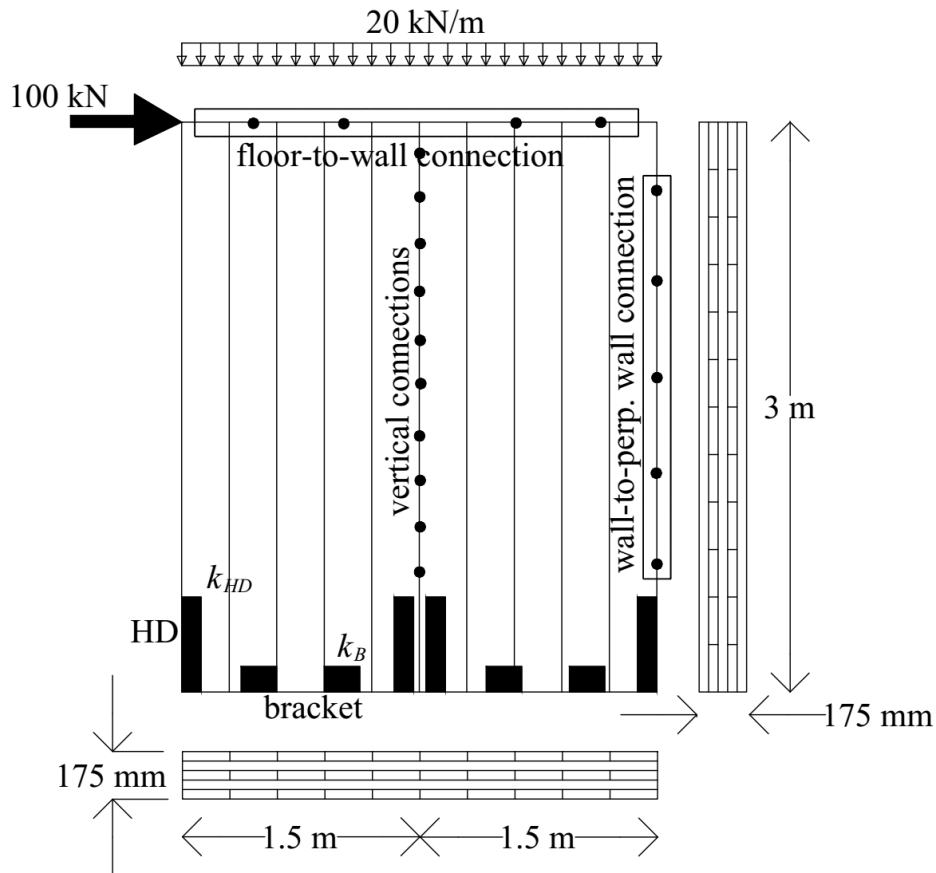


Figure B.6 Geometry and properties of coupled CLT shear walls with 4-HDs connected to perpendicular wall and floor above

Table C.4 Connection properties of CLT coupled shear wall-to-perp. wall and floor above

Properties	
Stiffness of CLT wall-to-floor above connections, k_{fi} [N/mm]	500
Stiffness of CLT wall-to-perp. wall connections, k_{wi} [N/mm]	500
Tensile stiffness of brackets in perpendicular wall, $k_{t,p}$ [N/mm]	1000
Shear stiffness of brackets in perpendicular wall, $k_{s,p}$ [N/mm]	1000
No. of brackets in the perp. wall, n_p	3
Spacing of STSs in CLT shear wall-to-perp. wall connections [mm]	50
Spacing of STSs in CLT shear wall-to-floor connections [mm]	50

Perpendicular wall configuration 1:

The deflection of the coupled shear wall can be calculated using Eq. 4.46 as:

$$\delta = \frac{F}{\sum K_i} - \frac{qh}{2k_{HD}} \frac{1}{r}$$

where

$$\frac{1}{K_i} = \frac{1}{K_{b,i}} + \frac{1}{K_{s,i}} + \frac{1}{K_{sl,i}} + \frac{1}{K_{r,i}}$$

Now, the bending, $K_{b,i}$, shear, $K_{s,i}$, sliding, $K_{sl,i}$ and rocking, $K_{r,i}$, stiffness of each wall segment can be calculated as:

$$K_{b,1} = K_{b,2} = \frac{3(EI_{eff})_i}{h^3} = \frac{3 \cdot 1.98 \times 10^{15}}{3000^3} = 220500 \text{ N/mm}$$

$$K_{s,1} = K_{s,2} = \frac{G_{CLT} \cdot t_{CLT} \cdot b_i}{h} = \frac{250 \cdot 175 \cdot 1500}{3000} = 21875 \text{ N/mm}$$

$$K_{sl,1} = n_{B,i}k_{B,i} + n_{f,i}k_{f,i} = 2*5000 + 2*500 = 11000 \text{ N/mm}$$

$$K_{sl,2} = n_{B,i}k_{B,i} + n_{w,i}k_{w,i} + n_{f,i}k_{f,i} = 2*5000 + 5*500 + 2*500 = 13500 \text{ N/mm}$$

$$\begin{aligned} r &= \left[1 + \frac{1}{b^2} \left(\sum_{i=1}^{n_f} x_i^2 k_{fi} + \sum_{i=1}^{n_w} y_i^2 k_{wi} \right) \frac{1}{k_{HD}} \right]^{-1} \\ &= \left[1 + \frac{1}{1500^2} (500(500^2 + 1000^2 + 1500^2 + 2000^2 + 2500^2)) \frac{1}{6000} \right. \\ &\quad \left. + \frac{1}{1500^2} (500(500^2 + 1000^2 + 2000^2 + 2500^2)) \frac{1}{6000} \right]^{-1} \\ &= 0.52 \end{aligned}$$

$$\begin{aligned} r' &= \left[1 + \frac{1}{b^2} \left(\sum_{i=1}^{n_f} x_i^2 k_{fi} \right) \frac{1}{k_{HD}} \right]^{-1} \\ &= \left[1 + \frac{1}{1500^2} (500(500^2 + 1000^2 + 2000^2 + 2500^2)) \frac{1}{6000} \right]^{-1} \\ &= 0.7 \end{aligned}$$

$$K_{r,1} = \left(\frac{b^2 k_{HD,i}}{h^2} \right) \frac{1}{r'} = \frac{1500^2 * 6000}{3000^2} \frac{1}{0.7} = 2143 \text{ N/mm}$$

$$K_{r,2} = \left(\frac{b^2 k_{HD,i}}{h^2} \right) \frac{1}{r} = \frac{1500^2 * 6000}{3000^2} \frac{1}{0.52} = 2885 \text{ N/mm}$$

The total stiffness of the left wall panel is:

$$\frac{1}{K_1} = \frac{1}{K_{b,1}} + \frac{1}{K_{s,1}} + \frac{1}{K_{sl,1}} + \frac{1}{K_{r,1}} = \frac{1}{1645} \Rightarrow K_1 = 1645 \text{ N/mm}$$

The total stiffness of the right wall panel is:

$$\frac{1}{K_2} = \frac{1}{K_{b,2}} + \frac{1}{K_{s,2}} + \frac{1}{K_{sl,2}} + \frac{1}{K_{r,2}} = \frac{1}{2123} \Rightarrow K_1 = 2123 \text{ N/mm}$$

Therefore, the total stiffness of the CLT coupled wall can be calculated as:

$$\frac{1}{K_{wall}} = \frac{1}{\sum K_i} = \frac{1}{1645 + 2123} \Rightarrow K_{wall} = 3768 \text{ N/mm}$$

Therefore, the deflection of the coupled shear wall with perpendicular wall and HDs can be estimated as:

$$\delta = \frac{F}{\sum K_i} - \frac{qh}{2k_{HD}} \frac{1}{r} = \frac{100 \times 10^3}{3768} - \frac{20 \times 3000}{2 \times 6000} \frac{1}{0.52} = 16.9 \text{ mm}$$

Perpendicular wall configuration 2:

The deflection of the coupled shear wall can be calculated using Eq. 4.53 as:

$$\delta = \frac{F}{\sum K_i} - \frac{qh}{2k'_{HD}} \frac{1}{r'}$$

The stiffness of wall segments can be calculated:

$$\frac{1}{K_i} = \frac{1}{K_{b,i}} + \frac{1}{K_{s,i}} + \frac{1}{K_{sl,i}} + \frac{1}{K_{r,i}}$$

Now, the bending, $K_{b,i}$, shear, $K_{s,i}$, sliding, $K_{sl,i}$ and rocking, $K_{r,i}$, stiffness of each wall segment can be calculated as:

$$K_{b,1} = K_{b,2} = \frac{3(EI_{eff})_i}{h^3} = \frac{3 \times 1.98 \times 10^{15}}{3000^3} = 220500 \text{ N/mm}$$

$$K_{s,1} = K_{s,2} = \frac{G_{CLT} \cdot t_{CLT} \cdot b_i}{h} = \frac{250 \times 175 \times 1500}{3000} = 21875 \text{ N/mm}$$

$$K_{sl,1} = n_{B,i} k_{B,i} + n_{f,i} k_{f,i} = 2 \times 5000 + 2 \times 500 = 11000 \text{ N/mm}$$

$$K_{sl,2} = n_{B,i} k_{B,i} + n_{f,i} k_{f,i} + n_p k_{s,p} = 2 \times 5000 + 2 \times 500 + 3 \times 1000 = 14000 \text{ N/mm}$$

$$\begin{aligned}
r' &= \left[1 + \frac{1}{b^2} \left(\sum_{i=1}^{n_f} x_i^2 k_{fi} \right) \frac{1}{k'_{HD}} \right]^{-1} \\
&= \left[1 + \frac{1}{1500^2} (500(500^2 + 1000^2 + 2000^2 + 2500^2)) \frac{1}{6000} \right]^{-1} \\
&= 0.7
\end{aligned}$$

$$K_{r,1} = \left(\frac{b^2 k'_{HD,i}}{h^2} \right) \frac{1}{r'} = \frac{1500^2 * 6000}{3000^2} \frac{1}{0.7} = 2143 \text{ N/mm}$$

$$k'_{HD} = k_{HD} + n_p k_{t,p} = 6000 + 3 * 1000 = 9000 \text{ N/mm}$$

$$K_{r,2} = \left(\frac{b^2 k'_{HD,i}}{h^2} \right) \frac{1}{r'} = \frac{1500^2 * 9000}{3000^2} \frac{1}{0.7} = 3214 \text{ N/mm}$$

The total stiffness of the left wall panel is:

$$\frac{1}{K_1} = \frac{1}{K_{b,1}} + \frac{1}{K_{s,1}} + \frac{1}{K_{sl,1}} + \frac{1}{K_{r,1}} = \frac{1}{1645} \Rightarrow K_1 = 1645 \text{ N/mm}$$

The total stiffness of the right wall panel is:

$$\frac{1}{K_2} = \frac{1}{K_{b,2}} + \frac{1}{K_{s,2}} + \frac{1}{K_{sl,2}} + \frac{1}{K_{r,2}} = \frac{1}{2211} \Rightarrow K_2 = 2211 \text{ N/mm}$$

Therefore, the total stiffness of the CLT coupled wall can be calculated as:

$$\frac{1}{K_{wall}} = \frac{1}{\sum K_i} \Rightarrow K_{wall} = 3856 \text{ N/mm}$$

Therefore, the deflection of the coupled shear wall with perpendicular wall and HDs can be estimated as:

$$\delta = \frac{F}{\sum K_i} - \frac{qh}{2k'_{HD}} = \frac{100 \times 10^3}{3856} - \frac{20 * 3000}{2 * 9000} \frac{1}{0.7} = 21.17 \text{ mm}$$

Appendix B5: Coupled CLT shear wall with 2-HDs connected to a perpendicular wall

The deflection of coupled CLT shear wall with 2-HDs as shown in Figure 5.17B.7 can be estimated using the equation of single CLT shear wall. The properties of the wall and connectors is described in Table B.3 and Table B4.

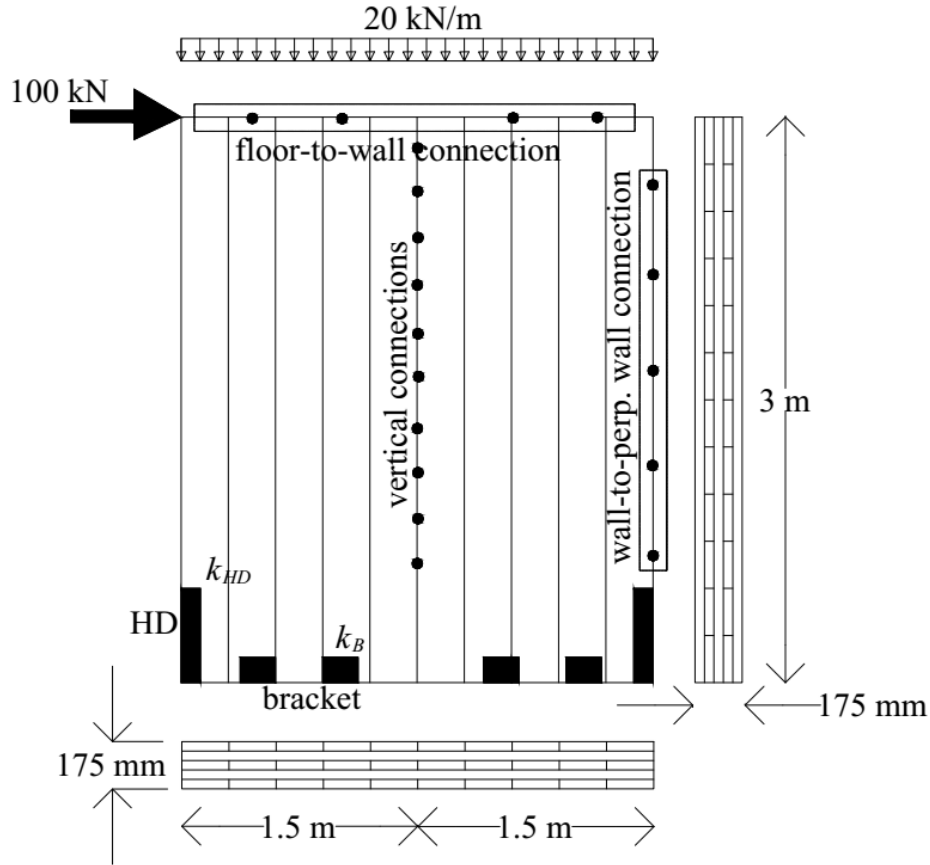


Figure B.7 Geometry and properties of coupled CLT shear walls with 2-HDs connected to perp. wall and floor above

The deflection of coupled CLT shear wall with 2-HDs and without any perpendicular wall or floor above:

$$\delta = \frac{Fh^3}{3EI_{eff}} + \frac{Fh}{G_{CLT}t_{CLT}b} + \frac{F}{n_Bk_B} + \left(\frac{Fh^2}{b^2} - \frac{qh}{2} \right) \frac{1}{k_{HD}} = 21.1 \text{ mm}$$

The deflection of coupled CLT shear wall with 2-HDs and with perpendicular wall configuration 1 (Figure 4.3a) and floor above:

$$\delta = \left(\frac{Fh^3}{3EI_{eff}} + \frac{F \cdot h}{G_{CLT} \cdot t_{CLT} \cdot b} + \frac{F}{n_B k_B + n_w k_w + n_f k_f} + \left(\frac{F \cdot h^2}{b^2} - \frac{qh}{2} \right) \frac{1}{k_{HD}} \left[1 + \frac{1}{b^2} \left(\sum_{i=1}^{n_f} x_i^2 k_{fi} + \sum_{i=1}^{n_w} y_i^2 k_{wi} \right) \frac{1}{k_{HD}} \right]^{-1} \right)$$

$$\Rightarrow \delta = 0.45 + 2.29 + 5.1 + 9.45 = 17.3 \text{ mm}$$

The deflection of coupled CLT shear wall with 2-HDs and with perpendicular wall configuration 2 (Figure 4.3b) and floor above:

$$\delta = \left(\frac{Fh^3}{3EI_{eff}} + \frac{F \cdot h}{G_{CLT} \cdot t_{CLT} \cdot b} + \frac{F}{n_B k_B + n_f k_f + n_p k_{sl,p}} + \left(\frac{F \cdot h^2}{b^2} - \frac{qh}{2} \right) \frac{1}{k_{HD} + n_p k_{t,p}} \left[1 + \frac{1}{b^2} \left(\sum_{i=1}^{n_f} x_i^2 k_{fi} \right) \frac{1}{k_{HD} + n_p k_{t,p}} \right]^{-1} \right)$$

$$\Rightarrow \delta = 0.45 + 2.29 + 5.0 + 7.3 = 15.0 \text{ mm}$$

Appendix C: Examples on Lateral Resistance of CLT Shear Walls

Appendix C1: Single CLT Shear Wall with Brackets

Find the lateral resistance of the single CLT shear wall with brackets as shown in Figure C.1. The wall is 3×3 m with a 5-layer of CLT panel. The properties of the wall is described in Table C.1.

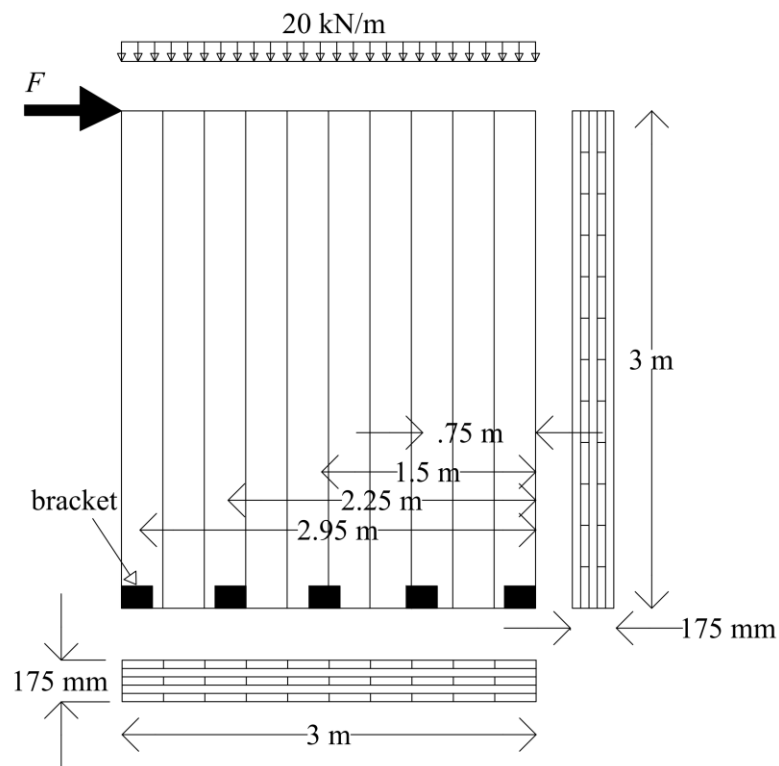


Figure C.1 Lateral resistance calculation in a single CLT shear wall with brackets

Table C.1 Properties of CLT shear wall

Parameters	
Length, b [mm]	3000
Height, h [mm]	3000
No. of brackets, n_B	3
Stiffness of bracket, k_B [N/mm]	5000
Stiffness of hold-downs, k_{HD} [N/mm]	6000
No of layer in CLT panel, n	5
Total thickness of CLT panel, t_{CLT} [mm]	175
Vertical loading, q [kN/m]	20
Fasteners in brackets	12-16d SN 3.9×89 mm
Fasteners in HDs	18-16d SN 3.9×89 mm

Lateral Resistance of the Fasteners:

Fasteners type: spiral nails 16d-3.9×89 mm

According to CSA O86-16, the factored resistance of the fasteners can be calculated as:

$$N_R = \phi n_u n_F n_S J_F$$

$$N_u = n_u (K_D K_{SF} K_T)$$

where

ϕ = resistance factor ($\phi = 0.8$)

N_R = factored lateral resistance of nails

N_u = specified lateral resistance of nails

n_u = unit lateral resistance

n_F = number of fasteners in the connection

n_s = number of shear planes per nail

$$J_F = J_E J_A J_B J_D$$

J_E = end grain factor = 1.0

J_A = toe-nailing factor = 1.0

J_B = nail clinching factor = 1.0

J_D = factor for diaphragm and shear wall construction = 1.3

K_D = load duration factor ($K_D = 1.15$)

K_{SF} = service condition factor for fastening

K_T = Preservative and fire-retardant treatment factor ($K_T = 1.0$)

The unit lateral resistance, n_u can be calculated from the smallest value of the following equations:

(a) $f_1 d_F t_1$

(b) $f_2 d_F t_2$

(c) $\frac{1}{2} f_2 d_F t_2$

(d) $f_1 d_F^2 \left(\sqrt{\frac{1}{6} \frac{f_3}{f_1 + f_3} \frac{f_y}{f_1}} + \frac{1}{5} \frac{t_1}{d_F} \right)$

(e) $f_1 d_F^2 \left(\sqrt{\frac{1}{6} \frac{f_3}{f_1 + f_3} \frac{f_y}{f_1}} + \frac{1}{5} \frac{t_2}{d_F} \right)$

(f) $f_1 d_F^2 \frac{1}{5} \left(\frac{t_1}{d_F} + \frac{f_2}{f_1} \frac{t_2}{d_F} \right)$

(g) $f_1 d_F^2 \left(\sqrt{\frac{2}{3} \frac{f_3}{f_1 + f_3} \frac{f_y}{f_1}} \right)$

where

d_F = nail diameter (mm)

t_l = steel thickness (mm)

t_2 = length of penetration into wood (mm)

f_l = embedment strength of steel (MPa) = $3(\Phi_{\text{steel}} / \Phi_{\text{wood}}) f_u$

f_2 = embedment strength of wood (MPa) = $50G(1 - 0.01d_F)J_x$

f_3 = embedment strength of wood where failure is fastener yielding (MPa) = $110G^{1.8}(1 - 0.01d_F)J_x$

f_y = nail yield strength (MPa) = $50(16 - d_F)$

f_u = ultimate tensile strength of steel (MPa) = ASTM A36 = 400 MPa

G = mean relative density of lumber

Table D.2 Properties of the connections: nail fasteners 16d-3.9×89 mm

Parameters	
d_f [mm]	3.9
t_l [mm]	3
t_2 [mm]	86
f_u [N/mm ²]	400
G	0.42
n_s	1
n_f (HDs)	18
n_f (brackets)	12
K_d	1.15
K_{SF}	1
K_T	1
J_F	1.3
J_X	0.9
Φ_{steel}	0.67
Φ_{wood}	0.8

The embedded strength can be calculated as:

$$f_1 = 3(\Phi_{\text{steel}} / \Phi_{\text{wood}}) f_u = 3(0.67 / 0.8) 400 = 1005 \text{ N/mm}^2$$

$$f_2 = 50G(1 - 0.01d_F) J_x = 50 * 0.42(1 - .01 * 3.9) 0.9 = 18.2 \text{ N/mm}^2$$

$$f_3 = 110G^{1.8}(1 - 0.01d_F) J_x = 110 * 0.42^{1.8}(1 - .01 * 3.9) * 0.9 = 19.96 \text{ kN/mm}^2$$

The unit lateral resistance, n_u :

$$(a) f_1 d_F t_1 = 11.8 \text{ kN}$$

$$(b) f_2 d_F t_2 = 6.1 \text{ kN}$$

$$(d) f_1 d_F^2 \left(\sqrt{\frac{1}{6} \frac{f_3}{f_1 + f_3} \frac{f_y}{f_1}} + \frac{1}{5} \frac{t_1}{d_F} \right) = 3.03 \text{ kN}$$

$$(e) f_1 d_F^2 \left(\sqrt{\frac{1}{6} \frac{f_3}{f_1 + f_3} \frac{f_y}{f_1}} + \frac{1}{5} \frac{t_2}{d_F} \right) = 68.1 \text{ kN}$$

$$(f) f_1 d_F^2 \frac{1}{5} \left(\frac{t_1}{d_F} + \frac{f_2}{f_1} \frac{t_2}{d_F} \right) = 3.57 \text{ kN}$$

$$(g) f_1 d_F^2 \left(\sqrt{\frac{2}{3} \frac{f_3}{f_1 + f_3} \frac{f_y}{f_1}} \right) = 1.35 \text{ kN}$$

Therefore, the minimum unit lateral resistance, $n_u = 1.35 \text{ kN}$

Factored lateral resistance of a single nail:

$$N_R = \phi n_u n_F n_S J_F = 0.8(1.35 * 1.15 * 1 * 1) * 1 * 1 * 1.3$$

$$\Rightarrow N_R = 1.61 \text{ kN}$$

Now, the lateral resistance of the brackets and HDs:

$$N_B = 12 * N_R = 19.3 \text{ kN} \quad N_{HD} = 18 * N_R = 29 \text{ kN}$$

Lateral resistance of Single CLT wall with brackets:

Now the rocking resistance the single CLT shear wall with brackets can be calculated as:

$$\begin{aligned} F_r &= \frac{N_B}{h x_1} \left(\sum_1^{n_B} x_i^2 \right) + q \frac{b^2}{2h} \\ &\Rightarrow \frac{19.3}{3 * 2.95} (2.95^2 + 2.25^2 + 1.5^2 + 0.75^2) + 20 \frac{3^2}{2 * 3} \\ &\Rightarrow 66.2 \text{ kN} \end{aligned}$$

The combined rocking-sliding of the single CLT shear wall with brackets can be calculated as:

$$F_{r-sl} = \frac{N_B - N_{B,sl}}{h x_1} \left(\sum_1^{n_B} x_i^2 \right) + q \frac{b^2}{2h}$$

Now the ratio of the sliding-to-rocking reactions of the bracket at the ultimate resistance of the wall can be calculated using following formula:

$$\begin{aligned} \frac{N_{B,sl}}{N_{B,r}} &= \frac{\frac{F}{n_B k_B}}{\left(\frac{F \cdot h^2}{b^2} - \frac{qh}{2} \right) \frac{1}{k_B}}; \text{ where } F \leq F_r \\ &\Rightarrow \frac{N_{B,sl}}{N_{B,r}} = \frac{\frac{66.2 \times 10^3}{5 * 5000}}{\left(\frac{66.2 \times 10^3 * 3000^2}{3000^2} - \frac{20 * 3000}{2} \right) \frac{1}{5000}} = 0.37 \end{aligned}$$

The sliding and rocking reactions can be calculated using the linear interaction formula:

$$\begin{aligned} \frac{N_{B,sl}}{N_B} + \frac{N_{B,r}}{N_B} &\leq 1.0 \\ &\Rightarrow N_{B,sl} = 5.17 \text{ kN} \\ &\Rightarrow N_{B,r} = 14.13 \text{ kN} \end{aligned}$$

Therefore, the combined rocking-sliding of the single CLT shear wall with brackets:

$$F_{r-sl} = \frac{19.3 - 5.17}{3 * 2.95} (2.95^2 + 2.25^2 + 1.5^2 + 0.75^2) + 20 \frac{3^2}{2 * 3} = 56.47 \text{ kN}$$

Appendix C2: Single CLT Shear Wall with Brackets and Hold-downs

Find the lateral resistance of the single CLT shear wall with brackets and 2-HDs at the corner as shown in Figure C.2. The wall is 3×3 m with a 5-layer of CLT panel. The properties of the wall is described in Table C.1.

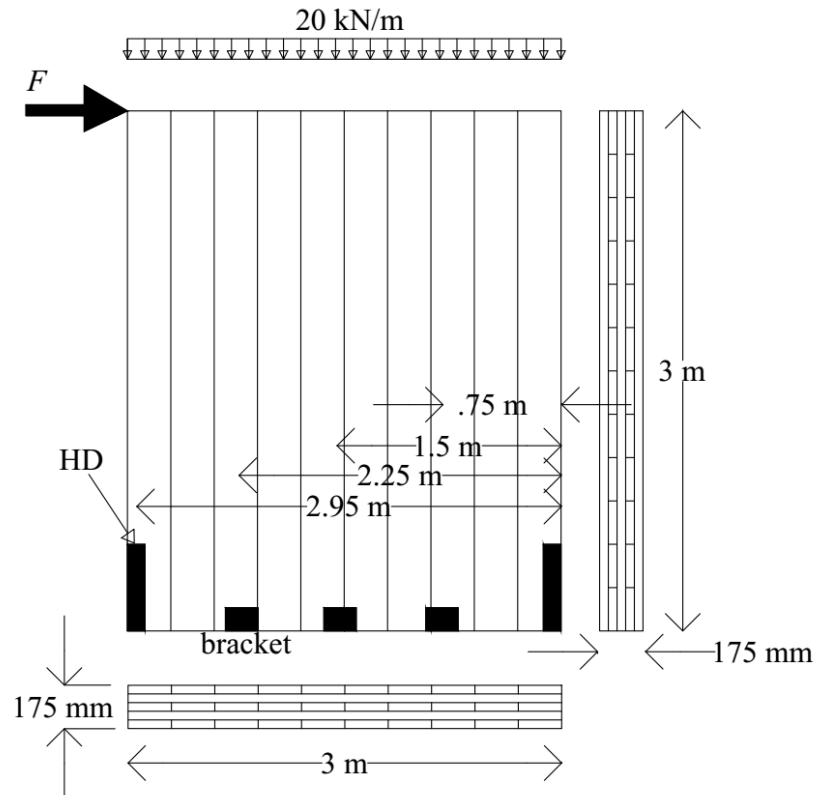


Figure C.2 Lateral resistance calculation in a single CLT shear wall with brackets and HDs

Lateral resistance of Single CLT wall with brackets and HDs:

The factored lateral resistance of the brackets and HDs:

$$N_B = 19.3 \text{ kN} ; N_{HD} = 29 \text{ kN}$$

Now the rocking resistance the single CLT shear wall with brackets and HDs can be calculated as:

$$F_r = \frac{N_{HD}x_1}{h} + \frac{N_B}{x_1h} \left(\sum x_i^2 \right) + q \frac{b^2}{2h}$$

$$\Rightarrow \frac{29*2.95}{3} + \frac{19.3}{3*2.95} (2.25^2 + 1.5^2 + 0.75^2) + 20 \frac{3^2}{2*3}$$

$$\Rightarrow 75.7 \text{ kN}$$

The combined rocking-sliding of the single CLT shear wall with brackets and HDs can be calculated as:

$$F_{r-sl} = \frac{N_{HD}x_1}{h} + \frac{N_B - N_{B,sl}}{x_1h} \left(\sum x_i^2 \right) + q \frac{b^2}{2h}$$

Now the ratio of the sliding-to-rocking reactions of the bracket at the ultimate resistance of the wall can be calculated using following formula:

$$\frac{N_{B,sl}}{N_{B,r}} = \frac{\frac{F}{n_B k_B}}{\left(\frac{F \cdot h^2}{b^2} - \frac{qh}{2} \right) \frac{1}{k_{HD}}} ; \text{ where } F \leq F_r \Rightarrow \frac{N_{B,sl}}{N_{B,r}} = \frac{\frac{75.7 \times 10^3}{3 * 5000}}{\left(\frac{75.7 \times 10^3 * 3000^2}{3000^2} - \frac{20 * 3000}{2} \right) \frac{1}{7500}} = 0.83$$

The sliding and rocking reactions can be calculated using the linear interaction formula:

$$\frac{N_{B,sl}}{N_B} + \frac{N_{B,r}}{N_B} \leq 1.0$$

$$\Rightarrow N_{B,sl} = 8.7 \text{ kN}$$

$$\Rightarrow N_{B,r} = 10.6 \text{ kN}$$

Therefore, the combined rocking-sliding of the single CLT shear wall with brackets and HDs:

$$F_{r-sl} = \frac{29*2.95}{3} + \frac{19.3-8.7}{3*2.95} (2.25^2 + 1.5^2 + 0.75^2) + 20 \frac{3^2}{2*3} = 67.2 \text{ kN}$$

Appendix C3: Coupled CLT Shear Wall with Brackets and 2-HDs

Find the lateral resistance of a coupled CLT shear wall with brackets and 2-HDs at the corner as shown in Figure C.3. The wall contains two panels of each 2.1 m length with a 5-layer of CLT panel. The properties of the wall is described in Table C.1. The panels are connected by lap joints with STSs of 10-8×120 mm.

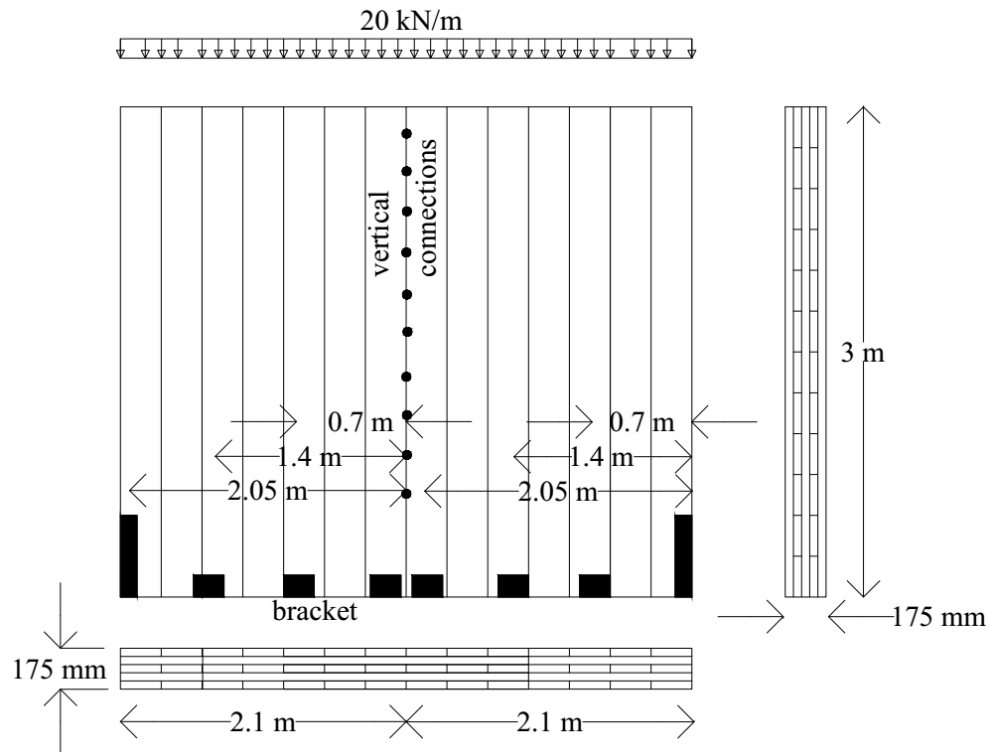


Figure C.3 Lateral resistance calculation in a coupled CLT shear wall with brackets and 2-HDs

Lateral Resistance of the Fasteners:

The factored lateral resistance of the brackets and HDs:

$$N_B = 19.3 \text{ kN} ; N_{HD} = 29 \text{ kN}$$

Lateral Resistance of Vertical Joints:

Fasteners type: STSs of 10-8×120 mm.

Table C.3 Properties of the vertical joints: STSs 10-8×120 mm

Parameters	
d_f [mm]	8
t_1 [mm]	87.5
t_2 [mm]	32.5
G	0.42
n_s	1
n_f	10
K_d	1.15
K_{SF}	1
K_T	1
J_F	1.3
J_X	0.9

The embedded strength can be calculated as:

$$f_1 = 50G(1 - 0.01d_F)J_x = 50 * 0.42(1 - .01 * 8)0.9 = 17.4 \text{ N/mm}^2$$

$$f_2 = 50G(1 - 0.01d_F)J_x = 50 * 0.42(1 - .01 * 8)0.9 = 17.4 \text{ N/mm}^2$$

$$f_3 = 110G^{1.8}(1 - 0.01d_F)J_x = 110 * 0.42^{1.8}(1 - .01 * 8) * 0.9 = 19.1 \text{ kN/mm}^2$$

The unit lateral resistance, n_u :

$$(a) f_1 d_F t_1 = 12.1 \text{ kN}$$

$$(b) f_2 d_F t_2 = 4.5 \text{ kN}$$

$$(d) f_1 d_F^2 \left(\sqrt{\frac{1}{6} \frac{f_3}{f_1 + f_3} \frac{f_y}{f_1}} + \frac{1}{5} \frac{t_1}{d_F} \right) = 4 \text{ kN}$$

$$(e) f_1 d_F^2 \left(\sqrt{\frac{1}{6} \frac{f_3}{f_1 + f_3} \frac{f_y}{f_1}} + \frac{1}{5} \frac{t_2}{d_F} \right) = 2.48 \text{ kN}$$

$$(f) f_1 d_F^2 \frac{1}{5} \left(\frac{t_1}{d_F} + \frac{f_2}{f_1} \frac{t_2}{d_F} \right) = 3.34 \text{ kN}$$

$$(g) f_1 d_F^2 \left(\sqrt{\frac{2}{3} \frac{f_3}{f_1 + f_3} \frac{f_y}{f_1}} \right) = 3.15 \text{ kN}$$

Therefore, the minimum unit lateral resistance, $n_u = 2.48 \text{ kN}$

Factored lateral resistance of a screw:

$$N_R = \phi n_u n_F n_S J_F = 0.8(2.48 * 1.15 * 1 * 1) * 1 * 1 * 1.3$$

$$\Rightarrow N_R = 2.97 \text{ kN}$$

Now, the lateral resistance of the vertical STS joints:

$$N_S = 10 * N_R = 29.7 \text{ kN}$$

Lateral resistance of Coupled CLT wall with brackets and 2-HDs:

The rocking resistance the coupled CLT shear wall with brackets and 2-HDs can be calculated as:

$$F_r = \frac{1}{h} \left[\frac{N_{HD} b}{2} + \frac{2N_B}{b} \left(\sum x_i^2 \right) + q \frac{b^2}{4} + \frac{N_S b}{2} \right]$$

$$\Rightarrow \frac{1}{3} \left[\frac{29 * 4.2}{2} + \frac{2 * 19.3}{4.2} (1.4^2 + 0.7^2 + 2.05^2 + 1.4^2 + 0.7^2) + 20 \frac{4.2^2}{4} + \frac{29.7 * 4.2}{2} \right]$$

$$\Rightarrow 98.4 \text{ kN}$$

The combined rocking-sliding of the single CLT shear wall with brackets and HDs can be calculated as:

$$F_{r-sl} = \frac{1}{h} \left[\frac{bN_{HD}}{2} + \frac{2(N_B - \max \{N_{B,sl,i}\})}{b} \left(\sum x_i^2 \right) + q \frac{b^2}{4} + \frac{N_S b}{2} \right]$$

Now the ratio of the sliding-to-rocking reactions of the bracket at the ultimate resistance of the wall can be calculated using following formula:

$$\frac{N_{B,sl}}{N_{B,r}} = \frac{\frac{F_i}{n_B k_B}}{\left(\frac{F_i h^2}{b^2} - \frac{qh}{2} \right) \frac{1}{k_{HD}}}; \text{ where } F_i \leq F_{r,i}$$

$$\Rightarrow \frac{N_{B,sl}}{N_{B,r}} = \frac{\frac{(98.4/2) \times 10^3}{3 \times 5000}}{\left(\frac{(98.4/2) \times 10^3 \times 3000^2}{2100^2} - \frac{20 \times 3000}{2} \right) \frac{1}{7500}} = 0.35$$

The sliding and rocking reactions can be calculated using the linear interaction formula:

$$\frac{N_{B,sl}}{N_B} + \frac{N_{B,r}}{N_B} \leq 1.0 \Rightarrow N_{B,sl} = 5 \text{ kN} \Rightarrow N_{B,r} = 14.3 \text{ kN}$$

Therefore, the combined rocking-sliding of the single CLT shear wall with brackets and HDs:

$$F_{r-sl} = \frac{1}{h} \left[\frac{b N_{HD}}{2} + \frac{2(N_B - \max \{N_{B,sl,i}\})}{b} \left(\sum_{i=1}^{n_B} x_i^2 \right) + q \frac{b^2}{4} + \frac{N_S b}{2} \right]$$

$$\Rightarrow F_{r-sl} = \frac{1}{3} \left[\frac{29 \times 4.2}{2} + \frac{2 \times (19.3 - 5)}{4.2} (1.4^2 + 0.7^2 + 2.05^2 + 1.4^2 + 0.7^2) + 20 \frac{4.2^2}{4} + \frac{29.7 \times 4.2}{2} \right]$$

$$\Rightarrow 91.2 \text{ kN}$$

Check for the yielding of STSs:

In order to ensure that the vertical joints yield first, the following inequalities must satisfy:

$$N_S < N_{HD} + \frac{N_B}{b_1} \left(\sum_{i=1}^{n_{B1}} x_i \right) + q b_1$$

$$\Rightarrow N_S (= 29.7) < 29 + \frac{19.3}{2.1} (1.4 + 0.7) + 20 \times 2.1$$

$$\Rightarrow N_S (= 29.7) < 90.2 \Rightarrow \text{ok}$$

Appendix C4: Coupled CLT Shear Wall with Brackets and 4-HDs

Find the lateral resistance of a coupled CLT shear wall with brackets and 4-HDs at the corner as shown in Figure C.4. The wall contains two panels of each 2.1 m length with a 5-layer of CLT panel. The properties of the wall is described in Table C.1. The panels are connected by lap joints with STSs of 10-8×120 mm.

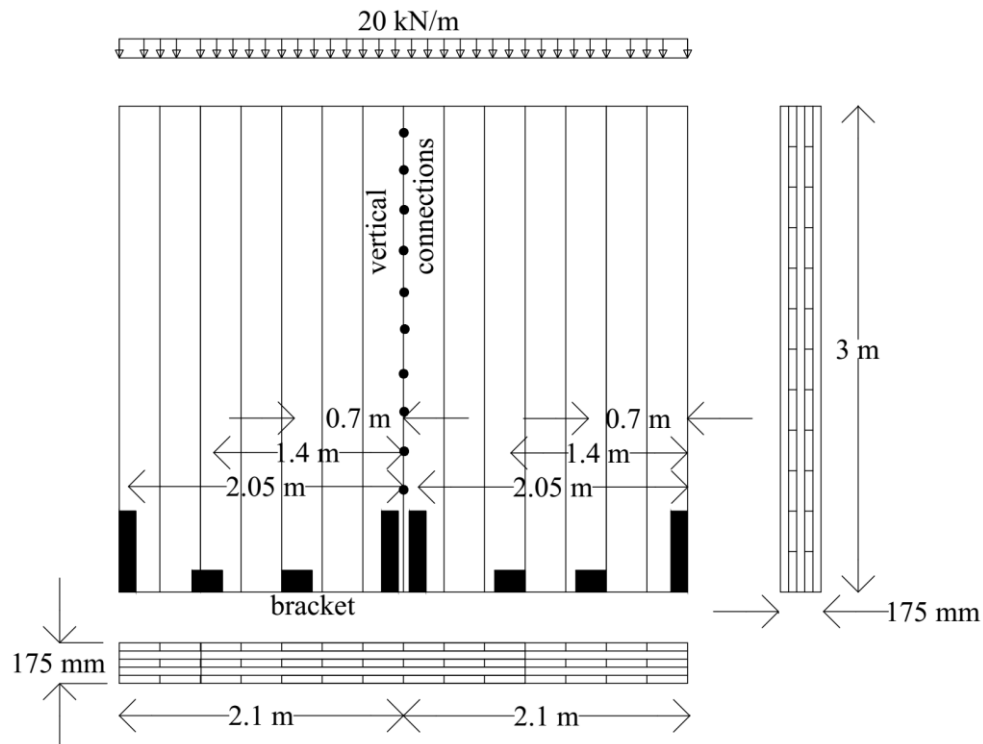


Figure C.4 Lateral resistance calculation in a coupled CLT shear wall with brackets and 4-HDs

Lateral Resistance of the Fasteners:

The factored lateral resistance of the brackets, HDs and STS joints:

$$N_B = 19.3 \text{ kN} ; N_{HD} = 29 \text{ kN} ; N_S = 29.7 \text{ kN}$$

Lateral resistance of Coupled CLT wall with brackets and 4-HDs:

The rocking resistance the coupled CLT shear wall with brackets and 2-HDs can be calculated

as:

$$\begin{aligned} F_r &= \frac{1}{h} \left[N_{HD} b + \frac{2N_B}{b} \left(\sum_{i=1}^{n_B} x_i^2 \right) + q \frac{b^2}{4} + \frac{N_s b}{2} \right] \\ &\Rightarrow \frac{1}{3} \left[29 * 4.2 + \frac{2 * 19.3}{4.2} (1.4^2 + 0.7^2 + 1.4^2 + 0.7^2) + 20 \frac{4.2^2}{4} + \frac{29.7 * 4.2}{2} \right] \\ &\Rightarrow 105.8 \text{ kN} \end{aligned}$$

The combined rocking-sliding of the single CLT shear wall with brackets and HDs can be calculated as:

$$F_{r-sl} = \frac{1}{h} \left[N_{HD} b + \frac{2(N_B - \max \{N_{B,sl,i}\})}{b} \left(\sum_{i=1}^{n_B} x_i^2 \right) + q \frac{b^2}{4} + \frac{N_s b}{2} \right]$$

Now the ratio of the sliding-to-rocking reactions of the bracket at the ultimate resistance of the wall can be calculated using following formula:

$$\begin{aligned} \frac{N_{B,sl}}{N_{B,r}} &= \frac{\frac{F_i}{n_B k_B}}{\left(\frac{F_i h^2}{b^2} - \frac{qh}{2} \right) \frac{1}{k_{HD}}}; \text{ where } F_i \leq F_{r,i} \\ &\Rightarrow \frac{N_{B,sl}}{N_{B,r}} = \frac{\frac{(105.8/2) \times 10^3}{2 * 5000}}{\left(\frac{(105.8/2) \times 10^3 * 3000^2}{2100^2} - \frac{20 * 3000}{2} \right) \frac{1}{7500}} = 0.51 \end{aligned}$$

The sliding and rocking reactions can be calculated using the linear interaction formula:

$$\frac{N_{B,sl}}{N_B} + \frac{N_{B,r}}{N_B} \leq 1.0$$

$$\Rightarrow N_{B,sl} = 6.5 \text{ kN}$$

$$\Rightarrow N_{B,r} = 12.8 \text{ kN}$$

Therefore, the combined rocking-sliding of the single CLT shear wall with brackets and HDs:

$$F_{r-sl} = \frac{1}{h} \left[bN_{HD} + \frac{2(N_B - \max\{N_{B,sl,i}\})}{b} \left(\sum_{i=1}^{n_B} x_i^2 \right) + q \frac{b^2}{4} + \frac{N_S b}{2} \right]$$

$$\Rightarrow F_{r-sl} = \frac{1}{3} \left[29 * 4.2 + \frac{2 * (19.3 - 6.5)}{4.2} (1.4^2 + 0.7^2 + 1.4^2 + 0.7^2) + 20 \frac{4.2^2}{4} + \frac{29.7 * 4.2}{2} \right]$$

$$\Rightarrow 100.7 \text{ kN}$$

Check for the yielding of STSs:

In order to ensure that the vertical joints yield first, the following inequalities must satisfy:

$$N_S < N_{HD} + \frac{N_B}{b_1} \left(\sum_{i=1}^{n_{Bl}} x_i \right) + qb_1$$

$$\Rightarrow N_S (= 29.7) < 29 + \frac{19.3}{2.1} (1.4 + 0.7) + 20 * 2.1$$

$$\Rightarrow N_S (= 29.7) < 90.2 \Rightarrow \text{ok}$$

Appendix D: Parametric studies on Resistance of CLT Shear Walls

Appendix D1: CLT single shear walls

Wall ID	P_{peak} kN	$F_{d,sl}$ kN	$F_{d,r}$ kN	$F_{d,r-sl}$ kN	$P_{peak}/$ $F_{d,sl}$	$P_{peak}/$ $F_{d,r}$	$P_{peak}/$ $F_{d,r-sl}$
W.4B ₁	99.6	90.8	58.3	49.7	1.1	1.7	2.0
W.5B ₁	113.6	113.5	65.6	56.8	1.0	1.7	2.0
W.6B ₁	132.6	136.2	72.9	63.3	1.0	1.8	2.1
W.7B ₁	153.9	158.9	80.4	68.7	1.0	1.9	2.2
W.4B ₂	97.8	115.2	67.8	56.8	0.8	1.4	1.7
W.5B ₂	117.4	144.0	77.0	65.9	0.8	1.5	1.8
W.6B ₂	134.9	172.8	86.4	74.1	0.8	1.6	1.8
W.7B ₂	155.0	201.6	95.8	81.0	0.8	1.6	1.9
W.4B ₃	92.9	94.8	59.9	50.8	1.0	1.6	1.8
W.5B ₃	113.7	118.5	67.4	58.3	1.0	1.7	2.0
W.6B ₃	131.2	142.2	75.1	65.1	0.9	1.7	2.0
W.7B ₃	150.0	165.9	82.9	70.8	0.9	1.8	2.1
W.4B ₄	99.3	48.4	41.8	37.2	2.1	2.4	2.7
W.5B ₄	118.1	60.5	45.7	41.0	2.0	2.6	2.9
W.6B ₄	134.7	72.6	49.6	44.5	1.9	2.7	3.0
W.7B ₄	152.1	84.7	53.6	47.4	1.8	2.8	3.2
W.2HD ₁ .2B ₁	103.9	45.2	51.3	45.2	2.3	2.0	2.3
W.2HD ₁ .3B ₁	119.9	67.8	58.5	50.0	1.8	2.0	2.4
W.2HD ₁ .4B ₁	146.1	90.4	65.8	54.1	1.6	2.2	2.7
W.2HD ₁ .5B ₁	176.4	113.0	73.2	57.4	1.6	2.4	3.1
W.2HD ₁ .2B ₂	104.6	57.6	54.7	46.0	1.8	1.9	2.3
W.2HD ₁ .3B ₂	118.8	86.4	63.9	51.7	1.4	1.9	2.3
W.2HD ₁ .4B ₂	141.2	115.2	73.3	56.8	1.2	1.9	2.5
W.2HD ₁ .5B ₂	156.7	144.0	82.7	60.9	1.1	1.9	2.6
W.2HD ₁ .2B ₃	107.2	47.4	51.9	45.4	2.3	2.1	2.4
W.2HD ₁ .3B ₃	121.1	71.1	59.4	50.4	1.7	2.0	2.4
W.2HD ₁ .4B ₃	135.6	94.8	67.1	54.6	1.4	2.0	2.5
W.2HD ₁ .5B ₃	154.7	118.5	74.9	58.1	1.3	2.1	2.7
W.2HD ₁ .2B ₄	104.3	24.2	45.4	43.2	4.3	2.3	2.4
W.2HD ₁ .3B ₄	121.7	36.3	49.3	46.1	3.4	2.5	2.6
W.2HD ₁ .4B ₄	136.2	48.4	53.2	48.4	2.8	2.6	2.8
W.2HD ₁ .5B ₄	156.3	60.5	57.2	50.2	2.6	2.7	3.1

Wall ID	P_{peak} kN	$F_{d,sl}$ kN	$F_{d,r}$ kN	$F_{d,r-sl}$ kN	$P_{peak}/$ $F_{d,sl}$	$P_{peak}/$ $F_{d,r}$	$P_{peak}/$ $F_{d,r-sl}$
W.2HD ₁ .2B ₅	75.2	28.8	46.7	43.7	2.6	1.6	1.7
W.2HD ₁ .3B ₅	107.2	43.2	51.3	47.1	2.5	2.1	2.3
W.2HD ₁ .4B ₅	117.8	57.6	56.0	49.8	2.0	2.1	2.4
W.2HD ₁ .5B ₅	131.7	72.0	60.7	51.9	1.8	2.2	2.5
W.2HD ₂ .2B ₁	110.3	45.2	47.4	40.4	2.4	2.3	2.7
W.2HD ₂ .3B ₁	126.2	67.8	54.6	44.8	1.9	2.3	2.8
W.2HD ₂ .4B ₁	146.6	90.4	61.9	48.7	1.6	2.4	3.0
W.2HD ₂ .5B ₁	161.4	113.0	69.3	52.0	1.4	2.3	3.1
W.2HD ₁ .2B ₂	113.5	57.6	50.8	41.0	2.0	2.2	2.8
W.2HD ₂ .3B ₂	134.9	86.4	60.0	46.2	1.6	2.2	2.9
W.2HD ₂ .4B ₂	152.2	115.2	69.4	50.9	1.3	2.2	3.0
W.2HD ₂ .5B ₂	169.2	144.0	78.8	54.9	1.2	2.1	3.1
W.2HD ₂ .2B ₃	113.8	47.4	48.0	40.5	2.4	2.4	2.8
W.2HD ₂ .3B ₃	135.2	71.1	55.5	45.1	1.9	2.4	3.0
W.2HD ₂ .4B ₃	154.0	94.8	63.2	49.2	1.6	2.4	3.1
W.2HD ₂ .5B ₃	169.5	118.5	71.0	52.5	1.4	2.4	3.2
W.2HD ₂ .2B ₄	114.0	24.2	41.5	38.8	4.7	2.7	2.9
W.2HD ₂ .3B ₄	132.4	36.3	45.4	41.6	3.6	2.9	3.2
W.2HD ₂ .4B ₄	155.9	48.4	49.3	43.9	3.2	3.2	3.6
W.2HD ₂ .5B ₄	168.8	60.5	53.3	45.7	2.8	3.2	3.7
W.2HD ₂ .2B ₅	74.6	28.8	42.8	39.3	2.6	1.7	1.9
W.2HD ₂ .3B ₅	105.7	43.2	47.4	42.5	2.4	2.2	2.5
W.2HD ₂ .4B ₅	111.1	57.6	52.1	45.1	1.9	2.1	2.5
W.2HD ₂ .5B ₅	118.3	72.0	56.8	47.3	1.6	2.1	2.5

Appendix D2: CLT coupled shear walls

Wall ID	P_{peak}	$F_{d,sl}$	$F_{d,r}$	$F_{d,r-sl}$	$P_{peak}/$	$P_{peak}/$	$P_{peak}/$
	kN	kN	kN	kN	$F_{d,sl}$	$F_{d,r}$	$F_{d,r-sl}$
W.2HD ₁ .4B ₁ .WW ₁	100.2	90.4	48.8	42.7	1.1	2.1	2.3
W.2HD ₁ .4B ₂ .WW ₁	101.8	115.2	52.2	43.5	0.9	1.9	2.3
W.2HD ₁ .4B ₃ .WW ₁	103.0	94.8	49.4	42.8	1.1	2.1	2.4
W.2HD ₁ .4B ₄ .WW ₁	103.1	48.4	42.9	40.4	2.1	2.4	2.6
W.2HD ₁ .4B ₅ .WW ₁	97.8	57.6	44.2	41.2	1.7	2.2	2.4
W.2HD ₁ .4B ₁ .WW ₂	78.0	90.4	48.8	42.7	0.9	1.6	1.8
W.2HD ₁ .4B ₂ .WW ₂	84.8	115.2	52.2	43.5	0.7	1.6	2.0
W.2HD ₁ .4B ₃ .WW ₂	82.8	94.8	49.4	42.8	0.9	1.7	1.9
W.2HD ₁ .4B ₄ .WW ₂	82.1	48.4	42.9	40.4	1.7	1.9	2.0
W.2HD ₁ .4B ₅ .WW ₂	71.3	57.6	44.2	41.2	1.2	1.6	1.7
W.2HD ₂ .4B ₁ .WW ₁	100.4	90.4	52.2	47.3	1.1	1.9	2.1
W.2HD ₂ .4B ₂ .WW ₁	103.4	115.2	55.7	48.4	0.9	1.9	2.1
W.2HD ₂ .4B ₃ .WW ₁	103.9	94.8	52.8	47.5	1.1	2.0	2.2
W.2HD ₂ .4B ₄ .WW ₁	104.0	48.4	46.4	44.6	2.1	2.2	2.3
W.2HD ₂ .4B ₅ .WW ₁	99.2	57.6	47.6	45.3	1.7	2.1	2.2
W.2HD ₂ .4B ₁ .WW ₂	81.4	90.4	52.2	47.3	0.9	1.6	1.7
W.2HD ₂ .4B ₂ .WW ₂	84.7	115.2	55.7	48.4	0.7	1.5	1.7
W.2HD ₂ .4B ₃ .WW ₂	86.4	94.8	52.8	47.5	0.9	1.6	1.8
W.2HD ₂ .4B ₄ .WW ₂	82.7	48.4	46.4	44.6	1.7	1.8	1.9
W.2HD ₂ .4B ₅ .WW ₂	73.5	57.6	47.6	45.3	1.3	1.5	1.6
W.4HD ₁ .4B ₁ .WW ₁	127.6	135.6	67.9	56.4	0.9	1.9	2.3
W.4HD ₁ .4B ₂ .WW ₁	134.1	172.8	74.5	57.9	0.8	1.8	2.3
W.4HD ₁ .4B ₃ .WW ₁	134.3	142.2	69.1	56.7	0.9	1.9	2.4
W.4HD ₁ .4B ₄ .WW ₁	133.3	72.6	56.8	52.5	1.8	2.3	2.5
W.4HD ₁ .4B ₅ .WW ₁	110.1	86.4	59.2	53.6	1.3	1.9	2.1
W.4HD ₁ .4B ₁ .WW ₂	117.2	135.6	67.9	56.4	0.9	1.7	2.1
W.4HD ₁ .4B ₂ .WW ₂	121.4	172.8	74.5	57.9	0.7	1.6	2.1
W.4HD ₁ .4B ₃ .WW ₂	121.8	142.2	69.1	56.7	0.9	1.8	2.1
W.4HD ₁ .4B ₄ .WW ₂	121.1	72.6	56.8	52.5	1.7	2.1	2.3
W.4HD ₁ .4B ₅ .WW ₂	113.1	86.4	59.2	53.6	1.3	1.9	2.1

Wall ID	P_{peak}	$F_{d,sl}$	$F_{d,r}$	$F_{d,r-sl}$	$P_{peak}/$	$P_{peak}/$	$P_{peak}/$
	kN	kN	kN	kN	$F_{d,sl}$	$F_{d,r}$	$F_{d,r-sl}$
W.4HD ₂ .4B ₁ .WW ₁	142.9	135.6	74.8	65.4	1.1	1.9	2.2
W.4HD ₂ .4B ₂ .WW ₁	148.6	172.8	81.4	67.6	0.9	1.8	2.2
W.4HD ₂ .4B ₃ .WW ₁	149.8	142.2	76.0	65.8	1.1	2.0	2.3
W.4HD ₂ .4B ₄ .WW ₁	147.6	72.6	63.7	60.4	2.0	2.3	2.4
W.4HD ₂ .4B ₅ .WW ₁	133.6	86.4	66.1	61.7	1.5	2.0	2.2
W.4HD ₂ .4B ₁ .WW ₂	130.1	135.6	74.8	65.4	1.0	1.7	2.0
W.4HD ₂ .4B ₂ .WW ₂	134.6	172.8	81.4	67.6	0.8	1.7	2.0
W.4HD ₂ .4B ₃ .WW ₂	136.0	142.2	76.0	65.8	1.0	1.8	2.1
W.4HD ₂ .4B ₄ .WW ₂	133.7	72.6	63.7	60.4	1.8	2.1	2.2
W.4HD ₂ .4B ₅ .WW ₂	123.0	86.4	66.1	61.7	1.4	1.9	2.0